JYU DISSERTATIONS 523

Andreas Eriksson

A Multi-Omics Approach to Understand PAH Toxicity in Rainbow Trout (*Oncorhynchus mykiss*) Alevins

UNIVERSITY OF JYVÄSKYLÄ
FACULTY OF MATHEMATICS
AND SCIENCE

JYU DISSERTATIONS 523

Andreas Eriksson

A Multi-Omics Approach to Understand PAH Toxicity in Rainbow Trout (*Oncorhynchus mykiss*) Alevins

Esitetään Jyväskylän yliopiston matemaattis-luonnontieteellisen tiedekunnan suostumuksella
julkisesti tarkastettavaksi yliopiston Ylistönrinteen salissa YAA303
kesäkuun 10. päivänä 2022 kello 12.

Academic dissertation to be publicly discussed, by permission of
the Faculty of Mathematics and Science of the University of Jyväskylä,
in Ylistönrinne, auditorium YAA303, on June 10, 2022 at 12 o'clock noon.

JYVÄSKYLÄN YLIOPISTO
UNIVERSITY OF JYVÄSKYLÄ

JYVÄSKYLÄ 2022

Editors
Anssi Lensu
Department of Biological and Environmental Sciences, University of Jyväskylä
Ville Korkiakangas
Open Science Centre, University of Jyväskylä

ISBN 978-951-39-9159-3 (PDF)
URN:ISBN:978-951-39-9159-3
ISSN 2489-9003

Permanent link to this publication: http://urn.fi/URN:ISBN:978-951-39-9159-3

ABSTRACT

Eriksson, Andreas
A multi-omics approach to understand PAH toxicity in rainbow trout (*Oncorhynchus mykiss*) alevins
Jyväskylä: University of Jyväskylä, 2022, 111 p.
(JYU Dissertations
ISSN 2489-9003; 523)
ISBN 978-951-39-9159-3 (PDF)
Yhteenveto: Omiikat apuna PAH-yhdisteiden toksisuusmekanismien selvittämiseen kirjolohen (*Oncorhynchus mykiss*) poikasissa
Diss.

Polycyclic aromatic hydrocarbons (PAHs) are a group of environmental contaminants originating from incomplete combustion or pyrolysis of organic material, as well as intentional or accidental release of crude oil or industrial spillage and effluents. Exposure to PAHs is known to cause toxicity in developing fish larvae, which includes reduced heart rate, increased occurrence of blue sac disease (BSD) symptoms, as well as altered morphology and behavior. The exact mechanisms of PAH-mediated toxicity, in fish larvae, are still not fully understood, even after decades of research. In this doctoral thesis, the toxicity of two PAHs, with different modes of action (retene: an aryl hydrocarbon receptor 2, Ahr2, agonist; and fluoranthene: a weaker Ahr2 agonist and a cytochrome P450a1, Cyp1a, inhibitor), either alone or as a mixture, were investigated in newly hatched rainbow trout (*Oncorhynchus mykiss*) alevins. Multiple endpoints, including development and growth, BSD, heart function and PAH accumulation, were investigated in relation to how the cardiac transcriptome, proteome, and metabolome responded. Each treatment resulted a unique toxicity profile, while that the mixture was more potent at inducing toxicity than the components. The transcriptome, proteome and metabolome responded in an exposure specific manner. Alterations in heart function and accumulation of the PAHs were a direct consequence of, and could be explained by, changes in the exposure specific upregulations and enrichments. Additionally, we found a specific metabolite, known as FICZ (an Ahr2 agonist that causes PAH and dioxin-like toxicity), which could contribute to toxicity, accumulated following exposure to the mixture. Restrictions in energy availability is implied as per numerous enrichments and upregulations, suggesting impaired yolk consumption, which in turn could influence growth and development negatively. These findings, as presented within this doctoral thesis, extend our understanding of how PAH, alone or as a mixture, induces toxicity in developing rainbow trout alevins.

Keywords: Cardiotoxicity; metabolome; mixture; PAHs; proteome; rainbow trout; transcriptome.

Andreas Eriksson, University of Jyväskylä, Department of Biological and Environmental Science, P.O. Box 35, FI-40014 University of Jyväskylä, Finland

TIIVISTELMÄ

Eriksson, Andreas
Omiikat apuna PAH-yhdisteiden toksisuusmekanismien selvittämiseen kirjolohen (*Oncorhynchus mykiss*) poikasissa
Jyväskylä: Jyväskylän yliopisto, 2022, 111 p.
(JYU Dissertations
ISSN 2489-9003; 523)
ISBN 978-951-39-9159-3 (PDF)
Yhteenveto: Omiikat apuna PAH-yhdisteiden toksisuusmekanismien selvittämiseen kirjolohen (*Oncorhynchus mykiss*) poikasissa
Diss.

Polyaromaattiset hiilivedyt (PAH-yhdisteet) ovat vierasaineita, jotka päätyvät ympäristöön orgaanisen aineksen epätäydellisen palamisen tai tahallisen tai tahattoman öljy- tai jätevesipäästön seurauksena. PAH-yhdisteet aiheuttavat kehittyville kalanpoikasille toksisuutta, joka ilmenee hitaampana pulssina, ruskuaispussitaudin oireina ja muutoksina morfologiassa ja käyttäytymisessä. PAH-yhdisteiden toksisuusmekanismeja kalanpoikasissa ei vielä vuosikymmenten tutkimuksen jälkeenkään tunneta kunnolla. Tässä väitöskirjassa tutkittiin vastakuoriutuneissa kirjolohen (*Oncorhynchus mykiss*) poikasissa kahden eri mekanismilla toimivan PAH-yhdisteen toksisuutta yksittäin ja seoksena. Tutkittavat yhdisteet olivat reteeni (aryylihiilivetyreseptori 2 -proteiinin, Ahr2:n, agonisti) ja fluoranteeni (heikompi Ahr2-agonisti ja Cyp1a-proteiinin inhibiittori). Tutkittavia vasteita olivat kehitys, kasvu, ruskuaispussitauti, sydämen toiminta ja PAH-yhdisteiden kertyminen, ja näitä verrattiin sydämen transkriptomin, proteomin ja metabolomin vasteisiin. Jokainen käsittely aiheutti omanlaisensa toksisuusprofiilin, ja seos aiheutti suuremmat vasteet kuin yksittäiset aineet. Altistusspesifiset geeni- proteiini- ja metaboliittiprofiilit saivat aikaan myös uniikit yliedustusprofiilit. Muutokset sydämen toiminnassa ja PAH-yhdisteiden kertymisessä selittyivät altistusspesifisillä muutoksilla omiikkaprofiileissa. Lisäksi saimme selville, että sisäsyntyinen metaboliatuote FICZ (Ahr2-agonisti, joka saa aikaan dioksiinityyppistä toksisuutta) kertyi seosaltistuksen seurauksena. Monien geenien ja proteiinien voimistava säätely viittaa energiansaannin rajoituksiin, joka saattaa johtua ruskuaisen imeytymisen häiriöistä ja vaikuttaa negatiivisesti kasvuun ja kehitykseen. Nämä havainnot lisäävät ymmärrystämme siitä, miten PAH-yhdisteet erikseen ja seoksena saavat aikaan toksisuutta kirjolohen poikasissa.

Avainsanat: kirjolohi; metabolomi; PAH-yhdisteet; proteomi; seos; sydäntoksisuus; transkriptomi.

Andreas Eriksson, Jyväskylän yliopisto, Bio- ja ympäristötieteiden laitos PL 35, 40014 Jyväskylän yliopisto

Author's address Andreas (Nils Mauritz) Eriksson
Department of Biological and Environmental Science
P.O. Box 35
FI-40014 University of Jyväskylä
Finland
andreas.n.m.eriksson@jyu.fi

Supervisors Docent Eeva-Riikka Vehniäinen, PhD
Department of Biological and Environmental Science
P.O. Box 35
FI-40014 University of Jyväskylä
Finland

Dr. Cyril Rigaud
Department of Biological and Environmental Science
P.O. Box 35
FI-40014 University of Jyväskylä
Finland

Associate Professor Lotta-Riina Sundberg
Nanoscience Center
P.O. Box 35
FI-40014 University of Jyväskylä
Finland

Reviewers Professor Jérôme Cachot
Université de Bordeaux
Bâtiment B2, 1er étage est
Avenue des Facultés
33405 Talence Cedex
France

Professor Lynn Weber
Department of Veterinary Biomedical Sciences
University of Saskatchewan
52 Campus Drive, Room 1319
Saskatoon, SK S7N 5B4T
Canada

Opponent Associate Professor Katja Anttila
University of Turku
Vesilinnantie 5
FI-20500 Turku
Finland

CONTENTS

LIST OF ORIGINAL PUBLICATIONS

This doctoral thesis is based on the following original papers, which will be referred to in the text by their Roman numerals (I – III). The responsibilities and contributions of co-authors for each publication are denoted in Table 1.

I Eriksson A.N.M., Rigaud C., Krasnov A., Wincent E. & Vehniäinen E-R. 2022. Exposure to retene, fluoranthene, and their binary mixture causes distinct transcriptomic and apical outcomes in rainbow trout (*Oncorhynchus mykiss*) yolk sac alevins. *Aquatic Toxicology* 244: 106083. https://doi.org/10.1016/j.aquatox.2022.106083

II Eriksson A.N.M., Rigaud C., Rokka A., Skaugen M., Lihavainen J.H. & Vehniäinen E-R. 2022. Changes in cardiac proteome and metabolome following exposure to the PAHs retene and fluoranthene and their mixture in developing rainbow trout alevins. *Science of the Total Environment* 830: 154846. https://doi.org/10.1016/j.scitotenv.2022.154846

III Eriksson A.N.M., Rigaud C., Wincent E., Pakkanen H., Salonen P. & Vehniäinen E-R. Endogenous AhR agonist FICZ accumulates in rainbow trout (*Oncorhynchus mykiss*) alevins exposed to a mixture of two PAHs, retene and fluoranthene. Submitted manuscript.

TABLE 1 Co-author responsibilities and contributions for publications I–III. Author initials: AE = Andreas Eriksson; AK = Aleksey Krasnov; CR = Cyril Rigaud; ERV = Eeva-Riikka Vehniäinen; EW = Emma Wincent; HP = Hannu Pakkanen; JL = Jenna Lihavainen; PS = Pihla Salonen; AR = Anne Rokka; SM = Morten Skaugen. Column abbreviations: Exp. design = Experimental Design; Trans = Transcriptomics; Prot = Proteomics; Meta = Metabolomics. A dash (-) denotes that the specified analytical approach was not part of said experiment.

	Exp. Design	Exposure and Sampling	qPCR	Body burden	Morph	Trans	Prot	Meta	Primary author
I	AE, CR, ERV	AE, CR, ERV	CR, ERV	AE, EW	AE	AE, CR, AK	-	-	AE
II	AE, CR, ERV	AE, CR, ERV	-	AE, EW	AE	-	AE, CR, SM, AR	AE, CR, JL	AE
III	AE, CR, ERV	AE, CR, ERV	CR	AE, EW, HP, PS	AE, CR	-	-	-	AE

ABBREVIATIONS

ACN	Acetonitrile
BP	Biological Process
BPM	Beats per minute
CC	Cellular component
cDNA	Complementary DNA
cRNA	Complementary RNA
DEG(s)	Differentially expressed gene(s)
DEP(s)	Differentially expressed protein(s)
DNA	Deoxyribonucleic acid
DMSO	Dimethyl sulfoxide
ECHA	European Chemical Agency
EEA	European Environment Agency
EU	European Union
Flu	Fluoranthene
GC-MS	Gas Chromatography-Mass Spectrometry
GO	Gene Ontology
HPLC	High Performance Liquid Chromatography
H_2O_2	Hydrogen peroxide
KEGG	Kyoto Encyclopedia of Genes and Genomes
LC/MS-MS	Liquid Chromatography–Mass Spectrometry–Mass Spectrometry
LRTAP	Geneva Convention on Long-Range Transboundary Air Pollution
MF	Molecular Function
Mix	Mixture (retene + fluoranthene)
MS	Mass spectrometry
NASA	National Aeronautics and Space Administration
OECD	Organization for Economic Co-operation and Development
ORA	Over Representation Analysis
PAH(s)	Polycyclic aromatic hydrocarbon(s)
PCB	Polychlorinated biphenyl
qPCR	quantitative Polymerase Chain Reaction
Ret	Retene
RNA	Ribonucleic acid
SFS	Synchronous Fluorescence Spectroscopy
UV	Ultraviolet light

1 INTRODUCTION

1.1 Polycyclic Aromatic Hydrocarbons

1.1.1 An overview

Polycyclic aromatic hydrocarbons (PAHs) are a diverse group of environmental pollutants of either natural or anthropogenic origins. The defining feature of PAHs is the two or more fused aromatic rings (Collier *et al.* 2013). PAHs are naturally occurring compounds that have been detected in interstellar space (Salama 2008, Tielens 2008), on stellar objects other than the Earth (Sagan *et al.* 1993), and have even been proposed as a hypothetical origin for the formation of life (Ehrenfreund *et al.* 2006). Ultimately, it is estimated by NASA that approximately 20 % of all carbon in the universe is present in the form of PAHs (Hoover 2014).

In nature, PAHs always occur as a complex mixture, but the composition of said mixture differs from source to source, and thus, the PAH composition can function as a fingerprint for the identification of the origin of environmental contamination (Ravindra *et al.* 2008). For example, PAHs formed during the incomplete combustion of coniferous wood contain an elevated proportion of the PAH retene (Gabos *et al.* 2001), whereas the PAH composition of petroleum products varies regarding origin and level of refinement. Both of the aforementioned sources of PAHs are influenced by anthropogenic activity (Wild and Jones 1995, Pacyna *et al.* 2003). Certain industrial activities can lead to the formation of volatilized PAHs which, if not treated during the production phase, would be deposited over a large area, whether terrestrial or aquatic (Behera *et al.* 2018). Nevertheless, legislative and technological developments aimed at reducing environmental deposition of PAHs from industrial processes have been successfully implemented, which is exemplified by how changes in production methodology resulted in an 87 % reduction of the national industrial emissions of PAH between 2008 and 2009 in Sweden, as reported by the Swedish Environmental Protection Agency (Naturvårdsverket 2021). Similar results have been observed within the European Union, as the emissions

of any PAH decreased by 77.7 % from 1990 to 2017, as studied and reported by the European Environment Agency (EEA 2019). Even so, environmental deposition of PAHs is rising globally, as the primary source of contamination has shifted from industrial activity to urban sprawl and heating (van der Gon *et al.* 2007). Yet, industrial emissions and effluents are still a prevalent source (Wickström and Tolonen 1987, Van Metre *et al.* 2000). Reliable data from outside the developed world is currently limited but steadily growing in quantity and quality.

The fate of environmentally deposited PAHs depends on multiple factors, such as molecular weight, number of aromatic rings, and in which specific strata the PAHs are deposited. In general, PAHs with lower molecular weight (< 6 fused aromatic rings) are typically volatilized, whereas heavier PAHs (≥ 6 fused aromatic rings) typically become associated with particles (Ravindra *et al.* 2008). Once the PAHs have entered the atmosphere, they can be environmentally deposited either through wet or dry processes. The former represents processes where the PAHs are "scrubbed" from the air by precipitation, whereas the latter involves processes where PAHs adsorb to particles in the atmosphere and are deposited on the ground or in water without precipitation, as per the U.S. Environmental Protection Agency (US EPA 2007). The half-life of volatilized PAHs is typically shorter than in other strata due to photo-oxidation (McConkey *et al.* 2002), although PAHs bound to volatilized particles are more resistant to degradation than those that are not (Falk *et al.* 1956). Terrestrially and aquatically deposited PAHs, irrespective of source, can form so-called legacy deposits, as optimal biological mineralization and degradation of PAHs requires microbial aerobic metabolism (Cerniglia 1993, Jonker *et al.* 2006). It is noteworthy that microbial metabolism and degradation of PAHs is primarily effective at degrading low molecular PAHs, whereas metabolism and mineralization of heavier PAHs is less effective *in situ* (Wilson and Jones 1993, Collier *et al.* 2013). The fate of aquatically deposited PAHs is further complicated by several factors, such as abiotic factors and differences in strata distribution. As a result, the concentration of PAHs is typically highest in sediment, lowest in the water column, and somewhere in between these extremes in suspended particles (Qiu *et al.* 2009, Adeniji *et al.* 2019). As a consequence, the accumulation of PAHs in fish is typically lower in species inhabiting the pelagic zone and greater in those species who prey upon organisms inhabiting contaminated sediment. Another issue associated with PAHs deposited (or spilled) in the aquatic strata is weathering; that is, how weather, waves, sunlight and microbial degradation affect the PAHs (and crude oil) *in situ*. Hence, the higher the proportion of weathered PAHs to unweathered, the older the contamination, as per the US National Oceanic and Atmospheric Administration (NOAA 2015). Subsequently and due to weathering, the proportion of alkylated to un-alkylated PAHs increases with time, which in turn has been linked with increased toxicity compared to the parental compound (Carls *et al.* 1999). Furthermore, the toxicity of unweathered and weathered PAHs (and oil) is 2 to 1000 times stronger in the presence of UV-irradiation (Pelletier *et al.* 1997, Calfee *et al.* 1999), further complicating the

situation while stressing the need for speedy and efficient cleanup following contamination.

The toxicity of PAHs has been under scientific investigation for more than a century, ever since Yamagiwa and Ichikawa (1918) determined that coal tar, which contains high levels of PAHs, is carcinogenic when applied topically to the ear of a domesticated rabbit (*Oryctolagus cuniculus domesticus*), thereby causing the development of squamous cell carcinomas. Prior to this discovery, it was well known within the medical establishment, through epidemiological investigations, that chimney sweeps often developed a rare form of scrotal carcinomas and soot was considered the causative agent (Pott 1974). Unbeknownst at the time, soot contains high levels of PAHs which contributes to the formation of tumors (Richter and Howard 2000).

Over the last five decades, much attention and effort have been focused on PAH toxicity in different organisms at different stages of development. To this end, the US EPA developed a priority list in the early 1970s containing 16 PAHs that should be focused on during toxicological screening; a review covering the background and history is presented by Keith (2015). However, this priority list suffered from two distinct faults: 1) the PAHs included on the list were primarily decided based upon supplier and standard availability in relation to, at the time, known environmental or toxicological relevance, and 2) the list focused primary on individual PAHs rather than complex and simple mixtures of environmental relevance. This list is still considered a guiding document, although it has been heavily criticized and challenged (Andersson and Achten 2015), and remains in use due to its legacy.

Since the inception of the priority list by the US EPA, the toxicity of environmentally deposited PAHs has been extensively investigated, especially following the environmental catastrophe of the grounding of Exxon Valdez off the Alaskan coast in 1989, which contaminated the local environment with 37 000 tons of crude oil (the equivalent of 41 000 m^3). As a result, the local environment, stock of fish, and wildlife were heavily contaminated and damaged (Wolfe *et al.* 1994). Regrettably, the catastrophe occurred during the spawning season for several endemic salmonid species, which in turn resulted in a severely reduced recruitment of new fish stocks, stocks which were already under pressure from overfishing (Thorne and Thomas 2008). Those fish larvae that survived suffered signs of chronic developmental toxicity, signs that were observed in sampled fish over the coming years and beyond (Rice *et al.* 2001, Peterson *et al.* 2003, Ward *et al.* 2017). The observed symptoms of toxicity have been replicable in a laboratory setting, confirming the effects of exposure in relation to toxicological outcomes (Heintz *et al.* 2000). Similar observations have since been reported following numerous catastrophic PAH and crude oil contaminations in recent times, e.g. the Deepwater Horizon catastrophe as reviewed by Pulster *et al.* (2020).

1.1.2 PAH Toxicity

From a toxicological perspective, 3 to 5-ringed PAHs are more biologically available and relevant, as they easily accumulate in organisms compared to larger PAHs, whereas PAHs with ≥ 4 rings are considered to be carcinogenic to humans (Knafla *et al.* 2006). Yet, when considering the octanol-water partition coefficient (log K_{ow}), larger PAHs, which have a greater coefficient than smaller PAHs, should be more biologically and toxicologically relevant, as they accumulate more easily in lipophilic tissue and cellular structures. Inversely, a compound with a greater log K_{ow} equates to poorer water solubility, and therefore tends to become less readily available for biological accumulation and uptake. In general, PAHs have been considered to induce toxicity through two distinct pathways: non-specifically (narcosis) and receptor-specifically. However, the notion of non-specific narcosis toxicity has recently been challenged in a review by Incardona (2017), who presents compelling evidence for PAH-specific hydrophobicity as the driving factor. Rather than interacting with the cell membrane non-specifically, as previously considered the primary mode of action under the narcosis model of toxicity, lipoproteins in the cell membrane are suggested as the plausible target of non-specific PAH toxicity. The main consequence of such toxicity is ultimately the disruption of the flow of ions over the cell membrane which, in turn, would impact multiple intracellular processes that rely upon a normalized ion gradient. Yet, even after decades of research, non-specific PAH toxicity, in developing fish larvae, is still poorly understood and investigated, as indicated by Incardona's review (2017).

In contrast, receptor-specific PAH toxicity has been extensively investigated in fish larvae; the most extensively studied pathway being the activation of aryl hydrocarbon receptor 2 (Ahr2). This pathway is activated when a PAH (or other xenobiotic agonists, such as dioxins, or endogenous metabolites, such as 6-formylindolo[3,2-b]carbazole) binds to Ahr2, thereby acting as a transcription factor that can govern and induce a wide range of downstream gene expressions (Abnet *et al.* 1999).

First and foremost, it must be noted that fish species carry 3 different paralogues of genes that encode for 3 different forms of aryl hydrocarbon receptors: *ahr1a* and *b*, as well as *ahr2* (each presenting multiple isoforms) (Abnet *et al.* 1999, Doering *et al.* 2013). The additional forms of *ahr* among fish, relative to other taxa, are hypothesized to have evolved as consequence of gene duplication during early fish evolution (Hansson *et al.* 2003). The Ahr1 isoforms (a and b), although poorly investigated, are both less prevalent than Ahr2, which is present in 4 isoforms (Hansson and Hahn 2008), as tissue distribution and prevalence of Ahr1 is primarily confined to the liver and hepatocytes (Andreasen *et al.* 2002). Interestingly, it has been proposed that Ahr2 counteracts xenobiotics at lower concentrations, whereas Ahr1b only becomes activated at higher concentrations (Karchner *et al.* 2005), thereby fulfilling different roles of xenobiotic metabolism. This stems from the fact that the relationship between Ahr1a and b, and subsequent toxicity, is complex and, in some instances, contradictory and is both species and xenobiotic-specific, as

reviewed by Shankar *et al.* (2020). From a toxicological perspective, knockdown of *ahr1a* in zebrafish larvae is associated with some protection against cardiac, hepatic, and developmental toxicity following exposure to pyrene (a 4-ringed PAH) (Incardona *et al.* 2006). Knockdown of *ahr1a* and *cyp1a* were associated with delayed pyrene-mediated mortality (exposure to 5 mg l^{-1}), which highlights increased resistance to toxicity. This is further complicated by research published by Garner *et al.* (2013), who report that knockdown of *ahr1a* in zebrafish embryos did not affect fluoranthene and benzo[a]pyrene (BaP) toxicity, albeit increased the expression of *cyp1a*, whereas *ahr1b* knockdown protected against both PAH and polychlorinated biphenyl-126 (PCB) induced cardiotoxicity. Additionally, simultaneous knockdown of *ahr1a* and *b* resulted in protection against PCB-126 mediated toxicity but only intermediate resistance against PAH toxicity. Interestingly, knockdown of *ahr1a* alongside exposure to fluoranthene + benzo(k)fluoranthene but not fluoranthene + benzo[a]pyrene was reported to result in stronger cardiotoxicity than among exposed but mock-injected individuals. Souder and Gorelick (2019), on the other hand, report that knockout of *ahr1a* and *b* did not confer any protection against the dioxin 2,3,7,8-Tetrachlorodibenzo-*p*-dioxin (TCDD) mediated cardiac and developmental toxicity in zebrafish embryos. Knockout of *ahr2*, in contrast, facilitated protection against TCDD-mediated toxicity. An *in vitro* cross-species assessment of Ahr found a linear and significant relationship between Ahr2 activation and early life mortality, but not for Ahr1 (Doering *et al.* 2018).

The function of Ahr2 in developing fish has been reported to regulate heart tissue development (Gasiewicz *et al.* 2008) as well as numerous other biological processes (Lu *et al.* 2020). Constant activation of Ahr2 by, for example, PAHs has therefore been linked to downstream impacts on the whole organ and development, as per improper receptor activation and incorrectly triggered molecular signaling (Zodrow and Tanguay 2003). Even though Ahr2 controls a wide selection of biological functions, the best studied function regarding binding and activation by PAHs (and other agonists) is the binding of the agonist-receptor complex to the xenobiotic response element, which facilitates transcription and translation of cytochrome P450a (Cyp1a) (Danielson 2002). This specific enzyme allows for phase I metabolism of xenobiotics (and endogenic compounds), a process which serves to increase hydrophilicity of the substrate by addition of hydroxyl group(s) (Zanger and Schwab 2013), thereby facilitating further metabolism (conjugation with glutathione, sulfur-based groups, and (or) glucuronic acid) before excretion (Almazroo *et al.* 2017, Huang *et al.* 2017). Induction of *cyp1a* is a tightly regulated process, which requires the translocation of the substrate, bound to Ahr2 (and other co-factors), to the nucleus (Fig. 1; exemplified using the PAHs of interest for this thesis: retene and fluoranthene). Once translocated, the co-factors dissociate, and the complex binds to the xenobiotic response element in the genome, which in turn facilitates the transcription of *cyp1a* (Denison *et al.* 1988, Krishnan *et al.* 1995, Ma and Whitlock 1997).

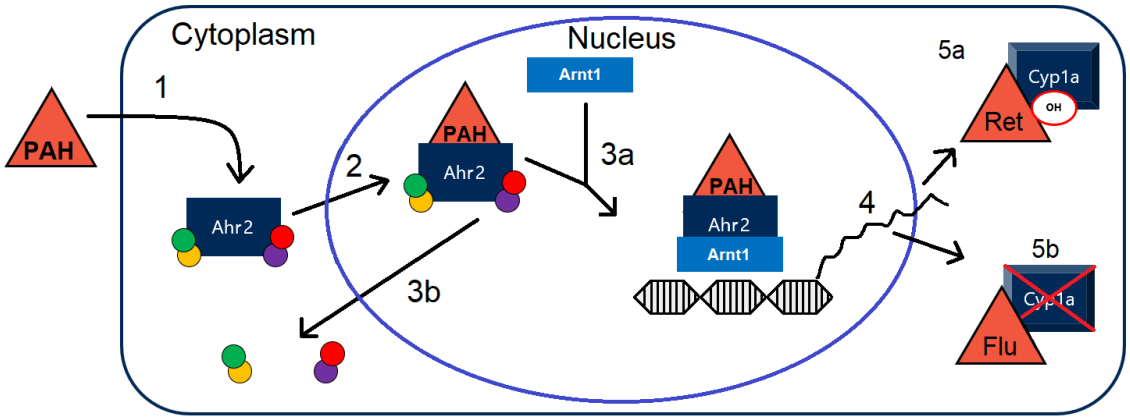

FIGURE 1 Visualization of PAH-mediated activation of Ahr2 and subsequent phase I metabolism in fish, as exemplified by the PAHs retene (Ret) and fluoranthene (Flu). 1: the PAH passes through the cell membrane to the cytoplasm, where it associates with the aryl hydrocarbon receptor 2 (Ahr2) and co-factors. 2: the complex is translocated to the nucleus. There, the Arnt1 associates with the PAH+Ahr2 complex (3a), which forces the co-factors to dissociate (3b). The PAH+Ahr2+Arnt1 binds to the xenobiotic response element, which facilitates the transcription of *cyp1a* and the subsequent translation and post-translational modification (4). The functional Cyp1a enzyme facilitates the hydroxylation of the PAH (e.g. retene) or endogenous metabolites (e.g. FICZ) (5a). However, PAHs (such as fluoranthene) can inhibit the function of Cyp1a (5b), which results in constant Ahr2 activation and only partial metabolism. This figure is inspired by Schmidt and Bradfield (1996) and Fujii-Kuriyama and Kawajiri (2010).

From the perspective of developmental toxicity in fish larvae, it is known that knockdown of *ahr2* and *cyp1a* (to a certain degree), but not *ahr1*, prevents induction of toxicity. This fact highlights the necessity of a functional Ahr2 for the induction of PAH toxicity (Incardona *et al.* 2006, Scott *et al.* 2011, Garner *et al.* 2013). Additionally, a recent hypothesis suggests that improper activation of cyclooxygenase-2 (Cox2) could be involved in PAH toxicity (Doering *et al.* 2019). The expression of *cox2*, just like *cyp1a*, is controlled by Ahr2 activation, and should therefore be sensitive to improper activation by said receptor (Teraoka *et al.* 2008, Teraoka *et al.* 2014). Under normal circumstances, Cox2 is important during early life development, although less essential than Cox1 (Grosser *et al.* 2002), while facilitating the transformation of arachidonic acid to prostaglandin. Prostaglandins are hormone-like molecules, depending on type and tissue, that are important for the maintenance of normal heart function and cardiovascular circulation. Functionally, prostaglandins facilitate cardiovascular dilation, prevent blood platelets from aggregating, and promote both inflammatory responses and muscle relaxation (Ricciotti and FitzGerald 2011). How Cox2 contributes to PAH-induced toxicity is currently only partially understood. From an empirical perspective, there is ample evidence for the involvement of Cox2 in PAH-mediated toxicity in developing fish larvae. As a result, the empirical evidence is deemed moderate to high (Ahr2 activation, upregulation of *cox2*, cardiotoxicity). However, the quantitative understanding of how Cox2 contributes to toxicity is considered low to moderate, as per indirect relationships between exposure, upregulation, and early life stage

mortality (Doering *et al.* 2019). Hence, more quantitative research on how Cox2 can contribute to toxicity is required before any final conclusion can be established.

1.1.3 Retene and fluoranthene

Two PAHs of scientific and environmental interest are retene (Fig. 2a) and fluoranthene (Fig. 2b), both with regards to toxicological properties and environmental relevance. Retene, as part of a PAH mixture, is primarily associated with incomplete pyrolysis or combustion of wood (Ramdahl 1983, Leppänen and Oikari 2001). Hence, it is a useful biomarker for the identification of ongoing forest fires, but it has been detected in crude oil as well (Binjie and Xinyu 1994). Retene is also readily present in the wastewater effluent from paper and pulp mills, but it may also be observed following the microbial degradation of resin acids (from coniferous trees), such as dehydroabietic acid (Leppänen and Oikari 1999). From a toxicological perspective, retene is fairly lipophilic (estimated log K_{ow} of 6.35) and has a strong affinity for Ahr2 (Barron *et al.* 2004). As such, retene is well known to induce cardiotoxicity in developing fish larvae (Billiard *et al.* 1999; Scott and Hodson 2008; Vehniäinen *et al.* 2016; Rigaud *et al.* 2020a).

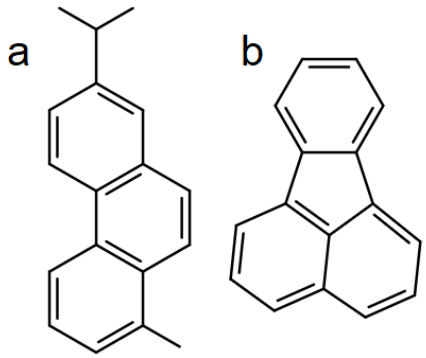

FIGURE 2 The chemical structure of (a) retene and (b) fluoranthene. The figures were created using the online platform https://www.chem-space.com/search.

Fluoranthene, on the other hand, is present in virtually any PAH mixture, whether that be petroleum products, effluent, soot, or exhaust. Less lipophilic than retene (log K_{ow} = 5.16), fluoranthene has, from a toxicological perspective, less affinity for Ahr2 than retene (Barron *et al.* 2004). An interesting and secondary characteristic of fluoranthene is its ability to physically block the active site of Cyp1a, thus reducing the rate at which phase I metabolism occurs (Fig. 1, step 5b) (Willett *et al.* 1998, Fent and Bätscher 2000). No investigative study on the mixture toxicity of retene and fluoranthene has been performed as of yet in developing fish larvae.

From the perspective of environmental toxicology, the European Chemical Agency (ECHA) categorizes fluoranthene as a substance of *very high concern* due to properties of being environmentally (very) persistent, (very) bioaccumulative, and toxic (ECHA 2018). Hence, fluoranthene is covered by

European Union Directive 2008/105/EC as a proxy for other, more potent, PAHs. Reported half-life ranges from > 7.8 years in soil (*in situ*) (Wild *et al.* 1991), whereas a laboratory experiment, under ideal conditions, yielded a mean half-life of 137 ± 35 days (Wild and Jones 1995). Overall, the larger the PAH, the longer the half-life in soil. In aquatic sediment, the half-life of fluoranthene is reported to be > 1250 days, which should be compared to a half-life of 200 days in water, assuming ongoing sediment-water partitioning (Mackay 2006). Hence, the environmental presence of fluoranthene is greatly dependent on the specific environmental strata. Even though fluoranthene only makes up 1.7 – 2 % of the PAH content of crude oil (Almeda *et al.* 2013), once associated with soil and sediment, fluoranthene can become persistent and an environmental problem if disturbed and remobilized. Therefore, the maximum limit of fluoranthene emissions to surface water, within the European Union, is set to 120 ng l^{-1} per emission source, compared to the reported (average) emission of 6.3 ng l^{-1}; Annex I of the Water Environmental Quality Standards Directive; 2008/105/EC, Part A. No such harmonized classification is available for retene, as per the Substance Infocard provided by the ECHA (2022). However, the environmental presence of retene has been measured at concentrations of 3.3 mg g^{-1} in contaminated sediment (dry weight) (Leppänen and Oikari 1999) and 0.31 ng kg^{-1} in fresh snow melted to water (Northern Highland State Forest, Wisconsin, USA), whereas fluoranthene (median concentration) was measured at 0.42 ng kg^{-1} in melted snow, as per the same study (von Schneidemesser *et al.* 2008). In contrast, PAHs emitted into the atmosphere are covered by the *Convention on Long Range Transboundary Air Pollution on Persistent Organic Pollutants* (LRTAP; which has been in effect since March 16, 1983; codified by the European Union under decision 81/462/EEC), which covers PAHs as a group, rather than as individual compounds. LRTAP considers PAHs, since the implementation of the 1998 Aarhus Protocol to the convention, as persistent organic pollutants to be reduced from the emissions of stationary sources. This decision was codified by the European Union in 2004 (protocol 22004A0319(01)). As a result, the emissions of PAHs within the European Union have decreased by 77.7 % since 1990 (EEA Report No 5/2020).

1.2 The effects of PAHs on fish

Numerous studies have investigated the impact of PAHs and petroleum products on developing and adult fish belonging to a wide range of species. What can be concluded is that tolerance to PAHs is endpoint and species-specific. Yet, heart development and function are especially sensitive to the influence of PAHs among developing fish larvae, as both bradycardia and arrhythmia have been reported in multiple species following exposure (Incardona *et al.* 2006, 2009, 2014, Sørhus *et al.* 2017). Long-term exposure to PAH(s) can, therefore, have downstream consequences for the developing larvae, as cardiovascular output and circulation are impacted. The exact

underlying mechanisms leading up to PAH-induced cardiotoxicity are not fully known, but interactions between parental or metabolized PAH(s) and cardiac calcium and potassium ion channels and the subsequent disruption in the propagation of action potential have been suggested as a plausible explanation. This is supported by *in vitro* patch-clamp assessment of PAH-exposed and separate cardiac cells, which has shown that exposure to PAHs impairs and alters the repolarization of the action potential in a compound-specific fashion (Ainerua *et al.* 2020). In the case of separated cardiac cells from rainbow trout (*Oncorhynchus mykiss*), following exposure to retene, the repolarization event is shortened in a dose-response fashion compared to the control group (Fig. 3; Vehniäinen *et al.* 2019), whereas exposure to fluoranthene extended the repolarization event (Vehniäinen; unpublished data). The impact of PAHs on the cardiac transcriptome and proteome has been investigated in rainbow trout alevins exposed to retene, pyrene, or phenanthrene (alone, Rigaud *et al.* 2020a, 2020b) and in zebrafish larvae (*Danio rerio*; benzo[a]pyrene and fluoranthene, alone or as a mixture, Jayasundara *et al.* 2014), which revealed exposure-specific alterations in the expression of the components constituting the aforementioned ion channels. However, it is not fully known if, or how, these transcriptome or proteome changes are related to the impaired repolarization of the action potential; although, it is plausible that these alterations are compensatory rather than a direct effect of exposure. Ultimately, the consequence of PAH-mediated cardiotoxicity is impaired and altered heart structure, function, and capacity, which translates to decreased circulation of nutrients and hormones, as well as reduced gas exchange.

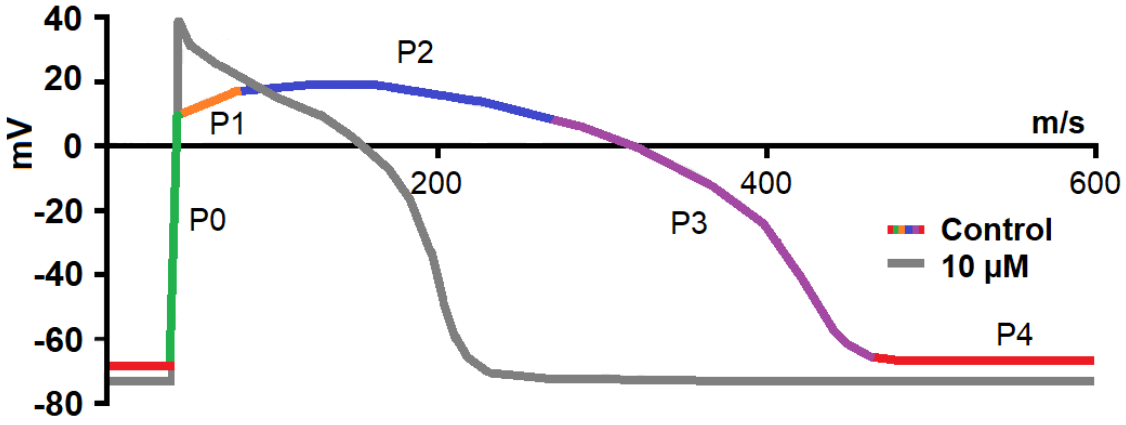

FIGURE 3 "Normal" *in vitro* cardiac action potential and repolarization in rainbow trout exposed to DMSO (multi-colored as per the different phases; P0 to P4; *in vitro*) compared to the influence of 10 µM of retene (grey). This figure is adapted from Vehniäinen *et al.* (2019). Unpublished results by Vehniäinen report that exposure to fluoranthene prolonged the repolarization of the cardiac action potential.

Another commonly assessed endpoint associated with PAH toxicity and dioxins (TCDD; Cook *et al.* 2003, King-Heiden *et al.* 2012), which are also Ahr2 agonists in developing fish larvae, is the so-called Blue Sac Disease (BSD). BSD is an umbrella term, which encompasses symptoms of toxicity that range from

craniofacial deformities, pericardial and yolk sac edema, hemorrhage, and fin rot to curved spine (Billiard *et al.* 1999). The primary advantage of assessing BSD is that it is easily performed, even with the unaided eye, and the results correlate well with actual exposure. However, the chain of events leading up to increased occurrence of BSD-related symptoms, following activation of Ahr2 by PAH(s), is poorly understood from a molecular perspective. Research has indicated that there might be a link between impaired cardiovascular function and the occurrence of BSD (Fleming and Di Giulio 2011, Sørhus *et al.* 2016), which suggests Ahr2-mediated toxicity, plausibly related to Cox2. It is suggested, and plausible, that the impairment or saturation of other organs involved in the metabolism and excretion of xenobiotics, such as the kidneys and liver, is also involved in the formation of BSD-related symptoms. More research is required before any final conclusion can be made. What is clear, though, is that a systemic approach is needed in order to understand the cause of Blue Sac Disease-related symptoms in developing fish larvae.

Other reported symptoms and consequences of PAH or oil-mediated toxicity in fish are decreased growth and development (Heintz *et al.* 2000), impaired inflation of the air bladder (Price and Mager 2020), decreased immune response, genotoxicity, altered behavior (Honkanen *et al.* 2004, Brown *et al.* 2016a), and a decreased survival rate among adult fish that were exposed during their early life development to PAHs or crude oil as per catch-and-release studies (Heintz *et al.* 2000, Laurel *et al.* 2019).

However, the majority of laboratory-based toxicological investigations on the effects of PAHs on fish have primarily focused on either individual PAHs or petroleum products, rather than binary or simple mixtures. From a toxicological and realistic perspective, this makes sense, as the data is highly applicable, both for the understanding of why a certain PAH becomes toxic but also for environmental risk assessors. This can be exemplified by exposure to crude oil, which, besides PAHs, contains a wide range of elements, such as heavy metals, that can modulate and further influence toxicity (Meador and Nahrgang 2019). Additionally, exposure *in situ* often encompasses environmental factors, which in turn can reduce an organism's resistance to the influence and stress caused by xenobiotics (Martin *et al.* 2014, Allmon *et al.* 2021). Yet, the few available laboratory studies on the topic of binary and simple PAH mixture toxicity report that the mixture is often more potent than the individual components. This aspect of toxicology highlights the necessity of why it is important to assess mixtures as well, especially when considering mechanisms of toxicity. Assessing two PAHs with the same mode of action and toxicological outcome is often straightforward in the sense of extrapolation. However, assessing two PAHs with different modes of action and toxicological outcomes is demanding, as toxicity cannot be predicted from the additive effect of the individual compounds. We know from Geier *et al.* (2018) that certain components of a PAH mixture contribute more to toxicity than other components in zebrafish. Other studies focusing on binary (PAH) mixture toxicity in developing fish report a stronger and synergized toxicity response than among those exposed to the individual components, especially if one of the components can inhibit Cyp1a

(Hodson *et al.* 2007, Timme-Laragy *et al.* 2007, Wills *et al.* 2009, Fleming and Di Giulio 2011, Scott *et al.* 2011, Van Tiem and Di Giulio 2011, Curtis *et al.* 2017). This is exemplified by Geier *et al.* (2018) but also by studies on zebrafish co-exposed to benzo[a]pyrene and fluoranthene (Jayasundara *et al.* 2014) or benzo[k]fluoranthene and fluoranthene (B[k]P + Flu) (Van Tiem and Di Giulio 2011) relative to those exposed to the individual components. Interestingly, knockdown of Ahr2 prevented the formation of pericardial edema and weakened the phase I and II metabolic responses following exposure to the B[k]P + Flu mixture. This finding highlights the interaction between Ahr2 and PAHs as a pre-requisite for the formation of developmental toxicity. Therefore, understanding the mechanisms of toxicity of binary mixtures, as a proxy for complex mixtures, is essential for the understanding of subsequent toxicodynamics, kinetics, and mechanics *in vivo* and in relation to *in situ*.

A relatively recent discovery on the topic of PAH-mediated toxicity in developing fish larvae is the impairment of lipid metabolism following exposure to crude oil (Laurel *et al.* 2019). During normal circumstances and development, fish larvae maintain normal growth and development by consuming yolk, which is rich in lipids, cholesterol, fatty acids, and other essential nutrients. By the time the yolk is fully consumed, the fish larva should be able to ingest feed on its own. Hence, the consumption of yolk by a developing organism is strictly regulated, as knockdown of individual genes controlling certain aspects of energy and lipid metabolism, in zebrafish larvae, either results in stalled growth and development or death from starvation (Pickart *et al.* 2006, Anderson *et al.* 2011). This finding, that crude oil can impact lipid metabolism, has been observed both indirectly, through transcriptomic over-representation analysis of whole-body Atlantic haddock larvae (*Melanogrammus aeglefinus*) exposed to crude oil (Sørhus *et al.* 2017), and directly, in whole-body Polar cod larvae (*Boreogadus saida*) exposed to crude oil as per Laurel *et al.* (2019). In the latter study, the long-term survival rate among exposed larvae decreased, while the levels of triglycerides, fatty acids, and sterols were enriched in developing larvae, which implies a decreased rate of consumption. Towards the end of their study's duration, the stores of triglycerides in exposed fish were significantly reduced compared to control. Additionally, research by Sørhus *et al.* (2021) highlights that exposure to the PAH phenanthrene, weathered crude oil, and nicardipine hydrochloride (Nic; a pharmaceutical vasodilator which specifically targets and inhibit the voltage-dependent calcium ion channels in heart tissue) results in exposure and tissue specific fatty acid and cholesterol profiles in developing Atlantic haddock embryos (*Melanogrammus aeglefinus*). These altered lipidomics profiles were accompanied by compensatory over-representations of pathways related to fatty acid metabolism and cholesterol biosynthesis in eye tissue, which suggests disrupted mobilization of lipids from the yolk sac that, in turn, forces the localized catabolism. Albeit relatively poorly investigated and mechanistically understood, it appears quite likely that the energy and lipid metabolism (in fish larvae) are impacted by exposure to PAH(s). However, the long-term impact(s)

on the wellbeing of the exposed fish, exposed to PAHs as larvae, is likely to be negative.

1.3 FICZ

There are other compounds that can act agonistically with Ahr2, be they of exogenous or endogenous origin. One endogenous activator of Ahr2 is the tryptophan metabolite 6-formylindolo[3,2-b]carbazole (FICZ), which has a high affinity for the aforementioned receptor, whereby keeping the levels of FICZ close to zero following phase I metabolism by Cyp1a (Wincent *et al.* 2009) and excretion. It is therefore hypothesized that endogenously derived FICZ is constantly formed during normal cellular metabolism and is considered the primary reason behind a constant Cyp1a expression (Wei *et al.* 1998).

Formation of endogenous FICZ is associated with increased photo irradiation, oxidative stress, or enzymatic activity (Smirnova *et al.* 2016, Rannug and Rannug 2018). Previous research has reported that exposure to exogenous FICZ alongside knockdown of *cyp1a* or co-exposed with a Cyp1a inhibitor (alpha-naphthoflavone) induced developmental toxicity similar to the symptoms of PAHs or dioxin toxicity (TCDD) in zebrafish embryos (Wincent *et al.* 2012). Knockdown of *ahr2*, on the other hand, protected against FICZ toxicity in a similar fashion as observed by Incardona *et al.* (2006) in PAH-exposed zebrafish. Hence, if endogenous FICZ is formed and accumulates in PAH-exposed developing fish larvae, it is plausible to assume that such could contribute to Ahr2-dependent developmental toxicity and also possibly contribute to elevated or even synergized PAH toxicity (Scott and Hodson 2008, Geier *et al.* 2018). So far, this aspect is purely hypothetical, yet holds scientific merit.

2 OBJECTIVES

The primary aim of this doctoral thesis is to explore the mechanism(s) of PAH-induced toxicity by retene and fluoranthene (individual PAHs with different modes of action or as a mixture) in newly hatched and developing rainbow trout alevins (*Oncorhynchus mykiss*). Exposure-specific toxicity was investigated at multiple levels of biological organization, ranging from how the cardiac transcriptome, proteome, and metabolome responded to exposure to observing heart function and the effects on the whole organism (growth, yolk consumption, PAH accumulation, and Blue Sac Disease Index). Specifically, the aims of performed studies were to:

1) Investigate and identify the cardiac transcriptomic, proteomic, and metabolomic responses in PAH-exposed and developing rainbow trout alevins.
2) Assess how these omics responses translate to exposure-specific over-representation profiles; which functions are affected by exposure?
3) Investigate how exposure affects heart rate and if any changes in the transcriptome and/or proteome could contribute to cardiotoxicity.
4) Compare morphological endpoints, such as growth, development and planar yolk area, to exposure-specific omics responses.
5) Investigate the temporal shift of exposure on body burden and if omics responses could provide correlations with the exposure-specific body burden profiles.
6) Investigate if a tryptophan metabolite, FICZ, can accumulate following exposure to the PAHs, individually or as a mixture. If present, could accumulation contribute to synergism, thereby aggravating toxicity?

3 MATERIAL AND METHODS

3.1 Overview

Exposures were conducted in the winter and spring of 2017 (I, II) and the early spring of 2018 (III) at the Ambiotica building, Ylistö Campus, University of Jyväskylä, Central Finland. The experimental setup and exposure methodology applied in these studies were based upon OECD Guideline 210 (Fish, Early-life Stage Toxicity Test; OECD 1992). The number of alevins used per treatment, with the correlating number of replicates, is stated in Table 2, and a summary of investigated endpoints per study is presented in Table 3.

TABLE 2 Summary of exposure concentrations of retene and fluoranthene (µg l^{-1}) used in relation to the number of treatments, replicates, and alevins per study.

Study	Retene (µg l^{-1})	Fluoranthene (µg l^{-1})	Number of treatments	Number of replicates per treatment	Number of alevins per replicate	Number of alevins per treatment
I	32	50	4	8 or 12*	15	120 – 180**
II	32	50	4	8 or 12*	15	120 – 180***
III	32	50	4	3	15	45

* 8 replicates per treatment in the 14-day exposures, and 12 replicates per treatment in the 1, 3, and 7-day exposures.

** 120 alevins per treatment in the 14-day exposure, and 180 alevins per treatment in the 1, 3, and 7-day exposures.

*** 120 alevins per treatment in the 14-day exposure, and 180 alevins per treatment in the 7-day exposures (7 day exposed alevins were the same as in I).

TABLE 3 Summary of investigated endpoints in relation to sample type and in which study said endpoint was included (I, II, III).

Source	Investigated endpoints
Exposure water	Exposure concentrations (I, II)
	Oxygen, pH, and conductivity (I, II, III)
Whole alevins	PAH body burden(s) (I, II, III)
	Body length (I, II)
	Planar yolk area (I, II)
	Blue Sac Disease symptoms (I, II, III)
	Development (I, II)
	qPCR (whole-body; III)
	Presence and body burden of FICZ (III)
Heart tissue	Transcriptomics (I)
	Proteomics (II)
	Metabolomics (II)
	qPCR (heart; I)

3.2 Setup, exposure, and sampling

Newly hatched and healthy rainbow trout alevins, supplied by Hanka-Taimen Oy fish farm (Central Finland), were exposed semi-statically for 1, 3, 7, and 14 days (I, II) and 1, 3, and 7 days (III) to two model PAHs of environmental and toxicological relevance: retene (CAS-number 483-65-3) and fluoranthene (CAS-number 206-44-0). Exposure to the PAHs was conducted either to the individual compound or to the binary mixture (I, II, III) at concentrations of 32 and 50 µg l^{-1} respectively and in relation to control (DMSO; 0.002 %; CAS-number 67-68-5). It must be noted that besides these aforementioned concentrations of retene and fluoranthene, 3.2 and 10 µg l^{-1} of retene as well as 5 and 500 µg l^{-1} of fluoranthene were investigated, alone or as binary mixtures (III). But for the sake of comparability with I and II, results related to the additional exposures (3.2 and 10 µg l^{-1} of retene, and 5 and 500 µg l^{-1} of fluoranthene) are omitted from this thesis. The only exception being the body burden of FICZ, which is presented in full, in Chapter 5. Stock solutions were prepared by dissolving the PAHs in DMSO at room temperature (nominal retene stock concentration at 3.2 mg ml^{-1} and fluoranthene 5 mg ml^{-1}). The 20 µl of pure or PAH-fortified DMSO added to the exposure bowls (20 µl per litre) is far below the recommended levels set by the OECD (100 µl DMSO per litre; OECD 2013) and should therefore not contribute to toxicity (Maes *et al.* 2012, Kais *et al.* 2013, Christou *et al.* 2020).

Each exposure study was performed in filtered lake water, which was transported from the Konnevesi Research Station (Central Finland) in sealed, plastic 25-litre buckets. Once delivered to the Ambiotica building, the sealed

buckets were stored in the same room as exposures were to be conducted in. Water that was set to be used within 24 hours was aerated for this duration. Note that negligible concentrations of retene (~30 ng l^{-1}), fluoranthene (~130 ng l^{-1}), and other PAHs were detected in the water collected at the research station. Furthermore, The Finnish Environment Institute (SYKE) reports that water from Lake Konnevesi contains 7 to 14 µg l^{-1} ammonium (as nitrogen), 0.13 to 0.19 mmol l^{-1} alkalinity, and has a Ca+Mg hardness of 0.12 mmol l^{-1} (Hertta database).

Twenty-four hours prior to the initiation of exposure, each replicate bowl (1.5-litre Pyrex glass tray) was filled with 1 litre of water and pre-saturated with the corresponding chemicals, as per Table 4.

TABLE 4 Summary of stock solutions, volume added to the exposure bowls, nominal concentrations, purity, and supplier. Note that 136.65 nM of retene = 32 µg l^{-1} and 247.2 nM of fluoranthene = 50 µg l^{-1}.

Exposure	Stock solution concentration (µM)	Volume added (µL)	Nominal PAH + DMSO exposure concentrations (nM)	Purity (%)	Supplier
Control	Pure DMSO	0 + 20	0 + 256	≥ 99.9	Sigma Aldrich
Retene + DMSO	13655	10 + 10	136.7 + 128	98	MP Biomedical
Fluoranthene + DMSO	24720	10 + 10	247.2 + 128	≥ 98	Sigma Aldrich
Retene + Fluoranthene	As above	10 + 10	136.7 + 247.2	As above	As above

Each bowl was continuously aerated through a glass Pasteur pipette connected via rubber tubing to an air pump; each pump aerated four replicates. These pumps were, in turn, placed upon a stack of paper tissue so as to eliminate vibrations upon the metal shelves hosting the exposure bowls. Furthermore, an additional replicate per treatment, without alevins, was maintained in order to monitor and assess possible absorption of the PAHs to the glass surfaces and microbial degradation. The replicates were placed in Latin square formations so as to minimize the effect of replicate placement upon exposure, as the temperature varied a few tenths of a degree within the exposure room due to how the air was circulated by the cooling system. The rooms hosting the exposures were illuminated by artificial yellow lighting 16 hours per day, followed by 8 hours of darkness, throughout the exposure duration.

On the day of exposure initiation, following the 24 hours of saturation, water and exposure solutions were renewed, and 15 newly hatched and healthy rainbow trout alevins were transferred to each replicate. Selected alevins were free of hemorrhages, edemas of any sort, spinal curvature, craniofacial abnormalities, polycephaly, and any other developmental abnormality. Throughout the exposure durations, water temperature was maintained within

an interval ranging from 10 to 12 °C as per daily measurement of control bowls prior to the complete renewal of water and chemicals (I: 11.7 ± 0.4°C; II: 11.6 ± 0.3°C; III: 10.8 ± 0.3°C). Complete renewal of water and chemicals was achieved by temporarily transferring the alevins to a 50 ml Falcon tube, collected using a 5 ml plastic Pasteur pipet with a broaden tip. The whole process took less than 30 seconds per replicate.

In order to assess actual exposure concentrations, exposure water was sampled (before renewal) after 1, 3, 5, 7, 10, and 14 days of exposure and subsequently stored in a 1:1 mixture with ethanol (99.5 % purity) at 4°C for later synchronous fluorescence spectroscopy (SFS; I, II) or in a 1:1 mixture with acetonitrile (70 % purity) for later high-performance liquid chromatography analysis (HPLC; III). Water quality was assessed on an equally regular basis so as to validate the relative oxygen saturation, pH, and conductivity of stock water. Alevins found dead throughout the exposure were checked for symptoms related to the Blue Sac Disease Index (BSD; yolk and pericardial edema, curved spine, and hemorrhaging) or other potential developmental defects.

Sampling was performed after 1, 3, 7, and 14 days of exposure. Alevins sampled after 1 and 3 days were done according to a timetable as to adjust sampling in relation to initiation of exposure. The sampling procedure was initiated by a visual assessment for symptoms of BSD (yolk and pericardial edema, and hemorrhaging), followed by photographing in groups of three to five alevins next to millimeter scale paper for later *in silico* measurements of standard length, yolk area, yolk morphology, and pigmentation development (I, II, III). In experiments investigating the transcriptome (I), proteome, and metabolome (II), four replicates of cardiovascular tissue per treatment were produced, processed, and analyzed. Each replicate was created using hearts excised from either 30 alevins (sampled after Day 14; every alevin from 2 replicates pooled) or 45 alevins (sampled after Days 1, 3, and 7; every alevin from 3 replicates pooled), which were pooled in a microcentrifuge tube, snap-frozen in liquid nitrogen, and stored at –80 °C for later omics analysis. The remaining alevin carcasses were pooled in a microcentrifuge tube (based upon replicate), snap-frozen in liquid nitrogen, and stored at –80 °C for later assessment of body burden.

A similar methodology was applied when sampling alevins exposed to broader exposure gradients (III). These alevins were sampled in two groups. The first group, consisting of five randomly selected alevins from the same replicate, was sedated lightly and individually in MS-222 (20 mg l^{-1}) and subsequently placed on individual glass Petri dishes under an illuminated stereo microscope. Heart rate was recorded using a digital camera before transferring the alevins to a light table, where they were photographed one by one next to millimeter scale paper. These five alevins were then placed in individual microcentrifuge tubes, which were snap-frozen in liquid nitrogen and then stored at –80 °C for later whole-body qPCR-analysis. The remaining alevins were sedated together in MS-222 and, once sedated, transferred to a glass Petri dish in groups of five to be photographed before being pooled in a

microcentrifuge tube, snap-frozen in liquid nitrogen, and stored at –80 °C for later body burden analysis.

3.3 Morphological measurements

3.3.1 Calculating the Blue Sac Disease Index

The occurrence of symptoms related to Blue Sac Disease (BSD) is known to become more frequent, relative to control, in developing fish larvae exposed to PAHs, oil, and dioxin-like compounds. The current convention on the calculation of the BSD-index was established by Villalobos *et al.* (2000) and later modified by Scott and Hodson (2008). In order to make the results from the different studies (I, III) comparable, only yolk sac, pericardial edema (YE; PE; scored 0–1), and hemorrhaging (HM; scored 0–1) were assessed and calculated as per Eq. 1. Note that assessment of BSD symptoms was performed during sampling (I, II) and *in silico* after sampling in (III).

$$BSD = \frac{\Sigma\, PE + \Sigma\, HM + \Sigma\, YE}{Maximum\ score\ per\ replicate} \quad (1)$$

It must be acknowledged that inconsistent scoring during sampling resulted in half of the replicates from the 3 and 7-day exposures being omitted (I). Regarding the alevins exposed for 14 days, all BSD data had to be omitted but was replaced with assessment of the pigmentation intensity of the dorsal fin and the lateral side (I). Furthermore, additional endpoints (craniofacial deformities and yolk edema severity score) were assessed *in silico* but omitted in the calculation of BSD so as to make the results comparable between the investigations (III). A curved spine, which is a common hallmark of BSD (and commonly observed among the PAH-exposed alevins), was not assessed, as it presents poorly once an alevin is out of water.

3.3.2 Measuring standard length, yolk area, and development

Photographs of exposed alevins were analyzed *in silico* through ImageJ (v1.51k using Java 1.6.0_24; 64-bit; National Institutes of Health, USA). Using the millimeter scale as a known length reference, both the standard length and planar yolk area could be measured with high precision (3 decimals) and good resolution (30 pixels per mm). Furthermore, *in silico* analysis allowed for easy assessment of possible yolk sac edema, yolk sac edema severity, and hemorrhaging. However, as the temperature within the exposure room varied (due to the air flow from the cooling systems and tank placement), standard length and yolk area measurements were normalized against the average

temperature of the closest control tank replicate. By doing so, it was possible to compensate for the effect of temperature variation on growth.

As mentioned in Chapter 3.3.1, data from the 14-day exposure had to be omitted due to inconsistent scoring of BSD symptoms. Instead, general development was evaluated according to Vernier's salmonid developmental catalogue from 1977. Focusing on the pigmentation intensity of both the lateral side and dorsal fin as developmental cues, intensities were scored as either "high or low intensity" or "absent or present," respectively. The utilization of a developmental assessment approach alongside the direct measurement of standard length allows for a more comprehensive evaluation of the effect of PAH(s) on morphology. In other words, are the shorter alevins simply shorter compared to control, or are they at an earlier developmental stage than control?

In addition to the aforementioned developmental markers and endpoints, yolk sac morphology was assessed with regards to if the yolk extended beyond the posterior-most point of attachment (Day 7; III). Such approach could highlight effects of exposure upon yolk absorption and development in general.

3.3.3 Heart rate measurement

Measurements of heart function were performed in accordance with Incardona *et al.* (2009) on video recordings of lightly sedated alevins *in silico* using the OpenShot Video Editor. In short, the average number of frames between each of the 31 first heartbeats were counted and converted, first to frames per second and then to beats per minute (BPM). Calculation of BPM allowed for identification of potential bradycardia or tachycardia caused by exposure. Interbeat variability was established from the average standard deviation of the number of seconds between each beat. A higher interbeat variability equates to a higher standard deviation and a greater variation between heartbeats, thereby indicating altered cardiac function, such as arrhythmia.

3.4 HPLC, SFS, and LC/MS-MS

3.4.1 Overview and considerations

Both HPLC and SFS were employed for the measurement of actual PAH concentration in exposure water (SFS: I, II; HPLC: III) and body burden (HPLC; I, II, III). Body burden was established by whole-body carcasses, whereas exposure water was collected prior to the renewal of water and PAHs, then subsequently stored until analysis.

3.4.2 PAH concentration(s) in exposure water (SFS)

As mentioned previously, the measurement of PAH concentration(s) in exposure water was performed through SFS analysis (PerkinElmer Instruments LS55 luminescence Spectrometer, USA). Exposure water was sampled on Days 1, 3, 7, 10, and 14, diluted 1:1 in 99.5 % ethanol (20 ml scintillation vials), and stored at 4 °C until analysis. SFS and PAH-specific parameters (Watson *et al.* 2004, Turcotte *et al.* 2011) are available in Table 5. All LS55 measurements were performed in quartz cuvettes (Quartz SUPRASIL® High Precision Cell, Hellma Analytics, Germany; I, II).

TABLE 5 LS55 luminescence spectrometer parameters used in order to identify and quantify retene and fluoranthene in exposure water. Abbreviations: excitation, emission, and spectral width (I).

Treatment	Wavelengths measured (nm)	Delta wavelength (Δλ; nm)	Peak (nm)	Excitation slit (nm)	Emission slit (nm)	Scan speed (nm/min)
Retene	250-350	50	290-315	5	5	300
Fluoranthene	200-500	155	270-292	2.5	5	240

As an SFS approach is precise but labor intensive, the analytical methodology was changed from SFS to the less labor intensive HPLC approach (III). Retene and fluoranthene concentrations were measured in the same fashion as when analyzing the body burden of the PAHs, and final concentrations were calculated against the standard curves (as presented in 3.4.2).

3.4.3 Body burden analysis

Rainbow trout alevin carcasses, stored at –80 °C post-sampling, were thawed, counted, and transferred to a fresh microcentrifuge tube with screw-on cap. Before the tube was sealed, 600 ml 70 % acetonitrile (ACN; diluted in de-ionized water; CAS-number: 75-05-08; Fisher Scientific) together with 2–8 one mm ⌀ and 1–4 two mm ⌀ zirconium pellets were added. The tubes were then placed in a bullet blender (standard model, Next Advance) at max setting for 2 minutes. The ensuing homogenate was then centrifuged four times at 14 000 rounds per minute for 10 minutes at 4 °C (Centrifuge 5415 R, Eppendorf, Germany). Between each round of centrifugation, the supernatant was collected and pooled in a 2 ml microcentrifuge tube, and the pellet was resuspended mechanically in 400 µl of 70 % ACN. In order to minimize the amount of debris in the pooled supernatant, approximately 1800 µl of supernatant were centrifuged again at the aforementioned setting; 1500 µl of the supernatant were then collected and transferred to a clean microcentrifuge tube, which was, in turn, subsequently stored at –20 °C until HPLC analysis.

HPLC-ready samples (to be analyzed for retene and fluoranthene content) were diluted 1:100 in 70 % ACN, whereas analysis for FICZ was

performed on undiluted samples. Diluted and undiluted samples (final volume: 120 µl) were loaded into 250 µl conical glass inserts (Agilent Technologies, German), each of which was placed inside an amber glass vial with a screw-on cap (Agilent Technologies, Poland). In each analytical round, 10 µL of supernatant aliquot were injected onto a 150-mm long ACE C18-AR column (5 µm particular size filter; Advanced Chromatography Technologies LTD, Scotland, UK) and analyzed by a Shimadzu U-HPLC Nexera system connected to an RF-20A xs Prominence fluorescence detector (Shimadzu, Japan). The analytic protocol and constitution of the mobile phase gradient allowed for separation of the PAHs' and FICZ's retention time and, thus, accurate measurement in a time efficient fashion (Table 6). The flow rate of the mobile phase was set to 1 ml per minute and started at a 50:50 mixture of 70 % ACN together with deionized water (both spiked with 1.5 mM formic acid; Fischer Scientific; CAS-number: 64-18-6) to reach 100 % ACN (70 %) after 15 minutes, before reverting to the 50:50 ratio over 4 minutes, starting at the 16-minute mark. A blank sample, 70 % ACN, was analyzed after every 8th supernatant sample so as to rinse and maintain system integrity, while also avoiding carry-over from one analysis to another. Fortunately, carry-over from one analytical run to another was never observed in the chromatograms yielded from analysis of blanks.

TABLE 6 HPLC parameters used for the detection of retene, fluoranthene, and FICZ (emission, excitation, and retention time) as well as limit of detection (LOD) and limit of quantification (LOQ) for each of the investigated compounds.

Compound	Emission (nm)	Excitation (nm)	Retention time (minutes)	LOD (pM)	LOQ (pM)
Retene	370	259	14.99 ± 0.02	0.13	0.38
Fluoranthene	525	288	12.17 ± 0.03	150.70	456.66
FICZ	525	390	8.38 ± 0.01	6.02	18.25

Body burden was calculated as follows: The measured area under the curve (AUC), as per chromatograms, was manually adjusted following each analysis in order to make the measurement exact. Background compensation was achieved by the subtraction of the average peak AUC from control samples (based upon the retention time of the PAHs and FICZ) from the AUC of alevins exposed to retene, fluoranthene, and mixture. The background-compensated AUC was then adjusted for dilution, number of alevins, and fitted to a standard curve.

Processing fish carcasses in acetonitrile, for the making of supernatant, is associated with loss of PAHs. Assessment of the recovery of retene and fluoranthene was performed by the addition of 10 µL of 105.96 nM of retene or 335.88 nM of fluoranthene to both DMSO-exposed alevins carcasses and an empty microcentrifuge tube. These two tubes were then processed in the same fashion as stated before, and the recovery was calculated. Analysis was performed twice in accordance with aforementioned procedures in order to

generate technical replicates. The recovery of retene was 14.3 % and fluoranthene 13.4 %, which suggests that most of the PAHs were (or became) bound to the pellet, even after two rounds of re-suspension. The recovery of FICZ is unknown, as no FICZ could be identified in the technical replicates of ACN fortified with FICZ. However, preliminary assessment of the recovery of FICZ yielded a rate of > 77 % after one round of resuspension (n = 2).

3.4.4 LC-MS/MS

In order to validate and confirm the presence of FICZ (according to HPLC), undiluted supernatant was analyzed using liquid chromatography–mass spectrometry–mass spectrometry (LC/MS–MS; Agilent 1290 ultra-high pressure LC system coupled to an Agilent 6460 triple quadruple (QQQ) mass spectrometer; Agilent Technologies. Inc., Palo Alto, CA, USA) using a sample from the standard curve as a known reference. Sample separation was performed through ultra-HPLC on a Zorbax Eclipse Plus C18 column (100 mm × 2.1 mm, 1.8 µm at 30 °C; Agilent, USA), and the column was, in turn, protected by a Zorbax SB-C18 ultra-HPLC Guard (2.1 mm × 5 mm, 1.8 µm). In every analytical run, 3 µl of sample were injected and analyzed over a mobile phase consisting of water and 70 % ACN with a flow rate of 0.35 ml minute^{-1} (both components of the mobile phase were spiked with 1.5 mM formic acid; Table 7).

TABLE 7 The relationship between the components of mobile phase in LC-MS/MS; water and acetonitrile. This table is obtained from Table s3, Manuscript III.

Time (minute)	Water (%)	Acetonitrile (%)
0.0	50	50
1.0	50	50
9.0	5	95
10.0	5	95
10.5	50	50
11.0	50	50

With such a setup, the retention time of FICZ was 3.54 minutes; eluate until 2.6 minutes and after 4.6 minutes was directed to the waste container. After each analytical run, the column was allowed to stabilize for 2.5 minutes. Using the Agilent 6460 QQQ, operating on negative electrospray mode with multiple reaction monitoring, it was possible to detect and confirm FICZ in the supernatant.

3.5 Gene expression analysis

3.5.1 Samples and RNA extraction

Gene expression analyses were performed on cardiac tissue (I; microarray and qPCR) and whole-body carcasses (III; qPCR). In the case of the former, both qPCR and microarray approaches were employed. Unfortunately, microarray validation by qPCR proved to be unreliable due to data variation. Hence, the microarrays were validated by comparing results from retene exposure with those reported by Rigaud *et al.* (2020a). The number of investigated gene expressions through qPCR was eight (I) and one (III) following 1, 3, 7, and 14 days of exposure to DMSO, retene, fluoranthene, and the mixture of the two PAHs (a 14-day exposure duration was only conducted in I).

3.5.2 RNA extraction preparation and analysis

The protocol utilized for RNA extraction is based upon Sivula *et al.* (2018) and adapted for rainbow trout by Rigaud *et al.* (2020a). In short, RNA was extracted from pooled cardiac tissue (I) or from whole carcasses (III). In the case of the former, hearts from 45 (Days 1 through 7; 3 replicates per treatment pool, yielding 4 pools of heart tissue) or 30 alevins (Day 14; 2 replicates per treatment pool, yielding 4 pools of heart tissue) were produced. In case of the latter, 15 whole alevins per treatment (hence 5 per replicate) were sampled. Cardiac tissue and carcasses were mechanically homogenized in TRI Reagent (Molecular Research Center, USA). RNA concentration, purity (NanoDrop 1000 and 2000; Thermo Fisher Scientific), and RNA integrity score (Bioanalyzer RNA 6000 Nano assay kit; Agilent Technologies) were evaluated following the manufacturer's instructions. Extracted RNA meant for qPCR was treated with DNase (Thermo Scientific), reverse transcribed to cDNA (iScript cDNA Synthesis Kit, Bio-Rad, USA), and diluted 1:10 in autoclaved sterile water for subsequent qPCR analysis. Samples destined for microarray analysis were not treated in the aforementioned fashion.

3.5.3 Microarray preparation and analysis

Analysis of how exposure affected cardiac gene expressions was performed using a custom microarray (Agilent 4x44K, Salgeno Design ID 082522). Material preparation and analysis were performed at NOFIMA (Ås, Norway) and in accordance with methodology developed by Krasnov *et al.* (2011). In short, 220 ng of RNA per replicate were labelled with Cy3 dye (Agilent Low Input Quick Amp Labeling Kit; product number 5190-2305), amplified, and purified (Qiagen RNeasy Mini Kit, Qiagen, Germany). cRNA concentration averaged at 266.3 ± 48.9 ng μl^{-1} (according to NanoDrop measurement), and Cy3 labelling activity averaged at 12.9 ± 2.5 pmol per µg of cRNA.

Each labeled, amplified, and purified sample was hybridized overnight at 65 °C using the Agilent Gene Expression Hybridization Kit (product number 5188-5242). Following hybridization, the microarrays were washed using the Agilent Gene Expression Wash Buffer Kit (product number 5188-5327). The washed and hybridized microarrays were analyzed using a SureScan Microarray Scanner, and the raw data output was processed using Nofima's bioinformatics package, based upon intensity levels (Krasnov *et al.* 2011). Nofima's bioinformatics package allowed for normalization of gene expression, identification of DEG compared to control (Student's *t*-test; $p \leq 0.05$)), and $\log_2$-transformation of the raw data output. The raw data output is currently available at the transcriptomic repository ArrayExpress (E-MTAB-8980).

3.5.4 Over-representation analysis

The raw data output was further processed through over-representation analysis (ORA) using the R-packages Bioconductor (v3.7) and clusterProfiler (v3.8.1) (Boyle *et al.* 2004, Yu *et al.* 2012). In order to perform ORA, gene ontology (GO; includes biological process (BP), molecular function (MF), cellular component (CC)), KEGG (Kyoto Encyclopedia of Genes and Genomes) (Ashburner *et al.* 2000), and Reactome annotations were attributed for each feature of the microarray. However, no gene annotation database was available for rainbow trout in AnnotationHub at the time of analysis. To circumvent this issue, the corresponding zebrafish RefSeq gene ID and symbols were used as substitutes, which in turn were linked to each feature on the microarray. Such was accomplished by utilizing NCBI BLAST software 2.7.1 (National Center for Biotechnology Information, Bethesda, MD, USA). Based upon BLAST output, it was possible to create an ORA background database containing a grand total of 19 025 unique zebrafish gene IDs. Significantly impacted terms and pathways were identified and adjusted for multiple comparisons according to the Benjamini and Hochberg method (Benjamini and Hochberg 1995; $p \leq 0.05$). Over-represented terms and pathways were then manually assessed so as to identify how the exposure impacted the involved genes.

3.5.5 qPCR analysis

Each qPCR reaction was performed in triplicate on a mixture containing 5 µl of diluted cDNA, 1.5 µl of forward and reverse primers (Table 8; final concentration 300 nM), 4.5 µl of sterile H_2O, and 12.5 µl of iQ SYBR Green Supermix (Bio-Rad). The qPCR mixture was processed on a CFX96 Real-Time PCR cycler (Bio-Rad) set to the following protocol: 3 minutes at 95 °C; 40 cycles (10 seconds at 95 °C followed by 10 seconds at 58 °C, which continued with 30 seconds at 72 °C); and a melting curve ranging from 65 °C to 95 °C with increments of 0.5 °C. A single melting temperature peak was detected in the dissociation curves for each of the target genes. No template controls were applied, and the cycle threshold values were always over 38. The gene expressions of the target genes were calculated using Bio-Rad CFX Manager

software (v.3.1) with the following reference genes: NADH dehydrogenase [ubiquinone] 1 alpha sub-complex subunit 8 (*ndufa8*) and 60S ribosomal protein L27 (*rl17*), as preliminary experiments indicate these two genes are stable at transcript level (data not shown).

Validation of the microarray results was performed through two methods: either by 1) assessing the Spearman's correlation between specific DEGs with the corresponding qPCR results; or by 2) correlation analysis of shared microarray results (for retene) reported by Rigaud *et al.* (2020a) and those reported within this thesis (I).

TABLE 8 Gene-specific primer sequences, product base pair length (PL; bp), and efficiencies (Eff) for the eight investigated genes following qPCR (I; note that the *cyp1a* expression was measured in whole-body carcasses in III).

Gene	Accession	Primers	PL (bp)	Eff (%)
crabp	NM_001140880.2	F: CTTCCAAAGTGGGAGACAGACAGT R: AATGAGCTCGCCGTCATTGGTT	111	96.6
cxcr4	NM_001124342.2	F: AGATGCACTGGCTGTCAACAGTAG R: ACTTGAGGACTCGGATTCAGTGGA	97	92.1
cyp1a	XM_021607648.1	F: CAGTCCGCCAGGCTCTTATCAAGC R: GCCAAGCTCTTGCCGTCGTTGAT	94	96.9
fah	XM_021586746.1	F: GACAGATGAGACCCGACCAA R: AGAATGCCATCTCCAGCTCA	81	97.6
frim	XM_014187871.1	F: AGGACATCACGAAGCCAGAA R: GGGCCTGGTTCACATTCTTC	93	90.9
mt2	XM_021597409.1	F: TCCTTGTGAATGCTCCAAAACT R: TGCTTTCTTACAACTGGTGCA	88	101.1
txn	XM_021577868.1	F: CTTCTTCAAAGGGCTGTCGG R: GGAACGTTGGCATGCATTTG	119	86.4
txnrd1	XM_021568557.1	F: AGAGTTCATCGAGCCACACA R: ACTCTTTGTCTCCGGGGATG	131	97.2
rl17	NM_001195159.2	F: ATCGAGCACATCCAGGTAACAAG R: AATGTGGCAAGGGGAGCTCATGTA	99	110.1
ndufa8	NM_001160582.1	F: TTCAGAGCCTCATCTTGCCTGCT R: CAACATAGGGATTGGAGAGCTGTACG	119	114

Correlation analysis was performed day-by-day for qPCR results, whereas every shared DEGs (identified by microarray analysis) were assessed together (irrespective of exposure duration).

HPLC GmbH, Ammerbuch-Entringen, Germany). The mobile phase was constructed from deionized water (Solution 1) and an 80:20 mix of ACN:water (v/v; Solution 2), both spiked with 0.1 % formic acid. Each HPLC analytic run took 125 minutes; during the first 85 minutes, Solution 2 increased from 5 % to 28 %, followed by an additional increase from 28 % to 40 % over the next 35 minutes. Finally, the sample was washed in 100 % of the ACN:water solution

for 5 minutes in order to prepare the system for the next run. Each sample was analyzed twice in order to create technical replicates.

3.6 Protein expression analysis

3.6.1 Overview

Compared to the cardiac transcriptome (which was investigated after 1, 3, 7, and 14 days of exposure to DMSO, retene, fluoranthene, and the binary mixture of the two PAHs), the cardiac proteome was only investigated after 7 and 14 days of exposure. Note that the cardiac proteome and transcriptome are derived from the same alevins, which allows for direct comparisons between gene and protein expressions.

3.6.2 Proteomic material preparation and analysis

Material preparation for proteomic analysis (obtained from the TRI reagent extraction) was initiated by the removal of the aqueous phase by the addition of ethyl-alcohol (99.5 % purity), precipitation, and the removal of DNA from the remaining organic and interphase. The remaining proteins were precipitated by the addition of isopropanol; the protein pellet was then washed in 0.3 M guanidine hydrochloride (dissolved in 95 % ethyl alcohol), directly followed by an additional wash in 99.5 % ethanol. The washed protein pellet was then dissolved in a 1 M Tris-HCl buffer (pH 8.0) solution containing 8 M urea and 2 M thiourea. The ensuing protein samples (comprising 15 µg) were then reduced for one hour in dithiothreitol (37 °C), followed by alkylation by the addition of iodoacetamide at room temperature for one hour. Once reduced and alkylated, the urea concentration in each sample was diluted to ≤ 1 M by the addition of 50 mM Tris-HCl. The protein samples were then digested for 16 hours at 37 °C by the addition of trypsin (1:30 w/w), desalted using a SepPak C18 96-well plate according to manufacturer's instructions (Waters, Milford, MA, USA), and dried through evaporation by the application of a SpeedVac (Thermo Fisher Scientific). Finally, the dried protein samples were dissolved in 0.1 % formic acid before mass spectrometry (MS) analysis. The sample concentration of peptides was established through absorbance measured at 280 nm in a NanoDrop (Thermo Fisher Scientific), and the concentration was adjusted to 100 ng μl^{-1}.

The cardiac proteome was processed using liquid chromatography-electrospray ionization-mass spectrometry/mass spectrometry analysis (LC-ESI-MS/MS), and subsequent measurements were performed using a nanoflow HPLC system (Easy-nLC1200, Thermo Fisher Scientific) coupled to a Q Exactive HF mass spectrometer (Thermo Fisher Scientific) coupled to a nano-electrospray ionization source. A prepared protein solution dissolved in 0.1 % formic acid was injected onto a trapping column and separated inline on a 15

cm C18 column (75 µm x 15 cm, ReproSil-Pur 5 µm 200 Å˚ C18-AQ, Dr. Maisch HPLC GmbH, Ammerbuch-Entringen, Germany). The mobile phase was constructed from deionized water (Solution 1) and an 80:20 mix of ACN:water (v/v; Solution 2), both spiked with 0.1 % formic acid. Each HPLC analytic run took 125 minutes; during the first 85 minutes, Solution 2 increased from 5 % to 28 %, followed by an additional increase from 28 % to 40 % over the next 35 minutes. Finally, the sample was washed in 100 % of the ACN:water solution for 5 minutes in order to prepare the system for the next run. Each sample was analyzed twice in order to create technical replicates.

3.6.3 Proteomic analysis

Protein identification and label-free quantification were performed on the raw output from the LC-ESI-MS/MS analysis using MaxQuant v1.6.14.0 (Cox and Mann 2008). MaxQuant allowed for the assignment of RefSeq identification codes to each protein for both rainbow trout and Atlantic salmon (*Salmo salar*) using the integrated Andromeda search engine (Cox *et al.* 2011). The processed MaxQuant output was further analyzed using the Perseus platform v1.6.7.0, which is a proteomic analytical and computational platform developed by Tyanova *et al.* (2016). Such allows for fast and reliable identification of differentially expressed proteins (DEPs) relative to a control through a statistical approach (ANOVA combined with Tukey's *post hoc* test). In order to perform statistical analysis, and thereby identify DEPs, imported data was $\log_2$-adjusted, filtered for blanks, and protein annotations for rainbow trout were added (the annotation database was obtained at https://www.datashare.biochem.mpg.de).

The Perseus output was manually assessed for exposure-specific alterations, whereas over-representation analysis was performed using the online platform Metascape (Zhou *et al.* 2019). In order to perform such analysis, each DEPs' UnitProt identification code was translated to the equivalent zebrafish gene Ensembl identification code (obtained from https://www.zfin.org). Significantly impacted terms and pathways, as per Metascape, were filtered for false positives by considering the corresponding q value. Therefore, any impacted term, with a q value ≤ 0.05, was considered affected by exposure.

The proteome database was uploaded to the repository service PRIDE (https://www.ebi.ac.uk/pride) and made available under the project code: PXD026443.

3.7 Metabolome

3.7.1 Overview and considerations

Cardiac material meant for metabolome analysis was sampled from alevins exposed for 14 days to retene, fluoranthene, and the mixture of the two PAHs and then normalized in relation to DMSO-exposed (control) alevins (II). It must be noted that the alevins analyzed for their metabolome are not the same as those analyzed for their proteome and transcriptome. Supplied by the same company, these alevins were exposed in the same fashion under near-to-exact conditions but 2.5 months later than those sampled for their cardiac transcriptome and proteome.

3.7.2 Metabolomic material preparation and analysis

The metabolome was analyzed from 3 to 4 pooled samples of rainbow trout alevin hearts (45 hearts per pool) per treatment. The hearts were homogenized by bead mill (2×2 mm and 1×5 mm stainless steel beads, 2×15 seconds at 20 Hz, Qiagen TissueLyser II) in cold methanol (CAS number: 67-56-1, Merck, Germany), fortified with 0.1 % of the following components: formic acid, benzoic-d5 acid (as an internal standard; CAS number: 1079-02-3, Sigma-Aldrich, Germany), glycerol-d8 (CAS number: 7325-17-9, Sigma-Aldrich, Germany), and 4-methylumbelliferone (CAS number: 90-33-5, Sigma-Aldrich). The homogenate was vortexed, followed directly by centrifugation, and the generated supernatant was transferred to a clean test tube. Cold methanol spiked with 0.1 % formic acid was added to the supernatant, which was re-vortexed, re-centrifuged, separated into 200 µl aliquots, and dried in a vacuum for 40 minutes at 35 °C. The dried samples were further treated by the addition of methoxyamine hydrocloride (CAS number: 593-56-6, Sigma-Aldrich) and pyridine (CAS number: 110-86-1, VWR, USA) under continuous shaking at 37 °C. After 90 minutes of shaking, the samples were silylated by the addition of MSTFA (CAS number: 24589-78-4, Thermo Scientific, Germany) with 1 % of TMSC (CAS number: 106018-85-3, Thermo Scientific) at 37 ^{o}C and then shaken for an additional 60 minutes. Before being analyzed through GC-MS, the samples were treated with alkane series in hexane (C7-C30) and hexane.

Prepared metabolite samples were analyzed using GC-MS (Agilent 7890A chromatography system coupled with an Agilent 7000 Triple quadrupole mass spectrometer and GC PAL autosampler and injector; CTC Analytics). Each analytical run was initiated by the injection of 1 µl of sample at 260 ^{o}C. The helium flow rate in the guard column (Agilent Ultimate Plus) and in the analytical column (Agilent HP-5MS UI) was set at 1.2 ml minute^{-1} and purge flow at 46 ml minute^{-1} while helium flow in the restrictor column was 1.3 ml minute^{-1}. Mass spectra were collected with a scan range of 55–550 m/z, whereas AMDIS (version 2.68, NIST) and a metabolite detector (versions 2.06 beta and

2.2N; Hiller *et al.* 2009) were used for deconvolution, component detection, and metabolite quantification.

Metabolite levels were calculated as the peak area of the metabolite, normalized against the peak area of the internal standard (benzoic-d5 acid) and the dry weight of the sample. Subsequent average metabolite levels were then normalized against the average of control, thereby assessing the impact of exposure. Annotation of metabolites was based upon spectra and retention time matched to reference compounds and the Golm Metabolome Database (Hummel *et al.* 2007), the NIST mass spectral database (version 2.0, Agilent), and the Fiehn Library (Agilent). It must be noted that the samples were adjusted based upon wet weight as well. However, said approach results in increased variation and overlapping results, with respect to exposure, and is therefore omitted from this thesis.

3.7.3 Bioinformatic metabolome analysis (II)

Metabolome output, based upon dry weight of the samples, was averaged per exposure, normalized against control, with statistical differences between the peak area, relative to control, identified using the non-parametric Mann-Whitney U-test, and the *p*-value adjusted for multiple comparisons using the Bonferroni method. Metabolites with an average enrichment of ≥ 200 % or ≤ 50 % depletion, compared to control, were identified. The latter approach is less reliable due to few replicates and is therefore only presented in this thesis as a comparison with the statistical approach.

3.8 Statistics and synergism

3.8.1 Statistics

Every statistical analysis was performed in R v.4.0.3 (The R Foundation for Statistical Computing, 2020) and RStudio v.1.2.5042 (RStudio Team 2020), apart from protein and metabolite expressions which were statistically analyzed using Perseus v.1.6.7.0. (Tyanova *et al.* 2016) and Simca P+ version 16 (Umetrics, Sartorius), respectively. Mortality and developmental cues were statistically analyzed using Fisher's exact test, whereas dataset normality was assessed using Shapiro Wilk's test. The dataset was considered normally distributed (parametric) if $p \geq 0.05$, unless the number of replicates were ≤ 4; then, the dataset was considered non-parametric by default in order to avoid drawing false positive conclusions on normality. When comparing the effect of exposure on a specific endpoint, *t*-test and one-way ANOVA with Tukey's *post hoc* test were employed if the data was parametric, whereas Mann-Whitney's U-test and Kruskal-Wallis (KW) with Dunn's *post hoc* test were used if the dataset was non-parametric, depending on dataset configuration and number of treatments compared. In the case of correlation, Pearson's correlation analysis was used if

the data was normally distributed, but Spearman's rho if not. Two-way ANOVA analysis was performed on every investigated endpoint from the multi-concentration exposure (III).

3.8.2 Assessment of synergism

Synergistic impact on endpoints following exposure to the mixture compared to the effect of the components was validated using the Bliss independent approach and combination index (reviewed by Foucquier and Guedj 2015). The combination index is calculated as per Eq. 2:

$$Combination\ index = \frac{A_a + B_b}{AB_{ab}} \quad (2)$$

Where A_a is the measured effect in alevins exposed to retene at concentration "a," whereas B_b is the corresponding effect in alevins exposed to fluoranthene. AB_{ab} is the measured effect in alevins exposed to the binary mixture of retene (at concentration a) and fluoranthene (at concentration b). If the calculated combination index is < 1, then the effect of the mixture is considered as synergistic when compared to the combined effect of the components.
Applying the Bliss independence adjustment approach yields a more precise prediction of synergism compared to the combination index approach and is calculated as per Eq. 3: (3)

$$Combination\ index\ (Bliss) = \frac{A_a + B_b - (A_a B_b)}{AB_{ab}} \quad (3)$$

Where A_a, B_b, and AB_{ab} represent the same parameters as in Eq. 2. Synergism caused by the mixture, relative to the components, is assumed if the subsequent score is < 1.

4 RESULTS AND DISCUSSION

4.1 Mortality

Exposure to retene and fluoranthene, alone or as a binary mixture, independent of exposure duration, did not significantly increase mortality compared to DMSO-exposed control alevins. Such was expected, as the concentrations employed were selected to be sub-lethal in developing alevins, as per preliminary experiments with fluoranthene (exposure for 11 days to ≤ 500 μg l^{-1} of fluoranthene caused 0 % mortality; unpublished data) and previously published studies on retene toxicity (Hodson *et al.* 2007, Scott and Hodson 2008, Vehniäinen *et al.* 2016). The only significant difference regarding mortality was observed between alevins exposed to retene (5.56 %) and fluoranthene (0.56 %) for 7 days (I). Although mere speculation, it is plausible that mortality could increase if the semi-static exposure was maintained for a longer duration than 14 days, especially when considering latent developmental toxicity, which could be manifested at a later occasion, as some biological responses take additional time to develop in PAH-exposed and growing fish larvae (Laurel *et al.* 2019).

4.2 Omics responses

4.2.1 Overview and considerations

First and foremost, significant alterations in the cardiac transcriptome, proteome, and metabolome, in relation to treatment and exposure duration, will be discussed in detail with regards to the investigated endpoints, rather than by themselves. Thus, Chapter 4.2 will focus primarily on microarray validation, exposure-specific omics, and over-representation profiles rather than their subsequent biological impacts.

4.2.2 Microarray validation (I)

Validation of the microarray results was performed by qPCR as well as by comparison with microarray results from retene exposure reported by Rigaud *et al.* (2020a). Overall, validating the microarray results by qPCR did not yield strong or consistent correlations over time (r = 0.39, –0.05, 0.65, and 0.37 on Days 1, 3, 7, and 14, respectively; Pearson's product-moment correlation). It must be noted that the correlation between qPCR and the microarray results was significant only by Day 7 but lacked results from the retene exposure. Therefore, the higher r of 0.65 should be considered carefully.

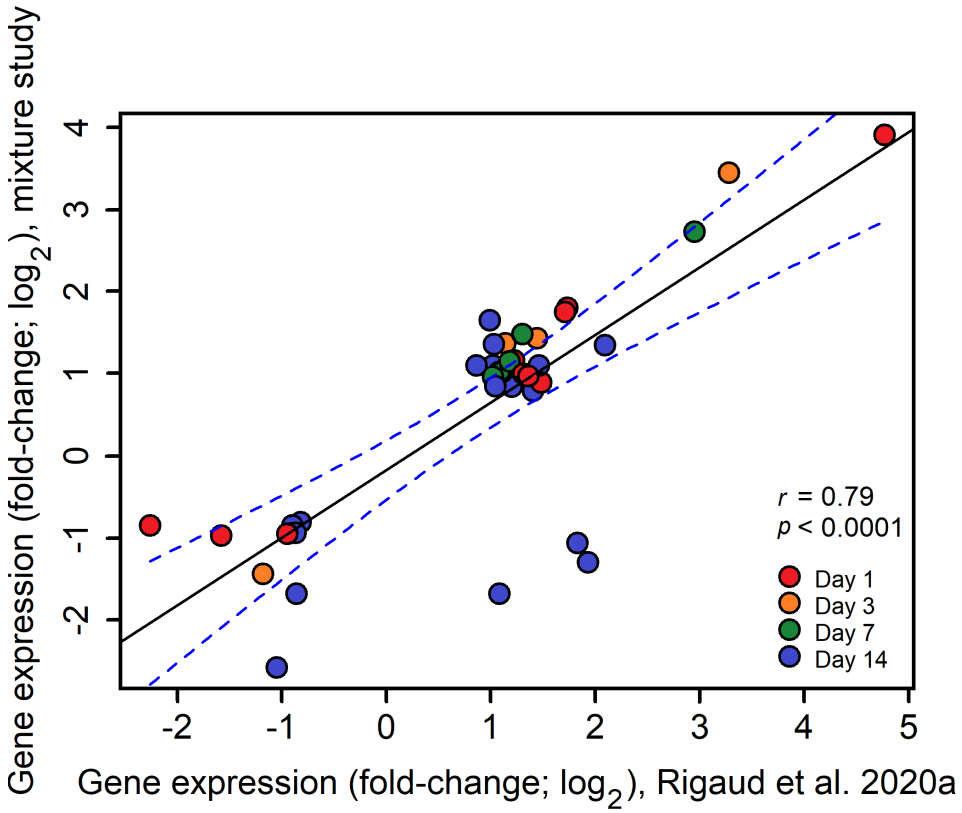

FIGURE 4 Regression analysis (± 95 % confidence interval; blue dashed line) between the shared DEGs induced by exposure to retene (I), and the corresponding DEGs reported by Rigaud *et al.* (2020a). Exposure duration is color-coded, as per the index. The 3 DEGs observed to be expressed in different directions (upregulated in Rigaud *et al.* but downregulated in I) by Day 14 were: *DKEY-90G20.1*, *tmco3*, and *muc5.1*.

In contrast, when the microarray profiles (from retene-exposed alevins) were compared with those reported by Rigaud *et al.*, a strong and significant correlation was obtained (r = 0.79; p < 0.0001; Fig. 4). It is unknown why the correlation between qPCR and the microarray was so poor, especially when considering that the microarray – microarray correlation provided a good validation. Possible explanations to the difference could stem from the microarray probe sensitivity in comparison to the qPCR primers, the latter usually being more precise than the former. Few replicates could also affect qPCR analysis. Additionally, material

degradation could also influence the results, as the qPCR analysis was performed 12–18 months after material extraction and microarray preparation. Additionally, qPCR preparation and analyses required multiple thawing and re-freezing. In the end, the microarray results can be considered reliable as per the microarray – microarray correlation assessment.

4.2.3 Transcriptomic responses and over-representation analysis

Cardiac transcriptomic responses were, to a great extent, exposure-specific, irrespective of exposure duration, and in total, 1986 DEGs were identified across the PAH exposures (Fig. 5; I). Exposure to retene (32 µg l^{-1}) resulted in 937 differentially expressed genes, whereas exposure to fluoranthene (50 µg l^{-1}) affected 344 DEGs. The binary mixture of the two PAHs resulted in 615 differentially expressed genes. The number of differentially expressed genes varied with exposure and duration. Nevertheless, only six differentially expressed genes were shared between the exposures, and only *cyp1a* was consistently upregulated by every treatment, independent of exposure duration. The other genes were nebulette (*nebl*), slow myosin heavy chain b (*smyhc2*), cholesteryl ester transfer protein (*cetp*), zinc finger protein (*D. rerio* gene id: 103910593), and C1q and TNF-like domains (*cbln11*).

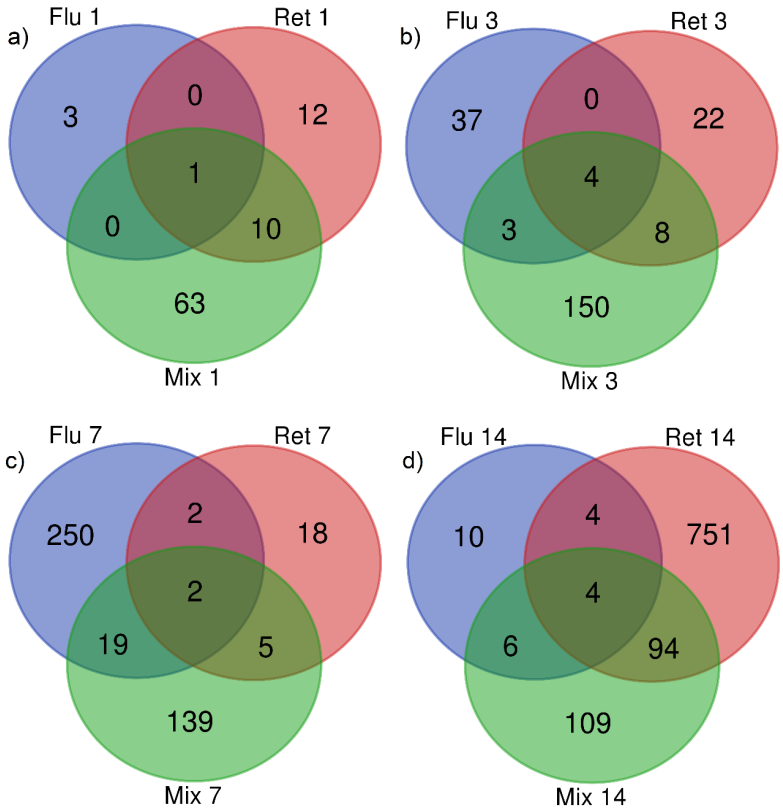

FIGURE 5 Venn diagrams representing the number of differentially expressed cardiac genes following exposure to fluoranthene (50 µg l^{-1}; Flu), retene (32 µg l^{-1}; Ret), and the binary mixture of the two PAHs (Mix) sampled after 1 (a), 3 (b), 7 (c), and 14 (d) days of exposure (I). These Venn diagrams were created using the online tool provided by https://www.bioinformatics.psb.ugent.be/webtools/Venn/.

These exposure-specific transcriptome profiles translated to unique pathway and GO-term profiles, as per over-representation analysis. Exposure to fluoranthene resulted in the over-representation of terms related to GABA-signaling (involved genes were, to a large extent, upregulated) and, to a lesser extent, different forms of metabolism (Fig. 6; Flu 3 to 14). Contrastingly, exposure to retene resulted in over-representation of G-protein signaling (genes primarily downregulated) but also a wide set of pathways related to chondrocyte morphogenesis (Fig. 6; Ret 1 to 14). The relevance of the latter over-representation is dubious due to low gene count, only facilitated by the downregulation of collagen, type XII, alpha 1a, 1b (*col12a1a* and *col12a1b*; retene and mixture) and matrilin 4 (*matn4*; mixture). In zebrafish, matrilin 4 protein is associated with the development of the eye, myoseptum, and to a lesser extent, the skeleton (Ko *et al.* 2005). Collagen XII proteins, in contrast, are abundant in the extracellular matrix of skeletal muscles and in bone tissue (Chiquet *et al.* 2014) but have also been reported to be important in zebrafish heart regeneration following cryoinjury (Marro *et al.* 2016).

An interesting aspect of GABA-signaling over-representation (by fluoranthene) and G-protein signaling (by retene) is the overlapping and shared genes; those genes that fluoranthene upregulated were downregulated by retene, which implies exposure-specific impacts upon these signaling pathways. The biological consequences of these over-representations are unknown and require further investigation. However, it is possible that increased GABA receptor activation would result in decreased parasympathetic stimulus upon blood pressure and heart function by the vagus nerve (Bentzen and Grunnet 2011, Leite *et al.* 2009). Downregulation of genes encoding for components of the G-protein receptors, on the other hand, could be due to previously increased expressions (Tsao and von Zastrow 2000). Further scientific inquiry and investigation are required in order to unveil the exact impact of exposure to retene and fluoranthene upon G-protein and GABA signaling, respectively.

Although the binary mixture only altered the expression of 615 genes, it over-represented the greatest number of GO-terms and pathways. These over-representations varied and covered functions which ranged from growth and development to chondrocyte morphogenesis, phase I and II xenobiotic metabolic processes, iron ion metabolism, and anti-oxidative processes (Fig. 6; Mix 1 to 14).

4.2.4 Proteomic responses and over-representations (II)

Exposure to the PAHs resulted in less extensive impacts upon the cardiac proteome when compared to the cardiac transcriptome. The Perseus platform identified 65 differentially expressed proteins after 7 days of exposure and 82 by Day 14. When these DEPs were separated based upon treatment, fluoranthene significantly affected 11 and 19 proteins after 7 and 14 days of exposure, whereas retene impacted 29 and 23 proteins when sampled after the same exposure duration. Exposure to the binary mixture altered the expression of 44 and 82 proteins, respectively (Fig. 7). Some overlapping protein

expressions were identified between Days 7 and 14, as exposure to fluoranthene resulted in 3 shared DEPs, whereas retene resulted in 4 DEPs and the binary mixture in 23 shared DEPs. Validation of the proteomic results were performed in the same fashion as for the transcriptomic results (Fig. 8). Over-representation analysis of the DEPs, converted to their respective zebrafish Ensembl ID, produced exposure-specific profiles (Table 9).

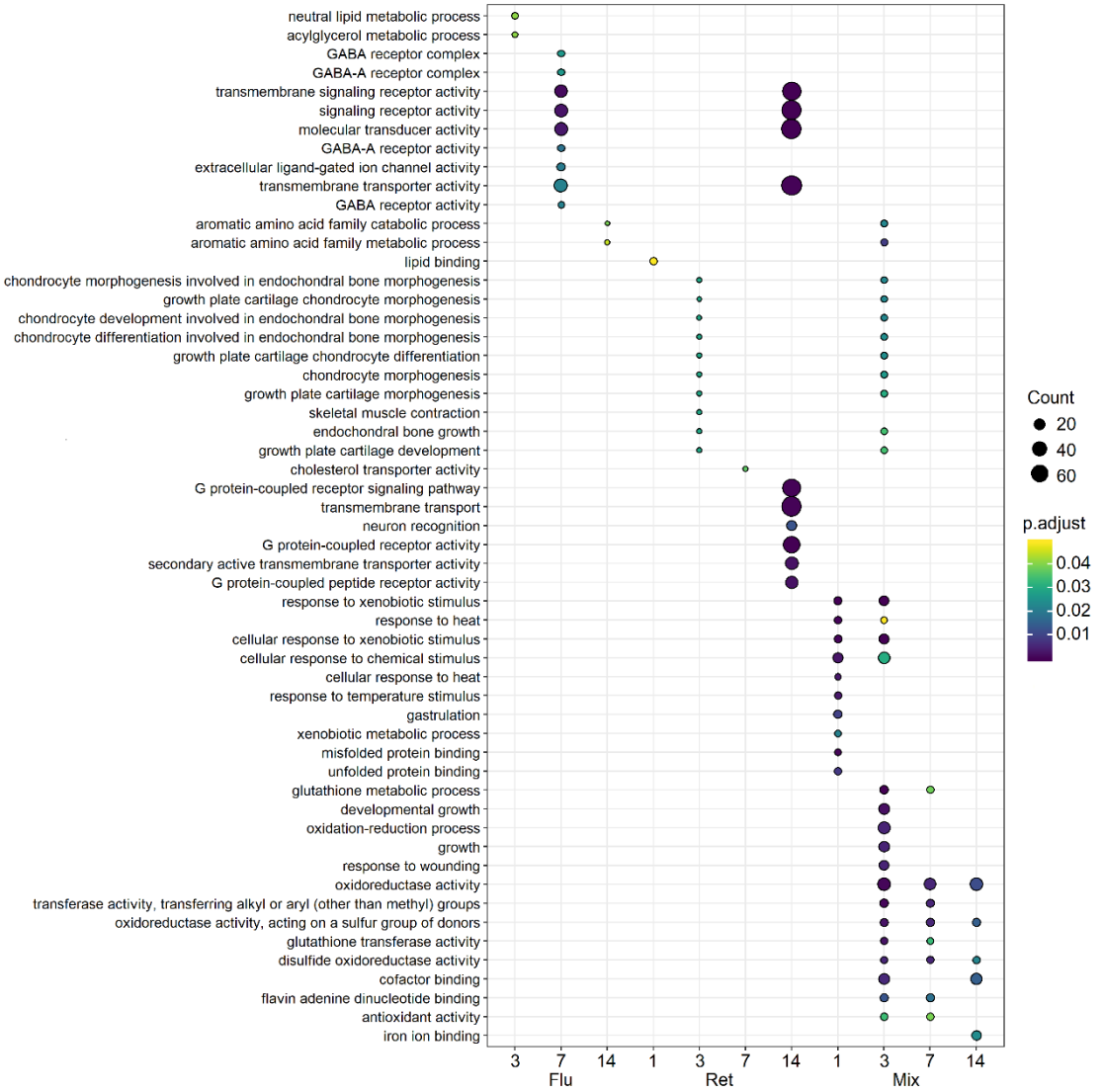

FIGURE 6 Over-represented GO-terms following exposure to fluoranthene (Flu), retene (Ret), and the binary mixture of the two PAHs (Mix) in rainbow trout alevins sampled after 1, 3, 7, and 14 days of exposure. The larger the dot, the greater the number of genes involved, whereas the darker the dot, the more significant the impact of exposure upon the specific term (I). Note that exposure to fluoranthene, for 1 days, did not result in any over-representations, and is therefore omitted from this figure.

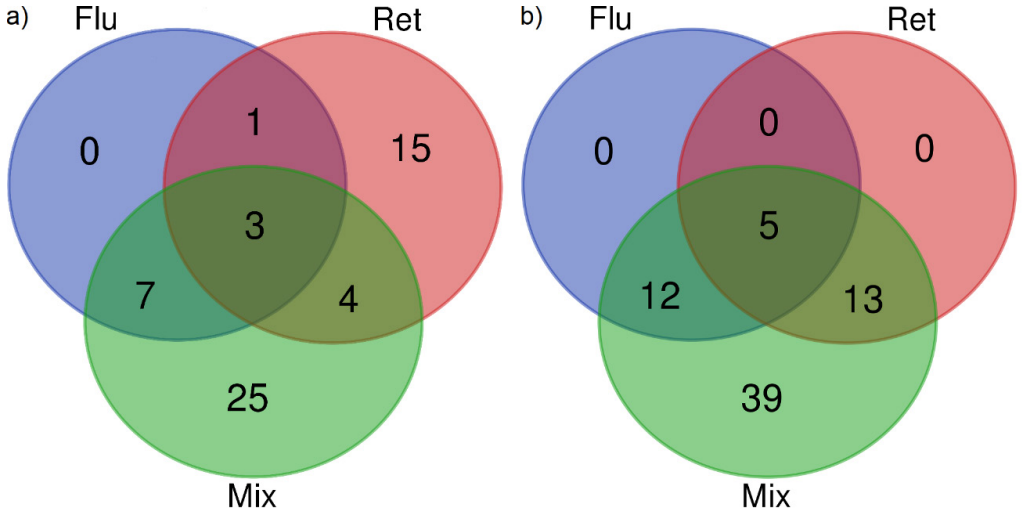

FIGURE 7 Venn diagrams representing the number of differentially expressed cardiac proteins following exposure to fluoranthene (50 µg l^{-1}; Flu), retene (32 µg l^{-1}; Ret), and the binary mixture of the two PAHs (Mix) sampled after 7 (a) and 14 (b) days of exposure (data in II). These Venn diagrams were created using the online tool provided by https://www.bioinformatics.psb.ugent.be/webtools/Venn/.

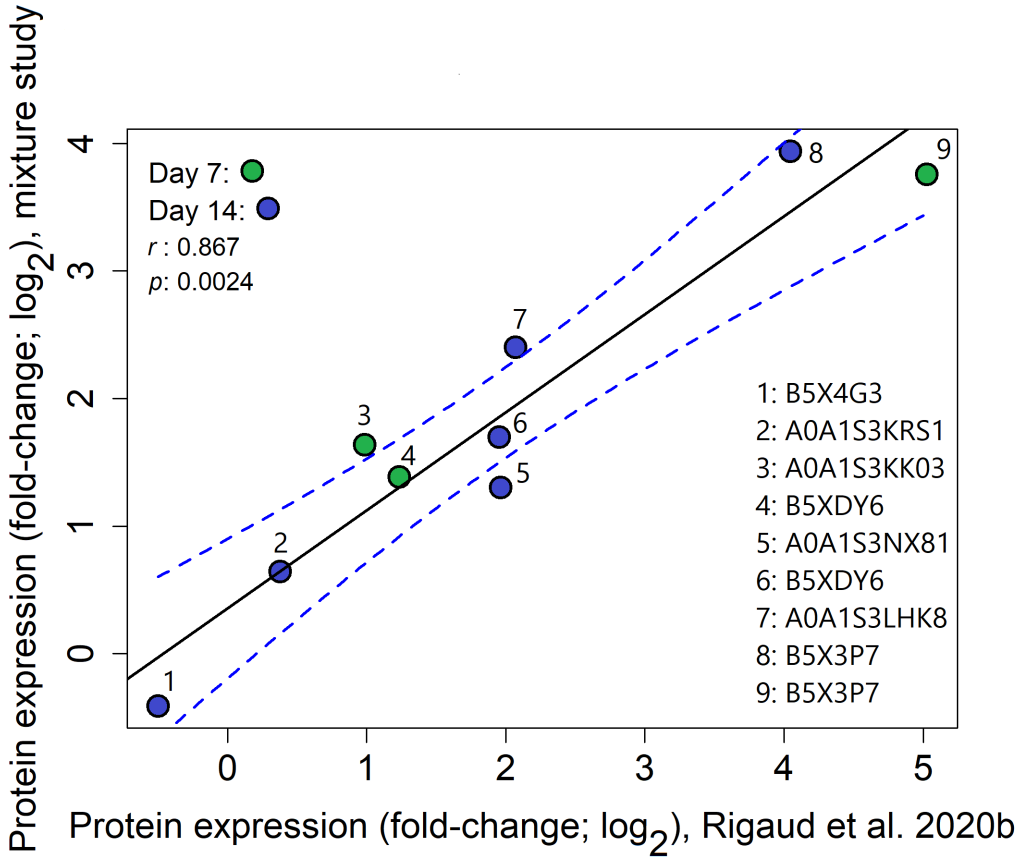

FIGURE 8 Regression analysis (± 95 % confidence interval; blue dashed line) between the shared DEPs induced by exposure to retene (III), and the corresponding DEPs reported by Rigaud *et al.* (2020b). Exposure duration is color-coded as per the index.

TABLE 9 Summary of significantly impacted ($p \leq 0.05$) and over-represented gene ontology (GO), KEGG (dre), and Reactome terms (R-DRE) with a q value ≤ 0.05, as per the cardiac proteome. The cardiac proteome was sampled from rainbow trout alevins that were exposed for 7 and 14 days to fluoranthene (50 µg l^{-1}; Flu), retene (32 µg l^{-1}; Ret), and the binary mixture (Mix) of the two PAHs. Over-representation analysis was performed using the web-based platform Metascape. Note that in order to perform the over-representation analysis, each differentially expressed protein was translated to the equivalent zebrafish Ensembl ID, which in turn was utilized for the over-representation analysis (II).

Duration	Exposure	Term ID	Term description	*P*–value	*q*–value
Day 7	Ret	R-dre-8963898	Plasma lipoprotein assembly	< 0.0001	0.003
	Flu	No over-representations identified			
	Mix	dre00980	Metabolism of xenobiotics by cytochrome P450	< 0.0001	< 0.0001
		GO:0006267	Pre-replicative complex assembly involved in nuclear cell cycle DNA replication	< 0.0001	0.001
Day 14	Ret	No over-representations identified			
	Flu	dre00980	Metabolism of xenobiotics by cytochrome P450	< 0.0001	0.018
	Mix	GO:0050878	Regulation of body fluid levels	< 0.0001	< 0.0001
		GO:0010466	Negative regulation of peptidase activity	< 0.0001	< 0.0001
		dre00980	Metabolism of xenobiotics by cytochrome P450	< 0.0001	< 0.0001
		GO:0045454	cell redox homeostasis	< 0.0001	< 0.0001
		GO:0006267	Pre-replicative complex assembly involved in nuclear cell cycle DNA replication	< 0.0001	0.002
		GO:0031589	Cell-substrate adhesion	< 0.0001	0.013
		GO:0072376	Protein activation cascade	0.0001	0.037
		GO:0051186	Cofactor metabolic process	0.0002	0.040

4.2.5 Metabolomic responses (II)

Exposure to the PAHs had minimal impact upon the cardiac metabolome as per statistical analysis (levels adjusted for wet weight, as data adjusted for dry weight was too varied as per principal component analysis, PCA). Based upon the PCA, 50.1% of the variation in the metabolomic data is caused by exposure to the PAHs relative to control (Fig. 9a; component 1 relative component 2). In contrast, Component 1 compared to Component 3 suggests that the metabolomic profile of the mixture is more similar to that of retene than to fluoranthene (Fig. 9b).

In total, 57 different cardiac metabolites were identified using reference libraries. Even so, only 5 significantly affected metabolites were identified following statistical analysis. Exposure to retene resulted in no significantly impacted metabolites. Exposure to fluoranthene enriched two metabolites significantly (relative to control): glucuronic acid and arabitol (a sugar alcohol). Alevins exposed to the binary mixture presented significantly depleted levels of methionine, putrescine, and hypotaurine, whereas the amino acid phenylalanine was near-to-significantly depleted (p = 0.054; Table 10). However, the metabolomic analysis utilized few replicates per treatment (n = 4), and large variation in the data could, therefore, obscure the analysis and subsequent results. Hence, these results should be considered carefully.

By comparison, if the qualifier of what constitutes an enriched or depleted metabolite is changed from a statistical approach (Mann-Whitney compensated for multiple comparisons; $p \leq 0.05$) to an average cut-off set at ≥ 200 % enrichment or ≤ 50 % depletion relative to the average control, a wider set of alterations are identified. Through such an approach, exposure to fluoranthene resulted in 8 depleted and 6 enriched metabolites, retene 1 and 5, whereas the mixture affected 12 and 4, respectively (Table 10). However, such an approach failed to take data variation into account. This is perfectly exemplified by the enrichment of tyrosine, which presented a greater standard deviation than the average, irrespective of treatment. Therefore, this is merely a comparison, and any further discussion on the topic of metabolomics will focus on the significantly enriched and depleted metabolites. The impact of exposure upon the cardiac metabolome, in relation to toxicity, will be discussed as part of subsequent sections of this thesis, especially in relation to growth, energy consumption, and cardiac function, but also with regards to body burden and xenobiotic metabolism.

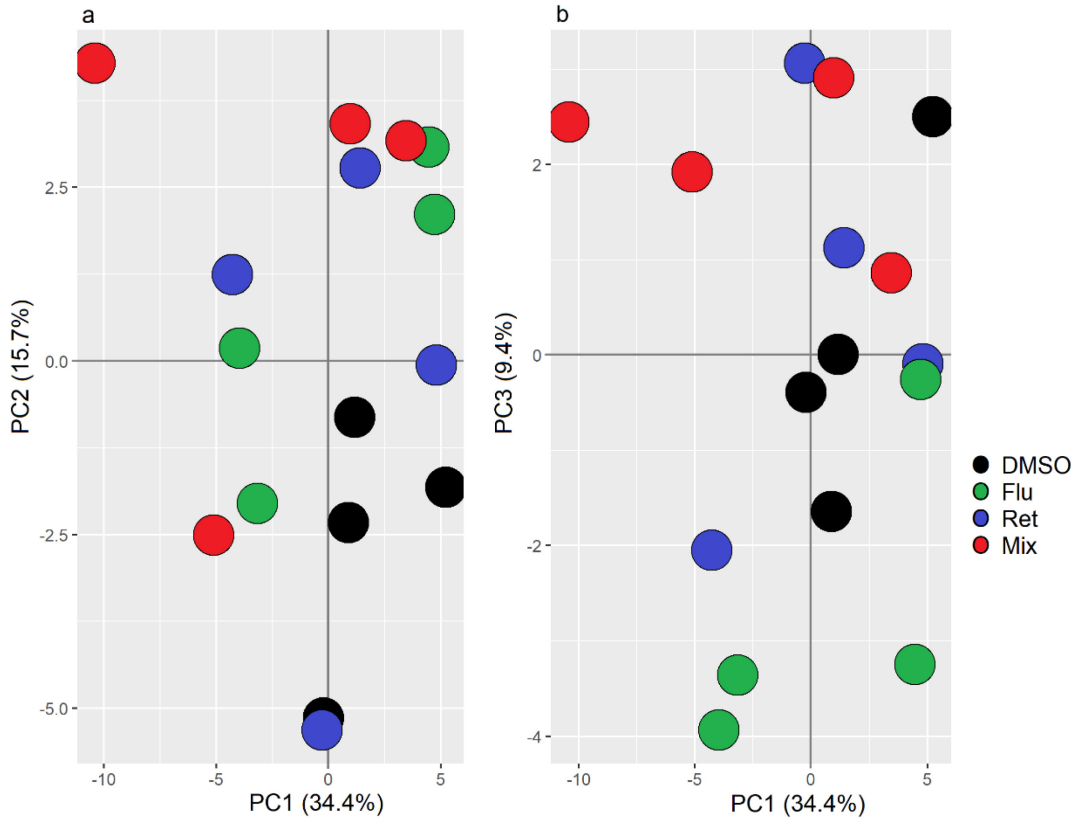

FIGURE 9 Principal component analysis of the metabolomic data adjusted for wet weight between a) Components 1 and 2 or b) Components 1 and 3. Each dot represents one replicate per treatment of either control (DMSO), fluoranthene (Flu), retene (Ret), or the binary mixture of the two (Mix).

4.3 Xenobiotic metabolism (I, II, III)

4.3.1 Body burden and xenobiotic metabolism

The relationship between the accumulation of PAH(s), measured as body burden, and the subsequent activation of phase I and II metabolic processes (as per the transcriptome and proteome) resulted in the strongest cause-and-effect relationship observed between omics responses and an investigated endpoint. Exposure to retene or fluoranthene alone resulted in the formation of exposure-specific body burden profiles over time, whereas when co-exposed, the subsequent profiles were modulated (I, III). Alevins exposed to 32 µg l^{-1} retene and sampled after 1, 3, and 7 days produced non-significantly fluctuating body burden profiles, which by Day 14 had decreased significantly compared to Day 1 (Fig. 10a, grey-filled boxes). Exposure to 50 µg l^{-1} fluoranthene produced a completely different body burden profile; as fluoranthene accumulated with time, the body burden increased significantly from Day 7 onward as compared to Day 1 (Fig. 10b; grey-filled boxes).

TABLE 10 A summary of enriched and depleted metabolites (data normalized against control; average ± SD) following 14 days of exposure to fluoranthene, retene, and the binary mixture of the two PAHs. Metabolites that are significantly affected by exposure, as per Mann-Whitney's U-test and adjusted for multiple comparisons using Bonferroni's method, are denoted with an *. Metabolites that are on average enriched by ≥ 200 % or depleted by ≤ 50 %, relative to control, are denoted by either ↑ or ↓, respectively. The number of replicates per treatment = 4 (II). NA = not available.

	Normalized metabolite abundance, relative to control		
Metabolite	Retene	Fluoranthene	Mixture
Adenine	NA	NA	0.39 ± 0.20 ↓
Alanine	0.53 ± 0.17	0.05 ± 0.02 ↓	0.42 ± 0.33 ↓
Arabitol	1.37 ± 0.79	23.63 ± 9.25 ↑ *	2.95 ± 1.17 ↑
Aspartic acid	0.84 ± 0.33	0.83 ± 0.27	0.47 ± 0.22 ↓
Glucopyranose	1.55 ± 0.34	1.17 ± 0.39	2.11 ± 1.57 ↑
Glucuronic acid	1.69 ± 0.86	11.14 ± 3.73 ↑ *	1.70 ± 0.90
Glutamic acid	0.86 ± 0.30	0.77 ± 0.29	0.49 ± 0.19 ↓
Glycericacid-3-phosphate	0.53 ± 0.66	0.39 ± 0.48 ↓	0.55 ± 0.36
Heneicosanoic acid	0.39 ± 0.25 ↓	0.18 ± 0.09 ↓	0.41 ± 0.30 ↓
Hypotaurine	0.76 ± 0.15	0.72 ± 0.22	0.62 ± 0.09 *
Isoleucine	0.69 ± 0.45	0.87 ± 0.29	0.49 ± 0.34 ↓
Lysine	5.03 ± 5.91 ↑	1.09 ± 0.45	NA
Mannose	6.50 ± 4.20 ↑	2.66 ± 2.91 ↑	4.46 ± 4.80 ↑
Methionine	0.85 ± 0.38	0.86 ± 0.17	0.60 ± 0.16 *
N-acetyl-aspartic acid	0.87 ± 0.31	0.67 ± 0.31	0.47 ± 0.20 ↓
N-Carboxyglycine	0.93 ± 0.23	1.19 ± 0.73	2.74 ± 1.98 ↑
Octadecenoic acid	0.98 ± 0.20	1.17 ± 0.23	0.46 ± 0.44 ↓
Proline	0.61 ± 0.38	0.95 ± 0.44	0.49 ± 0.38 ↓
Putrescine	0.79 ± 0.25	0.83 ± 0.12	0.50 ± 0.15 ↓ *
Threonic acid	2.61 ± 2.88 ↑	3.00 ± 4.15 ↑	1.62 ± 0.72
Tyrosine	11.98 ± 12.63 ↑	10.02 ± 16.43 ↑	6.88 ± 11.42 ↑

However, when the rainbow trout alevins were exposed to both retene and fluoranthene at the same time, the body burden of the PAHs changed drastically. When comparing the body burden of retene in mixture-exposed alevins with those exposed to retene alone, the body burden increased significantly by 352.6 % after a single day of exposure, and by Day 14 had increased by 363.9 % (Fig. 10a; gray-filled boxes compared to white ones). This pattern was inverted for fluoranthene, where the body burden was significantly reduced by 60 % in mixture-exposed alevins after one day of exposure, when compared to alevins exposed to fluoranthene alone. By Day 14, the gap in body

burden of fluoranthene had increased and was 94 % on average when comparing those exposed to fluoranthene alone to those exposed to the mixture (Fig. 10b; gray-filled boxes compared to white ones).

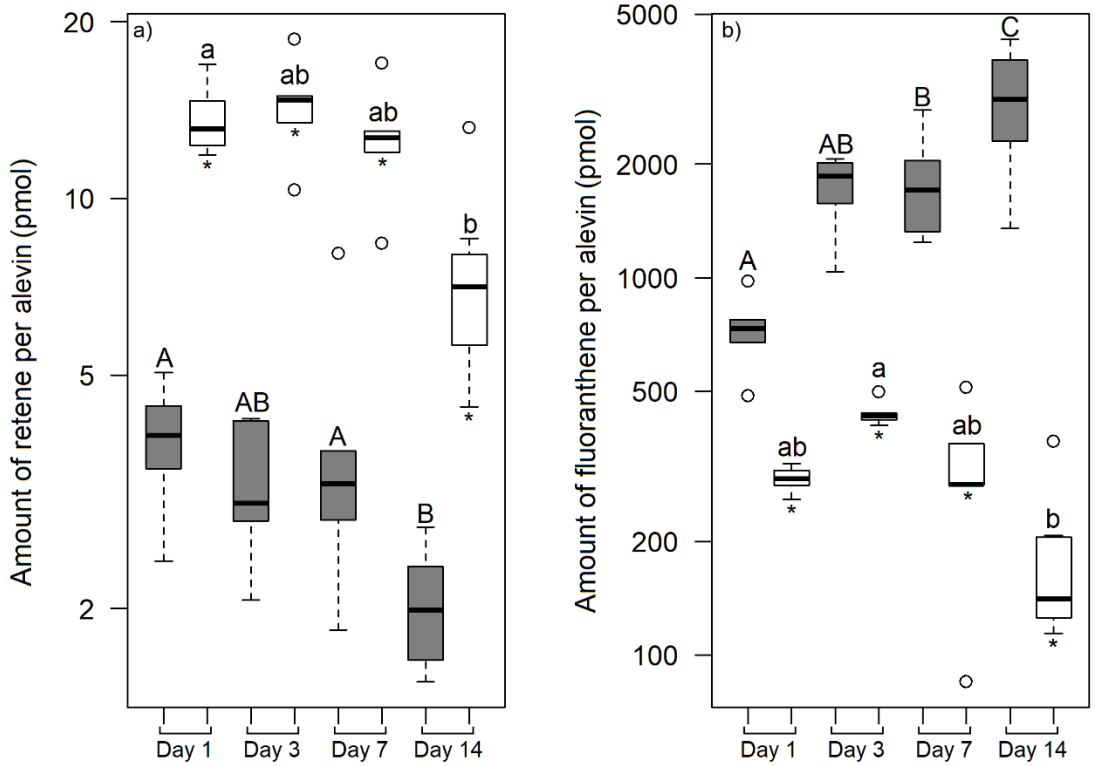

FIGURE 10 Boxplot representations of how the body burden (per alevin) of retene (a) and fluoranthene (b) changed with time in rainbow trout alevins when exposed for 1, 3, 7, and 14 days to the PAH alone (grey boxes) or as a binary mixture (white boxes). Significant differences in body burden over time are denoted by upper-case letters, and lower-case letters depend on whether the alevins were exposed to the PAHs alone or as a mixture, respectively. Significant differences between the body burden of alevins exposed to the PAH alone or as a mixture are marked with an * (I; *t*-test).

Interestingly, but in line with accumulation, fluoranthene was detected in the cardiac metabolome of alevins exposed to fluoranthene (alone) but not following exposure to the mixture (assessed as below the limit of detection). By comparison, retene was not detected in the cardiac metabolome of alevins exposed to the mixture or retene alone. Accumulation of fluoranthene in the heart tissue is likely to reflect whole body accumulation. Yet, it cannot be established if certain tissue(s) and organs are more prone than others at accumulating retene and fluoranthene. Radiolabeled PAHs and subsequent assessment of exposed alevins through autoradiography could yield interesting results with regards to tissue distribution. Bakke *et al.* (2016), albeit utilizing adult polar cod (*Boreogadus saida*), report that ingested C-14 labeled benzo[a]pyrene and phenanthrene primarily become associated with the intestines and gall bladder, highlighting enterohepatic circulation and restricted metabolism with time. Utilizing labeled Cyp1a as a proxy for assessing tissue-

specific accumulation of PAH, Sørhus *et al.* (2016) observed that Atlantic haddock larvae, exposed to artificially weathered crude oil, produced exposure and tissue-specific Cyp1a profiles. Exposed larvae presented labeled accumulation of Cyp1a in the liver and throughout the skin, but not in the heart, which is contradictory to the proteomic results, as presented within this thesis (Table 11; II). These differences could potentially be due to species-specific sensitivity, rainbow trout being especially sensitive to PAH-induced cardiotoxicity. Hence, it is unclear if similar patterns of PAH distribution occurred in retene and fluoranthene-exposed alevins. Further research is required in order to assess plausible exposure and tissue-specific PAH distribution.

These exposure-specific body burden profiles were expected as per previously published research (Geier *et al.* 2018), whereas the massive shift in accumulation following exposure to the mixture was unexpected and could not be predicted based upon exposure to the individual PAHs. The foremost explanation(s) to the differences in body burden among mixture-exposed alevins, relative to those exposed to the individual components, are present in the cardiac transcriptome and proteome, as well as in the subsequent over-representation profiles related to phase I and II metabolism. These profiles can be exemplified by the over-representation of cellular response to chemical stimulus (GO:0070887) and metabolism of xenobiotics by cytochrome P450 (dre00980); the genes constituting the aforementioned term and pathway are associated with the body burden profiles (I). Exposure to fluoranthene (alone) resulted in the upregulation of *cyp1a* and *gstp1*, whereas exposure to retene resulted in the upregulation of *cyp1a*, *ugt1a1,* and *cbr1l.* In contrast, exposure to the binary mixture upregulated all of the aforementioned genes alongside a whole battery of other genes that encode for proteins involved in xenobiotic metabolism: e.g., *cyp1b1*, *gsto1*, *sult1st2,* and many more. These exposure-specific activations of phase I and II metabolic responses were, to a great extent, present in the cardiac proteome (Table 11). Exposure to fluoranthene enriched Cyp1a, Gstp, and Ugt, whereas retene enriched Cyp1a, Sult, and Ugt. Exposure to the combination of retene and fluoranthene was more potent at enriching the aforementioned proteins after 7 or 14 days of exposure.

Yet, these transcriptomic and proteomic results must be considered in relation to the relatively low metabolic activity of cardiomyocytes, especially in relation to hepatocytes, which has a greater capacity for phase I and II metabolism. It is therefore plausible that similar omics-based investigations of other organs, in addition to the heart, could yield different over-representation profiles. This notion is supported by research by Sørhus *et al.* (2016), who reported tissue-specific upregulation of *cyp1a* (assessed by *in situ* hybridization) among Atlantic haddock larvae exposed to crude oil. They found that upregulation was restricted to the skin, hepatocytes, head kidney, and intestines, as well as the endothelium of the heart (after 1 day of exposure). At the end of their experiment (Day 18), the expression of *cyp1a* was, in addition to aforementioned tissues, also observed in the gall bladder, gills, and brain. Their

results suggest that the distribution of Ahr-agonists throughout an organism takes time and is likely to be tissue specific

TABLE 11 Average expressions (log_2 fold changes) of identified cardiac transcripts and proteins involved in phase I and II xenobiotic metabolism following exposure to fluoranthene, retene, and the mixture of the two (mixture) sampled after 7 and 14 days. Only DEGs and DEPs, relative to control, are presented, as per identification by the Perseus platform (built-in ANOVA with Tukey's *post hoc* test) and Nofima's bioinformatics package, developed by Krasnov *et al.* (2011), respectively. Non-significant differences are denoted by -.

Gene ID	Fluoranthene		Retene		Mixture	
Protein ID	Day 7	Day 14	Day 7	Day 14	Day 7	Day 14
cyp1a	2.42	2.68	2.73	1.35	3.63	1.30
cbr1l	-	-	-	0.82	2.50	2.08
gstp1	1.07	1.59	-	-	2.86	2.70
gsto1	-	-	-	-	1.61	1.23
sult1st2	-	-	1.43	1.10	2.33	2.92
ugt1a1	-	-	1.02	0.84	1.65	1.38
Cyp1a	3.82	3.83	3.76	3.94	5.19	4.60
Gsta	-	-	-	-	1.50	2.01
Gstp	-	1.40	-	-	2.25	3.17
Gshr	-	-	-	-	2.62	3.07
Sult[1]	-	-	1.39	1.70	2.24	2.20
Ugt[2]	-	0.72	0.52	1.30	2.12	2.36

1) UniProt ID: B5XDY6
2) UniProt ID: A0A1S3NX81

Hence, the omics data strongly suggests that the increasing body burden of fluoranthene is caused by two processes: 1) a weaker phase I and II metabolic response (compared to the other treatments) in combination with 2) physical inhibition of Cyp1a. However, even though exposure to 50 µg l^{-1} of fluoranthene resulted in accumulation over time, only weak symptoms of developmental toxicity were observed (see 4.5.1.; BSD-index). Furthermore, the body burden in relation to the proteome and transcriptome profiles strongly suggests that fluoranthene was slowly metabolized through conjugation with glutathione and, to a lesser extent, by glucuronic acids. These findings suggest that metabolism of fluoranthene gives rise to a soft electrophile (Ketterer *et al.* 1983). Yet, it is unclear if electrophilic fluoranthene is completely scavenged by phase II metabolic processes or able to contribute to toxicity by interaction with any unknown and unintentional molecular target (Boelsterli 2007). This is exemplified by sulfur- containing amino acids (cysteine and methionine), which can become targets for electrophilic attack, resulting in covalent bonds and potentially disrupted protein function. However, multiple factors affect the probability for such interactions, primarily the protein's three-dimensional folding but also tissue distribution and concentration, both of which relate

specifically to the electrophile's half-life. If and how electrophilic fluoranthene can interact with, and plausibly form covalent bonds with, proteins and cellular structures are interesting prospects that should be investigated further. Additionally, and observed among alevins exposed to fluoranthene, the expression of *cyp1a* remained fluctuating around an equilibrium throughout the exposure duration and had only increased by 2% by Day 14 compared to Day 1 (I). Corresponding enrichments of Cyp1a were observed in the cardiac proteome, thereby confirming the transcriptomic results.

In contrast, exposure to retene induced a stronger phase II metabolic response than fluoranthene, which facilitated xenobiotic metabolism and, therefore, a diminishing body burden with time. These specific upregulations, following exposure to retene, are in line with previous research published by Huang *et al.* (2017) and reflect both decreased levels of absorption from the water column and increased hepatic capacity as the alevins mature. These two factors are, in turn, reflected in the temporal expression of *cyp1a,* which decreased by 66 % in retene-exposed alevins sampled after 14 days of exposure compared to Day 1 and relative to control. Similar results, with respect to *cyp1a* expression over time (76 % reduction), were obtained from mixture-exposed alevins by Day 14 relative to Day 1. Phase II metabolism of retene suggests the formation of nucleophiles, as per upregulation and enrichment of enzymes that facilitate conjugation of the substrate with glucuronic acid and sulfo groups, rather than glutathione.

A distinct discontinuity between an upregulation gene and an enrichment protein, in relation to exposure, was observed for *cyp1a*/Cyp1a. Exposure to retene resulted in a 4.7 % enrichment of Cyp1a protein by Day 14 compared to Day 7, while the corresponding gene expression decreased by 50.6 % over the same time period. Exposure to fluoranthene lead to a 0.3 % enrichment, relative to a 10.7 % increased gene expression. Exposure to the mixture corresponded to a 11.4 % depletion of the Cyp1a protein, while the gene expression decreased by 64.2 % over the same period of time. These differences highlight the discrepancy between an upregulated gene and an enriched protein and the time-lag that can exist between transcription and a fully translated and functional active protein.

The broader activation of phase II metabolic processes in mixture-exposed alevins is likely a consequence of the formation of both electrophilic and nucleophilic PAH metabolites. This would, in turn, allow for efficient phase I and II metabolism, which to a certain degree overcame the inhibitory effect of fluoranthene on Cyp1a, thereby altering the subsequent body burden profiles. Enhanced hepatic function would also contribute to increased efficiency over time. Inversely, the significantly increased body burden of retene among mixture-exposed alevins, relative to those exposed to retene alone, is likely a consequence of differences in substrate affinity of activated phase I and II enzymes for the two PAHs alongside partial Cyp1a inhibition by fluoranthene. Similar shifts in the body burden of PAHs, as per exposure to a mixture relative the components, have previously been reported in PAH-exposed and developing zebrafish (Geier *et al.* 2018). These dynamic relationships between

the mixture and its component and subsequent alterations in body burden, cardiac transcriptome, and proteome have not been observed previously. These changes could not have been predicted from assessment of the additive effects exerted by the individual components alone.

4.3.2 Synergized xenobiotic metabolism and FICZ

An interesting aspect observed among alevins exposed to the mixture is the significantly increased (compared to alevins exposed to DMSO and fluoranthene) and synergized whole-body expression of c*yp1a*, relative to the combined additive effect of the components (Fig. 11; III). These findings could reflect the changes in PAH body burden among mixture-exposed alevins (Fig. 12a, b). Another plausible explanation that could contribute to synergism, which relates to the formation and accumulation of endogenous AhR-agonist(s), such as the tryptophan metabolite FICZ (Rannug and Rannug 2018). Exposure to the PAHs alone did not result in the accumulation of FICZ, whereas exposure to the mixture did (Fig. 12c). Additionally, when considering the extended exposure gradient (as mentioned in Chapter 3.2), it is clear that every mixture exposure containing 50 and 500 µg l^{-1} of fluoranthene caused accumulation of FICZ, irrespective of retene concentration (see Chapter 5; Fig. 16). This is an interesting aspect of toxicokinetics and dynamics that can impact how PAH-induced toxicity is perceived.

Endogenous FICZ is thought to be constantly formed during normal cellular metabolism and is considered the primary reason behind a constant Cyp1a expression *in vivo* (Wei *et al.* 1998). Normally, FICZ, which has high affinity for Cyp1a, is readily metabolized and excreted. However, due to increased substrate competition between the PAHs for Cyp1a and partial Cyp1a inhibition by fluoranthene, it is unsurprising that accumulation occurs. But which other processes promote FICZ to accumulate?

From a toxicokinetic and dynamic perspective, it is unknown if the rate at which FICZ is formed is elevated with increased nominal exposure concentration of the PAHs or not. From an exposure duration perspective, the body burden of FICZ probably peaked after 3 days of exposure before decreasing again by Day 7 (Fig. 12c). These temporal changes in the accumulation patterns of FICZ reflect well the development of the alevins, as they become more proficient at metabolizing both endo- and xenobiotics as the liver matures. Hence, the ratio between the rate at which FICZ is formed and metabolized varies dynamically with time. Yet, the notion that FICZ was formed following exposure to the individual PAHs cannot be rejected. Rather, it can only be concluded that exposure to retene and fluoranthene alone were unable to cause the accumulation of FICZ. Therefore, one can only deduce that if FICZ was formed, metabolism was facilitated, as exposures to these treatments were not able to saturate the metabolic capacity to such a degree that accumulation ensued.

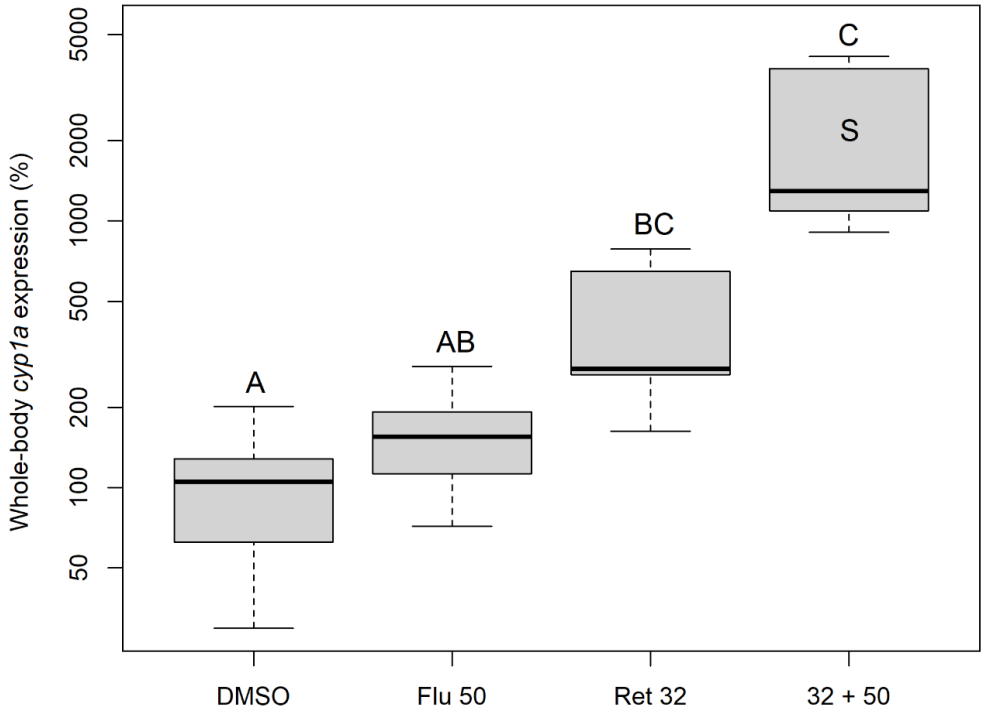

FIGURE 11 Boxplot representation of the whole-body *cyp1a* expression in rainbow trout alevins exposed to DMSO (n = 9), 50 µg l^{-1} of fluoranthene (Flu; n = 9), 32 µg l^{-1} of retene (Ret; n = 7), or the binary mixture of the two PAHs (presented as the nominal exposure concentration of retene + fluoranthene; n = 7; III). Alevins were sampled after 3 days. Significant differences in *cyp1a* expression between control alevins and those exposed to PAH(s) are denoted by different uppercase letters (KW + Dunn's *post hoc* test). A synergized expression of *cyp1a*, induced by the binary mixture, is indicated by the uppercase S.

It is not possible to fully attribute the synergized expression of *cyp1a* to the body burden of FICZ. Although accumulation of FICZ would contribute to upregulation, accumulation of the PAHs is essential, especially fluoranthene, which serves to inhibit some Cyp1a activity, thereby prolonging the duration between Ahr2 activation and subsequent metabolism of the PAHs and FICZ. Unpublished results from follow-up exposure investigation detected the accumulation of FICZ in alevins exposed to the mixtures of pyrene + fluoranthene and phenanthrene + fluoranthene; pyrene and phenanthrene are both relatively weak Ahr2 agonists (Barron *et al.* 2004). However, the accumulation of FICZ, following exposure to the aforementioned mixtures, is less than what was observed in retene + fluoranthene-exposed alevins. Thus, one can infer that the accumulation of FICZ occurs as a consequence of combined Ahr2 agonism alongside Cyp1a inhibition. It is therefore likely that exposure to crude (and weathered) oil or petroleum products could result in the accumulation of FICZ. This, however, must be confirmed before any extensive conclusion(s) can be made.

Previously published research on toxicokinetics and dynamics has reported that endogenously derived FICZ is primarily formed through three

distinct processes: enzymatic activity, UV-irradiation, and oxidative stress (Smirnova *et al.* 2016, Rannug and Rannug 2018). In this experimental setup, UV-irradiation, as the catalyst of FICZ formation, can be dismissed, as every experimental exposure was performed in windowless rooms lit by yellow fluorescent light-tubes. Such leaves increased enzymatic activity and oxidative stress as the most plausible promotors for the formation of FICZ *in vivo*. As neither direct measurement of enzymatic activity nor oxidative stress were performed, proxies must be considered and evaluated.

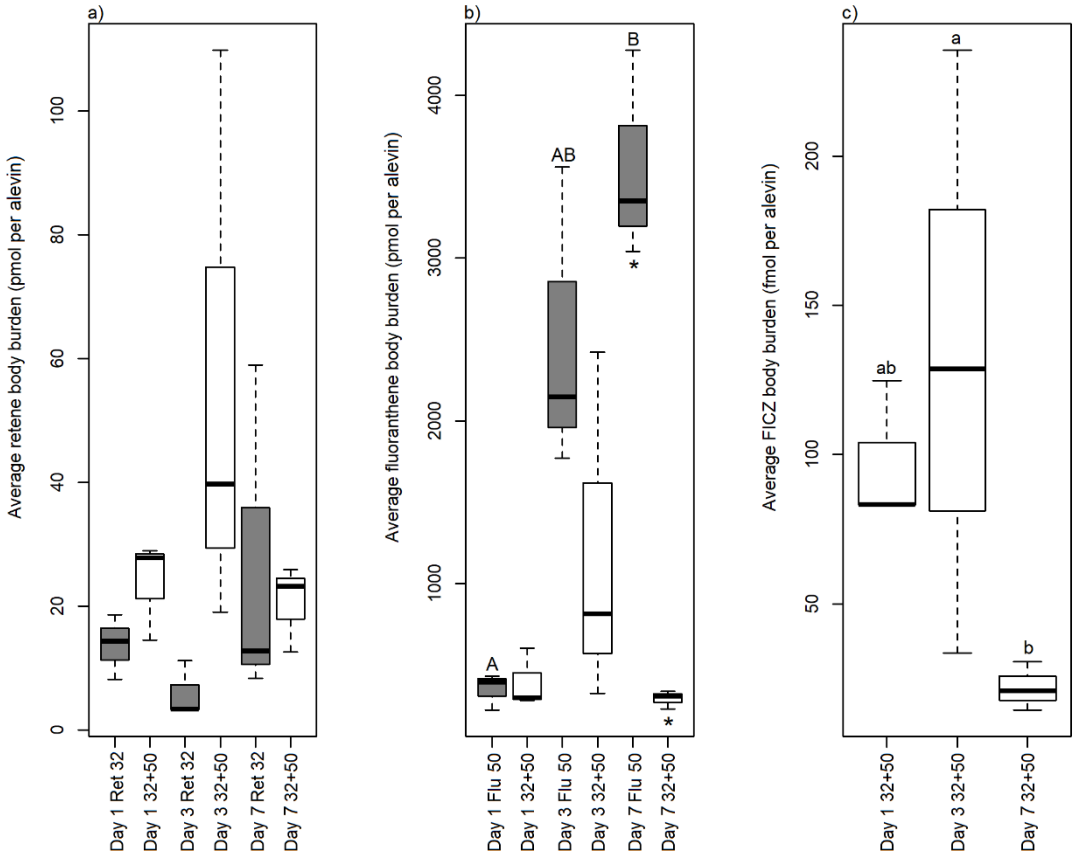

FIGURE 12 Boxplot representations of the body burden of (a) retene, (b) fluoranthene, and (c) FICZ as per rainbow trout alevin exposed to the PAH(s) alone (grey-filled boxes) and as a mixture (white-filled boxes) (III). Significant differences (KW + Dunn's *post hoc* test) between timepoints are denoted by uppercase (fluoranthene) and lowercase letters (FICZ). Significant differences between the body burden of alevins exposed to the PAH alone and the corresponding PAH in the binary mixture are marked with an * (Mann-Whitney's U-test). The number of replicates per treatment = 3.

4.4 Oxidative stress

Transcriptomic analysis revealed that exposure to fluoranthene and the mixture over-represented the GO-term oxidoreductase activity (GO:0016491) following 3 days of exposure and at subsequent sampling, whereas exposure to retene did

not (I). This specific over-representation was primarily promoted by the upregulation of thioredoxin reductase 1, thioredoxin-like, and peroxiredoxin 2. As a functional protein, peroxiredoxin is known to be involved in processes aimed at counteracting increased levels of oxidative stress caused by hydrogen peroxide (H_2O_2) (Rhee *et al.* 2001). It does so by catalyzing the reaction $2H_2O_2 \rightarrow 2\ H_2O + O_2$, while oxidizing itself in the process, thereby becoming inactive. Oxidized peroxiredoxin is re-reduced to its active form by reduced thioredoxin, which becomes oxidized. In turn, reduction of oxidized thioredoxin is facilitated by thioredoxin reductase (Mustacich and Powis 2000). Hence, upregulation of these three aforementioned genes suggests increased presence of H_2O_2 and, therefore, exposure-induced oxidative stress.

Additional support for the hypothesis of increased oxidative stress, following exposure to the mixture, is provided by the upregulation of several genes encoding for heatshock proteins (*hsp90A*1 (also among retene-exposed alevins), *hsp70L*, and *hspA8i)*. PAH-induced upregulation of *hsp* genes has previously been observed in developing fish larvae (Räsänen *et al.* 2012, Vehniäinen *et al.* 2016, Song *et al.* 2019), thereby providing additional support to the notion of ongoing oxidative stress and plausible protein damage (Sanders 1993).

Over-representation analysis of the proteome (translated to the corresponding zebrafish Ensembl IDs) revealed no impact on GO-terms or pathways involved in counteracting oxidative stress (II). However, manual assessment of the differentially expressed cardiac proteins indicates ongoing oxidative stress. Enrichment of peroxiredoxin (Prdx; B5X8H5) was observed among alevins exposed to the mixture for 7 and 14 days, as well as among alevins exposed to fluoranthene for 14 days. Further assessment of the proteome indicated that the abundance of hemopexin a (Hpxa; by fluoranthene and mixture) and ferritin (Frim; depleted by retene and enriched by mixture) were altered. These proteomic alterations indicate disrupted iron metabolism, which relates to oxidative stress, as hemopexin sequesters free and circulating heme, which, if left unchecked, has been linked to increased oxidative stress and cellular damage (Tolosano and Altruda 2002). The primary function of ferritin, on the other hand, is to store biologically available iron (Fe^{3+}) for biological functions in a safe and non-toxic form. Increased plasma levels of unbound iron are toxic and can function as a catalyst for the formation of reactive oxygen species, thereby resulting in increased oxidative stress (Orino *et al.* 2001). In this context, the exact underlying cause(s) leading up to the enrichment of Prdx and the upregulation of anti-oxidative processes is unknown, although a combination of pro-oxidants produced during phase I metabolism (Veith and Moorthy 2018), such as H_2O_2, alongside altered iron metabolism are likely to be involved, or even the causative factors. Other processes cannot be excluded, however.

Numerous studies have reported activation of oxidative countermeasures in fish larvae exposed to PAHs (as well as in other species and taxa, too) (Le Bihanic *et al.* 2014, Chong *et al.* 2019, Shankar *et al.* 2019, Xu *et al.* 2019). It is clear that an altered abundance of ferritin and hemopexin a may potentially

contribute to increased oxidative stress. Interestingly, exposure to the individual PAHs affected iron metabolism differentially, as fluoranthene depleted Hpxa (Day 14), whereas retene depleted ferritin (Day 7); co-exposure led to the depletion of both, irrespective of exposure duration. From a clinical perspective, depletion of hemopexin is associated with ongoing hemolysis and subsequently increased demand for the scavenging of free heme (reviewed by Delanghe and Langlois (2001)). From an environmental toxicological perspective, depletion of Hpxa has previously been reported in juvenile Atlantic cod (*Gadus morhua*) exposed to North Sea oil (Bohne-Kjersem *et al.* 2009).

Increased oxidative stress, alongside depletion of Hpxa by fluoranthene, is supported by the enrichment of the anti-oxidative enzyme Prdx. Interestingly, exposure to retene, which depleted ferritin, did not significantly alter the abundance of Prdx, which suggests that developing alevins are able to maintain oxidative stress at levels relative to control. Instead, exposure to retene resulted in the depletion of ferritin, which suggests past and/or ongoing mobilization of iron reserves, as levels of available iron are inadequate to maintain normal cellular functions, which could affect other biological processes, such as typical gas exchange. What causes the increased demand for iron is unknown, although previous studies have linked enrichment of ferritin to anoxia (Larade and Storey 2004) or exposure to oil (Troisi *et al.* 2007, Olsvik *et al.* 2012). In contrast to the individual PAHs, exposure to the mixture resulted in the depletion of hemopexin alongside enrichment of ferritin and Prdx. These findings could, therefore, reflect a continuously elevated demand for the proteins due to constant leakage of heme. The most plausible origin of leaked heme is damaged erythrocytes. If true, such would imply that PAH exposure disrupts erythrocyte cell membrane and/or cytoskeleton integrity to such a degree that leakage occurred. Nevertheless, the impact of PAH(s) on erythrocytes is poorly understood, but such seems to contribute to toxicity. Further studies are required.

4.5 Heart function

4.5.1 Overview and considerations

PAHs and crude oil are well known to affect both heart structure (Wills *et al.* 2009, Scott *et al.* 2011, Sørhus *et al.* 2017) and function in developing fish species, as per bradycardia and arrythmia (Brette *et al.* 2017, Incardona *et al.* 2011, Sørhus *et al.* 2017). The underlying mechanism(s) of PAH-induced bradycardia have been linked to altered heart structure (Incardona *et al.* 2004) as well as how PAHs interact with and affect cardiac calcium, potassium, and sodium ion channels, thus altering repolarization and disrupting propagation of the action potential (Vehniäinen *et al.* 2019, Ainerua *et al.* 2020).

4.5.2 Heart rate and interbeat variability

During normal development and under typical circumstances, heart rate increases significantly over time as the alevin grows (Fig. 13a; DMSO; unpublished results; III). Exposure to the individual PAHs did not prevent such increase, but exposure to the mixture did. Interestingly, exposure to retene and fluoranthene caused a significant reduction in heart rate among alevins sampled after 3 days of exposure, but not by Day 7. When co-exposed, a significant reduction of heart rate was observed among alevins sampled after 3 days of exposure. By Day 7, the heart rate was essentially the same (79.9 ± 8.4 BPM) as after 3 days of exposure (80.0 ± 5.4 BPM). These differences in heart rate between DMSO and PAH(s)-exposed alevins correspond to an average decrease of 5.4 %, 7.7 %, and 6.9 % among retene, fluoranthene, and mixture-exposed alevins by Day 3, and 4.8 %, 6.7 %, and 16.0 % decrease by Day 7, respectively.

These findings on exposure-induced bradycardia are comparable with previous research on PAH (and petroleum)-induced cardiotoxicity in fish larvae (Incardona *et al.* 2009, Xu *et al.* 2016, Li *et al.* 2021), whether an individual PAH (Incardona *et al.* 2009, Brette *et al.* 2017) or simple mixtures (Incardona *et al.* 2011, Jayasundara *et al.* 2014). What is evident from these articles is that multiple factors affect, govern and contribute to PAH-induced cardiotoxicity. Laurel *et al.* (2019) report compelling evidence on the development of bradycardia from crude oil-exposed polar cod (*Boreogadus saida*). They found that bradycardia reflected remodeling of cardiomyocytes' electrophysical properties rather than any acute impact on ion channel function, especially when considering the fact that heart defects were reported to be "permanent," even after exposure ceased. Yet, we know from Ainerua *et al.* (2020) and Vehniäinen *et al.* (2019) that exposure to PAH impacts cardiac ion channels, in vitro, and as a consequence, the propagation of the action potential is disrupted. Hence, it is possible that the remodeling of cardiomyocytes' electrophysical properties, as suggested by Laurel *et al.* (2019) is compensatory and a long-lasting consequence of exposure.

Arrythmia, which is reported to be a commonly observed sign of cardiotoxicity among fish larvae following exposure to PAHs and crude oil (Incardona *et al.* 2014), was not observed following exposure to these PAHs (Fig. 13b). No significant differences in interbeat variability were observed, be that after 3 or 7 days of exposure. However, it cannot be ruled out that an extended exposure duration or greater nominal exposure concentration(s) could cause arrythmia.

Nevertheless, the aforementioned results concerning PAH-induced cardiotoxicity tell us very little about the molecular factor(s) and mechanisms involved, merely that cardiotoxicity occurs as a consequence of exposure, relative to control. Therefore, cardiac transcriptomic and proteomic responses were investigated after 1, 3, 7, and 14 days of exposure in order to investigate the underlying mechanisms of cardiotoxicity (I, II). No single specific mechanism responsible for the induction of cardiotoxicity was identified in the

omics profiles. Rather, multiple biological functions and processes are compromised in parallel, although some may be directly involved, some compensatory, whereas others are affected indirectly as a downstream event, all of which contribute to the exposure-specific cardiotoxicity profiles.

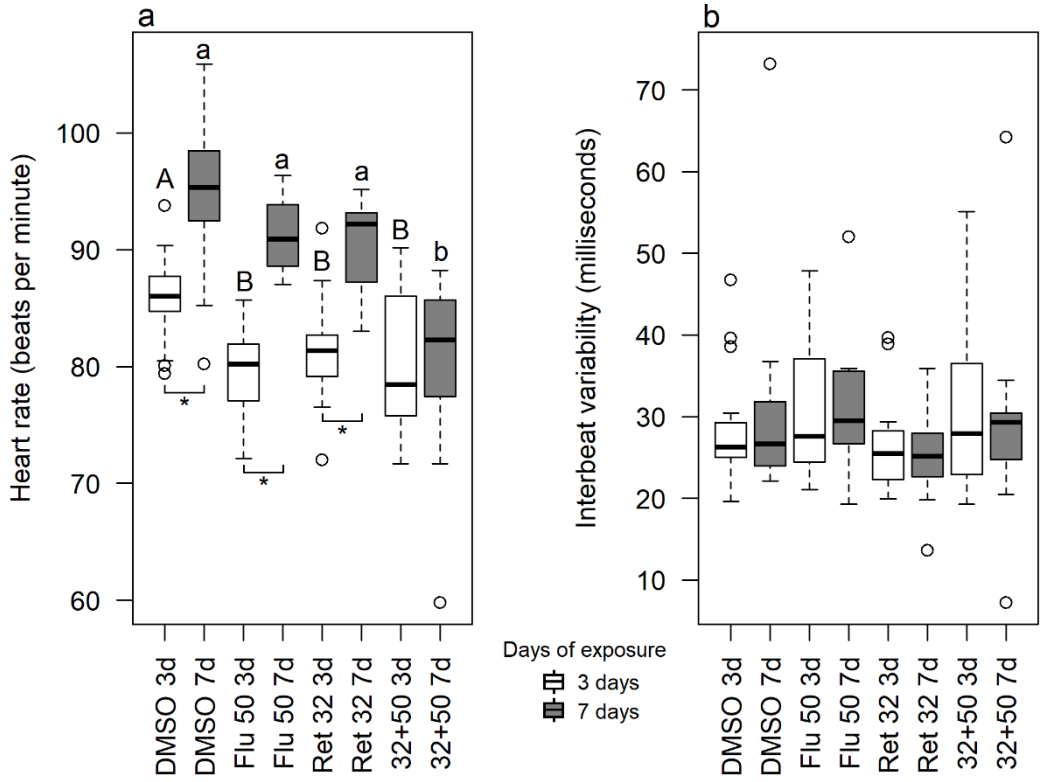

FIGURE 13 Boxplots representing the effect of PAH exposure on (a) heart rate and (b) interbeat variability in 3 (white) and 7 days old (grey) rainbow trout alevins. Exposure is denoted as Ret (retene; 32 µg l^{-1}) and Flu (fluoranthene; 50 µg l^{-1}) as well as the mixture of the two PAHs (presented as nominal exposure concentration of retene + fluoranthene; unpublished results associated with III). Significant differences following exposure are denoted with uppercase (3 days) and lowercase letters (7 days). Significant differences in heart rates, Day 3 to Day 7, are denoted by * (Mann-Whitney's U-test). The number of replicates per treatment = 15 (except for Flu (Day 7) and Mix (Days 3 and 7), which utilized 13 and 14 replicates, respectively).

Exposure to the individual PAHs, which induced bradycardia after 3 days of exposure, caused altered expression of a number of genes encoding for components of calcium (*cacna* genes) and potassium ion channels (*kcnq* genes). In the case of exposure to retene, numerous genes encoding for the aforementioned ion channel subunits were found to be downregulated, whereas exposure to fluoranthene downregulated *kcnq5b* but upregulated *cacna1*. These transcriptomic findings are, as previously mentioned, likely meant to offset the impact of PAHs on the propagation of action potential and cardiomyocyte remodeling (assuming that a differentially expressed gene results in an equally differentially expressed protein; a simplified notion). These specific differences in gene expression can, therefore, be considered as

"effective" with respect to maintaining normal heart rate and interbeat variability (non-significant relative to control). Similar transcriptomic changes in the expression of *cacna* and *kncq* genes have previously been observed by others (Jayasundara *et al.* 2014, Rigaud *et al.* 2020a). The former also reported that exposure to fluoranthene (500 µg l^{-1}) and the binary mixture of fluoranthene + B[a]P (100 µg l^{-1}) induced bradycardia in zebrafish larvae.

The shift from a significant reduction of heart rate by Day 3 to a non-significant reduction by Day 7 among alevins exposed to retene or fluoranthene alone indicates that these altered gene expressions could be able to compensate for the impact of exposure on the cardiac ion channels, thereby resulting in recovery from bradycardia while avoiding arrythmia. Furthermore, considering and extrapolating from the slight recovery in heart rate between Days 3 and 7, it is plausible that further recovery would occur with time, as the developing alevins are becoming less permeable and more efficient at xenobiotic metabolism and excretion.

Even though no transcriptomic alterations or subsequent over-representations related to heart function were observed following exposure to the mixture, said exposure induced bradycardia by Day 3, which remained stagnant by Day 7. Nonetheless, cardiac proteomic results from alevins exposed to the mixture for 7 and 14 days revealed several alterations that could have major repercussions for the structure and function of cardiomyocytes and, therefore, the capacity of the whole heart (II). The most striking finding was the depletion of several mini-chromosome maintenance factors (MCM), which are essential for the initiation of DNA replication together with the co-factors Cdc6 and Cdt1 (Dutta and Bell 1997, Cvetic and Walter 2006). Depletion of the MCM factors implies that cellular division is restricted at the earliest possible molecular event, thus limiting mitosis and organ growth. This finding is interesting and has not been reported previously. The plausible (and major) repercussion of MCM depletion is that fewer rounds of mitosis would have occurred in the hearts of mixture-exposed alevins compared to control. It is therefore possible that altered heart morphology, as per previous research (Brown *et al.* 2016b, Hicken *et al.* 2011, Wills *et al.* 2009), is, in part, related to restricted mitosis. This notion is supported by Incardona *et al.* (2004), who reported thinner heart walls and a dilated chamber in PAH-exposed zebrafish larvae; no recovery was observed upon transferal and recovery in clean water. Even so, depletion of MCM, in relation to heart structure, requires confirmation before any conclusion(s) can be established.

These findings on the impact of PAHs on heart function, *in vivo*, in relation to transcriptomic and proteomic alterations imply and provide additional support to the notion that growth and development of the heart is restricted following exposure to the PAH mixture. How the interaction between PAHs and ion channels (Ainerua *et al.* 2020, Vehniäinen *et al.* 2019) (Fig. 2) translates to long-term remodeling of cardiomyocytes *in vivo* and how the binary mixture of retene and fluoranthene would influence the repolarization of the action potential are unknown.

4.5.3 Cell membrane integrity and structure

Besides the depletion of MCM factors, it is plausible that the internal structure of cardiomyocytes was affected by exposure to the mixture, as both alpha and beta tubulins were significantly depleted relative to control. These two variants of tubulins form the microtubules, which are the foundation of the cytoskeleton (Nogales 2000) and therefore cellular integrity, while also being essential for successful mitosis (Mitchison and Kirschner 1984, Meunier and Vernos 2012). Depletion of the tubulins coincides well with the depletion of MCM, which when considered together, provides additional support to the notion that growth and development of the heart is restricted following exposure to the PAH mixture. It is, however, unclear how and if these depletions are related to the observed bradycardia. These depletions suggest that mixture-exposed alevins developed a smaller heart than those exposed to control or the individual components. If such is correct, it will have severe consequences for the organism as a whole. If the heart is both smaller and beats slower, as observed among mixture-exposed alevins (Fig. 13), the cardiac output per minute would translate to restricted circulation of nutrients, hormones, erythrocytes, and other freely circulating cells and molecules while restricting gas exchange. Decreased cardiac output and stroke volume have previously been reported by Incardona *et al.* (2011), who observed that zebrafish exposed to B[a]P and B[k]F suffered from both decreased cardiac output and slower heart rate. As a consequence, they highlight that even a modest reduction in cardiac output and heart rate has severe repercussions for the developing organism. This is exemplified by exposure to B[k]F, which reduced the average cardiac output by 22.2 % and heart rate by 27.3 %, which in turn translated to a 43.5 % reduction in stroke volume per minute compared to their control. Therefore, it is reasonable to assume that exposure to the mixture reduced the stroke volume per minute. However, this aspect remains fully speculative, as cardiac output was neither quantitatively nor qualitatively assessed in this thesis. Yet, when assessing the heart rate video recordings from alevins exposed to the largest mixture (32R + 500F mixture; III), it is clearly visible that exposure reduced the cardiac output considerably compared to control. Even so, until properly assessed, this observation will remain anecdotal.

In conjunction with the depletion of the tubulins and altered microtubule density was the reduction of three proteins composing different types of intermediate filaments of the cytoskeleton. Even though no over-representation related to cell membrane integrity was identified by Metascape, manual assessment of the DEPs identified keratin type I cytoskeletal 18(-like; K18), desmin(-like), and vimentin. These proteins are essential for normal cytoskeletal structure and function. K18, depleted following exposure to the mixture, is a type I intermediate filament that together with keratin 8 (a type II intermediate filament) forms the most abundant intermediate filament of epithelial cells (Paramio and Jorcano 2002). Distinguished from K18 and keratin 8 were vimentin (depleted following exposure to the mixture and retene) and desmin(-like; depleted by every PAH exposure), which are both type III intermediate

filaments. Functionally, vimentin provides fixation of organelles and contributes to cellular integrity (Katsumoto *et al.* 1990), whereas desmin is essential for muscle function, as it links myofibril to the Z-lines (Sequeira *et al.* 2014). Interestingly, depletion of desmin relates to the observed downregulation of the gene *nebl* (by every PAH exposure relative to control), as knockdown of the latter correlates with the widening of the Z-line in muscle tissue (Mastrototaro *et al.* 2015). Hence, analysis of the Z-line in cardiac muscle tissue of PAH-exposed fish larvae should be investigated further. It is therefore plausible that a broader Z-line could reflect a compensatory event, which suggest cardiac hypertrophy.

Depletion of the tubulins, alongside MCM, K18, vimentin, and desmin, in relation to the downregulation of *nebl*, is therefore likely to affect heart structure and function, although quantification of the absolute distribution and abundance of the aforementioned proteins, as well as the width of the Z-line, require confirmation before any conclusion(s) can be established. Yet, it is unknown, but likely, that these depletions are compensatory vis-à-vis exposure-related alterations of the action potential and its propagation, especially given that alteration of the action potential occurs shortly after exposure (Vehniäinen *et al.* 2019, Ainerua *et al.* 2020). This chain of events is supported by previous research, which reports that cardiac defects precede morphological aberrations in developing fish larvae exposed to PAH(s) (Incardona *et al.* 2004).

4.5.4 Coagulation

Alongside the reduction of heart rate and decreased abundance of tubulins and intermediate filaments was the over-representation of the GO-term body fluid levels (GO:0050878; II) following exposure to the mixture. The DEPs constituting this term were depleted and functionally related to coagulation processes. The depleted anti-coagulant proteins include antithrombin, plasminogen, protein C (vitamin K-dependent), and fibrinogen (gamma chain-like), whereas the depleted pro-coagulants were von Willebrand factor(-like; VVF) and coagulation factor VIII(-like). When these depletions are considered as an amalgamation, decreased coagulation capacity would be the ensuing result. Reduced abundance of the aforementioned anti- and pro-coagulants would, therefore, suggest either ongoing or past damage to the cardiovascular system, especially with regards to the depletion of pro-coagulants (Zimmerman and Edgington 1973, Weiss *et al.* 1977). Coagulation is a complex biological function, which relays upon multiple feedback pathways (Sang *et al.* 2021). In short and assuming damage to cardiovascular endothelium, coagulation is facilitated by the binding of circulating VVF to exposed collagen, present in the subendothelial matrix. In turn, activated VVF becomes accessible to circulating platelets, which aggregate to the damaged site. Once the damage is repaired, inhibitory feedback mechanisms prevent further aggregation of platelets.

It is unclear, though, how and why exposure to the mixture stimulated the aforementioned depletions related to coagulation. It is possible that there is a link between depletions of intermediate filaments over a period of time,

subsequent damage to cardiovascular tissue, and the abundance of anti- and pro-coagulants. Depletion of anti- and pro-coagulants has not been observed at a proteomic level before in developing fish exposed to PAHs, although downregulation of *vvf* has been reported to correlate with increased cardiotoxicity in mummichog embryos (*Fundulus heteroclitus*) (Bozinovic *et al.* 2021). Further studies on the dynamics between PAH exposure and cardiotoxicity in relation to the abundance of anti- and pro-coagulants and platelet count are required, especially in relation to PAH (or crude oil)-induced hemorrhaging, which is a symptom of Blue Sac Disease.

4.6 Morphology and development

4.6.1 Overview and considerations

Exposure to the PAH treatments caused multiple alterations to development and morphology, and in general, exposure to the mixture had a more profound effect on the developing alevins than the individual components. These observations are in accordance with previously published research on PAH mixture toxicity in developing fish larvae, as exemplified by Geier *et al.* (2018). Yet, it is clear that retene and fluoranthene contributed differentially to different developmental endpoints, as revealed by 2-way ANOVA analysis (Table 12; III). In general, exposure had a greater impact on the formation of BSD symptoms and heart rate than on body length, planar yolk area, and interbeat variability.

TABLE 12 Two-way ANOVA analysis highlighting the contributing impact of retene (R; 32 µg l^{-1}) and fluoranthene (F; 50 µg l^{-1}), individually or combined (M), on the outcome of the mixture. Endpoints were: interbeat variability (IBV), Blue Sac Disease (BSD) Index, heart rate (BPM), body length (BL), and planar yolk area (YA) in 7-day old, mixture-exposed alevins. Green-filled cells represent significant impacts ($p \leq 0.05$), relative to control, and the number of * represents the significance level (*** equates a p-value < 0.0001).

IBV			BSD			BPM			BL			YA		
R	F	M	R	F	M	R	F	M	R	F	M	R	F	M
	***			***	***	***	*	***						

4.6.2 Blue Sac Disease (I, III)

Assessing developing fish larvae for symptoms of Blue Sac Disease is a commonly employed practice following exposure to PAHs, dioxins, and petroleum products, an approach which carries many advantages. Primarily, it can be done *in situ* and unaided by technical hardware. Furthermore, assessing BSD does not require the animals to be sacrificed (unless sampled for other

biomarkers), and the results correlate well with actual contamination levels (Billiard *et al.* 1999, 2006, Colavecchia *et al.* 2006). However, the primary issues when assessing symptoms of BSD are related to the biases and experience of the investigator; what one investigator considers a yolk edema could be dismissed by another investigator. Investigator experience is likely to have influenced the assessment of BSD symptoms (I), and is the sole reason why BSD could not be calculated for alevins exposed for 14 days, as well as why only half of the replicates were used for assessment on Days 3 and 7. To compensate for the loss of data from the 14-day exposure, pigmentation of the dorsal fin and the lateral side was assessed instead (Table 13). Pigmentation intensity of the dorsal fin and lateral side highlight both exposure and batch-specific outcomes. Yet, when considering the effect of exposure on both the dorsal fin and the lateral side combined, such indicates that exposure to control and fluoranthene yielded stronger pigmentation intensity than exposure to retene and especially the mixture. A previous scientific investigation on how incorrect activation of Ahr2 in adult zebrafish exposed to TCDD resulted in hyperpigmentation of regrown caudal fin tissue (Zodrow and Tanguay 2003). Differences in developmental stage and investigated tissue could potentially explain certain aspects of hypopigmentation in relation to hyperpigmentation. Alternatively, it is equally plausible that retene and mixture-exposed alevins were at an earlier developmental stage, relative to control, whereas fluoranthene-exposed alevins were at a developmental stage more akin to the control alevins (II). These results on pigmentation will be discussed in relation to growth and development in Chapter 4.6.2 (Growth, development, and planar yolk area).

TABLE 13 Summary of dorsal fin and lateral side pigmentation (%) among rainbow trout alevins sampled for their cardiac transcriptome and proteome (I, II) as well as metabolome (II). Alevins were exposed to DMSO (control), retene (Ret), fluoranthene (Flu), and the binary mixture of the PAHs for 14 days. Significant differences are denoted with either different upper and lowercase Latin letters (I), or Greek letters and numbers (II), as per Fisher's exact test.

	Transcriptome and Proteome (I, II)		Metabolome (II)	
Treatment	Dorsal fin (%)	Lateral side (%)	Dorsal fin (%)	Lateral side (%)
DMSO	100 ^{A}	83 ^{a}	100 $^{\alpha}$	61 ^{1}
Ret	42 ^{C}	71 ^{ab}	100 $^{\alpha}$	17 ^{2}
Flu	88 ^{B}	67 ^{b}	89 $^{\beta}$	83 ^{3}
Mix	29 ^{C}	63 ^{b}	78 $^{\beta}$	11 ^{2}

The BSD results presented in this thesis (I, III) are comparable with each other when calculated using the same parameters (hemorrhaging, pericardial and yolk edemas; Table 14). No significant difference in BSD-index was observed after one day of exposure (I). By Days 3 and 7, alevins exposed to the mixture presented a significantly increased (relative to the control group) and plausibly synergized BSD-index, relative to the components (I). Note that true synergism

cannot be established due to the experimental design; rather, it is only possible to state that mixture-exposed alevins presented a BSD-index greater than the additive effect of the components. These results are in agreement with previous studies on PAH mixture toxicity, which reported that PAH mixtures can synergize the BSD-index compared to the components and that exposure to PAHs increases the index relative to control (Clark *et al.* 2013, Martin *et al.* 2014, Geier *et al.* 2018).

Furthermore, it is evident that retene is more potent than fluoranthene at inducing symptoms of BSD as per similar (average) BSD-indices (III). These findings support the notion that each PAH treatment increased the BSD-index through different processes related to differences in Ahr2 affinity and activation, measured as *cyp1a* upregulation over time. Spearman's correlation analysis, between the average BSD-indices and whole body *cyp1a* expression, yields a moderate R^2 of 0.40 and a non-significant p-value (0.75) on Day 3. In comparison, a stronger (R^2 = 0.80) yet non-significant correlation (0.20) was obtained from the microarray *cyp1a* expression correlated with BSD-indices (I). However, in order to understand how organ dysfunction and site-specific occurrence of BSD-related symptoms are induced, detailed investigation of molecular events is required, both systematically and organ-specifically.

TABLE 14 Summary of Blue Sac Disease (BSD) Indices in 3 and 7-day old rainbow trout alevins exposed to DMSO (control; 0.002 %), retene (32 µg l^{-1}), fluoranthene (50 µg l^{-1}), and the binary mixture of the two PAHs. Significantly different BSD-indices are denoted by different letters (I; ANOVA + Tukey / KW + Dunn) and with numbers (III; KW + Dunn). A BSD-index greater than the combined additive effect of the components, among mixture-exposed alevins, is denoted by an * as per Equation 3 (Bliss adjusted Combination Index). Control (baseline) adjusted BSD-indices are presented as well. I: *n* = 6; III, *n* = 3.

	Exposure	Concentration(s) (µg l^{-1})	Day 3 BSD	Day 7 BSD	Day 3 adjusted	Day 7 adjusted
Study I	DMSO	0R + 0F	0.20 ± 0.08 ^{a}	0.23 ± 0.11 ^{A}	-	-
	Retene	32	0.25 ± 0.08 ^{a}	0.29 ± 0.16 ^{AB}	0.05	0.06
	Fluoranthene	50	0.34 ± 0.17 ^{ab}	0.25 ± 0.06 ^{A}	0.14	0.02
	Mixture	32R + 50F	0.49 ± 0.09 ^{b}	0.43 ± 0.10 ^{B}	0.29 *	0.20 *
Study III	DMSO	0R + 0F	0.20 ± 0.12 ^{12}	0.24 ± 0.08	-	-
	Retene	32	0.33 ± 0.18 ^{12}	0.33 ± 0.12	0.13	0.09
	Fluoranthene	50	0.18 ± 0.10 ^{1}	0.33 ± 0.12	–0.02	0.09
	Mixture	32R + 50F	0.49 ± 0.10 ^{2}	0.44 ± 0.10	0.29 *	0.20 *

Additionally, it is also possible that the suggested impairments of heart structures and functions are indirectly involved. Systemic downstream events are likely to be linked to reduced kidney function, whether following exposure to PAHs (Incardona *et al.* 2004) or the dioxin TCDD (Hornung *et al.* 1999). Furthermore, the relationship between FICZ, oxidative stress, and the formation

of BSD-related symptoms will require future attention in order to understand early life developmental toxicity in fish.

4.6.3 Growth, development, and planar yolk area (I, III)

Considering the impact that exposure to the PAHs has on heart structure and function, subsequent effects of exposure on growth and development are expected. Such is particularly likely because normal heart function is essential for the efficient circulation of nutrients, hormones, erythrocytes, gas exchange, and other freely circulating cells and molecules throughout the organism. During the first few days of development post-hatching, gas exchange is maintained through simple diffusion, as the structure and function of the gills are not properly developed at this stage (Wells and Pinder 1996). But as the fish larva grows and develops, the oxygen requirements increase, and gas exchange is shifted from cutaneous respiration to the gills (Rombough and Moroz 1997). Therefore, reduced heart rate (as presented and discussed in Section 4.4 and 4.5.1) could contribute to a correspondingly reduced gas exchange and circulation of nutrients, as a reduced volume of blood is circulated per unit of time.

Developing fish larvae exposed to individual PAHs, mixtures thereof, or petroleum products are known to suffer from reduced or even impaired development and growth (Billiard *et al.* 1999, Heintz *et al.* 2000, Brown *et al.* 2016a, Geier *et al.* 2018). In the performed studies (I, III), exposure to fluoranthene alone for 3 days resulted in significantly shorter alevins relative to control (standard length; Table 15; I), but this effect had disappeared by Day 7 onwards. Interestingly, the follow-up investigation (III) reported significantly longer alevins following exposure to fluoranthene (Day 3), whereas alevins exposed to retene and the binary mixture were significantly shorter after 7 days of exposure (Table 15; III). By Day 14 (I), alevins exposed to retene and the mixture were significantly shorter when compared to control (I). No significant impact of exposure on standard length (II). Parameters related to growth and development were initially measured among alevins exposed for and sampled after 1 day. These results were excluded from analysis, as any significant effects observed on development and growth at that stage could not, with certainty, be attributed to exposure, as a longer exposure period would be required before being observable (Laurel *et al.* 2019, Price and Mager 2020). At any rate, reduced and impaired growth and development following exposure to retene, and the mixture, are likely related to impaired heart function and, therefore, reduced circulation of nutrients and gas exchange.

Essential to growth during early development is the consumption of yolk. During normal development, yolk serves as the sole source of nutrients before reaching the filter feeding developmental stage, a process that takes approximately two weeks for a newly hatched rainbow trout alevin to attain (assuming water temperature of 10 °C). Thus, measuring how the planar yolk area shrinks over time is a functional proxy of energy consumption. By extension, a significantly larger yolk area would indicate issues with yolk

absorption, whereas a smaller yolk area would indicate increased utilization (Hansen *et al.* 2019). Additionally, heart tissue is primarily dependent upon β-oxidation of fatty acids for sustained energy metabolism, although energy can be derived from glucose, pyruvate and lactate (Grynberg and Demaison 1996); fatty acids that originates from the consumption of yolk among developing fish larvae. Hence, the impact of exposure, vis-à-vis yolk absorption and consumption, as per difference planar yolk area, can result in localized or system compensatory responses, which forces shifts in energy metabolism at a molecular level.

Exposure to fluoranthene, irrespective of exposure duration, did not result in any significant impact on the planar yolk area compared to control (Table 16; I, II, III). Similar results were obtained from retene-exposed alevins, although a significantly larger area was observed among alevins exposed for 7 days (III). Exposure to the mixture resulted a significantly larger yolk area by Day 7 in relation to control (III) but not by Day 14 (I, II). Rather, the yolk area among retene-exposed alevins was significantly smaller compared to those exposed to the mixture on Day 14, which could suggest that exposure to the mixture impaired certain aspects of yolk consumption.

TABLE 15 Average standard length (± standard deviation; mm) among rainbow trout alevins exposed to the control (DMSO), the individual PAHs (retene or fluoranthene), as well as the mixture of the two PAHs for 3, 7, or 14 days. Significant differences are denoted by lower and uppercase Latin letters (I; Days 3 and 14, respectively; ANOVA + Tukey / KW + Dunn), numbers (II; KW + Dunn), or Greek letters (III; KW + Dunn). I: n = 18 (Days 3 and 7) and 24 (Day 14). II: n = 18. III: n = 44–45.

	Exposure	Concentration(s) (μg l^{-1})	Day 3 (mm)	Day 7 (mm)	Day 14 (mm)
Study I	DMSO	0R+0F	18.0 ± 1.0 ^{a}	18.9 ± 1.0	22.1 ± 1.0 ^{A}
	Retene	32	17.4 ± 0.9 ^{ab}	19.1 ± 1.1	20.9 ± 1.1 ^{B}
	Fluoranthene	50	16.8 ± 1.4 ^{b}	18.7 ± 1.2	21.8 ± 1.2 ^{AB}
	Mixture	32R+50F	16.9 ± 1.0 ^{b}	18.6 ± 1.1	21.0 ± 1.3 ^{B}
Study II	DMSO	0R+0F	Not analyzed in Study II		22.8 ± 1.2 ^{1}
	Retene	32			22.4 ± 1.1 ^{12}
	Fluoranthene	50			22.4 ± 1.1 ^{12}
	Mixture	32R+50F			21.6 ± 1.1 ^{2}
Study III$^{\Delta}$	DMSO	0R+0F	15.9 ± 1.3	18.1 ± 0.7 $^{\alpha}$	Not analyzed in Study III
	Retene	32	16.5 ± 1.1$^{\#}$	17.5 ± 0.9 $^{\beta\gamma}$	
	Fluoranthene	50	16.1 ± 0.8	17.6 ± 1.0 $^{\beta}$	
	Mixture	32R + 50F	16.0 ± 0.9	17.1 ± 0.9 $^{\gamma}$	

$^{\#}$ p = 0.058

Hence, no clear and finite conclusion(s) on yolk consumption can be established, as significant differences in area varied temporally. However, when

considering the trend towards a larger average yolk area among mixture-exposed alevins, in relation to control, it is plausible that exposure affected absorption. Furthermore, and supported by transcriptomic, proteomic, and metabolomic data, which suggests increased catabolism, it is very possible that exposure to the mixture altered energy metabolism as a whole (see Sections 4.2.3 and 4.5.3). This is supported by research on how PAHs (and crude oil) affect the fatty acid and cholesterol content in different compartments of Atlantic Haddock larvae (Sørhus *et al.* 2016). The yolk of larvae exposed to crude oil (100 µg l^{-1}) held 9 % and 10 % more fatty acids and cholesterol, respectively and relative to control. In contrast, larvae exposed to the PAH phenanthrene (200 µg l^{-1}) held 11 % and 12 % less fatty acids and cholesterol in the yolk, respectively and relative to control. These discrepancies were hypothesized to be related to the level of cardiotoxicity, as a greater impact of exposure on heart function translated to reduced blood flow. As a consequence, the mobilization and distribution of lipids from the yolk to the rest of the organism is impaired, which was highlighted by decreased levels of fatty acids and cholesterol in the eyes, head, and trunk, and transcriptomically as per activation of compensatory over-representations pathways and processes. However, additional studies focusing on energy metabolism in relation to PAH exposure are required before any final conclusion(s) can be proposed.

In addition to the differences in planar yolk area, yolk morphology was assessed based upon whether the yolk protruded beyond its posterior-most point of attachment. As the growing rainbow trout alevins develop, the yolk is absorbed, and over time, the sac shrinks past the posterior-most point of attachment. It was observed that a significantly greater proportion of alevins exposed to retene (30.2 %) and the mixture (52.3 %) presented said morphology relative to control (13.3 %; Fig. 14; III). No single cause of exposure to the aforementioned impact on yolk sac morphology can be concluded as per these experimental designs. However, impaired cardiac function would reduce blood flow, gas exchange, as well as the absorption and circulation of yolk. Furthermore, Serigstad (1987) showed that maximum oxygen demand during early life development coincides with a peak in yolk consumption. Therefore, it is possible that an altered yolk morphology reflects a reduction in the availability of oxygen. An alternative, yet simpler explanation to the exposure-specific difference in yolk sac morphology could be that these alevins are at an earlier developmental stage, as already suggested by differences in pigmentation patterns (I). However, this specific aspect is beyond the scope of this thesis but should be investigated further.

From a molecular perspective, absorption of yolk, just like nutrients from the intestines, is a strictly controlled process. The knockdown of genes encoding for proteins involved in lipid transfer and metabolism, such as apolipoproteins (*apo*), diglyceride acyltransferase (*dgat*), and microsomal triglyceride transfer protein (*mtp*), has been observed to prevent yolk absorption in fish larvae, thereby stunting growth and development, which in turn, results in premature death, as reviewed by Anderson *et al.* (2011). It is unknown how exposure to either retene or fluoranthene alone, or their binary mixture, would influence the

aforementioned genes in the liver, which is of higher metabolic relevance than the heart. However, the transcriptomic analysis revealed that exposure to retene downregulated the expression of *apoB* on Day 14; a downregulation that is potentially a compensatory mechanism rather than directly related to yolk consumption. How the downregulation of *apoB* relates to lipid transfer and metabolism in heart tissue is unknown. Yet, when considering the impact of exposure to retene on planar yolk area (only significantly smaller relative to alevins exposed to the mixture by Day 14; Table 16, I), it is plausible that said downregulation is compensatory as less yolk (area) is on average left to be consumed, relative to control. However, inferring that a cardiac gene expression is valid for other organs and tissues is a sweeping generalization that should be considered speculative, yet worthy of further investigation.

TABLE 16 Average planar yolk area (± standard deviation; mm²) among rainbow trout alevins exposed to the control (DMSO), the individual PAHs (retene and fluoranthene), as well as the mixture of the two PAHs for 3, 7, or 14 days. Significant differences are denoted by lowercase, uppercase, and Greek letters (I, II; Days 7 and 14, respectively; ANOVA+Tukeys / KW+Dunn) or with numbers (Day 7; III; KW+Dunn). I, II: *n* = 18 (Days 3 and 7) and 24 (Day 14). III: *n* = 44 – 45.

Study	Exposure	Concentration(s) (µg l^{-1})	Day 3 (mm²)	Day 7 (mm²)	Day 14 (mm²)
Study I	DMSO	0R+0F	17.5 ± 3.1	12.9 ± 2.3 ^{a}	11.5 ± 2.4 ^{AB}
	Retene	32	17.8 ± 3.1	15.4 ± 2.6 ^{b}	10.2 ± 1.7 ^{A}
	Fluoranthene	50	18.5 ± 2.3	14.1 ± 2.5 ^{ab}	11.8 ± 3.5 ^{AB}
	Mixture	32R+50F	17.7 ± 2.2	14.2 ± 2.2 ^{ab}	12.8 ± 2.6 ^{B}
Study II	DMSO	0R+0F	Not in Study II	Same as in Study I	8.8 ± 4.4 $^{\alpha\beta}$
	Retene	32			10.1 ± 2.6 $^{\alpha}$
	Fluoranthene	50			7.5 ± 1.9 $^{\beta}$
	Mixture	32R+50F			10.0 ± 3.6 $^{\alpha\beta}$
Study III$^{\Delta}$	DMSO	0R+0F	16.8 ± 2.4	14.3 ± 2.5 ^{1}	Not analyzed in Study III
	Retene	32	18.8 ± 3.4	15.2 ± 2.1 ^{2}	
	Fluoranthene	50	17.4 ± 2.1	15.1 ± 2.5 ^{12}	
	Mixtures	32R + 50F	18.4 ± 2.4	15.3 ± 2.4 ^{2}	

Δ Results associated with Study III.

Closely associated with yolk consumption is angiogenesis, as the establishment of new blood vessels is required for the absorption of yolk. Unfortunately, less extensive and detailed knowledge is available on rainbow trout alevin angiogenesis, especially in regard to toxicity, than among zebrafish. However, Isogai and Horiguchi (1997) produced an excellent guide on rainbow trout vascular development. There, they highlight that yolk sac is encased in a vascular network already before the alevin has hatched (stage 25, as per Vernier's developmental guide, which sets hatching at stage 30). Initiation of

yolk sac encasement starts with the vasculature sprouting from the sub-intestinal vein (SIV; from the posterior-most part of the yolk sac) from the vitelline vasculature. The ensuing irregular meshwork of vasculature unites with the marginal vein, which in turn transport venous blood to the heart.

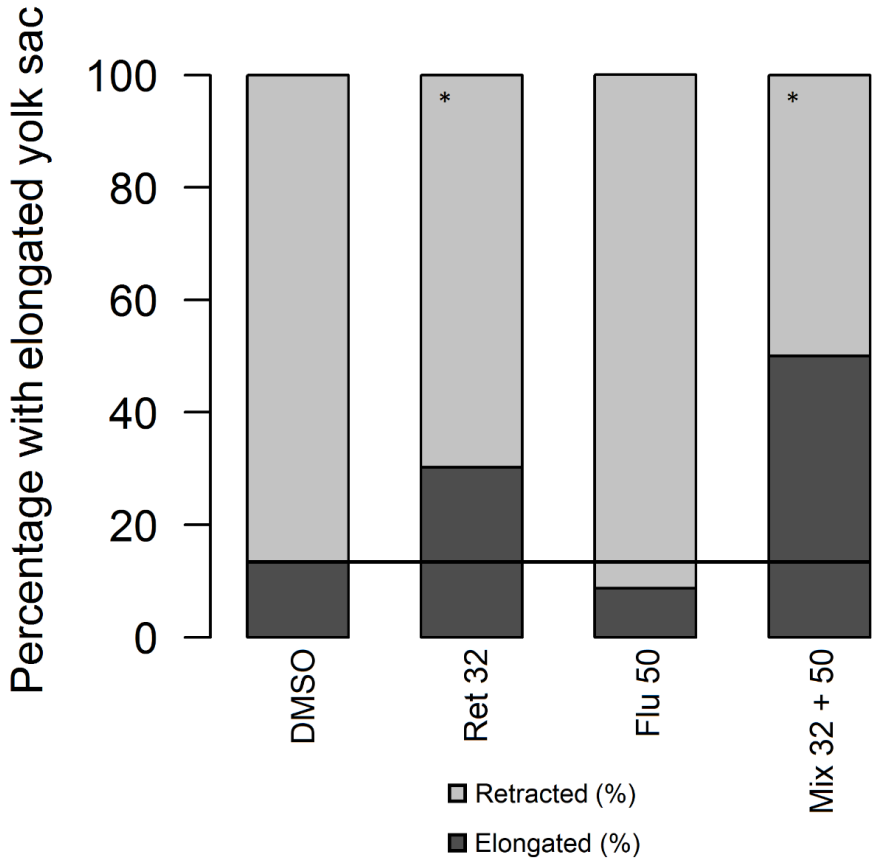

FIGURE 14 The proportion (%) of 7-day old rainbow trout alevins that presented a yolk sac extending beyond the posterior-most attachment (elongated; dark grey) compared to those alevins where the yolk sac was retracted anteriorly of this line (retracted; light grey). Alevins were exposed to DMSO (control), retene (Ret 32 µg l^{-1}), fluoranthene (Flu 50 µg l^{-1}), and mixture (Mix 32 + 50). Significant differences with regards to the impact of exposure on the proportion retracted to elongated compared to control are denoted with an * (Fisher's exact test). The solid black line represents the proportions among control alevins. n = 44 – 45 per treatment.

Contrastingly, more scientific literature on angiogenesis in zebrafish is available. Under normal circumstances, the sub-intestinal venous plexus (SIVP) sprouts posteriorly from the duct of Cuvier (Isogai *et al.* 2001), extends as a network over the yolk, which ultimately connects anteriorly with the cardinal vein, thereby closing the vascular loop (Nicoli and Presta 2007); outgoing blood from the SIVP connects to the hepatic portal veins and the liver. The process of SIVP angiogenesis is governed by numerous factors, as knockdown studies have identified vascular endothelial growth factor A (*vegfa*; promotes the sprouting and formation of inner blood vessels), *ahr*, and bone morphogenetic protein (*bmp*; regulates the outgrowth of SIVP over the yolk) as critical for

proper SIVP development (Goi and Childs 2016). It is unclear whether, but likely, these genes influence vascular development in rainbow trout alevins. As yolk is consumed, the left SIVP is retracted, and blood flow is redirected to the right SIVP. Once all of the yolk is consumed, the SIVP has facilitated the vascularization of the gut, liver, kidney, pancreas, and established the portal vein.

Zebrafish embryos exposed to the dioxin TCDD (1 μg l^{-1}) presented a severely altered SIVP network compared to control (Yue *et al.* 2021). It cannot be determined if exposure to the PAHs investigated in this thesis altered the vasculature development and network, although it is possible that similar results would be observed among mixture-exposed alevins as per a larger planar yolk area and the greater proportion of alevins with a protruding yolk morphology. However, as the vascular network is already established at the onset of exposure, restructuring rather than development would be affected. Additionally, even though the quality of the photographed alevins is good, visual inspection of blood vessels smaller than the vitelline vein is not possible due to resolution. Interestingly, transcriptomic analysis revealed that exposure to retene, but not the mixture, caused a significant downregulation of two genes involved in angiogenesis by Day 14: sphingosine 1-phosphate receptor 1 (*s1pr3a* and *5b*; the latter upregulated by fluoranthene on Day 14). Previous studies have reported that knockdown of sphingosine 1-phosphate results in hypervascularization and abnormal limb development in mice, as vascularization is promoted by reduced availability of oxygen (Chae *et al.* 2004, Takuwa *et al.* 2010). Downregulation of the gene encoding for the sphingosine receptors could, therefore, be associated with reduced availability of oxygen, which would promote vascularization and thereby improve the distribution of available oxygen, while at the same time causing vascular instability.

A major issue with regards to yolk consumption, and by extension energy consumption and metabolism, is that only a handful of studies have investigated it in relation to exposure to PAHs or petroleum products. Granted, yolk area and morphology are not standardized endpoints. Even so, previous exposure studies on fish larvae have reported that exposure has an effect on yolk consumption. For example, both Adams *et al.* (2020) and Carl *et al.* (1999) reported correlation between increasingly impaired yolk absorption in rainbow trout alevins and Pacific herring (*Clupea pallasi*), respectively, with increasing ∑PAH in oil. Moreover, rainbow trout alevins exposed to ≥ 180 μg l^{-1} of retene caused impaired yolk absorption to such a degree that the developing and exposed alevins starved to death (Billiard *et al.* 1999).

4.6.4 Energy metabolism and amino acid catabolism

As mentioned in the previous section, exposure affected a minor number of metabolites related to energy metabolism. To recapitulate, exposure to fluoranthene enriched both glucuronic acid and arabitol, whereas exposure to the mixture depleted methionine, putrescine, and hypotaurine significantly, whereas phenylalanine was (near-to-significantly) depleted. Furthermore,

altered energy metabolism is supported by transcriptomic and proteomic data (Fig. 15).

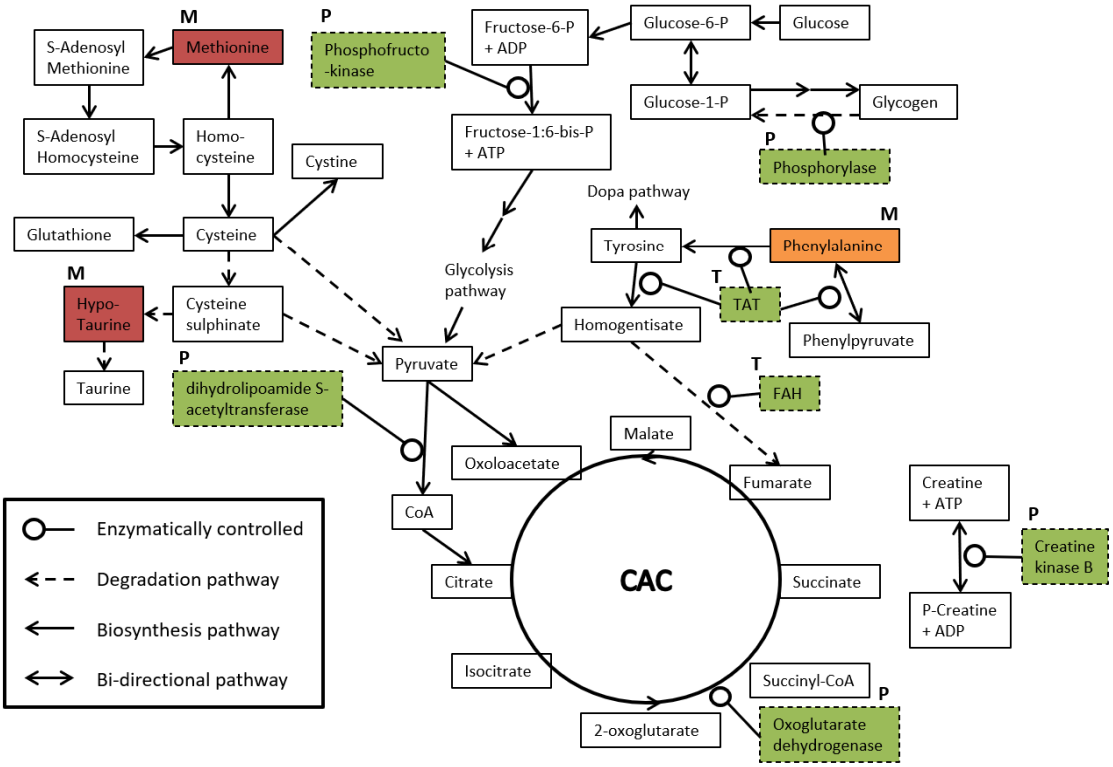

FIGURE 15 Simplified graphical representation of the impact of exposure to the binary mixture (32R + 50F) on energy and amino acid metabolism, as per the cardiac transcriptome (T), proteome (P), and metabolome (M), irrespective of exposure duration (I, II). Red-filled cells represent significant depletions; orange represents near-to-significant depletion, and green represents significant protein enrichment or gene upregulation. Highlighted enzymes are represented by dashed boxes, whereas components are represented by solid boxes. CAC = Citric Acid Cycle. Multiple consecutive arrows indicate multiple reactions that are not visualized. The figure is recreated from, and based upon, the interactive metabolic pathway map (https://www.biochemical-pathways.com), and the amino acid pathway map provided by https://www.wikipathways.org (pathway ID: WP3925).

These aforementioned findings highlight that exposure to the mixture induced catabolism of amino acid through multiple processes. Depletion of the amino acid methionine is likely related to the increased demand for cysteine (an amino acid) in glutathione (phase II) metabolism; depletion is facilitated through the SAM-e cycle (S-Adenosyl methionine), which in turn generates cysteine (Finkelstein and Martin 2000). Just like methionine, depletion of hypotaurine may also be linked to cysteine. Thus, depletion of hypotaurine is likely due to a reduced rate of formation, as utilization of cysteine is re-directed to glutathione metabolism (Fig. 15) (Stipanuk *et al.* 2006). Near-to-significant depletion of the amino acid phenylalanine could be linked to the upregulation of tyrosine aminotransferase (*tat*) (Dietrich 1992) and fumarylacetoacetate hydrolase (*fah*) (Bateman *et al.* 2001). The function of Tat and Fah is to facilitate the transformation of phenylalanine to tyrosine (by Tat) and tyrosine to fumarate

(by Fah), which in turn can be aerobically metabolized in the citric acid cycle or metabolized to coenzyme-A by dihydrolipoamide acetyltransferase (enriched by the mixture; Day 14). Furthermore, the proteomic data highlights the enrichment of 2-oxoglutarate dehydrogenase (by retene and the mixture; Day 14), which facilitates the citric acid cycle reaction of α-ketoglutarate + NAD^+ + Acetyl-CoA (CoA) → Succinyl CoA + CO^2 + NADH (Williamson 1979). Additionally, enrichment of creatine kinase B (-type; retene and mixture; Day 14) suggests increased activity of the ATP/ADP-dependent and reversible conversion of creatin ↔ phosphocreatine, which can produce a localized surge of ATP, when required (Oliver 1955).

Such an extensive impact of PAH exposure on multiple levels of molecular events related to energy metabolism has not previously been observed in developing fish larvae exposed to a simple binary PAH mixture, although the impact of exposure to individual PAHs upon transcriptome, proteome, and metabolome has previously been reported by Rigaud *et al.* (2020b). When considering the effects of PAH exposure on the whole organism in relation to the aforementioned alterations in energy metabolism, it is plausible that multiple processes are involved and are most likely compensatory with regards to the impaired consumption of yolk alongside impaired heart function and increased energy requirements by constant phase I and II metabolism in parallel to normal development and growth.

4.7 Future directions

As emphasized throughout this doctoral thesis, more questions arose than were answered. Due to the vast scope of biological systems and functions affected by exposure to the PAHs, alone or as a mixture, no one direction for future scientific inquiry on PAH toxicity in developing fish can be determined. Rather, this doctoral thesis highlights the importance of assessing multiple endpoints and the whole organism, in relation to exposure, rather than a limited set of outcomes. Such is especially true when considering a transcriptomic approach; although a powerful analytical tool, ensuing results are only indicative and do not necessarily represent any actual enrichments or depletion of proteins. However, the opposite is true for proteomics, which provide a molecular fingerprint of toxicity. Yet, depletions or enrichments of certain proteins and metabolites, present in low quantities or only transiently, are typically not identified and are therefore neglected.

Focusing on the specific endpoints, as presented within this thesis, highlights the nature of FICZ as the most pressing discovery for future inquiry, especially when considering its possible effect and influence on metabolism, toxicodynamics, and kinetics. Does exposure to other mixtures, petroleum products, and legacy deposits of PAHs result in accumulation of FICZ *in situ*? Are there differences in species and age tolerance to accumulation? To what extent does accumulation of FICZ actually contribute to (developmental)

toxicity? What molecular processes and reactions promote accumulation in the first place? Additionally, do other endogenous Ahr metabolites accumulate and contribute to toxicity?

Assessing the influence of PAH toxicity on multiple organs, not just the heart, through microarray and proteomic analytical approaches could unveil both organ-specific endpoints of toxicity but also shared mechanisms. Additionally, assessing multiple organs would allow for the assessment of feedback mechanisms between organs.

Although it is apparent that exposure to the mixture forced catabolism of amino acids, the analytical methodology was limited due to low number of replicates and, to a certain degree, by organ specificity. Dedicated whole-body amino acid quantification, in relation to exposure, could therefore contribute to, and improve upon, the combined omics approach, thereby filling in the blanks (Fig. 13).

Exposure to the PAHs, as per the cardiac proteome, highlighted multiple depletions of components essential to cellular structure and integrity. However, it cannot be established if these depletions arose as a consequence of fewer and / or smaller cells, or if their abundance was decreased irrespective of numbers and size. Immunohistochemistry alongside confocal microscopy of cardiomyocytes, extracted from exposed alevins, could contribute to our understanding of PAH-induced cardiotoxicity. Assessment of additional organs and tissues, alongside cardiomyocytes, could provide insights on plausible organ specificity.

In a natural setting, the body burden of PAHs diminishes with time after an acute exposure event, unless the individuals are exposed again. Therefore, it would have been interesting to assess the long-term impact of exposure: e.g., 2 weeks of exposure, followed by rearing in clean water for an additional 2 weeks. Would there be a difference in morphology, length, or weight? Would there be a lasting difference in the cardiac transcriptome, proteome, and metabolome? What about heart function; would the influence of PAH leave a significant mark, as per observed filament and tubulin depletions?

Finding that exposure resulted in the enrichment and depletion of pro- and anti-coagulants is a novel discovery of PAH toxicity. The mechanisms that promote these alterations are unknown but could be associated with cardiovascular damage. However, this hypothesis will remain speculative until confirmed and before any conclusion can be established.

Oxidative stress is an important factor to consider when assessing any type of toxicity. Although not assessed through direct means, as per this doctoral thesis, proxies in the transcriptome and proteome suggest increased levels of oxidative stress in heart tissue. No one mechanism, in relation to exposure, can be established. However, exposure-specific enrichment of enzymes evolved to counteract the presence of hydrogen peroxide, alongside upregulation of genes encoding for heatshock proteins, provides additional support to the notion that exposure to PAHs results in increased oxidative stress. The exact underlying mechanisms are unknown but should be investigated further.

The nature of electrophilic fluoranthene and nucleophilic retene could be an interesting prospect for further assessment of PAH toxicity. Assuming that exposure saturated the phase II metabolic capacity, it is possible that a certain proportion of electrophilic fluoranthene could start forming covalent adducts with sulfur-containing amino acids (nucleophilic targets) in proteins, which in turn can disrupt proper protein folding and function (Boelsterli 2007).

Over-representation of chondrocyte related GO-terms, following exposure to retene and the mixture (Day 3), although significant but of questionable relevance due to low gene count and organ specificity, could be an interesting prospect for further research, especially if such focused upon relevant organs and structures. It is well known that exposure to PAHs, oil, and TCDD affect the skeleton of developing fish larvae, causing skeletal and craniofacial deformities.

The nature of the exposure-specific over-representation of GABA and G-protein signaling by fluoranthene and retene, respectively, is somewhat of a mystery. What promotes these specificities, and is there an associated over-representation as per protein enrichment and depletions?

5 REMARKS

In total, approximately 8400 rainbow trout alevins were sacrificed for scientific purposes, in order to produce the scientific manuscripts covered within this doctoral thesis. No ethical approvals were required, as per the European Union Directive 2010/63/EU, Chapter 1, Article 1, point 3, which only covers: (a) "*live non-human vertebrate animals, including*:" (b) "*independently feeding larval forms*".

As briefly mentioned in the Materials and Methods (3.2 Setup, exposure, and sampling), the follow-up investigation (III) encompassed additional treatments not presented within this thesis. These additional exposures were 3.2 and 10 μg l^{-1} of retene and 5 and 500 μg l^{-1} of fluoranthene, alone or as any possible mixture (9 in total). Reported for the first time is the accumulation of endogenous FICZ. Exposure to any mixture containing 50 and 500 μg l^{-1} of fluoranthene, but not 5 μg l^{-1}, irrespective of contributing concentration of retene, resulted in the accumulation of endogenously derived FICZ. These trends were particularly prominent among alevins exposed to the mixtures containing 500 μg l^{-1} (Fig. 16), and especially among alevins exposed to the 32R + 500F mixture, which seems to saturate the metabolic capacity to such a degree that accumulation continues instead of peaking by Day 3. This data is, as of yet, unpublished.

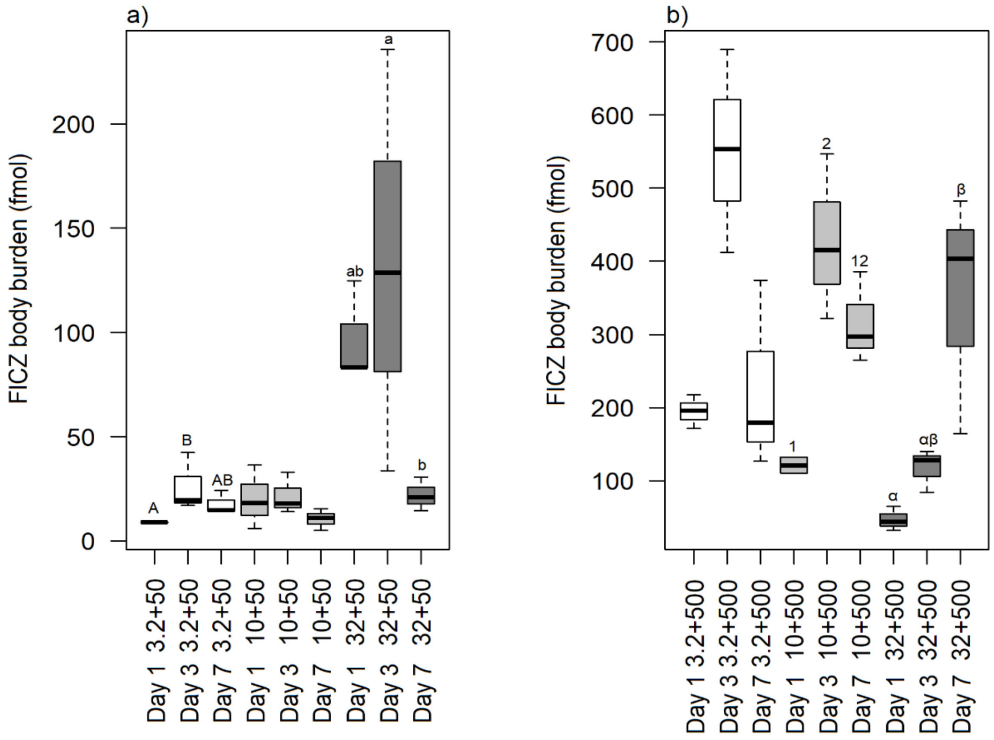

FIGURE 16 Boxplot visualization of the accumulation of FICZ in alevins exposed to mixtures containing (a) 50 and (b) 500 µg l^{-1} of fluoranthene. Significant differences are denoted with upper and lowercase Latin letters, numbers, and Greek letters (KW + Dunn's *post hoc* test). $n = 3$; $n = 2$ if a box is missing the bars.

6 CONCLUSIONS

The primary conclusion that can be drawn from the studies encompassed and presented within this doctoral thesis is that the toxicity of a PAH mixture cannot be predicted by the additive effects of the individual components, whether regarding the molecular level, organ function, or whole organism development. However, this does not mean that research on developmental toxicity in fish using individual PAHs is meaningless, as such research is important for the assessment of toxicological mechanisms. Instead, it highlights that health and environmental risk assessments on PAHs must be performed using what can be considered as realistic mixtures in order to maintain specificity and relevance, as a combination can affect endogenous processes.

By extension, it is clear that retene, fluoranthene, and the binary mixture of the two PAHs produce unique toxicity profiles, be that when considering the cardiac transcriptome, proteome, metabolome, body burden, or BSD and development. Exposure to the mixture resulted in synergized toxicity compared to the individual components, which is plausibly due to accumulation of endogenously derived FICZ alongside altered PAH body burden. The report of accumulated FICZ is a novel discovery that will impact how PAH mixture toxicity is perceived. However, and as stipulated in Chapter 4.7, how FICZ influences the toxicodynamics and kinetics is unknown and requires further scientific inquiry. Additionally, the body burden of the PAHs reflected well the exposure-specific activation of phase I and II metabolic processes.

Yet, there does not seem to be one single event that can explain the induction of PAH toxicity in developing rainbow trout alevins. Rather, the results presented within this doctoral thesis suggest that multiple and intertwined molecular processes were affected in parallel, that together resulted in the exposure-specific toxicity profiles.

It is unknown if the observed effects of PAH exposure and toxicity would result in recoverable or permanent developmental impairments. Yet, it is plausible to assume that some developmental impairment would persist with time, a notion supported by contemporary science (Heintz *et al.* 2000, Laurel *et*

al. 2019) but also acknowledged in the 19th century by Charles Darwin in his On the Origin of Species (2004 Ed.) as:

> *"Any change in the embryo or larva will almost certainly entail changes in the mature animal."*

Thus, the PAH-exposed alevins would likely suffer from long-term exposure-related issues, as per contemporary science, which include reduced survival, growth, and swimming ability, as well as altered pigmentation, potentially permanent cardiovascular defects, and behavioral changes, if reared in clean water following cessation of exposure.

In conclusion, the utilization and combination of transcriptomics, proteomics, and metabolomics, in relation to PAH-induced cardio and developmental toxicity, produced extensive perspectives on which molecular processes and apical responses were affected by exposure to retene and fluoranthene, alone or as a binary mixture. The results encompassed within this thesis report both previously known and novel mechanisms and outcomes of toxicity; knowledge that will be of importance so as to understand the nature of PAH toxicity in developing fish larvae. Yet, and as highlighted in Chapter 4.7, which covers future directions, more questions and considerations emerged than were answered by this doctoral thesis.

First and foremost, I would like to extend my thanks and appreciation to my supervisors: PhD and Academy Research Fellow Eeva-Riikka Vehniäinen and PhD Cyril Rigaud. You guys are fantastic supervisors, and I cannot explain how lucky I feel that I have had "sane" supervisors during my PhD years. I have heard so many horror stories from friends and colleagues. The time and effort you two spent helping me finish up the manuscripts (especially the transcriptomics manuscript, which was really tough to write) and giving feedback have really helped me develop as a doctoral student and researcher-in-training. Thank you!

I would also like to extend my appreciation and thanks to the members of my follow-up group: Associate Professor Lotta-Riina Sundberg, Professor Jussi Kukkonen, and PhD Päivi Meriläinen. I extend special thanks to Associate Professor Lotta-Riina Sundberg, who, besides partaking in the follow-up group, agreed to be my ceremonial supervisor following the termination of my contract with the Department in January 2021; and also to Jussi Kukkonen, who suggested that I should get involved in SETAC Europe.

Senior Lecturer Anssi Lensu for his thorough editing this doctoral thesis. Thank you so much for your effort.

PhD Emma Wincent at Karolinska Institutet. The times spent learning HPLC analysis from you and your co-workers were some of the most memorable of my PhD period, especially because I felt that we did something new despite a lot of trial and error before getting the process right. The days were long and intense, but I enjoyed them a lot.

PhD Hannu Pakkanen for helping out with and running the LC/MS-MS analysis, which allowed for the precise identification of endogenously formed and accumulated FICZ.

PhD Aleksei Krasnov for supervising and teaching me and PhD Cyril Rigaud how to prepare the microarrays at NOFIMA in Ås (Norway).

The laboratory technicians Emma Pajunen and Mervi Koistinen for always being friendly, cheerful, and helping out with experiments, sampling, material analysis, as well as coordinating different get-togethers at the section. It was always nice to see the two of you at work. No matter how much you had on your plates, you were always happy to talk, help out, or give instructions and directions.

The remaining co-authors that I never met in person, but without whom this doctoral thesis would not have become what it is today: PhD Jenna Lihavainen, PhD Anne Rokka, and PhD Morten Skaugen. Thank you for your expertise and input with regards to metabolomics and proteomics.

PhD Christopher Bishop for proofreading the English and checking the formatting of my doctoral thesis. Your help and input made sure that I could defend my thesis months earlier than what would otherwise be possible. Thank you also for the many great memories from our time at Uppsala University.

Professor Jérôme Cachot, at Université de Bordeaux, and Professor Lynn Weber, at the University of Saskatchewan, for taking on the role of external peer reviewers and assessors of this doctoral thesis. I hope that the two of you found the content of this thesis interesting.

Every bachelor and master student that I have had the pleasure to teach and supervise throughout the years.

To my fellow PhD students at the department: Thank you for interesting conversations throughout the years. Although I never really got to know many of you at a deeper level. However, I appreciated the pleasantries exchanged in the lunchroom, pubs, cantina, laboratories, and during the Sauna and Support meetings.

To my fellow members of the SETAC Student Advisory Council: Thanks for some of the most developing experiences of my time as a PhD student. Learning how to work and function in a cross-European and global organization, as well as organizing conferences and getting to know you all, has been an experience I would never trade away. You guys have given my time as a PhD student something extra that I could have otherwise easily missed out on. It has been tough but so worthwhile.

Many thanks and my eternal gratitude are extended to Erityis-koulutettujen työttömyys-kassa (ERKO) for financially supporting me after my contract with the University of Jyväskylä ended in mid-January of 2021. Without your financial allowances, I would not have been able to focus solely on my studies, manuscripts, and this thesis. Rather, it is very likely that I would have had to drop out due to financial reasons if it was not for the monthly allowances provided.

I would also like to extend several thanks to friends from outside of the academy. First and foremost is Freddie Johansson for helping me relocate from Uppsala to Jyväskylä back in early January of 2017, plus providing a place to stay while visiting Stockholm. Second are Gunnel and Roger Olausson for letting me stay at their place for a month while learning and performing HPLC analysis at Karolinska Institutet, Sweden.

Many thanks are extended to friends in Jyväskylä who is not affiliated to the academy, as well as my friends back in Uppsala, Sweden. You know who you all are.

Extra special thanks to my parents, Urban and Chatarina Eriksson, for supporting me since the early days and during every step along the long road that led to this dissertation.

Finally, thanks to my fiancée, Sonja Alasalmi, for supporting me in many ways throughout our years together.

YHTEENVETO (RÉSUMÉ IN FINNISH)

Sydäntoksisuus polyaromaattisille hiilivedyille altistuneissa kirjolohen (*Oncorhynchus mykiss*) poikasissa – moniomiikkatutkimus

Polyaromaattiset hiilivedyt (PAH-yhdisteet) ovat yhdisteitä, jotka koostuvat kahdesta tai useammasta aromaattisesta renkaasta. Näitä kemikaaleja syntyy erityisesti orgaanisen aineksen epätäydellisessä palamisessa, mutta niitä on myös öljyssä, muodostaen 15–60 % kokonaishiilestä. Ympäristön kannalta PAH-yhdisteet ovat ongelmallisia, koska öljypäästöt ja lyhyen ja pitkän matkan laskeuma (joka on peräisin lämmityksestä, liikenteestä ja teollisuudesta) voi aiheuttaa maaperän, veden ja sedimentin saastumisen. Erityisen huolestuttavaa on PAH-yhdisteiden kertyminen maaperään, sedimenttiin ja muihin anaerobisiin ympäristöihin, koska mikrobit tarvitsevat happea pystyäkseen hajottamaan PAH-yhdisteitä. Sen seurauksena saastuneen maaperän tai sedimentin liikuttelu voi saada aikaan PAH-yhdisteiden irtoamisen ja päätymisen ravintoketjuun, josta voi seurata toksisuutta. Erityisen herkkiä ovat maaperässä ja sedimentissä elävät eliöt, mutta myös kalanpoikaset. Tiedetään, että PAH-yhdisteille altistuneille kalanpoikasille kehittyy monenlaisia oireita, kuten nesteen kertymistä sydän- ja ruskuaispussiin, kallon epämuodostumia, selkärangan vääntymistä ja ihonalaisia verenpurkaumia (nämä oireet muodostavat ruskuaispussitaudin). Sen lisäksi PAH-yhdisteet aiheuttavat muutoksia käyttäytymisessä ja morfologiassa sekä sydäntoksisuutta ja kuolleisuutta. Kalanpoikasissa erityisesti sydämen rakenne, kehitys ja toiminta ovat herkkiä PAH-yhdisteille. Tämä on havaittu sekä laboratorio-olosuhteissa että suurten öljyonnettomuuksien jälkeen luonnossa.

Ei ole kuitenkaan selvää, miten PAH-yhdisteet aiheuttavat sydäntoksisuutta. Tiedetään, että aktiopotentiaalia kuljettavat ja ylläpitävät sydämen ionikanavat ovat alttiita altistukselle, ja seurauksena saattaa olla aktiopotentiaalin muutoksia, jotka voivat vaikuttaa sydämen syketiheyteen ja aiheuttaa bradykardiaa eli sydämen harvalyöntisyyttä. Niin kuin edellä kerrottiin, PAH-yhdisteet vaikuttavat myös sydämen rakenteeseen ja kehittymiseen, ei pelkästään toimintaan. Altistuksen myötä sydän muuttuu muodoltaan pidemmäksi ja ohuemmaksi, ja sykkii heikommin ja epätasaisemmin. Heikompi sydän johtaa verenkierron vähenemiseen, joka vaikuttaa kaasujen vaihtoon ja ravinteiden, hormonien, valkosolujen ja muiden molekyylien sekä veressä olevien solujen kulkeutumisen vähenemiseen. Näiden PAH-yhdisteiden aiheuttamien sydänvaikutusten taustalla olevat mekanismit tunnetaan joiltain osin hyvin. Toksisuutta ei kuitenkaan pystytä selittämään tarkasti; pikemminkin on luultavaa, että altistuksen vaikutukset kohdistuvat yhtä aikaa moniin prosesseihin. Eniten tutkittu molekulaarinen mekanismi PAH-yhdisteiden osalta on tietyn solunsisäisen reseptorin (aryylihiiliveryreseptori 2, Ahr2) aktivoituminen. Ahr2 säätelee sekä normaalia kehitystä ja kasvua että sytokromi P450a1 -entsyymin (Cyp1a, vierasainemetabolian I-vaiheen metabolia hydroksylaation kautta) välityksellä useiden sisäsyntyisten yhdisteiden ja vierasaineiden metaboliaa. Mielenkiintoista kyllä, jotkin PAH-yhdisteet

aktivoivat Ahr2:a ja inhiboivat Cyp1a:ta. Lisäksi on oletettu, että tiettyjen sisäsyntyisten metaboliittien, kuten FICZ:n (6-formyyli-indolo(3,2-b)karbatsoli), kertyminen voi olla osallisena Ahr2:n aktivoitumisessa ja toksisuudessa.

PAH-yhdisteiden aiheuttaman sydäntoksisuuden tuntemattomien (ja tunnettujen) mekanismien selvittämiseksi altistimme kirjolohen (*Oncorhynchus mykiss*) poikasia kahdelle PAH-yhdisteelle, joilla on eri toksisuusmekanismi (reteeni: Ahr2-aktivaattori; fluoranteeni: Ahr2-aktivaattori ja Cyp1a-inhibiittori) joko yksittäin tai seoksena. Altistukset kestivät 1, 3, 7 ja 14 päivää. Altistuksen lopussa poikaset valokuvattiin (myöhempiä *in silico* -mittauksia varten) ja sydämet kerättiin transkriptomiikkaa, proteomiikkaa ja metabolomiikkaa varten. Tämä mahdollistaa sen, että samalla kertaa voidaan analysoida tuhansia geenejä, proteiineja ja metaboliitteja ja sen jälkeen bioinformatiikan avulla voidaan määrittää, kuinka altistus vaikutti erilaisiin solunsisäisiin verkostoihin. Jäljelle jääneistä poikasen osista määritettiin PAH-yhdisteiden pitoisuudet. Myöhemmässä tutkimuksessa mitattiin altistuksen vaikutusta sydämen syketiheyteen ja sykkeen tasaisuuteen, poikasen kehitykseen ja kasvuun sekä FICZ:n määrään poikasessa.

Tulosten yhteenvedosta nähtiin, että jokaisella altistuksella oli oma toksisuusprofiilinsa. Oli myös selvää, että seokselle altistuminen aiheutti suurempaa toksisuutta kuin yksittäisille yhdisteille altistuminen yhteensä. Neljäntoista vuorokauden altistuksen jälkeen seokselle ja reteenille altistuneet poikaset olivat lyhyempiä ja ne olivat kuluttaneet eri määrän ruskuaista, ja seos aiheutti enemmän ruskuaispussitaudin oireita. Pigmentaatioon perustuen PAH-yhdisteille altistuneet poikaset näyttivät olevan varhaisemmassa kehitysvaiheessa kuin kontrollipoikaset. Altistus vaikutti sydämen toimintaan niin, että kolmen vuorokauden altistuksen jälkeen kaikki PAH-yhdisteet saivat aikaan bradykardian. Näitä vaikutuksia ei näkynyt yksittäisille PAH-yhdisteille altistuneissa poikasissa enää seitsemän vuorokauden altistuksen jälkeen. Sen sijaan seosaltistuksessa vastaavaa sydämen toiminnan palautumista ei havaittu. PAH-yhdisteiden kertyminen sai aikaan altistukselle ominaiset profiilit, joissa fluoranteenin määrä nousi koko ajan, kun taas reteenin määrä väheni ajan myötä. Sen sijaan seosaltistus sai aikaan fluoranteenin kertymisen vähenemisen, kun taas reteenin kertymisen käyrä pysyi samankaltaisena.

Sydämen transkriptomista havaittiin, että kaikki PAH-altistukset mukaanluettuna 1896 geenin transkriptiossa oli tilastollinen ero kontrolliin verrattuna. Bioinformatiikan avulla havaittiin, että altistus vaikutti useisiin molekulaarisiin verkostoihin. Fluoranteeni vaikutti vain muutamiin verkostoihin ja niistä suuri osa liittyi GABA-signalointiin, kun taas reteeni vaikutti G-proteiinivälitteiseen signaalinvälitykseen. Seoksella taas oli vaikutusta kasvuun, oksidatiiviseen stressiin ja vierasainemetabolian I- ja II-vaiheen verkostoihin. Mielenkiintoista kyllä, yksittäiset PAH-yhdisteet vaikuttivat useisiin geeneihin, jotka koodaavat ionikanavien proteiineja, mutta eivät silti saaneet aikaan bradykardiaa. Seos taas vaikutti päinvastoin. Tämä saattaa tarkoittaa, että nämä geenit toimivat kompensatorisesti. Vahvin yhteys löydettiin altistuksen, PAH-yhdisteen kertymisen ja vierasainemetabolian (I- ja II-vaiheen) väliltä. Fluoranteeni sai

aikaan *cyp1a*:n ja glutationimetaboliaan liittyvien geenien ekspression. Nämä prosessit eivät näyttäneet olevan riittävän tehokkaita metaboliaan ja erityksseen, koska fluoranteenin määrä poikasessa nousi koko ajan, mikä viittaa siihen, että fluoranteenia kertyi nopeammin kuin sitä pystyttiin poistamaan. Myös reteeni indusoi *cyp1a*:ta, mutta muita II-vaiheen entsyymejä kuin fluoranteeni, joka sai aikaan tehokkaamman metabolian. Seos puolestaan indusoi suurta määrää geenejä, jotka koodaavat I- ja II-vaiheeseen liittyviä enstyymejä, ja se sai aikaan PAH-yhdisteiden tehokkaan metabolian.

Sydämen proteomissa muutoksia havaittiin vähemmän kuin transkriptomissa: 65 proteiinia 7 päivän altistuksen jälkeen ja 82 proteiinia 14 päivän jälkeen. Proteomiikkatulokset ovat kuitenkin luotettavampia kuin transkriptomiikkatulokset, sillä geenieksprression muutokset eivät välttämättä aiheuta vastaavaa proteiinimäärän muutosta. Yksittäiset PAH-yhdisteet vaikuttivat vain harvoihin verkostoihin, kun taas seosaltistus näytti aiheuttavan vaikutuksia sydämen rakenteeseen (solufilamenttien ja lihasproteiinien väheneminen), vähentynyttä solujakautumista ja veren hyytymiskapasiteettia, muutoksia rautametaboliassa ja vahvempaa I- ja II-vaiheen metaboliaa. Transkriptomiin ja proteomiin verrattuna metabolomissa havaittiin vain viisi merkitsevästi muuttunutta metaboliittia (57 tunnistetusta metaboliitista). Kun transkriptomiikka- ja proteomiikkatulokset yhdistettiin, tuli selväksi, että seos sai aikaan energiametaboliaan liittyviä kompensatorisia mekanismeja. Näitä muutoksia näyttäisivät olevan aminohappojen katabolian kiihtyminen, kysteiinin tarpeen lisääntyminen (luultavasti glutationimetaboliaa varten) ja kreatiinin muuttuminen fosfokreatiiniksi, joka voi paikallisesti lisätä tarjolla olevan ATP:n määrää.

Lisäksi havaittiin, että altistus seokselle, muttei yksittäisille yhdisteille, sai aikaan endogeenisen FICZ:n määrän kasvun jo yhden päivän altistuksen jälkeen ja koko altistusajan. On luultavaa, että seokselle altistetuissa poikasissa havaittu suurempi toksisuus johtuu jossain määrin tästä kertymisestä. Transkriptomi- ja proteomiprofiilien mukaan FICZ:n määrän kasvu saattaa johtua oksidatiivisesta stressistä sekä substraattikilpailusta vierasainemetabolian I- ja II-vaiheen entsyymeistä.

Seos aiheutti selvästi voimakkaampaa toksisuutta kuin yksittäiset PAH-yhdisteet jokaisella biologisella organisaatiotasolla: geeni- ja proteiinieksprssiossa, sydämen toiminnassa (ja luultavasti myös rakenteessa), PAH-yhdisteiden, FICZ:n ja metaboliittien kertymisessä, kasvussa, kehityksessä ja energiankulutuksessa. Ympäristönsuojelun ja terveyden kannalta PAH-yhdisteiden riskinarviointia ei voi eikä pitäisi tehdä yksittäisten PAH-yhdisteiden toksisuuden perusteella vaan seoksiin pohjautuen (keinotekoisiin tai luonnossa esiintyviin). On silti tärkeää tutkia myös yksittäisiä PAH-yhdisteitä, jotta ymmärrettäisiin, miten ja miksi seokset saavat aikaan altistusspesifisen toksisuusprofiilin. On epäselvää, mitä kasvulle ja kehitykselle tapahtuu 14 vuorokauden altistuksen jälkeen. Kuitenkin jo Charles Darwin kirjoitti kirjassaan On the Origin of Species:

"Mikä tahansa muutos alkiossa tai toukkavaiheessa saa varmasti aikaan muutoksia täysikasvuisessa eläimessä. "

Sen vuoksi on luultavaa, että altistuksen aikaansaamat negatiiviset vaikutukset ovat pysyviä, kuten viimeaikainen PAH-toksisuustutkimus osoittaa.

SAMMANFATTNING (RÉSUMÉ IN SWEDISH)

Att förstå PAH toxicitet i regnbågslaxyngel (*Oncorhynchus mykiss*) med hjälp av olika omik-plattformar

Polycykliska aromatiska kolväten (PAH) är ett samlingsbegrepp för en viss typ av organiska ämnen bestående av två eller flera sammansatta aromatiska ringar. Dessa kemikalier uppkommer primärt till följd av ofullständig förbränning av organiskt material och industriella processer, men är även en komponent i petroleumolja där PAH bidrar med 15–60 % av kolmassan. Detta sagt, PAH:er är problematiska ur ett miljöperspektiv då spill av olja samt lång- och kortväga deponering via avgaser, rök och sot från uppvärmning, transporter och industri kan leda till kontaminering av mark, vatten och sediment. Speciellt bekymrande är ansamling av PAH:er i mark, sediment och annan anaerob miljö eftersom syre krävs för mikrobiell mineralisering och nedbrytning av PAH:er. Därmed kan användning och omsättning av förorenad mark och sediment leda till att PAH:er återinförs i näringskedjan och ökad bioackumulering. Särskilt sårbara är mark- och sedimentlevande organismer men även fiskyngel. Det är välkänt att PAH-exponerade fiskyngel utvecklar allvarliga symptom till följd av exponering; till exempel hjärt- och gulesäcködem, deformering av kranium, missbildad ryggrad och subkutana blödningar (dessa hittills nämnda symptom ingår i begreppet blue sac disease; BSD). Utöver dessa har även beteendeändringar, ändrad morfologi, kardiotoxicitet samt minskad överlevnad påvisats till följd av exponering. Hjärtat är ett kritiskt målorgan för PAH toxicitet, och effekter på hjärtats utveckling och funktion i fiskyngel har påvisats både i laboratoriemiljö och i naturen (till följd av massiva oljespill).

Det är dock inte helt fastställt mekanismerna bakom hur PAH orsakar kardiotoxicitet. Vad som är känt är att de olika jonkanalerna i hjärtceller, vilka propagerar och återställer aktionspotentialen och därmed upprätthåller hjärtfrekvens, kan påverkas av PAH-exponering vilket kan resultera i en ändrad slagfrekvens och orsaka bradykardi (långsammare frekvens) och arytmi. Som nämnts i ovanstående paragraf så påverkar även PAH:er hjärtats struktur och utveckling, och inte enbart funktionen. Detta manifesteras främst i att hjärtat blir långsmalt och tunnare. Som konsekvens av ett svagare hjärta följer minskat blodflöde vilket i sin tur påverkar gasutbytet, cirkulation av näringsämnen, hormoner, immunceller och andra molekyler och celler i blodet. De underliggande mekanismerna bakom dessa PAH-inducerade effekter på hjärtat är till viss del väl undersökta, men ännu finns ingen enskild mekanism som kan förklara toxiciteten i detalj, snarare lutar det åt att flera olika processer påverkas parallellt till följd av exponering. Den molekylära mekanism som studerats mest är aktivering en specifik cellulär receptor, aryl hydrokol receptor 2 (Ahr2), som i sin tur kontrollerar både normal utveckling och tillväxt (av bland annat hjärtat) men även metabolism av olika endo- och xenogena ämnen via induktion av enzymet cytokrom P450a1 (Cyp1a; fas I metabolism via hydroxylering). Samtidigt som PAH:er har visat sig aktivera Ahr2 i olika grad, och därmed öka

Cyp1a uttrycket, så kan även många PAH:er hämma funktionen av Cyp1a enzymet. Därutöver tillkommer endogena metaboliter som kan aktivera Ahr2-signalering vid ackumulation, till exempel FICZ (6-formylindolo(3,2-b)karbazol).

För att identifiera hittills okända (och kända) mekanismer av PAH-inducerad kardiotoxicitet så exponerades regnbågslaxyngel för två PAH:er med förväntat olika mekanismer (reten och fluoranten; båda aktiverar Ahr2 men fluoranten kan även hämma Cyp1a funktion), antingen enskilt eller som en binär blandning. Exponering pågick i 1, 3, 7 och 14 dagar. Efter exponering så fotograferades yngel (för senare dataanalys) och hjärtat dissekerades ut för så kallad transkriptomik-, proteomik- och metabolomikanalys. Med dessa typer av omik-analyser kan tusentals gener, proteiner och metaboliter analyseras i ett svep, för att sedan, med hjälp av bioinformatik identifiera hur olika molekylära nätverk påverkats av exponering. Kvarvarande vävnad sparades för att analysera hur mycket av PAH:erna som ackumulerats i ynglen över tid och i relation till behandling. I en senare studie så mättes effekter på hjärtfrekvens, tillväxt och utveckling, samt att vävnader analyserades för en specifik och hittills opåvisad endogen substans som också aktiverar Ahr2, och därmed potentiellt bidrar till observerad toxicitet, FICZ.

När resultaten av exponeringarna sammanställdes så framträdde exponerings-specifika toxicitetprofiler (jämfört med kontroll). Tydligt är att blandningen av retene och fluoranten orsakade kraftigare toxicitet än den adderade effekten av PAH:erna separat. Efter 14 dagar var yngel som exponerats för retene samt den binära blandningen signifikant kortare, hade förbrukat olika mängd gula. Det framgick även tydligt att blandningen orsakade allvarligare symptom av BSD. Baserat på pigmenteringsmönster så tycks även PAH-exponerade yngel vara i ett tidigare utvecklingsstadium än kontrollgruppen, dvs att deras utveckling försenats. Gällande hjärtats funktion, så bidrog exponering gentemot alla PAH:er, i 3 dagar, till signifikant bradykardi. Dessa signifikanta effekter observerades inte bland yngel efter 7 dagars exponering gentemot reten och fluoranten, men däremot bland blandningsexponerade yngel. Ackumulering av PAH:er skedde också exponeringsspecifikt där fluoranten ökade konstant medan reten minskade över tid. Exponering för blandningen av retene och fluoranten bidrog däremot till att ackumuleringen av fluoranten minskade över tid medan reten följde samma mönster som vid exponering mot reten enskilt, men visade signifikant högre nivåer.

Med avseende på hur exponering påverkade hjärtats transkriptom fann vi att 1896 gener, oavsett PAH-exponering, påvisade ett uttryck signifikant skilt från kontrollgruppen. Med hjälp av bioinformatik kunde ett stort antal molekylära nätverk påvisas påverkade. Exponering mot fluoranten påverkade få nätverk och dessa var till stor del involverade i GABA-signalering medan reten påverkade G-proteinkopplad signalering. Blandningen däremot påverkade nätverk relaterade till tillväxt, oxidativ stress, samt fas I och II metabolism. Intressant nog så påverkade de enskilda PAH:erna uttrycken av flera gener som kodar för komponenter i jonkannaler utan att resultera bradykardi. Exponering gentemot blandningen däremot orsakade bradykardi men påverkade inga av dessa gener. Detta tyder på att de ändrade genuttrycken är kompensatoriska och kan därmed

motverka ändrad slagfrekvens bland yngel exponerad gentemot the enskilda PAH:erna. Det starkaste orsakssambandet som observerades till följd av exponering var det mellan typ av exponering, grad och tids-profil av ackumulering, och aktivering av processer som är involverade i omsättning av xenobiotika (fas I och II metabolism). Fluoranten aktiverade generna för *cyp1a*- och enzym involverade i glutation metabolism. Dessa processer var tydligen inte kraftiga nog för att medföra effektiv metabolism och exkretion då fluoranthene ackumulerade med tid; blockering av Cyp1a är troligen en starkt bidragen faktor. Retene aktiverade också *cyp1a* men andra fas II enzymer vilket tillät effektivare metabolism över tid. Blandningen däremot aktiverade ett stort antal gener som kodar för enzym involverade i fas I och II metabolism, vilket tillät effektiv metabolism av PAH:erna, speciellt fluoranten.

Analys av hjärtproteomiken gav långt färre utslag än vad transkriptomiken gjorde: 65 och 82 proteiner efter 7, respektive 14 dagar. Däremot är proteomikresultaten mer konkreta jämfört med transkriptomiken, eftersom ett ändrat genuttryck inte nödvändigtvis motsvarar en ändring på proteinnivå. Klart är att de enskilda PAH:erna påverkade få nätverk medan exponering för blandningen tyder på ändrad hjärtstruktur (mindre mängd av olika cellulära filament och muskelkomponenter), begränsad celldelning, minskad koaguleringsförmåga, ändrad järnmetabolism samt starkare fas I och II metabolism. De enskilda PAH:erna påverkade dock endast ett fåtal enskilda (ovanstående) proteiner men, som sagt, inte nätverken. I motsats till transkriptomet och proteomet så påvisade metabolomet enbart 5 signifikant signifikanta utslag (utav 57 identifierade metaboliter). När resultaten från dessa omik-metoder kombineras så är det tydligt att exponering för blandningen påverkar tillgången av energimetabolismen. Dessa begränsningar tyder både på ökad katabolism av aminosyror, ökat behov av aminosyran cystein (troligen för glutation-metabolism) samt omvandling av kreatin till fosfatkreatin vilket bidrar med en lokal ökning tillgång på energi (ATP).

Utöver dessa resultat påvisades ackumulering av endogent FICZ, över tid, efter exponering gentemot blandningen, men inte de enskilda komponenterna, redan efter 1 dag av exponering och fram till dag 7 då exponeringen avslutades. Det är möjligt att den starkare toxiciteten till följd bladningsexponerade yngel är, till viss del, orsakad av just denna ackumulering. Mer forskning behövs dock för att kunna bekräfta detta. Ackumulering av FICZ är troligen en konsekvens av ökad oxidativ stress, påvisat av både transkriptomik och proteomik, och i kombination med hämmad metabolism.

Det är tydligt att blandningen av reten och fluoranten resulterade i en samverkande och starkare respons jämfört med de enskilda PAH:erna, och det på alla undersökta nivåer av biologisk organisation: från gen- och proteinuttryck, hjärtfunktion (och troligen även struktur), ackumulering av PAH:er, FICZ och metaboliter, till tillväxt, utveckling och energikonsumtion. Från ett miljö- och hälsoskyddsperspektiv bör därför inte riskbedömning utgå från enskilda PAH:er utan hellre se till blandningar (artificiella eller naturligt förekommande). Detta sagt så är det fortfarande nödvändigt att undersöka enskilda PAH:er för att förstå hur och varför blandningar resulterar i de toxicitetprofiler som observeras. Det är

dock oklart hur fortsatt exponerad eller oexponerad tillväxt och utveckling skulle kunna påverka fiskynglen efter 14 dagar. Charles Darwin påpekade redan i sin bok, Om Arternas Uppkomst (fritt översatt) att:

> "*Varje förändring i ett embryo eller yngel kommer med säkerhet att medföra förändringar hos det mogna djuret.*"

Med detta sagt så är det är troligt att de negativa effekterna av exponering kvarstår över en lång tid, vilket även påvisats av nutida forskning på PAH toxicitet.

REFERENCES

Abnet C.C., Tanguay R.L., Hahn M.E., Heideman W. & Peterson R.E. 1999. Two forms of aryl hydrocarbon receptor type 2 in rainbow trout (*Oncorhynchus mykiss*). Evidence for differential expression and enhancer specificity. *The Journal of biological chemistry* 274: 15159–15166.

Adams J.E., Madison B.N., Charbonneau K., Sereneo M., Baillon L., Langlois V.S., Brown R.S. & Hodson P.V. 2020. Effects on Trout Alevins of Chronic Exposures to Chemically Dispersed Access Western Blend and Cold Lake Blend Diluted Bitumens. *Environmental Toxicology and Chemistry* 39: 1620–1633.

Adeniji A.O., Okoh O.O. & Okoh A.I. 2019. Levels of Polycyclic Aromatic Hydrocarbons in the Water and Sediment of Buffalo River Estuary, South Africa and Their Health Risk Assessment. *Archives of Environmental Contamination and Toxicology* 76: 657–669.

Ainerua M.O., Tinwell J., Kompella S.N., Sørhus E., White K.N., Dongen B.E. van & Shiels H.A. 2020. Understanding the cardiac toxicity of the anthropogenic pollutant phenanthrene on the freshwater indicator species, the brown trout (*Salmo trutta*): From whole heart to cardiomyocytes. *Chemosphere* 239: 124608.

Allmon E., Serafin J., Chen S., Rodgers M.L., Griffitt R., Bosker T., Guise S. de & Sepúlveda M.S. 2021. Effects of polycyclic aromatic hydrocarbons and abiotic stressors on Fundulus grandis cardiac transcriptomics. *Science of The Total Environment* 752: 142156.

Almazroo O.A., Miah M.K. & Venkataramanan R. 2017. Drug Metabolism in the Liver. *Drug Hepatotoxicity* 21: 1–20.

Almeda R., Wambaugh Z., Wang Z., Hyatt C., Liu Z. & Buskey E.J. 2013. Interactions between Zooplankton and Crude Oil: Toxic Effects and Bioaccumulation of Polycyclic Aromatic Hydrocarbons. *PLOS ONE* 8: e67212.

Anderson J.L., Carten J.D. & Farber S.A. 2011. Chapter 5 - Zebrafish Lipid Metabolism: From Mediating Early Patterning to the Metabolism of Dietary Fat and Cholesterol Detrich H.W., Westerfield M. & Zon L.I. (eds.). *The Zebrafish: Cellular and Developmental Biology, Part B* 101: 111–141.

Andersson J.T. & Achten C. 2015. Time to Say Goodbye to the 16 EPA PAHs? Toward an Up-to-Date Use of PACs for Environmental Purposes. *Polycyclic Aromatic Compounds* 35: 330–354.

Andreasen E.A., Hahn M.E., Heideman W., Peterson R.E. & Tanguay R.L. 2002. The zebrafish (*Danio rerio*) aryl hydrocarbon receptor type 1 is a novel vertebrate receptor. *Molecular Pharmacology* 62: 234–249.

Ashburner M., Ball C.A., Blake J.A., Botstein D., Butler H., Cherry J.M., Davis A.P., Dolinski K., Dwight S.S., Eppig J.T., Harris M.A., Hill D.P., Issel-Tarver L., Kasarskis A., Lewis S., Matese J.C., Richardson J.E., Ringwald M., Rubin G.M. & Sherlock G. 2000. Gene Ontology: tool for the unification of biology. *Nature genetics* 25: 25–29.

Bakke M.J., Nahrgang J. & Ingebrigtsen K. 2016. Comparative absorption and tissue distribution of 14C-benzo(a)pyrene and 14C-phenanthrene in the polar cod (*Boreogadus saida*) following oral administration. *Polar Biology* 39: 1165–1173.

Barron M.G., Heintz R. & Rice S.D. 2004. Relative potency of PAHs and heterocycles as aryl hydrocarbon receptor agonists in fish. *Marine environmental research* 58: 95–100.

Bateman R.L., Bhanumoorthy P., Witte J.F., McClard R.W., Grompe M. & Timm D.E. 2001. Mechanistic inferences from the crystal structure of fumarylacetoacetate hydrolase with a bound phosphorus-based inhibitor. *The Journal of biological chemistry* 276: 15284–15291.

Behera B.K., Das A., Sarkar D.J., Weerathunge P., Parida P.K., Das B.K., Thavamani P., Ramanathan R. & Bansal V. 2018. Polycyclic Aromatic Hydrocarbons (PAHs) in inland aquatic ecosystems: Perils and remedies through biosensors and bioremediation. *Environmental Pollution* 241: 212–233.

Benjamini Y. & Hochberg Y. 1995. Controlling the False Discovery Rate: A Practical and Powerful Approach to Multiple Testing. *Journal of the Royal Statistical Society. Series B (Methodological)* 57: 289–300.

Bentzen B.H. & Grunnet M. 2011. Central and Peripheral GABA(A) Receptor Regulation of the Heart Rate Depends on the Conscious State of the Animal. *Advances in pharmacological sciences* 2011: 578273–578273.

Billiard S.M., Querbach K. & Hodson P.V. 1999. Toxicity of retene to early life stages of two freshwater fish species. *Environmental Toxicology and Chemistry* 18: 2070–2077.

Billiard S.M., Timme-Laragy A., Wassenberg D.M., Cockman C. & Di Giulio R.T. 2006. The Role of the Aryl Hydrocarbon Receptor Pathway in Mediating Synergistic Developmental Toxicity of Polycyclic Aromatic Hydrocarbons to Zebrafish. *Toxicological Sciences* 92: 526–536.

Binjie L. & Xinyu L. 1994. Characteristics of aromatic hydrocarbons in crude oils. *Chinese Journal of Geochemistry* 13: 97–106.

Boelsterli U. 2007. *Mechanistic Toxicology: The Molecular Basis of How Chemicals Disrupt Biological Targets*. Informa Healthcare, USA, Inc., New York, USA.

Bohne-Kjersem A., Skadsheim A., Goksøyr A. & Grøsvik B.E. 2009. Candidate biomarker discovery in plasma of juvenile cod (*Gadus morhua*) exposed to crude North Sea oil, alkyl phenols and polycyclic aromatic hydrocarbons (PAHs). *Marine environmental research* 68: 268–277.

Boyle E.I., Weng S., Gollub J., Jin H., Botstein D., Cherry J.M. & Sherlock G. 2004. GO::TermFinder--open source software for accessing Gene Ontology information and finding significantly enriched Gene Ontology terms associated with a list of genes. *Bioinformatics* 20: 3710–3715.

Bozinovic G., Shea D., Feng Z., Hinton D., Sit T. & Oleksiak M.F. 2021. PAH-pollution effects on sensitive and resistant embryos: Integrating structure and function with gene expression. *PLOS ONE* 16: e0249432.

Brette F., Shiels H.A., Galli G.L.J., Cros C., Incardona J.P., Scholz N.L. & Block B.A. 2017. A Novel Cardiotoxic Mechanism for a Pervasive Global Pollutant. *Scientific Reports* 7: 41476.

Brown D.R., Bailey J.M., Oliveri A.N., Levin E.D. & Di Giulio R.T. 2016a. Developmental exposure to a complex PAH mixture causes persistent behavioral effects in naive *Fundulus heteroclitus* (killifish) but not in a population of PAH-adapted killifish. *Neurotoxicology and teratology* 53: 55–63.

Brown D.R., Clark B.W., Garner L. & Di Giulio R.T. 2016b. Embryonic cardiotoxicity of weak aryl hydrocarbon receptor agonists and CYP1A inhibitor fluoranthene in the Atlantic killifish (*Fundulus heteroclitus*). *Comparative Biochemistry and Physiology Part C: Toxicology & Pharmacology* 188: 45–51.

Calfee R.D., Little E.E., Cleveland L. & Barron M.G. 1999. Photoenhanced toxicity of a weathered oil on *Ceriodaphnia dubia* reproduction. *Environmental Science and Pollution Research* 6: 207–212.

Carls M.G., Rice S.D. & Hose J.E. 1999. Sensitivity of fish embryos to weathered crude oil: Part I. Low-level exposure during incubation causes malformations, genetic damage, and mortality in larval pacific herring (*Clupea pallasi*). *Environmental Toxicology and Chemistry* 18: 481–493.

Cerniglia C.E. 1993. Biodegradation of polycyclic aromatic hydrocarbons. *Current opinion in biotechnology* 4: 331–338.

Chae S.-S., Paik J.-H., Allende M.L., Proia R.L. & Hla T. 2004. Regulation of limb development by the sphingosine 1-phosphate receptor S1p1/EDG-1 occurs via the hypoxia/VEGF axis. *Developmental biology* 268: 441–447.

Chiquet M., Birk D.E., Bönnemann C.G. & Koch M. 2014. Collagen XII: Protecting bone and muscle integrity by organizing collagen fibrils. *The international journal of biochemistry & cell biology* 53: 51–54.

Chong J., Wishart D.S. & Xia J. 2019. Using MetaboAnalyst 4.0 for Comprehensive and Integrative Metabolomics Data Analysis. *Current Protocols in Bioinformatics* 68: e86.

Christou M., Kavaliauskis A., Ropstad E. & Fraser T.W.K. 2020. DMSO effects larval zebrafish (*Danio rerio*) behavior, with additive and interaction effects when combined with positive controls. *Science of The Total Environment* 709: 134490.

Clark B., Cooper E., Stapleton H. & Di Giulio R. 2013. Compound- and mixture-specific differences in resistance to polycyclic aromatic hydrocarbons and PCB-126 among *Fundulus heteroclitus* subpopulations throughout the Elizabeth River estuary (Virginia, USA). *Environmental science & technology* 47.

Colavecchia M., Hodson P. & Parrott J. 2006. CYP1A Induction and Blue Sac Disease in Early Life Stages of White Suckers (*Catostomus commersoni*) Exposed to Oil Sands. *Journal of toxicology and environmental health. Part A* 69: 967–994.

Collier T.K., Anulacion B.F., Arkoosh M.R., Dietrich J.P., Incardona J.P., Johnson L.L., Ylitalo G.M. & Myers M.S. 2013. 4 - Effects on Fish of Polycyclic Aromatic Hydrocarbons (PAHs) and Naphthenic Acid Exposures. Tierney K.B., Farrell A.P. & Brauner C.J. (eds.). *Organic Chemical Toxicology of Fishes* 33: 195–255.

Cook P.M., Robbins J.A., Endicott D.D., Lodge K.B., Guiney P.D., Walker M.K., Zabel E.W. & Peterson R.E. 2003. Effects of aryl hydrocarbon receptor-mediated early life stage toxicity on lake trout populations in Lake Ontario during the 20th century. *Environmental Science & Technology* 37: 3864–3877.

Cox J. & Mann M. 2008. MaxQuant enables high peptide identification rates, individualized p.p.b.-range mass accuracies and proteome-wide protein quantification. *Nature biotechnology* 26: 1367–1372.

Cox J., Neuhauser N., Michalski A., Scheltema R.A., Olsen J.V. & Mann M. 2011. Andromeda: A Peptide Search Engine Integrated into the MaxQuant Environment. *Journal of Proteome Research* 10: 1794–1805.

Curtis L.R., Bravo C.F., Bayne C.J., Tilton F., Arkoosh M.R., Lambertini E., Loge F.J., Collier T.K., Meador J.P. & Tilton S.C. 2017. Transcriptional changes in innate immunity genes in head kidneys from *Aeromonas salmonicida*-challenged rainbow trout fed a mixture of polycyclic aromatic hydrocarbons. *Ecotoxicology and environmental safety* 142: 157–163.

Cvetic C.A. & Walter J.C. 2006. Getting a grip on licensing: mechanism of stable Mcm2-7 loading onto replication origins. *Molecular cell* 21: 143–144.

Danielson P.B. 2002. The cytochrome P450 superfamily: biochemistry, evolution and drug metabolism in humans. *Current drug metabolism* 6: 561.

Delanghe J.R. & Langlois M.R. 2001. Hemopexin: a review of biological aspects and the role in laboratory medicine. *Clinica Chimica Acta* 312: 13–23.

Denier van der Gon H., Bolscher M. van het, Visschedijk A. & Zandveld P. 2007. Emissions of persistent organic pollutants and eight candidate POPs from UNECE–Europe in 2000, 2010 and 2020 and the emission reduction resulting from the implementation of the UNECE POP protocol. *Atmospheric Environment* 41: 9245–9261.

Denison M.S., Fisher J.M. & Whitlock J.P. 1988. The DNA recognition site for the dioxin-Ah receptor complex. Nucleotide sequence and functional analysis. *Journal of Biological Chemistry* 263: 17221–17224.

Dietrich J.B. 1992. Tyrosine aminotransferase: a transaminase among others? *Cellular and molecular biology* 38: 95–114.

Doering J.A., Giesy J.P., Wiseman S. & Hecker M. 2013. Predicting the sensitivity of fishes to dioxin-like compounds: possible role of the aryl hydrocarbon receptor (AhR) ligand binding domain. *Environmental Science and Pollution Research* 20: 1219–1224.

Doering J., Hecker M., Villeneuve D. & Zhang X. 2019. Adverse Outcome Pathway on aryl hydrocarbon receptor activation leading to early life stage mortality, via increased COX-2IS 12.

Doering J.A., Wiseman S., Giesy J.P. & Hecker M. 2018. A Cross-species Quantitative Adverse Outcome Pathway for Activation of the Aryl Hydrocarbon Receptor Leading to Early Life Stage Mortality in Birds and Fishes. *Environmental Science & Technology* 52: 7524–7533.

Dutta A. & Bell S.P. 1997. Initiation of DNA replication in eukaryotic cells. *Annual Review of Cell and Developmental Biology* 13: 293–332.

ECHA. 2013. *Environmental-quality-standards - ECHA. Annex I, Part A, P.S. & P. in water*.

ECHA. 2022. Retene: Substance Information. URL https://echa.europa.eu/substance-information/-/substanceinfo/100.006.908 (accessed 2022.2.22).

ECHA. 2018. Fluoranthene: Substance information. URL https://echa.europa.eu/documents/10162/0d1ee6d4-1a47-0737-35c7-3503f0fca417 (accessed 2022.2.22)

Ehrenfreund P., Rasmussen S., Cleaves J. & Chen L. 2006. Experimentally Tracing the Key Steps in the Origin of Life: The Aromatic World. *Astrobiology* 6: 490–520.

EEA. 2021. *Persistent organic pollutant emissions* — European Environment Agency. https://www.eea.europa.eu/data-and-maps/indicators/eea32-persistent-organic-pollutant-pop-emissions-1/assessment-10 (accessed 2022.2.222)

Falk H., Markul I. & Kotin P. 1956. Aromatic hydrocarbons. IV. Their fate following emission into the atmosphere and experimental exposure to washed air and synthetic smog. *A.M.A.archives of industrial health* 13: 13.

Fent K. & Bätscher R. 2000. Cytochrome P4501A induction potencies of polycyclic aromatic hydrocarbons in a fish hepatoma cell line: Demonstration of additive interactions. *Environmental Toxicology and Chemistry* 19: 2047–2058.

Finkelstein J.D. & Martin J.J. 2000. Homocysteine. *The international journal of biochemistry & cell biology* 32: 385–389.

Fleming C.R. & Di Giulio R.T. 2011. The role of CYP1A inhibition in the embryotoxic interactions between hypoxia and polycyclic aromatic hydrocarbons (PAHs) and PAH mixtures in zebrafish (*Danio rerio*). *Ecotoxicology* 20: 1300–1314.

Foucquier J. & Guedj M. 2015. Analysis of drug combinations: current methodological landscape. *Pharmacology research & perspectives* 3: e00149–e00149.

Fujii-Kuriyama Y. & Kawajiri K. 2010. Molecular mechanisms of the physiological functions of the aryl hydrocarbon (dioxin) receptor, a multifunctional regulator that senses and responds to environmental stimuli. *Proceedings of the Japan Academy, Series B* 86: 40–53.

Gabos S., Ikonomou M.G., Schopflocher D., Fowler B.R., White J., Prepas E., Prince D. & Chen W. 2001. Characteristics of PAHs, PCDD/Fs and PCBs

in sediment following forest fires in northern Alberta. *Dioxin '99* 43: 709–719.

Garner L.V.T., Brown D.R. & Di Giulio R.T. 2013. Knockdown of AHR1A but not AHR1B exacerbates PAH and PCB-126 toxicity in zebrafish (*Danio rerio*) embryos. *Aquatic Toxicology* 142–143: 336–346.

Gasiewicz T.A., Henry E.C. & Collins L.L. 2008. Expression and activity of aryl hydrocarbon receptors in development and cancer. *Critical reviews in eukaryotic gene expression* 18: 279–321.

Geier M.C., Minick J.D., Truong L., Tilton S., Pande P., Anderson K.A., Teeguardan J. & Tanguay R.L. 2018. Systematic developmental neurotoxicity assessment of a representative PAH Superfund mixture using zebrafish. *Toxicology and applied pharmacology; Alternative Approaches to Developmental Neurotoxicity Evaluation* 354: 115–125.

Goi M. & Childs S.J. 2016. Patterning mechanisms of the sub-intestinal venous plexus in zebrafish. *Developmental biology* 409: 114–128.

Grosser T., Yusuff S., Cheskis E., Pack M.A. & FitzGerald G.A. 2002. Developmental expression of functional cyclooxygenases in zebrafish. *Proc Natl Acad Sci USA* 99: 8418.

Grynberg A. & Demaison L. 1996. Fatty acid oxidation in the heart. *Journal of Cardiovascular Pharmacology* 28 Suppl 1: S11-17.

Hansen B.H., Parkerton T., Nordtug T., Størseth T.R. & Redman A. 2019. Modeling the toxicity of dissolved crude oil exposures to characterize the sensitivity of cod (*Gadus morhua*) larvae and role of individual and unresolved hydrocarbons. *Marine pollution bulletin* 138: 286–294.

Hansson M.C. & Hahn M.E. 2008. Functional properties of the four Atlantic salmon (*Salmo salar*) aryl hydrocarbon receptor type 2 (AHR2) isoforms. *Aquatic Toxicology* 86: 121–130.

Hansson M.C., Wittzell H., Persson K. & Schantz T. von. 2003. Characterization of two distinct aryl hydrocarbon receptor (AhR2) genes in Atlantic salmon (*Salmo salar*) and evidence for multiple AhR2 gene lineages in salmonid fish. *Gene* 303: 197–206.

Heintz R.A., Rice S.D., Wertheimer A.C., Bradshaw R.F., Thrower F.P., Joyce J. & Short J. 2000. Delayed effects on growth and marine survival of pink salmon *Oncorhynchus gorbuscha* after exposure to crude oil during embryonic development. *Marine Ecology-progress Series - MAR ECOL-PROGR SER* 208: 205–216.

Hicken C.E., Linbo T.L., Baldwin D.H., Willis M.L., Myers M.S., Holland L., Larsen M., Stekoll M.S., Rice S.D., Collier T.K., Scholz N.L. & Incardona J.P. 2011. Sublethal exposure to crude oil during embryonic development alters cardiac morphology and reduces aerobic capacity in adult fish. *Proc Natl Acad Sci USA* 108: 7086.

Hiller K., Hangebrauk J., Jäger C., Spura J., Schreiber K. & Schomburg D. 2009. MetaboliteDetector: comprehensive analysis tool for targeted and nontargeted GC/MS based metabolome analysis. *Analytical Chemistry* 81: 3429–3439.

Hodson P.V., Qureshi K., Noble C.A.J., Akhtar P. & Brown R.S. 2007. Inhibition of CYP1A enzymes by alpha-naphthoflavone causes both synergism and antagonism of retene toxicity to rainbow trout (*Oncorhynchus mykiss*). *Aquatic Toxicology* 81: 275–285.

Honkanen J.O., Holopainen I.J. & Kukkonen J.V.K. 2004. Bisphenol A induces yolk-sac oedema and other adverse effects in landlocked salmon (*Salmo salar m. sebago*) yolk-sac fry. *Chemosphere* 55: 187–196.

Hoover R. 2014. Need to Track Organic Nano-Particles Across the Universe? NASA's Got an App for That. *NASA*. URL http://www.nasa.gov/ames/need-to-track-organic-nano-particles-across-the-universe-nasas-got-an-app-for-that (accessed 2022.2.21)

Hornung M.W., Spitsbergen J.M. & Peterson R.E. 1999. 2,3,7,8-Tetrachlorodibenzo-*p*-dioxin alters cardiovascular and craniofacial development and function in sac fry of rainbow trout (*Oncorhynchus mykiss*). *Toxicological Sciences* 47: 40–51.

Huang M., Mesaros C., Hackfeld L.C., Hodge R.P., Zang T., Blair I.A. & Penning T.M. 2017. Potential Metabolic Activation of a Representative C4-Alkylated Polycyclic Aromatic Hydrocarbon Retene (1-Methyl-7-isopropyl-phenanthrene) Associated with the Deepwater Horizon Oil Spill in Human Hepatoma (HepG2) Cells. *Chemical research in toxicology* 30: 1093–1101.

Incardona J.P. 2017. Molecular Mechanisms of Crude Oil Developmental Toxicity in Fish. *Archives of Environmental Contamination and Toxicology* 73: 19–32.

Hummel J., Selbig J., Walther D. & Kopka J. 2007. The Golm Metabolome Database: a database for GC-MS based metabolite profiling. In: Nielsen J. & Jewett M.C. (eds.), *Metabolomics: A Powerful Tool in Systems Biology*, Springer Berlin Heidelberg, Berlin, Heidelberg, pp. 75–95.

Incardona J.P., Collier T.K. & Scholz N.L. 2004. Defects in cardiac function precede morphological abnormalities in fish embryos exposed to polycyclic aromatic hydrocarbons. *Toxicology and Applied Pharmacology* 196: 191–205.

Incardona J.P., Day H.L., Collier T.K. & Scholz N.L. 2006. Developmental toxicity of 4-ring polycyclic aromatic hydrocarbons in zebrafish is differentially dependent on AH receptor isoforms and hepatic cytochrome P4501A metabolism. *Toxicology and applied pharmacology* 217: 308–321.

Incardona J.P., Carls M.G., Day H.L., Sloan C.A., Bolton J.L., Collier T.K. & Scholz N.L. 2009. Cardiac Arrhythmia Is the Primary Response of Embryonic Pacific Herring (*Clupea pallasi*) Exposed to Crude Oil during Weathering. *Environmental science & technology* 43: 201–207.

Incardona J.P., Linbo T.L. & Scholz N.L. 2011. Cardiac toxicity of 5-ring polycyclic aromatic hydrocarbons is differentially dependent on the aryl hydrocarbon receptor 2 isoform during zebrafish development. *Toxicology and applied pharmacology* 257: 242–249.

Incardona J.P., Gardner L.D., Linbo T.L., Brown T.L., Esbaugh A.J., Mager E.M., Stieglitz J.D., French B.L., Labenia J.S., Laetz C.A., Tagal M., Sloan C.A., Elizur A., Benetti D.D., Grosell M., Block B.A. & Scholz N.L. 2014. Deepwater Horizon crude oil impacts the developing hearts of large predatory pelagic fish. *Proc Natl Acad Sci USA* 111: E1510.

Isogai S. & Horiguchi M. 1997. The earliest stages in the development of the circulatory system of the Rainbow Trout *Oncorhynchus mykiss*. *Journal of Morphology* 233: 215–236.

Isogai S., Horiguchi M. & Weinstein B.M. 2001. The Vascular Anatomy of the Developing Zebrafish: An Atlas of Embryonic and Early Larval Development. *Developmental biology* 230: 278–301.

Jayasundara N., Van Tiem Garner L., Meyer J.N., Erwin K.N. & Di Giulio R.T. 2014. AHR2-Mediated Transcriptomic Responses Underlying the Synergistic Cardiac Developmental Toxicity of PAHs. *Toxicological Sciences* 143: 469–481.

Jonker M.T.O., Brils J.M., Sinke A.J.C., Murk A.J. & Koelmans A.A. 2006. Weathering and toxicity of marine sediments contaminated with oils and polycyclic aromatic hydrocarbons. *Environmental Toxicology and Chemistry* 25: 1345–1353.

Kais B., Schneider K.E., Keiter S., Henn K., Ackermann C. & Braunbeck T. 2013. DMSO modifies the permeability of the zebrafish (*Danio rerio*) chorion-

Implications for the fish embryo test (FET). *Aquatic Toxicology* 140–141: 229–238.

Karchner S.I., Franks D.G. & Hahn M.E. 2005. AHR1B, a new functional aryl hydrocarbon receptor in zebrafish: tandem arrangement of ahr1b and ahr2 genes. *The Biochemical Journal* 392: 153–161.

Katsumoto T., Mitsushima A. & Kurimura T. 1990. The role of the vimentin intermediate filaments in rat 3Y1 cells elucidated by immunoelectron microscopy and computer-graphic reconstruction. *Biology of the Cell* 68: 139–146.

Keith L.H. 2015. The Source of U.S. EPA's Sixteen PAH Priority Pollutants. 35: 147–160.

Ketterer B., Coles B. & Meyer D.J. 1983. The role of glutathione in detoxication. *Environmental Health Perspectives* 49: 59–69.

King-Heiden T.C., Mehta V., Xiong K.M., Lanham K.A., Antkiewicz D.S., Ganser A., Heideman W. & Peterson R.E. 2012. Reproductive and developmental toxicity of dioxin in fish. *Molecular and Cellular Endocrinology* 354: 121–138.

Knafla A., Phillipps K.A., Brecher R.W., Petrovic S. & Richardson M. 2006. Development of a dermal cancer slope factor for benzo[a]pyrene. *Regulatory Toxicology and Pharmacology* 45: 159–168.

Ko Y.-P., Kobbe B., Paulsson M. & Wagener R. 2005. Zebrafish (*Danio rerio*) matrilins: shared and divergent characteristics with their mammalian counterparts. *The Biochemical Journal* 386: 367–379.

Krasnov A., Timmerhaus G., Afanasyev S. & Jørgensen S.M. 2011. Development and assessment of oligonucleotide microarrays for Atlantic salmon (*Salmo salar* L.). *Comparative Biochemistry and Physiology Part D: Genomics and Proteomics; This Special Issue contains papers which stem from a presentation at the Genomics in Aquaculture symposium held in Bodø¸ on 5th-7th July 2009* 6: 31–38.

Krishnan V., Porter W., Santostefano M., Wang X. & Safe S. 1995. Molecular mechanism of inhibition of estrogen-induced cathepsin D gene expression by 2,3,7,8-tetrachlorodibenzo-*p*-dioxin (TCDD) in MCF-7 cells. *Molecular and cellular biology* 15: 6710–6719.

Larade K. & Storey K.B. 2004. Accumulation and translation of ferritin heavy chain transcripts following anoxia exposure in a marine invertebrate. *Journal of Experimental Biology* 207: 1353.

Laurel B.J., Copeman L.A., Iseri P., Spencer M.L., Hutchinson G., Nordtug T., Donald C.E., Meier S., Allan S.E., Boyd D.T., Ylitalo G.M., Cameron J.R., French B.L., Linbo T.L., Scholz N.L. & Incardona J.P. 2019. Embryonic Crude Oil Exposure Impairs Growth and Lipid Allocation in a Keystone Arctic Forage Fish. *iScience* 19: 1101–1113.

Le Bihanic F., Morin B., Cousin X., Le Menach K., Budzinski H. & Cachot J. 2014. Developmental toxicity of PAH mixtures in fish early life stages. Part I: adverse effects in rainbow trout. *Environmental Science and Pollution Research* 21: 13720–13731.

Leite C.A., Taylor E.W., Guerra C.D.R., Florindo L.H., Belão T. & Rantin F.T. 2009. The role of the vagus nerve in the generation of cardiorespiratory interactions in a neotropical fish, the pacu, *Piaractus mesopotamicus*. *Journal of Comparative Physiology A* 195: 721–731.

Leppänen H. & Oikari A. 1999. Occurrence of retene and resin acids in sediments and fish bile from a lake receiving pulp and paper mill effluents. *Environmental Toxicology and Chemistry* 18: 1498–1505.

Leppänen H. & Oikari A. 2001. Retene and resin acid concentrations in sediment profiles of a lake recovering from exposure to pulp mill effluents. *Journal of Paleolimnology* 25: 367–374.

Li X., Xiong D., Ju Z., Xiong Y., Ding G. & Liao G. 2021. Phenotypic and transcriptomic consequences in zebrafish early-life stages following exposure to crude oil and chemical dispersant at sublethal concentrations. *Science of The Total Environment* 763: 143053.

Lu J., Shang X., Zhong W., Xu Y., Shi R. & Wang X. 2020. New insights of CYP1A in endogenous metabolism: a focus on single nucleotide polymorphisms and diseases. *SI: Drug metabolism and disposition in diseases* 10: 91–104.

Ma Q. & Whitlock J.P. Jr. 1997. A Novel Cytoplasmic Protein That Interacts with the Ah Receptor, Contains Tetratricopeptide Repeat Motifs, and Augments the Transcriptional Response to 2,3,7,8-Tetrachlorodibenzo-*p*-dioxin. *Journal of Biological Chemistry* 272: 8878–8884.

Mackay D. (ed.). 2006. *Handbook of physical-chemical properties and environmental fate for organic chemicals*. CRC/Taylor & Francis, Boca Raton, FL.

Maes J., Verlooy L., Buenafe O.E., Witte P.A.M. de, Esguerra C.V. & Crawford A.D. 2012. Evaluation of 14 Organic Solvents and Carriers for Screening Applications in Zebrafish Embryos and Larvae. *PLOS ONE* 7: e43850.

Marro J., Pfefferli C., Charles A.-S. de P., Bise T. & Jaźwińska A. 2016. Collagen XII Contributes to Epicardial and Connective Tissues in the Zebrafish Heart during Ontogenesis and Regeneration. *PLOS ONE* 11: e0165497.

Martin J.D., Adams J., Hollebone B., King T., Brown R.S. & Hodson P.V. 2014. Chronic toxicity of heavy fuel oils to fish embryos using multiple exposure scenarios. *Environmental Toxicology and Chemistry* 33: 677–687.

Mastrototaro G., Liang X., Li X., Carullo P., Piroddi N., Tesi C., Gu Y., Dalton N.D., Peterson K.L., Poggesi C., Sheikh F., Chen J. & Bang M.-L. 2015. Nebulette knockout mice have normal cardiac function, but show Z-line widening and up-regulation of cardiac stress markers. *Cardiovascular research* 107: 216–225.

McConkey B.J., Hewitt L.M., Dixon D.G. & Greenberg B.M. 2002. Natural Sunlight Induced Photooxidation of Naphthalene in Aqueous Solution. *Water, air, and soil pollution* 136: 347–359.

Meador J.P. & Nahrgang J. 2019. Characterizing Crude Oil Toxicity to Early-Life Stage Fish Based On a Complex Mixture: Are We Making Unsupported Assumptions? *Environmental science & technology* 53: 11080–11092.

Meunier S. & Vernos I. 2012. Microtubule assembly during mitosis – from distinct origins to distinct functions? *Journal of cell science* 125: 2805.

Mitchison T. & Kirschner M. 1984. Dynamic instability of microtubule growth. *Nature* 312: 237–242.

Mustacich D. & Powis G. 2000. Thioredoxin reductase. *Biochemical Journal* 346: 1–8.

NOAA (National Oceanic and Atmospheric Administration). 2015. *What Is Weathering?* URL https://response.restoration.noaa.gov/oil-and-chemical-spills/significant-incidents/exxon-valdez-oil-spill/what-weathering.html (accessed 2022.2.22)

Naturvårdsverket. 2021. *PAH, utsläpp till luft*. URL https://www.naturvardsverket.se/data-och-statistik/luft/utslapp/pah-utslapp-till-luft/ (accessed 2022.2.22).

Nicoli S. & Presta M. 2007. The zebrafish / tumor xenograft angiogenesis assay. *Nature Protocols* 2: 2918–2923.

Nogales E. 2000. Structural Insights into Microtubule Function. *Annual Review of Biochemistry* 69: 277–302.

OECD. 1992. Test No. 210: Fish, Early-Life Stage Toxicity Test.

OECD. 2013. Test No. 236: Fish Embryo Acute Toxicity (FET) Test.

Oliver I.T. 1955. A spectrophotometric method for the determination of creative phosphokinase and myokinase. *Biochemical Journal* 61: 116–122.

Olsvik P.A., Lie K.K., Nordtug T. & Hansen B.H. 2012. Is chemically dispersed oil more toxic to Atlantic cod (*Gadus morhua*) larvae than mechanically dispersed oil? A transcriptional evaluation. *BMC Genomics* 13: 702.

Orino K., Lehman L., Tsuji Y., Ayaki H., Torti S.V. & Torti F.M. 2001. Ferritin and the response to oxidative stress. *The Biochemical journal* 357: 241–247.

Pacyna J.M., Breivik K., Münch J. & Fudala J. 2003. European atmospheric emissions of selected persistent organic pollutants, 1970–1995. *Dynamic processes of mercury and other trace contaminants in the marine boundary layer of european seas - ELOISE II* 37: 119–131.

Paramio J.M. & Jorcano J.L. 2002. Beyond structure: do intermediate filaments modulate cell signalling? *BioEssays* 24: 836–844.

Pelletier M.C., Burgess R.M., Ho K.T., Kuhn A., McKinney R.A. & Ryba S.A. 1997. Phototoxicity of individual polycyclic aromatic hydrocarbons and petroleum to marine invertebrate larvae and juveniles. *Environmental Toxicology and Chemistry* 16: 2190–2199.

Peterson C.H., Rice S.D., Short J.W., Esler D., Bodkin J.L., Ballachey B.E. & Irons D.B. 2003. Long-Term Ecosystem Response to the Exxon Valdez Oil Spill. *Science* 302: 2082–2086.

Pickart M.A., Klee E.W., Nielsen A.L., Sivasubbu S., Mendenhall E.M., Bill B.R., Chen E., Eckfeldt C.E., Knowlton M., Robu M.E., Larson J.D., Deng Y., Schimmenti L.A., Ellis L.B.M., Verfaillie C.M., Hammerschmidt M., Farber S.A. & Ekker S.C. 2006. Genome-Wide Reverse Genetics Framework to Identify Novel Functions of the Vertebrate Secretome. *PLOS ONE* 1: e104.

Pott P. 1974. Chirurgical observations relative to… cancer of the scrotum… *CA: A Cancer Journal for Clinicians* 24: 110–116.

Price E.R. & Mager E.M. 2020. The effects of exposure to crude oil or PAHs on fish swim bladder development and function. *Comparative Biochemistry and Physiology Part C: Toxicology & Pharmacology* 238: 108853.

Pulster E.L., Gracia A., Armenteros M., Toro-Farmer G., Snyder S.M., Carr B.E., Schwaab M.R., Nicholson T.J., Mrowicki J. & Murawski S.A. 2020. A First Comprehensive Baseline of Hydrocarbon Pollution in Gulf of Mexico Fishes. *Scientific Reports* 10: 6437.

Qiu Y.-W., Zhang G., Liu G.-Q., Guo L.-L., Li X.-D. & Wai O. 2009. Polycyclic aromatic hydrocarbons (PAHs) in the water column and sediment core of Deep Bay, South China. *Estuarine, Coastal and Shelf Science* 83: 60–66.

R Core Team (2020). R: A language and environment for statistical computing. R Foundation for Statistical Computing, Vienna, Austria. URL https://www.R-project.org/.

Ramdahl T. 1983. Retene—a molecular marker of wood combustion in ambient air. *Nature* 306: 580–582.

Rannug A. & Rannug U. 2018. The tryptophan derivative 6-formylindolo[3,2-b]carbazole, FICZ, a dynamic mediator of endogenous aryl hydrocarbon receptor signaling, balances cell growth and differentiation. *Critical reviews in toxicology* 48: 555–574.

Ravindra K., Sokhi R. & Van Grieken R. 2008. Atmospheric polycyclic aromatic hydrocarbons: Source attribution, emission factors and regulation. *Atmospheric Environment* 42: 2895–2921.

Rhee S.G., Kang S.W., Chang T.-S., Jeong W. & Kim K. 2001. Peroxiredoxin, a Novel Family of Peroxidases. *IUBMB life* 52: 35–41.

Ricciotti E. & FitzGerald G.A. 2011. Prostaglandins and Inflammation. *Arteriosclerosis, thrombosis, and vascular biology* 31: 986–1000.

Rice S.D., Thomas R.E., Carls M.G., Heintz R.A., Wertheimer A.C., Murphy M.L., Short J.W. & Moles A. 2001. Impacts to Pink Salmon Following the Exxon Valdez Oil Spill: Persistence, Toxicity, Sensitivity, and Controversy. *Rev.Fish.Sci.* 9: 165–211.

Richter H. & Howard J.B. 2000. Formation of polycyclic aromatic hydrocarbons and their growth to soot—a review of chemical reaction pathways. *Progress in Energy and Combustion Science* 26: 565–608.

Rigaud C., Eriksson A., Krasnov A., Wincent E., Pakkanen H., Lehtivuori H., Ihalainen J. & Vehniäinen E.-R. 2020a. Retene, pyrene and phenanthrene cause distinct molecular-level changes in the cardiac tissue of rainbow trout (*Oncorhynchus mykiss*) larvae, part 1 – Transcriptomics. *Science of The Total Environment* 745: 141031.

Rigaud C., Eriksson A., Rokka A., Skaugen M., Lihavainen J., Keinänen M., Lehtivuori H. & Vehniäinen E.-R. 2020b. Retene, pyrene and phenanthrene cause distinct molecular-level changes in the cardiac tissue of rainbow trout (*Oncorhynchus mykiss*) larvae, part 2 – Proteomics and metabolomics. *Science of The Total Environment* 746: 141161.

Rombough P. & Moroz B. 1997. The scaling and potential importance of cutaneous and branchial surfaces in respiratory gas exchange in larval and juvenile walleye. *The Journal of experimental biology* 200: 2459.

RStudio Team (2020). RStudio: Integrated Development for R. RStudio, PBC, Boston, MA URL http://www.rstudio.com/.

Räsänen K., Arsiola T. & Oikari A. 2012. Fast Genomic Biomarker Responses of Retene and Pyrene in Liver of Juvenile Rainbow Trout, *Oncorhynchus mykiss*. *Bulletin of environmental contamination and toxicology* 89: 733–738.

Sagan C., Khare B.N., Thompson W.R., McDonald G.D., Wing M.R., Bada J.L., Vo-Dinh T. & Arakawa E.T. 1993. Polycyclic Aromatic Hydrocarbons in the Atmospheres of Titan and Jupiter. *The Astrophysical Journal* 414: 399.

Salama F. 2008. PAHs in Astronomy - A Review. *Proceedings of the International Astronomical Union* 4: 357–366.

Sanders B.M. 1993. Stress Proteins in Aquatic Organisms: An Environmental Perspective. *Critical reviews in toxicology* 23: 49–75.

Sang Y., Roest M., Laat B. de, Groot P.G. de & Huskens D. 2021. Interplay between platelets and coagulation. *Blood Reviews* 46: 100733.

Schmidt J.V. & Bradfield C.A. 1996. Ah receptor signaling pathways. *Annual Review of Cell and Developmental Biology* 12: 55–89.

Schneidemesser E. von, Schauer J.J., Shafer M.M., Hagler G.S.W., Bergin M.H. & Steig E.J. 2008. A method for the analysis of ultra-trace levels of semi-volatile and non-volatile organic compounds in snow and application to a Greenland snow pit. *Polar Science* 2: 251–266.

Scott J.A. & Hodson P.V. 2008. Evidence for multiple mechanisms of toxicity in larval rainbow trout (*Oncorhynchus mykiss*) co-treated with retene and α-naphthoflavone. *Aquatic Toxicology* 88: 200–206.

Scott J.A., Incardona J.P., Pelkki K., Shepardson S. & Hodson P.V. 2011. AhR2-mediated, CYP1A-independent cardiovascular toxicity in zebrafish (*Danio rerio*) embryos exposed to retene. *Aquatic Toxicology* 101: 165–174.

Sequeira V., Nijenkamp L.L.A.M., Regan J.A. & Velden J. van der. 2014. The physiological role of cardiac cytoskeleton and its alterations in heart failure. *Biochimica et Biophysica Acta (BBA) - Biomembranes; Reciprocal influences between cell cytoskeleton and membrane channels, receptors and transporters* 1838: 700–722.

Serigstad B. 1987. Oxygen uptake of developing fish eggs and larvae. *Sarsia* 72: 369–371.

Shankar P., Geier M.C., Truong L., McClure R.S., Pande P., Waters K.M. & Tanguay R.L. 2019. Coupling Genome-wide Transcriptomics and Developmental Toxicity Profiles in Zebrafish to Characterize Polycyclic Aromatic Hydrocarbon (PAH) Hazard. *International journal of molecular sciences* 20: 2570.

Shankar P., Dasgupta S., Hahn M.E. & Tanguay R.L. 2020. A Review of the Functional Roles of the Zebrafish Aryl Hydrocarbon Receptors. *Toxicological Sciences* 178: 215–238.

Sivula L., Vehniäinen E.-R., Vehniäinen E.-R. & Kukkonen J.V.K. 2018. Toxicity of biomining effluents to *Daphnia magna*: Acute toxicity and transcriptomic biomarkers. *Chemosphere* 210: 304–311.

Smirnova A., Wincent E., Vikström Bergander L., Alsberg T., Bergman J., Rannug A. & Rannug U. 2016. Evidence for New Light-Independent Pathways for Generation of the Endogenous Aryl Hydrocarbon Receptor Agonist FICZ. *Chemical research in toxicology* 29: 75–86.

Song Y., Nahrgang J. & Tollefsen K.E. 2019. Transcriptomic analysis reveals dose-dependent modes of action of benzo(a)pyrene in polar cod (*Boreogadus saida*). *Science of The Total Environment* 653: 176–189.

Souder J.P. & Gorelick D.A. 2019. ahr2, But Not ahr1a or ahr1b, Is Required for Craniofacial and Fin Development and TCDD-dependent Cardiotoxicity in Zebrafish. *Toxicological Sciences* 170: 25–44.

Stipanuk M.H., Dominy J.E. Jr., Lee J.-I. & Coloso R.M. 2006. Mammalian Cysteine Metabolism: New Insights into Regulation of Cysteine Metabolism. *The Journal of nutrition* 136: 1652S-1659S.

Sørhus E., Incardona J.P., Karlsen Ø., Linbo T., Sørensen L., Nordtug T., Meeren T. van der, Thorsen A., Thorbjørnsen M., Jentoft S., Edvardsen R.B. & Meier S. 2016. Crude oil exposures reveal roles for intracellular calcium cycling in haddock craniofacial and cardiac development. *Scientific Reports* 6: 31058.

Sørhus E., Incardona J.P., Furmanek T., Goetz G.W., Scholz N.L., Meier S., Edvardsen R.B. & Jentoft S. 2017. Novel adverse outcome pathways revealed by chemical genetics in a developing marine fish. *eLife* 6: e20707.

Sørhus E., Meier S., Donald C.E., Furmanek T., Edvardsen R.B. & Lie K.K. 2021. Cardiac dysfunction affects eye development and vision by reducing supply of lipids in fish. *The Science of the Total Environment* 800: 149460.

Takuwa Y., Du W., Qi X., Okamoto Y., Takuwa N. & Yoshioka K. 2010. Roles of sphingosine-1-phosphate signaling in angiogenesis. *World journal of biological chemistry* 1: 298–306.

Teraoka T., Kubota A., Kawai Y. & Hiraga T. 2008. Prostanoid Signaling Mediates Circulation Failure Caused by TCDD in Developing Zebrafish. *Studies Environ. Chem. Biol. Resp. Chem. Pollut*: 61–80.

Teraoka H., Okuno Y., Nijoukubo D., Yamakoshi A., Peterson R.E., Stegeman J.J., Kitazawa T., Hiraga T. & Kubota A. 2014. Involvement of COX2–thromboxane pathway in TCDD-induced precardiac edema in developing zebrafish. *Aquatic Toxicology* 154: 19–26.

Thorne R.E. & Thomas G.L. 2008. Herring and the "Exxon Valdez" oil spill: an investigation into historical data conflicts. *ICES Journal of Marine Science* 65: 44–50.

Tielens A.G.G.M. 2008. Interstellar Polycyclic Aromatic Hydrocarbon Molecules. *Annual Review of Astronomy and Astrophysics* 46: 289–337.

Timme-Laragy A., Cockman C.J., Matson C.W. & Di Giulio R.T. 2007. Synergistic induction of AHR regulated genes in developmental toxicity from co-exposure to two model PAHs in zebrafish. *Aquatic Toxicology* 85: 241–250.

Tolosano E. & Altruda F. 2002. Hemopexin: Structure, Function, and Regulation. *DNA and cell biology* 21: 297–306.

Troisi G., Borjesson L., Bexton S. & Robinson I. 2007. Biomarkers of polycyclic aromatic hydrocarbon (PAH)-associated hemolytic anemia in oiled wildlife. *Environmental research* 105: 324–329.

Tsao P. & Zastrow M. von. 2000. Downregulation of G protein-coupled receptors. *Current opinion in neurobiology* 10: 365–369.

Turcotte D., Akhtar P., Bowerman M., Kiparissis Y., Brown R.S. & Hodson P.V. 2011. Measuring the toxicity of alkyl-phenanthrenes to early life stages of medaka (*Oryzias latipes*) using partition-controlled delivery. *Environmental Toxicology and Chemistry* 30: 487–495.

Tyanova S., Temu T., Sinitcyn P., Carlson A., Hein M.Y., Geiger T., Mann M. & Cox J. 2016. The Perseus computational platform for comprehensive analysis of (prote)omics data. *Nature Methods* 13: 731–740.

US EPA. 2007. *Survey of New Findings in Scientific Literature Related to Atmospheric Deposition to the Great Waters: Polycyclic Aromatic Hydrocarbons (PAH)*.

Van Metre P.C., Mahler B.J. & Furlong E.T. 2000. Urban Sprawl Leaves Its PAH Signature. *Environmental science & technology* 34: 4064–4070.

Van Tiem L.A. & Di Giulio R.T. 2011. AHR2 knockdown prevents PAH-mediated cardiac toxicity and XRE- and ARE-associated gene induction in zebrafish (*Danio rerio*). *Toxicology and applied pharmacology* 254: 280–287.

Vehniäinen E.-R., Bremer K., Scott J.A., Junttila S., Laiho A., Gyenesei A., Hodson P.V. & Oikari A.O.J. 2016. Retene causes multifunctional transcriptomic changes in the heart of rainbow trout (*Oncorhynchus mykiss*) embryos. *Environmental toxicology and pharmacology* 41: 95–102.

Vehniäinen E.-R., Haverinen J. & Vehniäinen E.-R. 2019. Polycyclic Aromatic Hydrocarbons Phenanthrene and Retene Modify the Action Potential via Multiple Ion Currents in Rainbow Trout *Oncorhynchus mykiss* Cardiac Myocytes. *Environmental Toxicology and Chemistry* 38: 2145–2153.

Veith A. & Moorthy B. 2018. Role of Cytochrome p450s in the Generation and Metabolism of Reactive Oxygen Species. *Current opinion in toxicology* 7: 44–51.

Vernier J.M. 1977. *Chronological Table of the Embryonic Development of Rainbow Trout, Salmo Gairdneri Rich. 1836*. Department of the Environment, Fisheries and Marine Service, Pacific Biological Station.

Villalobos S.A., Papoulias D.M., Meadows J., Blankenship A.L., Pastva S.D., Kannan K., Hinton D.E., Tillitt D.E. & Giesy J.P. 2000. Toxic responses of medaka, D-rR strain, to polychlorinated naphthalene mixtures after embryonic exposure by in ovo nanoinjection: A partial life-cycle assessment. *Environmental Toxicology and Chemistry* 19: 432–440.

Ward E.J., Adkison M., Couture J., Dressel S.C., Litzow M.A., Moffitt S., Hoem Neher T., Trochta J. & Brenner R. 2017. Evaluating signals of oil spill impacts, climate, and species interactions in Pacific herring and Pacific salmon populations in Prince William Sound and Copper River, Alaska. *PLOS ONE* 12: e0172898.

Watson G.M., Andersen O.-K., Galloway T.S. & Depledge M.H. 2004. Rapid assessment of polycyclic aromatic hydrocarbon (PAH) exposure in decapod crustaceans by fluorimetric analysis of urine and haemolymph. *Aquatic Toxicology* 67: 127–142.

Wei Y.-D., Helleberg H., Rannug U. & Rannug A. 1998. Rapid and transient induction of CYP1A1 gene expression in human cells by the tryptophan photoproduct 6-formylindolo[3,2-b]carbazole. *Chemico-biological interactions* 110: 39–55.

Weiss H.J., Sussman I.I. & Hoyer L.W. 1977. Stabilization of factor VIII in plasma by the von Willebrand factor. Studies on posttransfusion and dissociated factor VIII and in patients with von Willebrand's disease. *The Journal of clinical investigation* 60: 390–404.

Wells P. & Pinder A. 1996. The respiratory development of Atlantic salmon. I. Morphometry of gills, yolk sac and body surface. *The Journal of experimental biology* 199: 2725.

Wickström K. & Tolonen K. 1987. The history of airborne polycyclic aromatic hydrocarbons (PAH) and perylene as recorded in dated lake sediments. *Water, air, and soil pollution* 32: 155–175.

Wild S.R. & Jones K.C. 1995. Polynuclear aromatic hydrocarbons in the United Kingdom environment: A preliminary source inventory and budget. *Environmental Pollution* 88: 91–108.

Wild S.R., Berrow M.L. & Jones K.C. 1991. The persistence of polynuclear aromatic hydrocarbons (PAHs) in sewage sludge amended agricultural soils. *Environmental Pollution* 72: 141–157.

Willett K.L., Randerath K., Zhou G.-D. & Safe S.H. 1998. Inhibition of CYP1A1-Dependent Activity by the Polynuclear Aromatic Hydrocarbon (PAH) Fluoranthene. *Biochemical pharmacology* 55: 831–839.

Williamson J.R. 1979. Mitochondrial Function in the Heart. *Annual Review of Physiology* 41: 485–506.

Wills L.P., Zhu S., Willett K.L. & Di Giulio R.T. 2009. Effect of CYP1A inhibition on the biotransformation of benzo[a]pyrene in two populations of Fundulus heteroclitus with different exposure histories. *Aquatic Toxicology* 92: 195–201.

Wilson S.C. & Jones K.C. 1993. Bioremediation of soil contaminated with polynuclear aromatic hydrocarbons (PAHs): A review. *Environmental Pollution* 81: 229–249.

Wincent E., Amini N., Luecke S., Glatt H., Bergman J., Crescenzi C., Rannug A. & Rannug U. 2009. The Suggested Physiologic Aryl Hydrocarbon Receptor Activator and Cytochrome P4501 Substrate 6-Formylindolo[3,2-b]carbazole Is Present in Humans. *Journal of Biological Chemistry* 284: 2690–2696.

Wincent E., Bengtsson J., Bardbori A.M., Alsberg T., Luecke S., Rannug U. & Rannug A. 2012. Inhibition of cytochrome P4501-dependent clearance of the endogenous agonist FICZ as a mechanism for activation of the aryl hydrocarbon receptor. *Proc Natl Acad Sci USA* 109: 4479.

Wolfe D.A., Hameedi M.J., Galt J.A., Watabayashi G., Short J., O'Claire C., Rice S., Michel J., Payne J.R., Bradock J., Hanna S. & Sale D. 1994. The Fate of the Oil Spilled from the Exxon Valdez. *Environmental science & technology* 28: 560A-568A.

Xu E.G., Mager E.M., Grosell M., Pasparakis C., Schlenker L.S., Stieglitz J.D., Benetti D., Hazard E.S., Courtney S.M., Diamante G., Freitas J., Hardiman G. & Schlenk D. 2016. Time- and Oil-Dependent Transcriptomic and Physiological Responses to Deepwater Horizon Oil in Mahi-Mahi (*Coryphaena hippurus*) Embryos and Larvae. *Environmental science & technology* 50: 7842–7851.

Xu E.G., Khursigara A.J., Li S., Esbaugh A.J., Dasgupta S., Volz D.C. & Schlenk D. 2019. mRNA-miRNA-Seq Reveals Neuro-Cardio Mechanisms of Crude Oil Toxicity in Red Drum (*Sciaenops ocellatus*). *Environmental science & technology* 53: 3296–3305.

Yamagiwa K. & Ichikawa K. 1918. Experimental Study of the Pathogenesis of Carcinoma. *J Cancer Res* 3: 1.

Yu G., Wang L.-G., Han Y. & He Q.-Y. 2012. clusterProfiler: an R Package for Comparing Biological Themes Among Gene Clusters. *OMICS: A Journal of Integrative Biology* 16: 284–287.

Yue M.S., Martin S.E., Martin N.R., Taylor M.R. & Plavicki J.S. 2021. 2,3,7,8-Tetrachlorodibenzo-*p*-dioxin exposure disrupts development of the visceral and ocular vasculature. *Aquatic Toxicology* 234: 105786.

Zanger U.M. & Schwab M. 2013. Cytochrome P450 enzymes in drug metabolism: Regulation of gene expression, enzyme activities, and impact of genetic variation. *Pharmacology & therapeutics* 138: 103–141.

Zhou Y., Zhou B., Pache L., Chang M., Khodabakhshi A.H., Tanaseichuk O., Benner C. & Chanda S.K. 2019. Metascape provides a biologist-oriented resource for the analysis of systems-level datasets. *Nature communications* 10: 1523–1523.

Zimmerman T.S. & Edgington T.S. 1973. Factor VIII coagulant activity and factor VIII-like antigen: independent molecular entities. *The Journal of experimental medicine* 138: 1015–1020.

Zodrow J.M. & Tanguay R.L. 2003. 2,3,7,8-Tetrachlorodibenzo-*p*-dioxin Inhibits Zebrafish Caudal Fin Regeneration. *Toxicological Sciences* 76: 151–161.

ORIGINAL PAPERS

I

EXPOSURE TO RETENE, FLUORANTHENE, AND THEIR BINARY MIXTURE CAUSES DISTINCT TRANSCRIPTOMIC AND APICAL OUTCOMES IN RAINBOW TROUT (*ONCORHYNCHUS MYKISS*) YOLK SAC ALEVINS

by

Andreas N.M. Eriksson, Cyril Rigaud, Aleksei Krasnov, Emma Wincent & Eeva-Riikka Vehniäinen 2022

Aquatic Toxicology 244: 106083.

https://doi.org/10.1016/j.aquatox.2022.106083

Aquatic Toxicology 244 (2022) 106083

Contents lists available at ScienceDirect

Aquatic Toxicology

journal homepage: www.elsevier.com/locate/aqtox

Exposure to retene, fluoranthene, and their binary mixture causes distinct transcriptomic and apical outcomes in rainbow trout *(Oncorhynchus mykiss)* yolk sac alevins

Andreas N.M. Eriksson [a,*], Cyril Rigaud [a], Aleksei Krasnov [b], Emma Wincent [c], Eeva-Riikka Vehniäinen [a]

[a] Department of Biological and Environmental Sciences, University of Jyväskylä, P.O. Box 35, Jyväskylä FI-40014, Finland
[b] Fisheries and Aquaculture Research, Norwegian Institute of Food, Ås, Norway
[c] Institute of Environmental Medicine, Karolinska Institutet, Stockholm, Sweden

ARTICLE INFO

Keywords:
Transcriptome
Mixture
Retene
Fluoranthene
PAH
Rainbow trout
Oncorhynchus mykiss
Early life development

ABSTRACT

Polycyclic aromatic hydrocarbons (PAHs) are widely spread environmental contaminants which affect developing organisms. It is known that improper activation of the aryl hydrocarbon receptor (AhR) by some PAHs contributes to toxicity, while other PAHs can disrupt cellular membrane function. The exact downstream mechanisms of AhR activation remain unresolved, especially with regard to cardiotoxicity. By exposing newly hatched rainbow trout alevins (*Oncorhynchus mykiss*) semi-statically to retene (32 μg l^{-1}; AhR agonist), fluoranthene (50 μg l^{-1}; weak AhR agonist and CYP1a inhibitor) and their binary mixture for 1, 3, 7 and 14 days, we aimed to uncover novel mechanisms of cardiotoxicity using a targeted microarray approach. At the end of the exposure, standard length, yolk area, blue sac disease (BSD) index and PAH body burden were measured, while the hearts were prepared for microarray analysis. Each exposure produced a unique toxicity profile. We observed that retene and the mixture, but not fluoranthene, significantly reduced growth by Day 14 compared to the control, while exposure to the mixture increased the BSD-index significantly from Day 3 onward. Body burden profiles were PAH-specific and correlated well with the exposure-specific upregulations of genes encoding for phase I and II enzymes. Exposure to the mixture over-represented pathways related to growth, amino acid and xenobiotic metabolism and oxidative stress responses. Alevins exposed to the individual PAHs displayed over-represented pathways involved in receptor signaling: retene downregulated genes with a role in G-protein signaling, while fluoranthene upregulated those involved in GABA signaling. Furthermore, exposure to retene and fluoranthene altered the expression of genes encoding for proteins involved in calcium- and potassium ion channels, which suggests affected heart structure and function. This study provides deeper understanding of the complexity of PAH toxicity and the necessity of investigating PAHs as mixtures and not as individual components.

1. Introduction

Polycyclic aromatic hydrocarbons (PAHs) are a widespread group of environmental contaminants of either natural or anthropogenic origin. Always occurring as complex mixtures in nature, PAHs are generated in large quantities during combustion or pyrolysis of organic material and are present in petroleum products. The environmental prevalence of PAHs has increased over the last century due to increased anthropogenic activities (Wickström and Tolonen, 1987; Van Metre et al., 2000). The presence of PAHs is particularly problematic in anoxic strata as any degradation of PAHs *in situ* requires aerobic metabolism. Hence, PAH contamination can form legacy deposits that can pose long term environmental risks if remobilized or leached (Haritash and Kaushik, 2009).

Exposure to PAHs during early life development of fish is well known to result in a broad suite of defects at multiple levels of biological organization and consequently, increased mortality. Heart structure and function are especially sensitive to PAHs (Incardona et al., 2011), which has multiple down-stream consequences for the growing fish larvae as

* Correspondence author.
E-mail address: andreas.n.m.eriksson@jyu.fi (A.N.M. Eriksson).

https://doi.org/10.1016/j.aquatox.2022.106083
Received 14 May 2021; Received in revised form 11 January 2022; Accepted 18 January 2022
Available online 21 January 2022

circulation of nutrients and gas-exchange become restricted. Reduced growth and symptoms referred to as the blue sac disease (BSD; yolk sac and pericardial edemas, craniofacial and skeletal deformities, hemorrhaging and fin rot) are established hallmarks of PAH toxicity (Billiard et al., 1999; Colavecchia et al., 2006). Other developmental defects associated with PAH exposure are genotoxicity and behavioral alterations (Rhodes et al., 2005; Geier et al., 2018).

The exact mechanisms of PAH induced toxicity remain unresolved for most PAHs, although multiple molecular processes are known to contribute to the formation of toxicity in developing fish. What is known is that different PAHs have different modes of action and toxicity potential in different organs and species (Timme-Laragy et al., 2007; Geier et al., 2018). Furthermore, the composition of a PAH mixture affects toxicity as the toxicological potency of certain PAH mixtures has been observed to induce a stronger response than the combined effect of the components (Scott and Hodson, 2008; Brown et al., 2015). However, it must be noted that certain components contribute more to toxicity than others, as exemplified by Geier et al. (2018).

The most studied molecular response in PAH exposed and developing fish is the interaction between certain PAHs and the aryl hydrocarbon receptor 2 (AhR2); a receptor which regulates normal development and metabolism (Billiard et al., 2002). Note that not all PAHs have affinity for AhR2 (Barron et al., 2004), but those PAHs that do trigger its activation as a transcription factor. Activation induces the expression of, among other genes, cytochrome P450 (*cyp1a*) by associating with xenobiotic response elements. The activated form of CYP1a functions as a phase I metabolic enzyme that facilitates metabolism and excretion of a large set of xenobiotics through hydroxylation but also activation of endogenous molecules.

The PAH retene (1-methyl-7-isopropyl phenanthrene) is commonly associated with effluents from pulp- and paper mills as well as microbial metabolism of resin acids (Leppänen and Oikari, 1999) but can also function as a biomarker for forest fires (Gabos et al., 2001). Retene is a known AhR2 agonist with high affinity (Barron et al., 2004). However, the exact mechanisms leading up to cardiotoxicity are not fully understood for retene (Bauder et al., 2005; Hodson et al., 2007), as multiple intertwined processes are likely to be involved; exemplified by the Adverse Outcome Pathway 21 (AOP21) by Doering et al., 2019. From a toxicological perspective, knockdown of *ahr2*, but not *cyp1a*, in retene exposed zebrafish embryos (*Danio rerio*) prevented the formation of cardiac defects (Scott et al., 2011). However, as AhR2 controls a vast number of genes, knockdown does not highlight any underlying mechanism. One suggested downstream gene is cyclooxygenase-2, but the evidence and quantitative understanding for this pathway are currently only moderate, and there are also other pathways that may be involved (AOP21).

Another PAH of interest is fluoranthene, which occurs ubiquitously in any natural PAH mixture (Page et al., 1999). Although a weaker AhR2 agonist than retene (Barron et al., 2004), fluoranthene can impair CYP1a mediated metabolism by blocking the enzymes active site (Willett et al., 1998). The few laboratory studies on the impact of PAH mixtures containing fluoranthene on developing fish larvae report increased toxicity of fluoranthene-containing mixtures compared to the toxicity of the individual components (Wassenberg and Di Giulio, 2004; Geier et al., 2018). Nonetheless, the underlying mechanism(s) for the stronger toxicity of PAH mixtures containing fluoranthene, relative to the sum of toxicity of the individual mixture components, remains elusive. Consequently, it is important to understand how fluoranthene influences and potentiates the toxicity of a simple PAH mixture, especially from the perspective of environmental risk assessment.

Therefore, by exposing newly hatched and developing rainbow trout alevins (*Oncorhynchus mykiss*) to sub-lethal concentrations of retene and fluoranthene (individually or as a binary mixture), mechanisms related to cardiotoxicity were investigated at the transcriptomic level which in turn were related to effects on the whole organism. A targeted microarray approach was employed as per our previous experience with transcriptomic analysis (Rigaud et al., 2020; Vehniäinen et al., 2016). Rainbow trout was selected as test organism due to its (and other salmonid species') ecological, economical and scientific relevance for sub-arctic and boreal aquatic ecosystems. Cardiac tissue was chosen as the endpoint for transcriptomic investigation due to the heart being among the most sensitive organs to the exposure with PAHs. Differently expressed genes and subsequently over-represented terms and pathways were then compared with the effects on the whole organisms (growth and development, body burden and yolk consumption, the latter functioning as a proxy for energy consumption).

2. Materials and methods

2.1. Setup, maintenance, water analysis, animal care and sampling

Newly hatched (< 24 h) and healthy rainbow trout alevins (360°-days; supplied by Hanka-Taimen OY, Hankasalmi, Finland) were randomly selected and semi-statically exposed to dimethyl sulfoxide (DMSO, control), retene, fluoranthene or the binary mixture of the two PAHs (Table 1) and sampled after 1, 3, 7 and 14 days of exposure.

Exposure concentrations were selected in order to provoke toxicological responses, while avoiding exposure-related mortality. Both Billiard et al. (1999) and Vehniäinen et al. (2016) have reported that exposure to 32 μg l^{-1} of retene fulfills the abovementioned requirements while preliminary testing identified 50 μg l^{-1} of fluoranthene as suitable (unpublished data; exposure to 5, 50 and 500 μg l^{-1} of fluoranthene resulted in 0% mortality over a 11 day period; 3 replicates per concentration and 10 alevins per replicate).

Prior to the initiation of exposure, each exposure vessel was presaturated for 24 h with the corresponding chemicals. Stock water, meant for the exposure studies, was delivered from Konnevesi research station (Central Finland) in February and April 2017; the 14 days exposure took place in February, while the 1, 3 and 7 days exposures were performed in April, using different batches of alevins. Lake water was collected from a depth of 6 m and filtered for debris. The concentration of PAHs in the collected exposure water was below the level of detection. Every exposure was conducted in 1.5 L Pyrex glass bowls filled with 1 L of lake water and the corresponding exposure compound (s) while placed in a Latin square sequence (Fig. s1). Exposure was maintained in a semi-static fashion, which meant complete renewal of water and chemicals on a daily basis. Alevins were collected using a 5 ml plastic Pasteur pipet with a broadened tip and temporarily transferred to a 50 ml plastic centrifugation tube along with some exposure water while the exposure medium was renewed; a process that took less than 30 s per replicate.

In order to generate enough cardiac tissue for RNA extraction, 12 replicate bowls per treatment, (each replicate contained 15 alevins) were maintained for exposures lasting 1, 3 and 7 days while the exposure lasting for 14 days required 8 replicates per treatment, with the same number of alevins per replicate. This translated to 180 alevins per treatment lasting 1, 3 and 7 days while the 14 days exposure required 120 alevins per treatment. An additional bowl per treatment but without alevins was maintained and treated in the same fashion as those containing developing alevins to determine loss of PAHs due to microbial degradation, evaporation or adsorption to the glass bowl. Exposure water temperature, measured daily, was maintained at 11.7 ± 0.4 °C and photoperiodicity was set at 16:8 light to darkness. Water samples were collected prior to water and chemical renewal on Days 1, 3, 7, 10 and 14, diluted 50:50 in ethanol (99.5% purity) and stored at 4 °C for later synchronous fluorescence spectroscopy. Water quality, with regards to pH, conductivity and dissolved oxygen content in aerated stock water, was measured after 1, 3, 5, 7, 10 and 14 days of exposure. The Finnish Environment Institute's database Hertta reports that water from lake Konnevesi contains 7 to 14 μg l^{-1} ammonium (as nitrogen), 0.13 to 0.19 mmol l^{-1} alkalinity and has a Ca+Mg hardness of 0.12 mmol l^{-1}.

Table 1
DMSO, retene and fluoranthene stock solution concentrations (μM; dissolved in DMSO), volume of stock solution added per exposure bowl (μL), nominal exposure concentration (nM), chemical purity (%), supplier and CAS-number. Note: 136.6 nM of retene equals 32 μg L^{-1} while 247.2 nM of fluoranthene equals 50 μg L^{-1}. The nominal concentration of DMSO corresponds to 0.002% which is below the threshold of 0.01% solvent recommended by the OECD (2013) and is thus unlikely to contribute to, or increase, the toxicity of PAHs (Christou et al., 2020; Kais et al., 2013; Maes et al., 2012).

Exposure	Stock solution concentration (μM)	Volume added (μL)	Nominal PAH + DMSO exposure concentrations (nM)	Purity (%)	Supplier	CAS Number
DMSO	Pure DMSO	20	256	≥99.9	Sigma Aldrich	67-68-5
Retene +DMSO	13,655	10 + 10	136.6 + 128	98	MP Biomedical	483-65-3
Fluoranthene + DMSO	24,720	10 + 10	247.2 + 128	≥98	Sigma Aldrich	206-44-0
Retene + Fluoranthene	As above	10 + 10	136.6 + 247.2	As above	As above	As above

At sampling, exposed alevins were photographed next to millimeter scale paper, symptoms of BSD were assessed and hearts excised. Hearts from every alevin from 2 (alevins exposed for 14 days; 30 hearts in total per sample) or 3 (exposed for 1, 3 and 7 days; 45 hearts in total per sample) exposure replicates of the same treatment were pooled, snap frozen in liquid nitrogen and stored at −80 °C for later RNA extraction. Utilizing this approach yielded 4 replicates per treatment for transcriptomic analyzes, of which 3 were processed. The remaining alevins carcasses were pooled based upon replicate, snap frozen in liquid nitrogen and stored at −80 °C for later preparation and HPLC analysis.

2.2. Synchronous fluorescence spectroscopy (SFS) and water quality

This SFS protocol has previously been described by Rigaud et al. (2020), and outlines the analytical protocol for phenanthrene, pyrene and retene. The SFS parameters, although slightly adjusted, were obtained elsewhere (Watson et al., 2004; Turcotte et al., 2011) (Table 2). In short, exposure water from 4 replicates per treatment (selected at random) was sampled after 1, 3, 7, 10 and 14 days of exposure, collected in 20 ml scintillation bottles in a 50:50 mixture with ethanol (99.5% purity) and then stored at 4 °C until analysis. The concentration of retene and fluoranthene were measured using a LS55 Luminescence Spectrometer (PerkinElmer Instruments, USA). Every LS55 measurement was performed in quartz cuvettes (Quartz SUPRASIL® High Precision Cell, Hellma Analytics, Germany) as these PAHs have a low fluorescence at investigated exposure concentrations. Standard curves were created for each PAH which were used to calculate concentration regimes, once normalized against their respective control and using the peak area for retene (290–315 nm) and fluoranthene (270–292 nm).

2.3. Morphometric analyzes

Photos were analyzed utilizing ImageJ (v1.51j8, National Institutes of Health, USA). Using the millimeter paper as a known reference, standard length and planar yolk area were measured *in silico* with high accuracy (3 decimals) and resolution (30 pixels per mm). However, temperature and other abiotic factors are known to affect fish development and due to the architecture of the exposure room and the cooling system, the temperature in the exposure bowls varied spatially (1, 3 and 7 days exposure: 99.9–101.7% relative of replicate 1; 14 days exposure: 98.5–103.6% of control replicate 1; see Fig. s1). Therefore, standard length and yolk area were compensated for the influence of temperature by adjusting for the number of degree-days for every control replicate in relation to control replicate 1, as per Eq. (1):

$$Endpoint_{x-adj.} = Endpoint_X \Big/ \frac{DD_1}{DD_x} \quad (1)$$

Where DD_1 is the number of degree days in control replicate 1 and DD_x represents the degree days in the corresponding control $bowl_x$. The measured endpoint was then divided by the degree-day quota from the same $replicate_x$, thereby adjusting the measurements for the spatial temperature variation. The unadjusted results are presented in Fig. s2.

The BSD-index was established per replicate and calculated according to established convention (Eq. (2)) (Villalobos et al., 2000; Scott et al., 2011). Symptoms of pericardial edemas (PE; scored 0 or 1; not present or present), yolk sac edema (YE; scored 0 or 1) and hemorrhages (HM; scored 0 or 1) were assessed upon sampling. This procedure gave a maximum score of 45 per replicate. Additionally, the effect of the mixture on the BSD index, relative to the components (results adjusted for baseline toxicity among DMSO exposed alevins), was assessed as per combination index (Foucquier and Guedj, 2015).

$$\mathrm{BSD} = \frac{\sum \mathrm{PE} + \sum \mathrm{HM} + \sum YE}{\text{Maximum score}} \quad (2)$$

Inconsistencies in the assessment of BSD symptoms occurred during the sampling of alevins exposed. As a consequence, only half of the replicates were included in the calculation of the BSD-indices of alevins exposed for 1, 3 and 7 days. BSD-indices among alevins sampled after 14 days of exposure were completely omitted due to inconsistent scoring.

Alevins sampled after 14 days of exposure were developmentally assessed and scored based upon pigmentation intensity of the dorsal fin (present/not present) and the lateral side low/high intensity) in accordance with Vernier's rainbow trout developmental catalog (Vernier, 1977), as exemplified in Fig. s3. Formation and development of pigmentation is influenced by AhR2 and thus sensitive to the influence of AhR-agonists (Zodrow and Tanguay, 2003).

2.4. High-Performance liquid chromatography analysis

The body burden of retene and fluoranthene was assessed using a High-Performance Liquid Chromatography (HPLC) approach. For a detailed description on material preparation, analysis and recovery assessment, see supplementary material s1.1. In short, pooled alevin carcasses (10–13 per replicate) were homogenized in 70% acetonitrile (ACN; Fisher Scientific). The homogenate was centrifuged for 15 min at 14,000 rpm in 4 °C (Centrifuge 5415 R, Eppendorf, Germany) and the supernatant collected. The pellet was resuspended in 70% CAN, centrifuged and the supernatant collected and pooled. The resuspension

Table 2
LS55 luminescence synchronous fluorescence spectroscopy parameters used for the identification of retene and fluoranthene.

PAH	Wavelengths measured (nm)	Delta wavelength (Δλ; nm)	Peak (nm)	Excitation slit (nm)	Emission slit (nm)	Scan speed (nm/min)
Retene	250–350	50	290–315	5	5	300
Fluoranthene	200–500	155	270–292	2.5	5	240

processes of the pellet were repeated twice.

An aliquot of the collected supernatant (100 μl; the remaining supernatant was stored at −20 °C) was transferred to a 250 μL glass insert (Agilent Technologies, German) placed in an amber glass vial (Agilent Technologies, Poland). Ten μl of the aliquot were analysis using a Shimadzu U-HPLC Nexera system connected to a RF-20A xs Prominence fluorescence detector (Shimadzu, Japan) with a 150 mm long ACE C18-AR column with a particle size of 5 μm (Advanced Chromatography Technologies LTD, Scotland, UK). The analytical protocol developed allowed for simultaneous measurement of both PAHs in one run, thereby enabling detection of possible PAH cross-contamination. Retene was measured at excitation 259 nm and emission 370 nm with a retention time of 16.71 ± 0.09 min while fluoranthene was measured at excitation 288 nm and emission 525 nm after 13.5 ± 0.21 min. Chromatogram area under the curve (AUC) was manually adjusted and background- (by subtracting the average AUC from DMSO exposed alevins) and recovery compensated. The concentrations were then calculated according to the standard curves and the average PAH body burden (amount) calculated per fish.

2.5. Transcriptomic analysis

RNA was extracted from the pooled fish hearts with TRI Reagent (Molecular Research Center, USA). RNA was quantified using a NanoDrop 1000 v.3.8.1 and NanoDrop 2000 (Thermo Fisher Scientific, USA) and RNA integrity number (RIN) scored using Bioanalyzer RNA 6000 Nano assay kit (Agilent Technologies) according to manufacturer's instructions; lowest measured RIN was 9.8. Extracted RNA was then divided into two aliquots (one for microarray and one for qPCR validation analysis) and stored at −80 °C.

In brief, qPCR analysis was primarily meant as microarray validation, while methodology was first described by Rigaud et al. (2020). In total, 8 different genes related to xenobiotic, energy and iron metabolism, as well as oxidative stress, were analyzed, using *ndufa8* and *rl17* as references due to their transcript stability. For details, see supplementary material s1.2.

Microarray (Agilent 4 × 44 K, Salgeno Design ID 082,522) preparation and analysis were performed at NOFIMA (Ås, Norway) according to a previously developed protocol (Krasnov et al., 2011). First, 220 ng of RNA was labeled with one-color Cy3 dye (Agilent Low Input Quick Amp Labeling Kit; product number 5190–2305), amplified, and purified using Qiagen RNeasy Mini Kit (Qiagen, Germany). Based upon NanoDrop measurement the cRNA concentration (average 266.3 ± 48.9 ng μl^{-1}) and specific Cy3 activity was calculated (average 12.9 ± 2.5 ρmol per μg cRNA). Samples were hybridized overnight at 65 °C using Agilent Gene Expression Hybridization Kit (product number 5188–5242), and the hybridized microarrays were washed using the Agilent Gene Expression Wash Buffer Kit (product number 5188–5327). The hybridized microarrays were then analyzed using the Agilent SureScan Microarray Scanner and the gene expression readings were processed, analyzed and their intensity levels established using Nofima's bioinformatics package (Krasnov et al., 2011). Average microarray intensity levels were normalized and $\log_2$-transformed compared to controls. The bioinformatics package identified differentially expressed genes relative to control using Student's t-test ($p \leq 0.05$). Microarray raw data output is available at ArrayExpress (E-MTAB-8980).

2.6. Over-representation analyzes

Over-representation analyzes (ORAs) were performed using R (v.3.5.1., R Core Team, USA); extended by the packages Bioconductor v3.7 and clusterProfiler v3.8.1 (Boyle et al., 2004; Yu et al., 2012). Gene annotation in clusterProfiler was established using the AnnotationHub database. However, in accordance with Rigaud et al. (2020), as no gene annotation database were available for rainbow trout in AnnotationHub at the time of data analysis, we used zebrafish RefSeq gene ID and symbols and then attributed these to each feature of the microarray. This was achieved using the NCBI BLAST software 2.7.1 (National Center for Biotechnology Information, Bethesda, MD, USA). From the BLAST output, we generated an ORAs background database containing 19,025 unique zebrafish gene IDs (E-values $\geq 10^{-3}$ were removed). Over-representation- and pathway analysis were performed and include Gene Ontologies terms (GO), and KEGGs pathways. P-value cut-off was set to 0.05 and adjusted for multiple comparisons using Benjamini and Hochberg method (Benjamini and Hochberg, 1995). Once ORAs were performed, corresponding genes in relation to enrichment pathways were sorted based upon the exposure duration as to identify the specific genes involved in term- and pathways over-representations (Supplementary file 1).

The microarray profiles were validated by correlation analysis (Spearman's) with the corresponding qPCR results as well as the microarray results for retene, obtained from Rigaud et al. (2020) (Fig. s4).

2.7. Statistics

Statistical analyzes were performed in R-studio version 3.5.1. (R Core Team, USA). Gaussian distribution was tested using Shapiro-Wilk test and variance comparison was tested using one-way ANOVA with Tukey's post-hoc test (Tukey) if the data was normally distributed, otherwise, data were subjected to Kruskal–Wallis (KW) analysis of variance with Dunnett's post-hoc test (Dunn). Mortality and pigmentation were assessed using Fisher's exact test. Comparing the body burden between alevins exposed to retene and fluoranthene alone and part of the mixture was performed using t-test if the data was normally distributed and Mann-Whitney test (MW) if not. Significance- and cut-off value was set at $p \leq 0.05$. All numerical data are presented as mean ± standard deviation.

3. Results

3.1. Exposure parameters

Measured concentrations of PAHs in exposure water varied with time and treatment (Table 3). The concentrations of the two PAHs in exposure water were higher when co-exposed compared to the individual exposures. After 7 and 14 days of exposure, significantly more retene was measured in the samples from mixture exposure water than those from retene only exposures. The same pattern was observed regarding fluoranthene but only after 1 day of exposure. Water quality was within acceptable limits: conductivity 26.83 ± 4.35 mS m^{-1}; oxygen saturation 103.89 ± 5.32%; and pH 7.16 ± 0.10. The high oxygen saturation was due to constant aeration of stock water.

Table 3
Average measured (nM ± standard deviation) and average percentile of nominal concentration (within parentheses) of retene (Ret) and fluoranthene (Flu) in exposure water measured by synchronous fluorescence spectroscopy after 1, 3, 7, 10 and 14 days of exposure. For comparison, the developing alevins were exposed to 247.21 nM of fluoranthene and 136.55 nM of retene (nominally). Statistical differences between measured concentrations are denoted with ¤, * and # for fluoranthene Day 1, retene Day 7 and 14, respectively (*t*-test).

Concentration in nM, mean ± SD (% of nominal)					
	Day 1	Day 3	Day 7	Day 10	Day 14
Ret alone	35 ± 11 (26)	35 ± 11 (26)	30 ± 10 (22)*	26 ± 20 (19)	19 ± 14 (14)#
Ret mix	32 ± 7 (23)	39 ± 8 (29)	53 ± 28 (39)*	35 ± 12 (26)	47 ± 14 (35)#
Flu alone	37 ± 17 (15)¤	62 ± 32 (25)	88 ± 33 (36)	99 ± 75 (40)	113 ± 36 (46)
Flu mix	74 ± 38 (30)¤	76 ± 22 (31)	103 ± 44 (42)	108 ± 71 (44)	113 ± 42 (46)

3.2. Mortality and morphometrics

Mortality never exceeded 6% in any treatment or replicate. A significant difference was observed between alevins exposed to retene and fluoranthene individually and sampled on Day 7 (Table S2). Exposure to the binary mixture resulted in a significantly increased BSD-index on Day 3 and onward compared to control and the individual compounds on day 3 (retene) and 7 (fluoranthene), respectively (Table 4). The BSD-indices among mixture exposed alevins were, on average, greater than the combined additive effect exerted by the components following exposure for 3 and 7 days, when adjusted for baseline toxicity among DMSO exposed alevins.

Furthermore, alevins exposed to retene (for 14 days) and mixture (Days 3 and 14) were significantly shorter compared to control alevins (Fig. 1a). Fluoranthene exposed alevins were significantly shorter after 3 days of exposure compared to control. Retene-exposed alevins had significantly smaller planar yolk area than those exposed to mixture on Day 14 (Fig. 1b). Furthermore, no differences with regards to significances between the different treatments were observed between temperature adjusted and un-adjusted standard lengths (Fig. s2a) and planar yolk areas (Fig. s2b). Alevins exposed for 14 days to fluoranthene and mixture had reduced pigmentation intensity on their lateral side, and all PAH exposures caused hypopigmentation of the dorsal fin (Table 5; Fig. s3).

3.3. Body burden

Each PAH treatment produced exposure specific body burden profiles as exposure to the mixture altered the accumulation pattern of the PAHs compared to alevins exposed to the individual components. In the case of retene, the body burden was significantly increased by 353% after 1 day of exposure, which reached 364% by Day 14, compared to alevins exposed to retene alone (Fig. 2a). The body burden of fluoranthene by contrast was reduced significantly by 60% after 1 day of exposure and by Day 14, the reduction was 94% compared to alevins exposed to fluoranthene alone (Fig. 2b).

Low recovery rates of the two PAHs highlight that the absolute quantification should be considered carefully. Yet, the chromatograms yielded clear exposure specific peaks, which were 122 and 602 times greater for retene and fluoranthene, respectively, than background (control), already after 1 day of exposure.

3.4. Transcriptomic responses

Altogether, 1896 differently expressed genes (DEGs) were identified in rainbow trout heart tissue, independent of exposure duration and across all PAH treatments. Irrespective of exposure duration, exposure to fluoranthene, retene and the mixture results in 344, 937 and 615 DEGs, respectively. Few DEGs were shared among the different exposures and those that were shared were primarily between retene and mixture exposed alevins (Fig. 3a–d). The cardiac microarray results were validated by qPCR analysis as well as by comparing the shared DEGs reported for retene by Rigaud et al. (2020) with ours. In their study, rainbow trout alevins were exposed to retene under nearly identical conditions as those reported in this present study; the only difference being the additional 10 μl of DMSO added to the exposure replicate as per this study. Correlation analysis (Spearman) of the DEGs identified by microarray analysis provided a reliable approach for validation ($R^2 = 0.79$; $p < 0.0001$; Fig. s4) compared to qPCR analysis, which suffered from poorer matching ($R^2 = 0.39$, −0.05, 0.65 and 0.37 on Day 1, 3, 7 and 14, respectively; Table s3). Poorer correlation between the microarray and qPCR could stem from microarray probe sensitivity and specificity in relation to the qPCR primers but also possible degradation of the frozen material used for qPCR validation.

Of the 1896 DEGs identified by the microarray approach, only 6 DEGs were shared among the treatments; *cyp1a* being the only gene consistently upregulated by every treatment. The remaining 5 DEGs shared by all treatments were nebulette (*nebl*, downregulated, day 3), slow myosin heavy chain b (*smyhc2*, downregulated, Day 3), cholesteryl ester transfer protein (*cetp*, upregulated, Day 7), zinc finger protein (*Danio rerio* gene id: 103,910,593; downregulated by retene and upregulated by fluoranthene and mixture, Day 14) and C1q and TNF-like domains (*cbln11*, downregulated, Day 14).

Over-representation analysis revealed that exposure to fluoranthene altered the fewest number of pathways (Figs. 4, 5 and s5). Retene over-represented a vast number of GOs and KEGGs, although several were of low gene count and with overlapping functions. An interesting observation was that retene and fluoranthene over-represented different signaling pathways in a unique fashion and in opposite directions; retene over-represented G-protein signaling (downregulation) whereas fluoranthene affected GABA-signaling (upregulation). Another noteworthy effect of exposure to the individual components was that both exposures resulted in altered expression of genes encoding for components related to cardiac potassium- (*kcnq*) and calcium ion channels (*cacna*).

Exposure to the binary mixture did not over-represent any functions related to cardiac ion channels or signaling. However, the mixture over-represented a wide repertoire of terms and pathways related to metabolism of xenobiotics, amino acid metabolism and biosynthesis, oxidoreductase activity as well as growth and development (details are presented in Supplementary file 1). The most pronounced effect of exposure to the mixture was the stronger and broader upregulation of genes related to phase I and II metabolism compared to the individual PAHs: exposure to retene upregulated *cyp1a*, cytosolic sulfotransferase (*sult1*), UDP-glucuronosyltransferase (*ugtp1a1*) and carbonyl reductase (*cbr1l*) while fluoranthene only upregulated *cyp1a* and glutathione S-transferase P (*gstp*). Consequently, the mixture, but not the components, upregulated processes aimed at counteracting oxidative stress which

Table 4
Average blue sac disease index (BSD; ±SD) per treatment (control = DMSO, retene = Ret, Fluoranthene = Flu and mixture = Mix) sampled after 1, 3 and 7 days of exposure. Occurrence of BSD symptoms (pericardial and yolk sac edemas and hemorrhages) were scored during sampling (Villalobos et al., 2000; Scott et al., 2011). Assessment of BSD among alevins sampled on Day 14 are omitted due to inconsistent scoring during sampling. Significant differences between treatments are denoted with lowercase (Day 3) and uppercase letter (Day 7) ($p < 0.05$; KW + Dunn). Baseline adjusted BSD indices (average BSD index among control alevins subtracted from the average index among PAH exposed alevins) were utilized to assess the effect of the mixture relative to the components (combination index < 1; denoted + (Foucquier and Guedj, 2015)). Note, due to inconsistencies between the samplers, only half of the replicates are included in the calculation of BSD-index.

Exposure duration	BSD indices				Baseline adjustment			
	DMSO	Flu	Ret	Mix	Flu	Ret	Mix	Number of alevins
Day 1	0.03 ± 0.03	0.08 ± 0.10	0.07 ± 0.09	0.10 ± 0.06	0.05	0.04	0.07	90
Day 3	0.20 ± 0.08^{a}	0.34 ± 0.17^{ab}	0.25 ± 0.08^{a}	0.49 ± 0.09^{b}	0.14	0.05	0.29^{+}	90*
Day 7	0.23 ± 0.11^{A}	0.25 ± 0.06^{A}	0.29 ± 0.16^{AB}	0.43 ± 0.10^{B}	0.02	0.06	0.20^{+}	80–90**

*) Flu: $n = 89$.
**) Ret: $n = 80$; DMSO and Mix: $n = 87$; Flu: $n = 90$.
+) Mixture induced a BSD index greater than the additive effect of the components; combination index < 1.

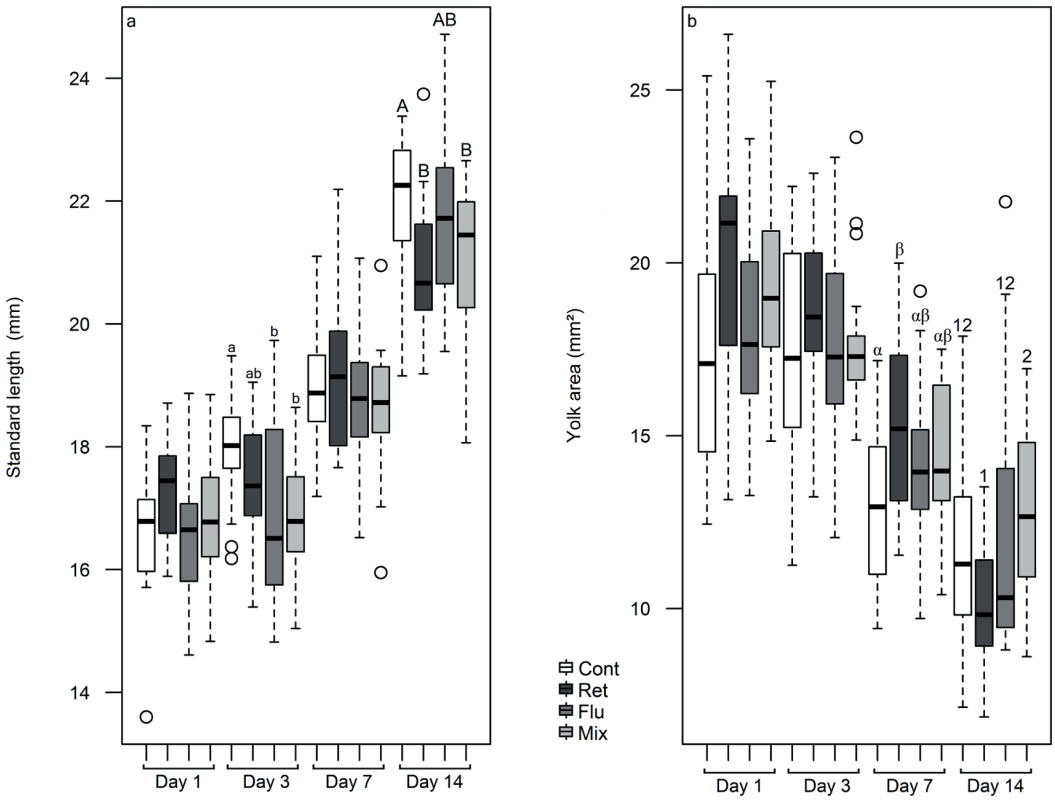

Fig. 1. Boxplot of rainbow trout alevin standard length (growth) (a) and planar yolk area (b) after 1, 3, 7 and 14 days of exposure to DMSO (Cont), retene (Ret), fluoranthene (Flu) and the binary mixture of the two PAHs (Mix). Significant differences ($p < 0.05$; depending on normality, either KW + Dunn or ANOVA + Tukey) are denoted using: (1) different lowercase Latin letters for standard length at Day 3; (2) uppercase Latin letters for standard length at Day 14; (3) Greek letters for yolk area at Day 7; and (4) numbers for yolk area at Day 14. A total of 18 alevins (3 alevins sampled from un-evenly numbered replicates) were analyzed per treatment and sampled after 1, 3 and 7 of exposure while 24 alevins (6 alevins sampled from un-evenly numbered replicates) exposed for 14 days were measured per treatment.

Table 5
Developmental observations (% ± SD) measured as pigmentation intensity of the lateral side (low - high) and the dorsal fin (yes - no) at sampling after 14 days of exposure to control (DMSO), fluoranthene (Flu), retene (Ret) and the binary mixture of the two PAHs (Mix). Significant differences are denoted using lower (lateral side) and uppercase letters (dorsal fin), as per Fisher's exact test. N per treatment = 24; 8 replicates and 3 alevins per replicate.

Tissue type	Outcome	DMSO	Flu	Ret	Mix
Pigmentation intensity of the lateral side	High (%)	83.3 ± 38.1^{a}	66.6 ± 48.2^{b}	70.8 ± 46.4^{ab}	62.5 ± 45.5^{b}
Pigmentation of the dorsal fin	Yes (%)	100^{A}	87.5 ± 33.8^{B}	41.7 ± 50.4^{C}	29.2 ± 46.4^{C}

included both antioxidative- and heat shock processes. Furthermore, exposure to the mixture also over-presented several terms related to growth and development which shifted from embryonic morphogenesis (GO:0048598) by Day 1 to formation- and development of extracellular structures (GO:0005615) and growth and development (GO:0040007 and GO:0048589) by Day 3.

4. Discussion

Exposure to retene and fluoranthene, alone or as a binary mixture, produced exposure specific toxicity profiles; both at the whole organism level and at the transcriptomic level. As expected per previous research (Billiard et al., 2008; Van Tiem and Di Giulio, 2011), the binary mixture produced a stronger toxicity response and a modulated body burden profile compared to exposure to the individual components (while retene being stronger than fluoranthene). Subsequent over-representation analysis of the cardiac transcriptome provided insights on multiple potential molecular responses that can explain the body burden profiles and contribute to the understanding on how PAH induced cardiotoxicity as well as how exposure impacts growth and development. The changes in gene expression are not, however, necessarily specific to the cardiac tissue, and may therefore suggest other types of toxicity as well.

4.1. Effect of exposure on genes involved in heart function and development

Exposure to the PAHs alone, but not the mixture, produced several DEGs that are known to be involved in maintaining heart function and development. Throughout the exposure duration, fluoranthene downregulated *kcnq5b* (Day 3; a component of the slow potassium ion channel which stabilizes the membrane potential (Jentsch, 2000)) and upregulated *cacna1* (Day 7; linked to calcium ion channel function (Grant, 2009)). Exposure to retene resulted in downregulation of 6 types of *kcnq* genes and 4 types of *cacna* genes by Day 14. These alterations suggest a delayed disruption of the action potential and heart function compared to fluoranthene. It is known that PAHs interact with cardiac ion channels which results in alterations of the action potential in cardiomyocytes (Incardona et al., 2011). Ventricular cardiomyocytes (from juvenile rainbow trout) exposed to retene, *in vitro*, resulted in shorter and altered action potential duration while exposure to phenanthrene had less impact (Vehniäinen et al., 2019). It is possible that altered expression pattern of *cacna*- and *kcnq* genes are compensatory mechanisms as to maintain normal heart functions. This assumption is supported by previous research where mice were administrated with the drug ivabradine

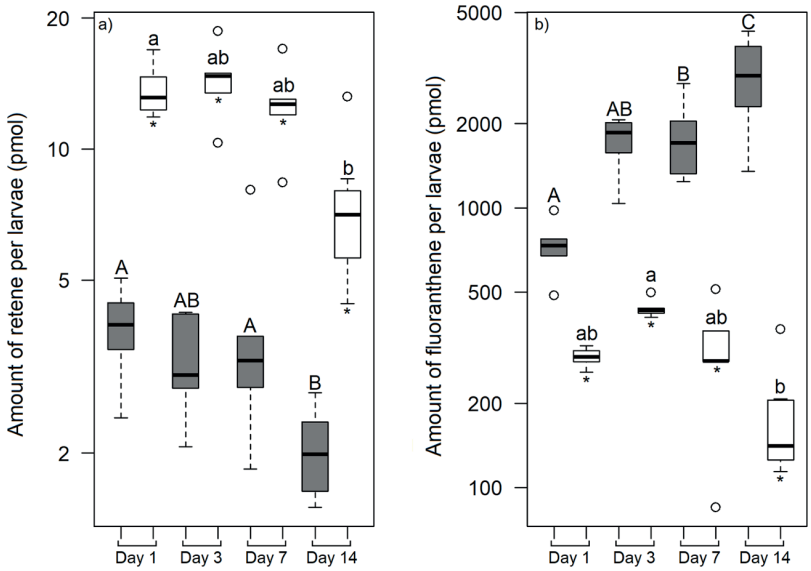

Fig. 2. Boxplot of retene (a; Ret; pMol fish^{-1}) and fluoranthene (b; Flu; pMol fish^{-1}) body burden in whole body rainbow trout alevin carcasses (background compensated) exposed for 1, 3, 7 and 14 days to the PAHs individually (filled boxes) or the binary mixture of the two (Mix, unfilled boxes). Significant differences ($p < 0.05$) in the body burden of retene and fluoranthene among mixture exposed alevins are denoted with lowercase letters, while uppercase letters denote significant differences in body burden among alevins exposed to the individual PAHs (Fluoranthene alone and in mixture: KW + Dunn; Retene alone and in Mix: ANOVA + Tukey). Significant differences in PAH body burden between single and mixture exposed alevins are denoted with a * underneath mixture box plots (Ret: *t*-test; Flu: MW). Note, alevins were exposed to 136.56 nM of retene and 247.21 nM of fluoranthene.

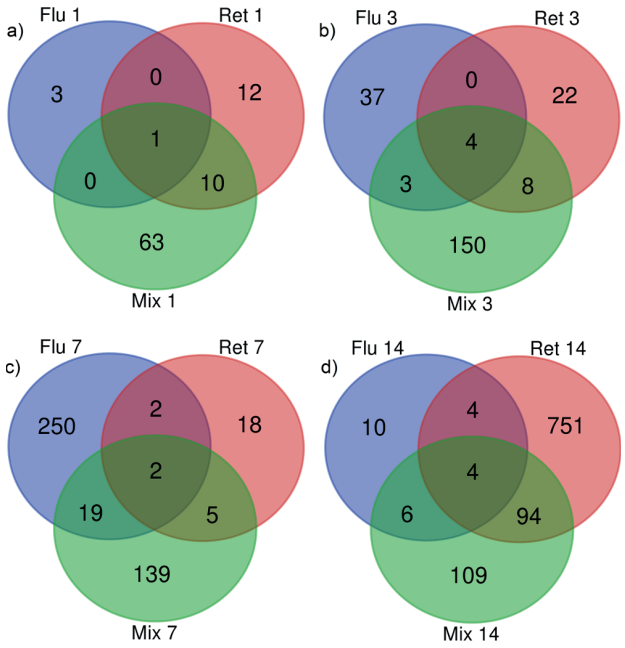

Fig. 3. Venn-diagrams representing the number of differently expressed cardiac genes affected by exposure to retene (Ret; red), fluoranthene (Flu; blue) and the mixture of the two PAHs (Mix; green) following 1 (a), 3 (b), 7 (c) and 14 (d) days of exposure. The Venn-diagram was created using the online platform provided by Bioinformatics & Evolutionary Genomics.

(reduces the heart rate by affecting the cardiac pacemaker cells (Bois et al., 1996)), which resulted in altered expression of a number of genes encoding for ion channels in the sinoatrial node of mouse heart and to a lesser extent, the ventricle (Leoni et al., 2006). In contrast to the individual PAHs, exposure to the mixture, independent of exposure duration, did not over-represent or alter the expression of any gene related to cardiac ion channels. However, it cannot be ruled out that exposure to the mixture affected heart function through other mechanisms without giving rise to a transcriptomic response(s).

Similar cardiac transcriptomic alterations have previously been reported in fish exposed to retene or fluoranthene. Jayasundara et al. (2014) exposed newly hatched zebrafish to a combination of benzo[*a*]pyrene and fluoranthene (albeit at much higher concentrations than used in this study) and identified a number of exposure-specific changes in the cardiac over-representation profiles and DEGs related to calcium ion homeostasis, embryonic development and cardiovascular system development and function. Both Vehniäinen et al. (2016) and Rigaud et al. (2020) exposed newly hatched rainbow trout alevins to retene (using the same setup as presented in this study) and assessed the cardiac transcriptome (the results reported by the latter correlated well with those presented here). Among the numerous over-representations related to cardiac function and development, the former reported over-representation of signaling transduction, growth, and cardiovascular development, while the latter reported over-representation of calcium, sodium, and potassium ion channel function, homeostasis and muscle contraction. Therefore, their results, when considered along those presented here, provide ample support to the notion that PAHs affect heart function through multiple pathways and that there is a transcriptomic component involved in the development of PAH induced cardiotoxicity. However, it is unknown if these DEGs are compensatory with regards to exposure or a direct effect of exposure, nor if they are specific to the heart only or differently expressed in a similar fashion in other tissues.

A striking difference in gene expression and over-representation was found in alevins exposed to fluoranthene or retene alone. Both exposures over-represented several terms and pathways related to cellular- and transmembrane signaling (high gene count and significance), including signaling receptor activity (GO:0038023) and neuroactive ligand receptor interactions (dre04080). The direction of expression of the involved DEGs constituting these terms and pathways were both exposure and signaling pathway specific, as exposure to fluoranthene (Day 7) resulted in the upregulation of involved DEGs involved in GABA receptor complex signaling (GO:1902710), while exposure to retene resulted in downregulation of G protein-coupled receptor signaling (GO:0007186; Day 14). These exposure specific impacts highlight potential exposure specific signaling disruption. Over-representation of GABA receptor complex and upregulation of the involved DEGs, following exposure to fluoranthene, suggests an increase in GABA receptor activation and consequently less parasympathetic influence on blood pressure and heart function through the vagus nerve (Leite et al., 2009; Bentzen and Grunnet, 2011). By contrast, prolonged saturation and activation of G-protein receptors can lead to downregulation of genes encoding for the receptors (Tsao and von Zastrow, 2000). Why

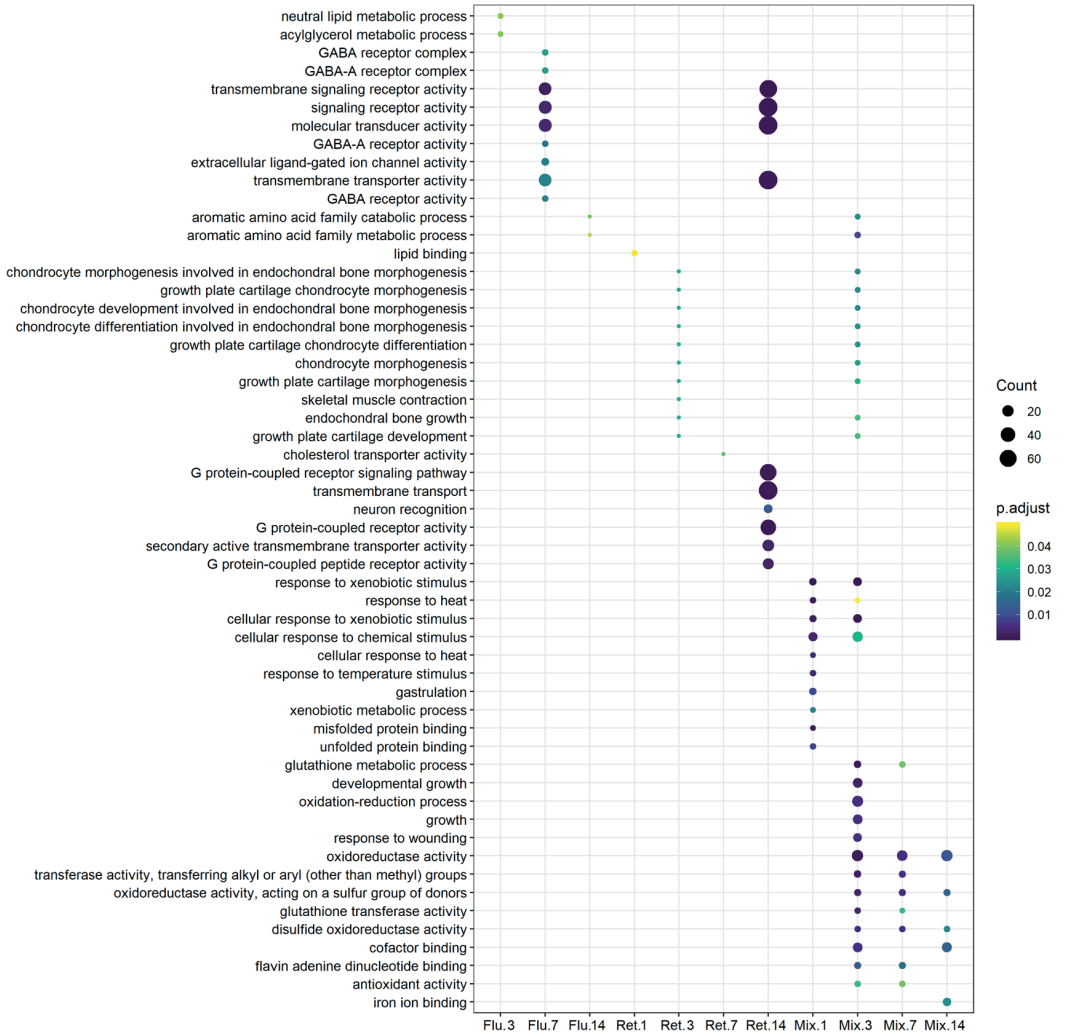

Fig. 4. Over-representation analysis of gene ontology (GO) groups following exposure to retene (Ret), fluoranthene (Flu) and the binary mixture (Mix) lasting for 1, 3, 7 and 14 days. Data was analyzed, p-value adjusted and plotted using clusterProfiler. The size of each dot equals the number of genes involved in each GO-term. Note: due to figure size limitations, Fig. 3 contains 54 out a total of 135 over-represented GO-term (whole data is presented in Fig. s5).

exposure to retene and fluoranthene over-represented signaling pathways so specifically is currently unknown but requires further investigation. However, it may be that the specificity is linked to how the PAHs interact with cardiomyocyte ion-channels and subsequently alter the repolarization of cardiac action potential, thus making these over-representations compensatory rather than a direct consequence of exposure. Yet, it is unknown if this phenomenon is heart-specific or if it could take place in other tissues as well. Additionally, the fact that these two over-representations only occurred among alevins exposed for 7 and 14 days supports the view that certain endpoints require extended exposure duration (or have to take place at a specific developmental stage) before the compensatory events become manifested in the developing organism (Price and Mager, 2020).

4.2. Body burden and xenobiotic metabolism

Unique and exposure specific body burden profiles were obtained already after 1 day of exposure and throughout the exposure duration, suggesting exposure specific phase I and II metabolic profiles. The body burden of retene was significantly reduced by Day 14, compared to Day 1, following exposure to retene alone or as a mixture (albeit significantly more abundant in mixture exposed alevins). By contrast, exposure to fluoranthene alone resulted in a significantly increased body burden by Day 7 and onward, which can be attributed to partial inhibition of the catalytic function of CYP1a by fluoranthene, alongside activation of a narrow suite of phase II metabolic processes. When co-administered with retene, the body burden of fluoranthene increased non-significantly from Day 1 to Day 3 before decreasing significantly with time. Similar changes in the body burden profiles of PAHs have previously been observed in rainbow trout exposed to a binary mixture of alpha-naphthoflavone (ANF; a CYP1a inhibitor) and retene (Hodson et al., 2007). Their specific binary mixture resulted in increased body burden of retene with increased dose of ANF. Changes in the body burden profiles of specific PAHs do not seem to be species specific as per previous observations in zebrafish exposed to a complex mixture of PAHs and a binary mixture of the AhR2 agonist beta-naphthoflavone and ANF (Timme-Laragy et al., 2007; Geier et al., 2018). Hence, the body burden of PAHs is both PAH and mixture specific while the underlying molecular processes resulting in the subsequent body burden profiles are related to accumulation in relation to metabolism. However, due to low recovery rates of the PAHs, the quantification of body burden should be considered carefully. Nonetheless, the low recovery rates appear justifiable in light of the similar recovery rates of retene (14.3%) and fluoranthene (14.6%) as well as the ratio between the subsequent

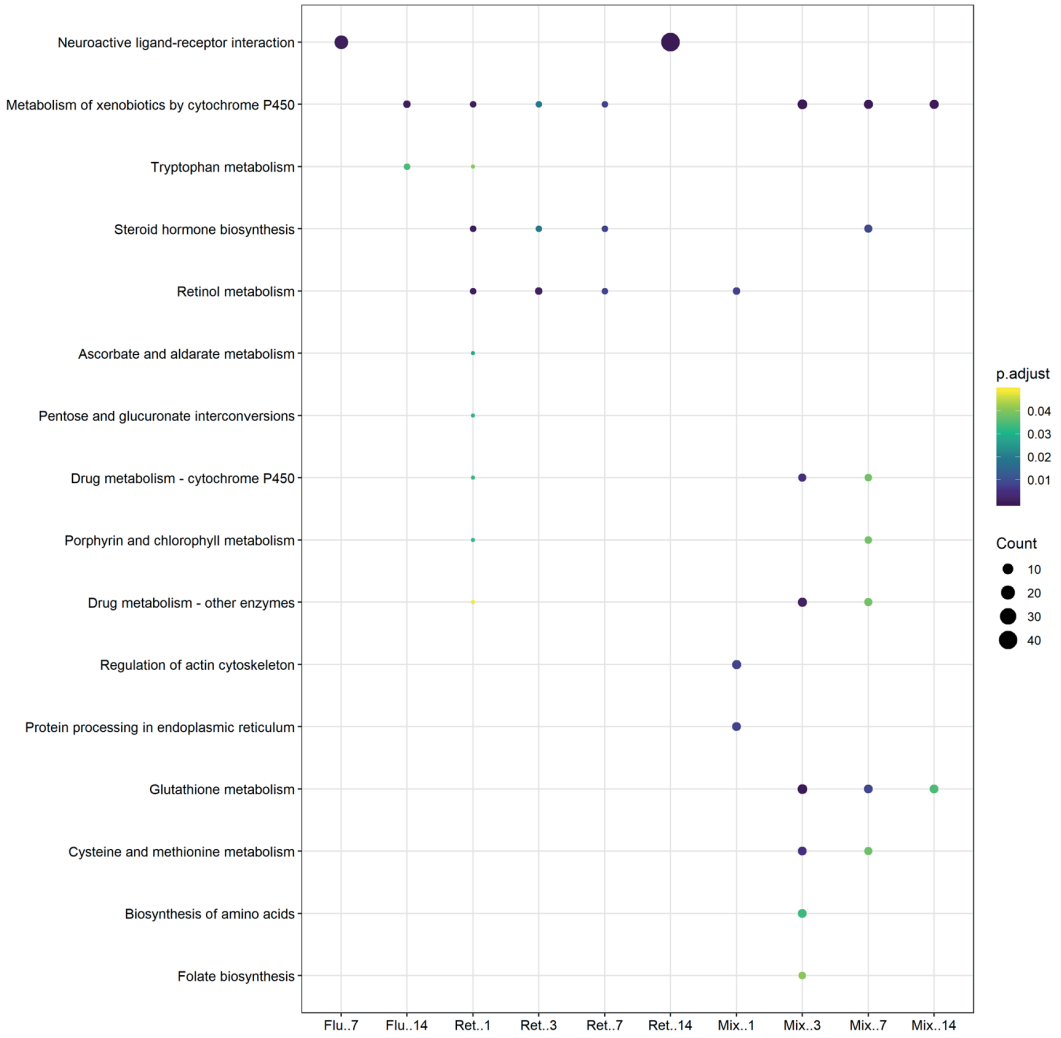

Fig. 5. Over-representation analysis of KEGG (Kyoto Encyclopedia of Genes and Genomes) pathways following exposure to retene (Ret), fluoranthene (Flu) and the binary mixture (Mix) lasting for 1, 3, 7 and 14 days. Data was analyzed, p-value adjusted and plotted using clusterProfiler. Dot size equals the number of genes involved in each KEGG-term.

body burden profiles (alevins exposed to the individual PAH compared to the mixture) and the exposure specific temporal accumulation patterns.

Possible molecular explanations to the exposure specific body burden profiles were present in the cardiac transcriptome. Through over-representation analysis, we found that the GO-term: cellular response to chemical stimulus (GO:0070887; mixture); and the KEGG: metabolism of xenobiotics by cytochrome P450 (dre00980; retene and mixture) best explained the body burden profiles. It must be noted that several uncertainties are involved when drawing conclusions on metabolism-related functions based upon a cardiac transcriptome, primarily that heart tissue is less metabolically active compared to the liver. Secondly, a differently expressed gene does not necessarily result in an equally enriched protein. However, the genes involved in above-mentioned GO-terms and KEGG pathways were upregulated in an exposure specific pattern, which suggests a strong relationship between the body burden profiles and expression of genes encoding for metabolic enzymes.

Fish exposed to certain PAHs are known to induce *cyp1a* (Nebert and Gonzalez, 1987; Shankar et al., 2019). Exposure to retene resulted in upregulation of *cyp1a* alongside cytosolic sulfotransferase (*sult1*), carbonyl reductase (*cbr1l*) and UDP-glucuronosyltransferase (*ugt1a1*), which is in accordance with the metabolism of retene as described by Huang et al. (2017). Exposure to fluoranthene over-represented no metabolism-related pathways but upregulated two genes related to xenobiotic metabolism: *cyp1a* (phase I) and glutathione s-transferase (*gst*; phase II), indicating AhR-activation and metabolism through oxidation, and conjugation by gst, which suggests that electrophiles are formed during phase I metabolism. However, as the body burden of fluoranthene constantly increased throughout the exposure period, it can be concluded that the capacity of the activated metabolic processes is rather low. These findings comply with the ability of fluoranthene to induce *cyp1a*-expression through AhR-activation alongside inhibition of the catalytic function of the corresponding enzyme, which together with a lower rate of metabolism would force fluoranthene to accumulate with time, as observed previously by Willet et al. (1998). Co-exposure upregulated abovementioned phase I and II metabolic genes plus a wider battery of genes involved in the metabolism of xenobiotics. This broader activation of phase I and II genes facilitated metabolism of both retene and fluoranthene as per the altered body burden profiles compared to those yielded from alevins exposed to the individual components.

An interesting aspect of *cyp1a* is how the expression varied with exposure and over time. Following exposure to retene and the mixture, the expression of *cyp1a* decreased with time and reached similar

expression levels by Day 14. In the case of retene the expression (log_2 fold change) decreased from 3.91 by Day 1 to 1.35 by Day 14, while the expression in mixture exposed alevins decreased from 5.35 to 1.30 over the same exposure duration. These trends of *cyp1a* expression correspond well with the decreasing body burden of retene with time (and fluoranthene when co-administrated with retene), yet it is plausible that the shift in metabolic capability is related to a more developed liver. Such correlation pattern was not present in alevins exposed to fluoranthene alone. Among those alevins, the expression of *cyp1a* remained stable over time, from an upregulation of 2.65 by Day 1 to 2.68 by Day 14, while the body burden of fluoranthene constantly increased. It is unclear if the hepatic expression of *cyp1a* would follow similar trends or increase throughout the exposure duration; an aspect that should be investigated further.

Activation of xenobiotic metabolism is associated with increased oxidative stress due to the formation of radical intermediates (Halliwell and Gutteridge, 1985). Exposure to the mixture (Day 3 and onward) resulted in the over-representation of the GO-term oxidoreductase activity (GO:0016491). In addition to metabolism-related genes, this specific GO-term highlighted DEGs encoding for proteins involved in oxidative stress response (*gsr, gsto1, nqo1, prdx1, txn*, and *txnrd3*). Said over-representation and upregulations suggest that exposure to the mixture resulted in increased oxidative stress. The underlying cause(s) can plausibly be linked to the metabolism of the xenobiotics, partial CYP1a-inhibition, accumulation of parental and metabolized PAHs and the formation of endogenous metabolites (Rannug and Rannug, 2018). In addition to these anti-oxidative responses, there is transcriptomic evidence that exposure to the mixture caused cellular stress as per increased expression of genes encoding for heat shock proteins: *hsp90A1,* (also among retene exposed alevins), *hsp70L* and *-A8*. Upregulation of *hsp*-genes and enrichment of the corresponding proteins are linked to increased oxidative stress and protein damage (Sanders, 1993). Similar upregulation of *hsp*-genes and proteins have been reported in different species of fish exposed to retene (Räsänen et al., 2012; Vehniäinen et al., 2016) and other PAHs (Song et al., 2019). Combined, upregulation of the abovementioned genes suggests that retene alone or combined with fluoranthene potentially increases cellular stress and protein damage during the first few days of exposure, before the liver reached a certain level of maturation.

4.3. Growth and development

Reduction of standard length was not consistent over time as significant impacts were observed after 3 days of exposure (fluoranthene and mixture exposed alevins relative to control), but not after 7 days. Interestingly, exposure to the mixture for 3 and 7 days, but not the components, resulted in a significantly increased BSD-index compared to control, which were also greater than additive effect of the components (adjusted for baseline toxicity of control). However, a greater BSD-index among mixture exposed alevins was expected and consistent with previous observations on PAH exposed and developing fish (Geier et al., 2018). By Day 14, alevins exposed to retene and the binary mixture were significantly shorter than control alevins, while retene exposed alevins had consumed significantly more yolk than alevins exposed to the mixture. This combination of reduced standard length but differently sized planar yolk areas highlight that growth and development were impacted in an exposure-specific fashion. These differences are plausibly related to the development and formation of sub-intestinal venous plexus which, with time, encases the yolk sac (Goi and Childs, 2016). Furthermore, based upon patterns and intensity of pigmentation, alevins exposed to any of the PAH treatments appeared to be at an earlier developmental stage by Day 14 compared to control, irrespective of how the exposure affected standard length and yolk consumption. This could have implications for the toxicological and transcriptional assessment; are the exposed alevins just shorter or at an earlier developmental stage. What caused hypopigmentation is unknown. However, considering that hyperpigmentation has been observed in zebrafish larvae exposed to the dioxin TCDD (Zodrow and Tanguay, 2003), it is plausible that the hypopigmentation observed in our study equates to an earlier developmental stage.

Central to maintaining normal development post hatching in fish larvae is the consumption of yolk, which is the sole source of energy during early life development before the larvae can actively feed. Impaired absorption of yolk would therefore affect the whole developing organism negatively (Laurel et al., 2019). Additional stress is exerted upon the developing organism due to increased energy requirements set by constantly maintained phase I and II metabolic activity, while at the same time counteracting increased oxidative stress. Over-representation analysis identified several impacted pathways that are involved in growth and development in mixture exposed alevins, but not following exposure to the individual components. After 1 day of exposure, embryonic morphogenesis (GO:0048598) was over-represented which shifted to developmental growth (GO:0048589), growth (GO:0040007) and extracellular region, parts and space (GO:0005615; GO:0005576; GO:0044421) by Day 3. These findings imply potential defects in cardiac development and growth, which could affect cardiac function and thereby the growth of the alevins. However, inferring that the identified alterations in the cardiac transcriptome serves as the principal origin for the impact on growth and development of the organism has several limitations: primarily due to the organ specificity, but also due to the fact that cross-communication between several organs and tissues, often along endocrine axes, is required to facilitate growth and development (Dickhoff et al., 1997).

Impaired heart function may restrict the circulation of nutrients and energy, which in turn could force amino acids catabolism as an alternative energy source. Restriction(s) in the availability of nutrients are suggested by upregulation of tyrosine aminotransferase (*tat*; mixture) and fumarylacetoacetate hydrolase (*fah*; mixture and fluoranthene). Upregulation of these genes indicate increased transformation rate of phenylalanine to tyrosine by Tat, which in turn is converted to fumarate or pyruvate by Fah. The latter two compounds are components that can fuel the citric acid cycle and thus provide energy. It is possible that impaired and decreased absorption of yolk, reduced availability of nutrients, and energy being reallocated away from growth to fuel metabolism could be part of the underlying rationale on why exposure affected development and growth.

5.1. Conclusive remarks

The cardiac transcriptome of rainbow trout alevins exposed jointly to retene and fluoranthene had few overlaps compared with alevins exposed to the individual compounds. This was especially evident in the expression of genes related to metabolism of xenobiotics (phase I and II), which in turn corresponded with, and explained the exposure-specific body burden profiles. The reduced standard length and slower development among retene and mixture exposed alevins could, partly, be caused by common mechanisms such as reallocation of energy to fuel xenobiotic metabolism and counteract increased oxidative stress. All in all, the combination of retene and fluoranthene increased the overall toxicity when compared to the individual components at several levels of biological organization, highlighting the fact that the toxicity of the mixture cannot be assessed from its individual components alone.

Ethical approval

Under the European Union Directive 2010/63/EU, Chapter 1, Article 1, point 3: no ethical approval is required for *in vivo* experiments on non-human vertebrates who fulfills their nutritional requirements through the consumption of yolk.

Funding sources

Academy of Finland project number: 285296, 294066 and 319284 granted to Eeva-Riikka Vehniäinen.

CRediT authorship contribution statement

Andreas N.M. Eriksson: Visualization, Writing – review & editing, Writing – original draft, Data curation, Resources, Investigation, Formal analysis, Conceptualization, Methodology, Validation. **Cyril Rigaud:** Writing – review & editing, Data curation, Resources, Investigation, Formal analysis, Conceptualization, Methodology, Validation. **Aleksei Krasnov:** Writing – review & editing, Data curation, Resources, Validation. **Emma Wincent:** Writing – review & editing, Methodology, Validation. **Eeva-Riikka Vehniäinen:** Supervision, Project administration, Funding acquisition, Writing – review & editing, Data curation, Resources, Validation.

Declaration of Competing Interest

The authors declare that they have no known competing financial interests or personal relationships that could have appeared to influence the work reported in this paper.

Acknowledgment

We acknowledge the contribution of laboratory technicians Mervi Koistinen, Emma Pajunen, Hannu Pakkanen and the laboratory personnel at Konnevesi research station for technical support as well as the master student Terhi Rahkonen for assessing fluoranthene lethality. We also like to thank Hanka-Taimen OY fish farm for supplying us with rainbow trout alevins for scientific purposes and research. Finally, we thank the anonymous peer reviewers who provided valuable feedback.

Supplementary materials

Supplementary material associated with this article can be found, in the online version, at doi:10.1016/j.aquatox.2022.106083.

References

Barron, M.G., Heintz, R., Rice, S.D., 2004. Relative potency of PAHs and heterocycles as aryl hydrocarbon receptor agonists in fish. Mar. Environ. Res. 58, 95–100.
Bauder, M.B., Palace, V.P., Hodson, P.V., 2005. Is oxidative stress the mechanism of blue sac disease in retene-exposed trout larvae? Environ. Toxicol. Chem. 24, 694–702.
Benjamini, Y., Hochberg, Y., 1995. Controlling the false discovery rate: a practical and powerful approach to multiple testing. J. R. Stat. Soc.Ser. B Methodol. 57, 289–300.
Bentzen, B.H., Grunnet, M., 2011. Central and peripheral GABA(A) receptor regulation of the heart rate depends on the conscious state of the animal. Adv. Pharmacol. Sci. 2011, 578273.
Billiard, S.M., Hahn, M.E., Franks, D.G., Peterson, R.E., Bols, N.C., Hodson, P.V., 2002. Binding of polycyclic aromatic hydrocarbons (PAHs) to teleost aryl hydrocarbon receptors (AHRs). Comp. Biochem. Physiol. Part B Biochem. Mol. Biol. 133, 55–68.
Billiard, S.M., Meyer, J.N., Wassenberg, D.M., Hodson, P.V., Di Giulio, R.T., 2008. Nonadditive effects of PAHs on early vertebrate development: mechanisms and implications for risk assessment. Toxicol. Sci. Off. J. Soc. Toxicol. 105, 5–23.
Billiard, S.M., Querbach, K., Hodson, P.V., 1999. Toxicity of retene to early life stages of two freshwater fish species. Environ. Toxicol. Chem. 18, 2070–2077.
Bois, P., Bescond, J., Renaudon, B., Lenfant, J., 1996. Mode of action of bradycardic agent, S 16257, on ionic currents of rabbit sinoatrial node cells. Br. J. Pharmacol. 118, 1051–1057.
Boyle, E.I., Weng, S., Gollub, J., Jin, H., Botstein, D., Cherry, J.M., Sherlock, G., 2004. GO:TermFinder–open source software for accessing gene ontology information and finding significantly enriched gene ontology terms associated with a list of genes. Bioinformatics 20, 3710–3715.
Brown, D.R., Clark, B.W., Garner, L.V.T., Di Giulio, R.T., 2015. Zebrafish cardiotoxicity: the effects of CYP1A inhibition and AHR2 knockdown following exposure to weak aryl hydrocarbon receptor agonists. Environ. Sci. Pollut. Res. 22, 8329–8338.
Christou, M, Kavaliauskis, A, Ropstad, E, Fraser, T.W.K, 2020. DMSO effects larval zebrafish (Danio rerio) behavior, with additive and interaction effects when combined with positive controls. Sci.Total Environ 709 (134490). https://doi.org/10.1016/j.scitotenv.2019.134490.
Colavecchia, M., Hodson, P., Parrott, J., 2006. CYP1A induction and blue sac disease in early life stages of white suckers (*catostomus commersoni*) exposed to oil sands. J. Toxicol. Environ. Health Part A 69, 967–994.
Dickhoff, W.W., Beckman, B.R., Larsen, D.A., Duan, C., Moriyama, S., 1997. The role of growth in endocrine regulation of salmon smoltification. Fish Physiol. Biochem. 17, 231–236.
Foucquier, J., Guedj, M., 2015. Analysis of drug combinations: current methodological landscape. Pharmacol. Res. Perspect. 3, e00149.
Gabos, S., Ikonomou, M.G., Schopflocher, D., Fowler, B.R., White, J., Prepas, E., Prince, D., Chen, W., 2001. Characteristics of PAHs, PCDD/Fs and PCBs in sediment following forest fires in Northern Alberta. Chemosphere 43, 709–719.
Geier, M.C., James Minick, D., Truong, L., Tilton, S., Pande, P., Anderson, K.A., Teeguardan, J., Tanguay, R.L., 2018. Systematic developmental neurotoxicity assessment of a representative PAH Superfund mixture using zebrafish. Toxicol. Appl. Pharmacol. 354, 115–125.
Goi, M., Childs, S.J., 2016. Patterning mechanisms of the sub-intestinal venous plexus in zebrafish. Dev. Biol. 409, 114–128.
Grant, A., 2009. Cardiac ion channels. Circ. Arrhythm. Electrophysiol. 2, 185–194.
Halliwell, B., Gutteridge, J.M.C., 1985. The importance of free radicals and catalytic metal ions in human diseases. Mol. Asp. Med. 8, 89–193.
Haritash, A.K., Kaushik, C.P., 2009. Biodegradation aspects of polycyclic aromatic hydrocarbons (PAHs): a review. J. Hazard. Mater. 169, 1–15.
Hodson, P.V., Qureshi, K., Noble, C.A.J., Akhtar, P., Brown, R.S., 2007. Inhibition of CYP1A enzymes by alpha-naphthoflavone causes both synergism and antagonism of retene toxicity to rainbow trout (*Oncorhynchus mykiss*). Aquat. Toxicol. 81, 275–285.
Huang, M., Mesaros, C., Hackfeld, L.C., Hodge, R.P., Zang, T., Blair, I.A., Penning, T.M., 2017. Potential metabolic activation of a representative C4-alkylated polycyclic aromatic hydrocarbon retene (1-methyl-7-isopropyl-phenanthrene) associated with the deepwater horizon oil spill in human hepatoma (HepG2) cells. Chem. Res. Toxicol. 30, 1093–1101.
Incardona, J.P., Linbo, T.L., Scholz, N.L., 2011. Cardiac toxicity of 5-ring polycyclic aromatic hydrocarbons is differentially dependent on the aryl hydrocarbon receptor 2 isoform during zebrafish development. Toxicol. Appl. Pharmacol. 257, 242–249.
Jayasundara, N., Van Tiem Garner, L., Meyer, J.N., Erwin, K.N., Di Giulio, R.T., 2014. AHR2-mediated transcriptomic responses underlying the synergistic cardiac developmental toxicity of PAHs. Toxicol. Sci. 143, 469–481.
Jentsch, T.J., 2000. Neuronal KCNQ potassium channels:physislogy and role in disease. Nat. Rev. Neurosci. 1, 21–30.
Kais, B, Schneider, K.E, Keiter, s, Henn, K, Ackermann, C, Braunbeck, T, 2013. DMSO modifies the permeability of the zebrafish (Danio rerio) chorion-Implications for the fish embryo test (FET). Aquatic Toxicology 140–141, 229–238. https://doi.org/10.1016/j.aquatox.2013.05.022.
Krasnov, A., Timmerhaus, G., Afanasyev, S., Jørgensen, S.M., 2011. Development and assessment of oligonucleotide microarrays for Atlantic salmon (*Salmo salar* L.). Comp. Biochem. Physiol. Part D Genom. Proteom. 6, 31–38 this special issue contains papers which stem from a presentation at the genomics in aquaculture symposium held in bodø, on 5th-7th July 2009.
Laurel, B.J., Copeman, L.A., Iseri, P., Spencer, M.L., Hutchinson, G., Nordtug, T., Donald, C.E., Meier, S., Allan, S.E., Boyd, D.T., Ylitalo, G.M., Cameron, J.R., French, B.L., Linbo, T.L., Scholz, N.L., Incardona, J.P., 2019. Embryonic crude oil exposure impairs growth and lipid allocation in a keystone arctic forage fish. Iscience 19, 1101–1113.
Leite, C.A., Taylor, E.W., Guerra, C.D.R., Florindo, L.H., Belão, T., Rantin, F.T., 2009. The role of the vagus nerve in the generation of cardiorespiratory interactions in a neotropical fish, the pacu, *Piaractus mesopotamicus*. J. Comp. Physiol. A 195, 721–731.
Leoni, A., Marionneau, C., Demolombe, S., Bouter, S.L., Mangoni, M.E., Escande, D., Charpentier, F., 2006. Chronic heart rate reduction remodels ion channel transcripts in the mouse sinoatrial node but not in the ventricle. Physiol. Genom. 24, 4–12.
Leppänen, H., Oikari, A., 1999. Occurrence of retene and resin acids in sediments and fish bile from a lake receiving pulp and paper mill effluents. Environ. Toxicol. Chem. 18, 1498–1505.
Maes, J, Verlooy, L, Buenafe, O.E, de Witte, P.A.M, Esguerra, C.V, Crawford, A.D, 2012. Evaluation of 14 Organic Solvents and Carriers for Screening Applications in Zebrafish Embryos and Larvae. PLOS ONE 7 (e43850). https://doi.org/10.1371/journal.pone.0043850.
Nebert, D., Gonzalez, F., 1987. P450 genes: structure, evolution, and regulation. Annu. Rev. Biochem. 56, 945–993.
Page, D.S., Boehm, P.D., Douglas, G.S., Bence, A.E., Burns, W.A., Mankiewicz, P.J., 1999. Pyrogenic polycyclic aromatic hydrocarbons in sediments record past human activity: a case study in Prince William sound, Alaska. Mar. Pollut. Bull. 38, 247–260.
Price, E.R., Mager, E.M., 2020. The effects of exposure to crude oil or PAHs on fish swim bladder development and function. Comp. Biochem. Physiol. Part C Toxicol. Pharmacol. 238, 108853.
Rannug, A., Rannug, U., 2018. The tryptophan derivative 6-formylindolo[3,2-b]carbazole, FICZ, a dynamic mediator of endogenous aryl hydrocarbon receptor signaling, balances cell growth and differentiation. Crit. Rev. Toxicol. 48, 555–574.
Räsänen, K., Arsiola, T., Oikari, A., 2012. Fast genomic biomarker responses of retene and pyrene in liver of juvenile rainbow trout, *oncorhynchus mykiss*. Bull. Environ. Contam. Toxicol. 89, 733–738.
Rhodes, S., Farwell, A., Mark Hewitt, L., MacKinnon, M., George Dixon, D., 2005. The effects of dimethylated and alkylated polycyclic aromatic hydrocarbons on the embryonic development of the Japanese medaka. Ecotoxicol. Environ. Saf. 60, 247–258.

Rigaud, C., Eriksson, A., Krasnov, A., Wincent, E., Pakkanen, H., Lehtivuori, H., Ihalainen, J., Vehniäinen, E., 2020. Retene, pyrene and phenanthrene cause distinct molecular-level changes in the cardiac tissue of rainbow trout (*Oncorhynchus mykiss*) larvae, part 1 – transcriptomics. Sci. Total Environ. 745, 141031.
Sanders, B.M., 1993. Stress proteins in aquatic organisms: an environmental perspective. Crit. Rev. Toxicol. 23, 49–75.
Scott, J.A., Hodson, P.V., 2008. Evidence for multiple mechanisms of toxicity in larval rainbow trout (*Oncorhynchus mykiss*) co-treated with retene and α-naphthoflavone. Aquat. Toxicol. 88, 200–206.
Scott, J.A., Incardona, J.P., Pelkki, K., Shepardson, S., Hodson, P.V., 2011. AhR2-mediated, CYP1A-independent cardiovascular toxicity in zebrafish (*Danio rerio*) embryos exposed to retene. Aquat. Toxicol. 101, 165–174.
Shankar, P., Geier, M.C., Truong, L., McClure, R.S., Pande, P., Waters, K.M., Tanguay, R. L., 2019. Coupling genome-wide transcriptomics and developmental toxicity profiles in zebrafish to characterize polycyclic aromatic hydrocarbon (PAH) hazard. Int. J. Mol. Sci. 20, 2570.
Song, Y., Nahrgang, J., Tollefsen, K.E., 2019. Transcriptomic analysis reveals dose-dependent modes of action of benzo(a)pyrene in polar cod (*Boreogadus saida*). Sci. Total Environ. 653, 176–189.
Timme-Laragy, A., Cockman, C.J., Matson, C.W., Di Giulio, R.T., 2007. Synergistic induction of AHR regulated genes in developmental toxicity from co-exposure to two model PAHs in zebrafish. Aquat. Toxicol. 85, 241–250.
Tsao, P., von Zastrow, M., 2000. Downregulation of G protein-coupled receptors. Curr. Opin. Neurobiol. 10, 365–369.
Turcotte, D., Akhtar, P., Bowerman, M., Kiparissis, Y., Brown, R.S., Hodson, P.V., 2011. Measuring the toxicity of alkyl-phenanthrenes to early life stages of medaka (*Oryzias latipes*) using partition-controlled delivery. Environ. Toxicol. Chem. 30, 487–495.
Van Metre, P.C., Mahler, B.J., Furlong, E.T., 2000. Urban sprawl leaves its pah signature. Environ. Sci. Technol. 34, 4064–4070.
Van Tiem, L.A., Di Giulio, R.T., 2011. AHR2 knockdown prevents PAH-mediated cardiac toxicity and XRE- and ARE-associated gene induction in zebrafish (*Danio rerio*). Toxicol. Appl. Pharmacol. 254, 280–287.
Vehniäinen, E., Bremer, K., Scott, J.A., Junttila, S., Laiho, A., Gyenesei, A., Hodson, P.V., Oikari, A.O.J., 2016. Retene causes multifunctional transcriptomic changes in the heart of rainbow trout (*Oncorhynchus mykiss*) embryos. Environ. Toxicol. Pharmacol. 41, 95–102.
Vehniäinen, E., Haverinen, J., Vehniäinen, E., 2019. Polycyclic aromatic hydrocarbons phenanthrene and retene modify the action potential via multiple ion currents in rainbow trout *oncorhynchus mykiss* cardiac myocytes. Environ. Toxicol. Chem. 38, 2145–2153.
Vernier, J.M., 1977. Chronological Table of the Embryonic Development of Rainbow Trout, Salmo Gairdneri Rich. 1836. Department of the Environment, Fisheries and Marine Service, Pacific Biological Station.
Villalobos, S.A., Papoulias, D.M., Meadows, J., Blankenship, A.L., Pastva, S.D., Kannan, K., Hinton, D.E., Tillitt, D.E., Giesy, J.P., 2000. Toxic responses of medaka, D-rR strain, to polychlorinated naphthalene mixtures after embryonic exposure by *in ovo* nanoinjection: a partial life-cycle assessment. Environ. Toxicol. Chem. 19, 432–440.
Wassenberg, D., Di Giulio, R., 2004. Synergistic embryotoxicity of polycyclic aromatic hydrocarbon aryl hydrocarbon receptor agonists with cytochrome P4501A inhibitors in *fundulus heteroclitus*. Environ. Health Perspect. 112, 1658–1664.
Watson, G.M., Andersen, O., Galloway, T.S., Depledge, M.H., 2004. Rapid assessment of polycyclic aromatic hydrocarbon (PAH) exposure in decapod crustaceans by fluorimetric analysis of urine and haemolymph. Aquat. Toxicol. 67, 127–142.
Wickström, K., Tolonen, K., 1987. The history of airborne polycyclic aromatic hydrocarbons (PAH) and perylene as recorded in dated lake sediments. Water Air Soil Pollut. 32, 155–175.
Willett, K.L., Randerath, K., Zhou, G., Safe, S.H., 1998. Inhibition of CYP1A1-dependent activity by the polynuclear aromatic hydrocarbon (PAH) fluoranthene. Biochem. Pharmacol. 55, 831–839.
Yu, G., Wang, L., Han, Y., He, Q., 2012. clusterProfiler: an R package for comparing biological themes among gene clusters. OMICS A J. Integr. Biol. 16, 284–287.
Zodrow, J.M., Tanguay, R.L., 2003. 2,3,7,8-tetrachlorodibenzo-p-dioxin inhibits zebrafish caudal fin regeneration. Toxicol. Sci. 76, 151–161.
Doering, J., Hecker, M., Villeneuve, D., Zhang, X., 2019. Adverse outcome pathway on aryl hydrocarbon receptor activation leading to early life stage mortality, via increased COX-2. IS 12.

SUPPORTING INFORMATION

Exposure to retene, fluoranthene, and their binary mixture causes distinct transcriptomic and apical outcomes in rainbow trout (Oncorhynchus mykiss) yolk sac alevins

Andreas N.M. Eriksson[a,*], Cyril Rigaud[a], Aleksei Krasnov[b], Emma Wincent[c], Eeva-Riikka Vehniäinen[a]

a Department of Biological and Environmental Sciences, University of Jyväskylä, P.O. Box 35, Jyväskylä FI-40014, Finland

b Fisheries and Aquaculture Research, Norwegian Institute of Food, Ås, Norway

c Institute of Environmental Medicine, Karolinska Institutet, Stockholm, Sweden

* Corresponding author: Andreas N.M. Eriksson. andreas.n.m.eriksson@jyu.fi.

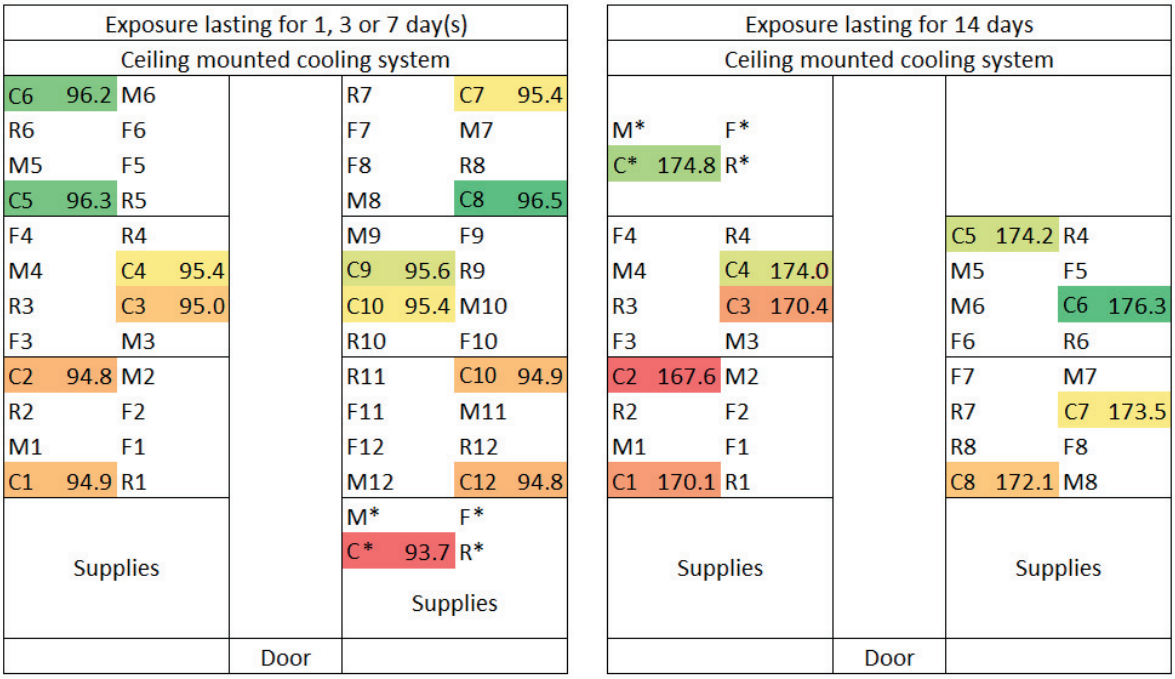

Figure s1. Top-down view of the experimental setup. Exposures lasting for 1, 3 and 7 days were conducted simultaneously in separate rooms, and the exposure lasting for 14 days was performed roughly 1 month prior to the other exposures. Bowls were placed in a Latin square sequence. C = control (DMSO), R = Retene, F = Fluoranthene, M = binary mixture and negative background control (bowls with water and chemicals only) are denoted with the corresponding letter and an *. In the 1, 3 and 7 days exposure study, which ran in parallel, negative control bowls were maintained in the 7 days exposure room. “Supplies” represents the areas where we kept supplies used for the exposure. Room temperature was maintained through a ceiling mounted cooling system with 3 fans connected to a thermostat. Degree days were calculated for each control replicate and the results for are presented for the 7 and 14 days exposures and presented as per the color scaled cells (red = lower degree days while green represents higher). Heart tissue was pooled according to the following pattern: exposures lasting for 1, 3 and 7 days, the hearts of fry from three bowls (replicate 1, 5, and 9; 2, 6, and 10; 3, 7, and 11; and 4, 8, and 12) were pooled together, resulting in four replicates for transcriptomic analyses. In the 14 days exposure setup, the hearts of fry from two bowls (replicate 1: 1 and 5; replicate 2: 2 and 6; replicate 3: 3 and 7; and replicate 4: 4 and 8) were pooled, resulting in four replicates per treatment.

s1.1. HPLC material preparation, analysis and recovery.

Pooled fish carcasses (10 – 13 per replicate) were transferred to a 2 ml Eppendorf tube together with eight 1 mm and four 2 mm Ø zirconium IV oxide beads (Next Advance, USA) and 600 µL of 70 % acetonitrile were added (ACN; Fisher Scientific). The samples were homogenized using a bullet blender (standard model, Next Advance) set at max setting for 5 minutes. The number of replicates per treatment was 6 for exposures lasting 1 to 7 days (except for the 7-day exposure to the mixture where N = 5) and 8 for the exposure lasting for 14 days. The homogenate was transferred to a clean Eppendorf tube and then rinsed with an additional 600 µL of 70 % ACN before being centrifuged for 15 minutes at 14 000 rpm in 4°C (Centrifuge 5415 R, Eppendorf, Germany). Following centrifugation, the supernatant was collected and the pellet re-suspended in 400 µL of 70 % ACN and centrifuged; this procedure was repeated twice and the collected supernatants were pooled and stored at -20 °C until further analysis. 100 µL of pooled supernatant were transferred to an amber glass vial (Agilent Technologies, Poland) with a 250 µL glass insert (Agilent Technologies, German) for analysis.

10 µL of the supernatant aliquot were injected into a Shimadzu U-HPLC Nexera system connected to a RF-20A xs Prominence fluorescence detector (Shimadzu, Japan) with a 150 mm long ACE C18-AR column with a particle size of 5 µm (Advanced Chromatography Technologies LTD, Scotland, UK). The analytical protocol developed allowed for simultaneous measurement of both PAHs in one run, enabling detection of possible PAH cross-contamination. Retene was measured at excitation 259 nm and emission 370 nm at 16.71 ± 0.09 minutes retention time with a limit of quantification (LOQ) = 3.45×10^{-16} M and a limit of detection (LOD) = 1.14×10^{-16} M based upon HPLC-measurements of spiked control carcasses. Fluoranthene was measured at excitation 288 nm and emission 525 nm at 13.5 ± 0.21 minutes retention time with a LOQ = 2.31×10^{-11} M and a LOD = 7.63×10^{-12} M based upon HPLC-measurements of spiked control carcasses. Flow rate was 1 mL per minute over a ddH_2O + 1.5 mM formic acid (Fischer Scientific)

together with 70 % acetonitrile fortified with 1.5 mM formic acid; the proportion of the gradient components started at 1:1 (fortified water : fortified 70 % ACN) and reached 0:1 by minute 15 before reverting to 1:1 from minute 16 to 20. Standard curves were created by spiking 70% ACN with 21.19, 4.24 and 0.85 nmol of retene and 67.18, 13.44 and 2.69 nmol of fluoranthene. Each sample was analyzed twice in order to generate technical replicates. Area under the curve was manually adjusted and background- (by subtracting the average area under the curve from DMSO exposed alevins) and recovery compensated. The concentrations were then calculated according to the standard curves and the average PAH body burden (amount) calculated per fish.

Preparation and processing of the fish carcasses could lead to loss of PAH(s), which was compensated for by recovery assessment of each PAH. In order to assess the loss, 7 alevins were pooled in a 2 ml microtube and fortified with 10 µL of 105.96 nM of retene or 335.88 nM of fluoranthene. The fortified alevins were processed and analyzed in the same fashion as stated above. An additional null-tube per PAH was processed in the same fashion as those containing alevins, the difference being that these tubes only contained 70 % acetonitrile (same final volume as those containing fish) and the abovementioned concentrations of PAH. Each sample was analyzed twice to generate a technical replicate. Based upon specific retention time of the PAHs, the resulting area under the curve was manually adjusted, background compensated (alevins fortified with 70 % acetonitrile and treated as stated above) and recovery was established by dividing the area under curve from PAH fortified alevins by the area of acetonitrile fortified with PAH. The recovery of retene was 14.3 % and fluoranthene 14.6 % which is low compared to other studies which utilizes an internal standard (Sørensen et al., 2017; Sørensen et al., 2016).

s1.2. qPCR verification of transcriptomics

Microarray results were confirmed using quantitative polymerase chain reaction (qPCR). In total, eight genes were selected for qPCR analysis. Primer sequences for genes investigated through qPCR were cellular retinoic acid binding protein (*crabp*), chemokine (C-X-C motif) receptor (*cxcr4*), cytochrome P450 1a (*cyp1a*), fumarylacetoacetate hydrolase (*fah*), ferritin (*frim*), metallothionein (*mt2*), thioredoxin (*txn*) and thioredoxin reductase (*txnrd1*); specs are presented in table s1. These selected genes cover a broad spectrum of processes known to be affected by exposure to PAH or important in developing fry, and based on microarray results, varied in the direction and magnitude of differential expression. The genes (in the order they are stated above) are involved in development, immune system, phase I metabolism, phenylalanine and tyrosine catabolism, iron storage capacity, metal binding and excretion and counteracting oxidative stress.

The qPCR protocol is based upon Sivula et al. (Sivula et al., 2018) protocol. In short: RNA was extracted from pooled heart tissue using TRI reagent (Molecular Research Centre) according to the manufacturer's instructions and the RNA concentration, purity (NanoDrop 1000, Thermo Fisher Scientific) and integrity (Agilent 2100 BioAnalyzer, Agilent) assessed and verified using the eukaryote total RNA 6000 Nano-kit (Agilent). The extracted RNA was then DNase treated (Dnase I, Fermentas) and reverse transcribed into cDNA (iScript cDNA Synthesis Kit, Bio-Rad, USA) and diluted 1:10 in nuclease-free water. Each qPCR reaction contained 5 µL of the diluted cDNA, 1.5 µL of forward and reverse primers (final concentration 300 nM), 4.5 µL sterile H_2O and 12.5 µL of iQ SYBR Green Supermix (Bio-Rad) for a total volume of 25 µL and processed on a CFX96 Real-Time PCR cycler (Bio-Rad). The protocol consisted of 3 minutes at 95 °C; 40 cycles (each cycle constituted of 10 seconds at 95 °C, 10 seconds at 58 °C, 30 seconds at 72°C) and the melting curve ranged from 65 °C to 95 °C with increments of 0.5 °C. No template controls (water instead of cDNA) were run on each plate for each gene, and the Ct values were always over 38. Once the presence of one PCR product was confirmed using the melting curves, the expression

of the target genes was calculated using Bio-Rad CFX Manager software (v.3.1). We used both *ndufa8* and *rl17* as reference genes as they were the most stable at transcript levels during our preliminary experiments (data not shown). Comparison with microarray data is presented in table s2 and most gene expressions are similar to the microarray data with the exception of day 1 expressions where several differences are present between the methods.

Table s1. Primer sequences, product base pair length (bp), efficiency for 8 genes investigated through qPCR while *rl17* and *ndufa8* were used as reference genes.

Gene	Accession	Primers	Product length (bp)	Efficiency (%)
crabp	NM_001140880.2	F: CTTCCAAAGTGGGAGACAGACAGT	111	96.6
		R: AATGAGCTCGCCGTCATTGGTT		
cxcr4	NM_001124342.2	F: AGATGCACTGGCTGTCAACAGTAG	97	92.1
		R: ACTTGAGGACTCGGATTCAGTGGA		
cyp1a	XM_021607648.1	F: CAGTCCGCCAGGCTCTTATCAAGC	94	96.9
		R: GCCAAGCTCTTGCCGTCGTTGAT		
fah	XM_021586746.1	F: GACAGATGAGACCCGACCAA	81	97.6
		R: AGAATGCCATCTCCAGCTCA		
frim	XM_014187871.1	F: AGGACATCACGAAGCCAGAA	93	90.9
		R: GGGCCTGGTTCACATTCTTC		
mt2	XM_021597409.1	F: TCCTTGTGAATGCTCCAAAACT	88	101.1
		R: TGCTTTCTTACAACTGGTGCA		
txn	XM_021577868.1	F: CTTCTTCAAAGGGCTGTCGG	119	86.4
		R: GGAACGTTGGCATGCATTTG		
txnrd1	XM_021568557.1	F: AGAGTTCATCGAGCCACACA	131	97.2
		R: ACTCTTTGTCTCCGGGGATG		
rl17	NM_001195159.2	F: ATCGAGCACATCCAGGTAACAAG	99	110.1
		R: AATGTGGCAAGGGGAGCTCATGTA		
ndufa8	NM_001160582.1	F: TTCAGAGCCTCATCTTGCCTGCT	119	114
		R: CAACATAGGGATTGGAGAGCTGTACG		

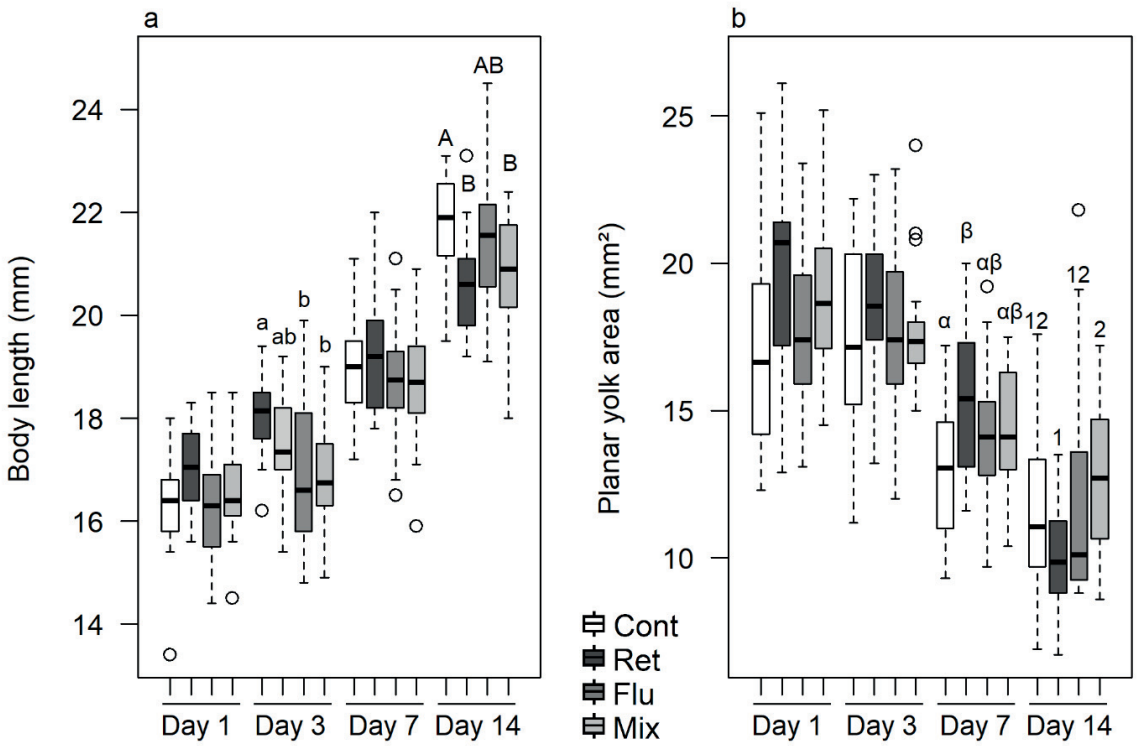

Figure s2. Boxplot presentation of the un-adjusted impact of exposure on a) standard length; and b) planar yolk area among rainbow trout alevins exposed to DMSO (Cont), retene (Ret), fluoranthene (Flu) and the mixture of the two PAHs (Mix). Alevins were sampled after 1, 3, 7 and 14 days of exposure. Significant differences are denoted using lower- and upper-case Latin letters (standard length day 3 and 14, respectively) as well as Greek letters (yolk area day 7) and numbers (yolk area day 14) (ANOVA + Tukey's test or Kruska-Wallis + Dunn's test depending on normality).

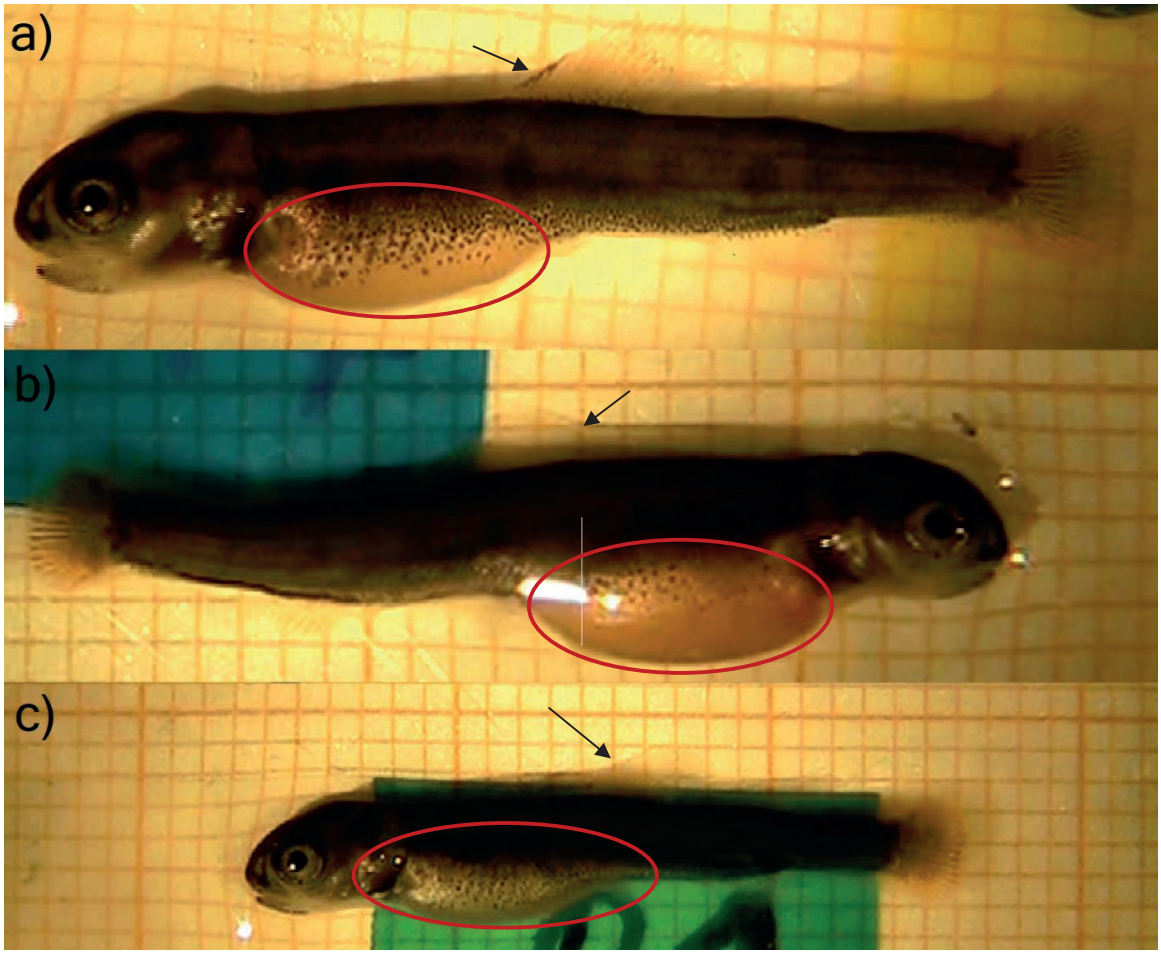

Figure s3. Pigmentation intensity of the lateral side of the yolk sac (red oval) and the dorsal fin (arrow) in a) control specimen and b) mixture exposed fry sampled on day 14. Control specimen a) have a high-density pigmentation of the lateral side and a clear pigmentation of the dorsal fin while mixture exposed specimen b) has a low density of pigmentation and no pigmentation of the dorsal fin. Fry with a fully pigmented yolk sac is silvery in appearance c) are scored as high intensity pigmentation; note that the pigmentation of the dorsal fin has not commenced.

Table s2. Cumulative mortality (%) and number of dead fish (in brackets) in relation to treatment. Fischer's exact test revealed a statistically significant difference in mortality between fluoranthene (Flu) and retene (Ret) after 7 days of exposure (denoted with different capital letters); however, no statistically significant difference was observed between control (DMSO) exposed fish and alevins exposed to PAH(s), irrespective of exposure duration.

Mortality in percentage and the numbers of dead in [brackets].					
Exposure duration	DMSO (%)	Flu (%)	Ret (%)	Mix (%)	N per treatment
Day 1	0 [0]	0 [0]	0 [0]	0 [0]	180
Day 3	0 [0]	0.56 [1]	0 [0]	0 [0]	180
Day 7	2.78 [5]^{AB}	0.56 [1]^{A}	5.56 [10]^{B}	2.22 [4]^{AB}	180
Day 14	3.31 [4]	2.50 [3]	1.67 [2]	3.33 [4]	120$^{\#}$

* p = 0.0106 using Fisher's exact test when comparing mortality of fluoranthene and retene.

DMSO exposure contained 121 fish and the rest 120 per treatment.

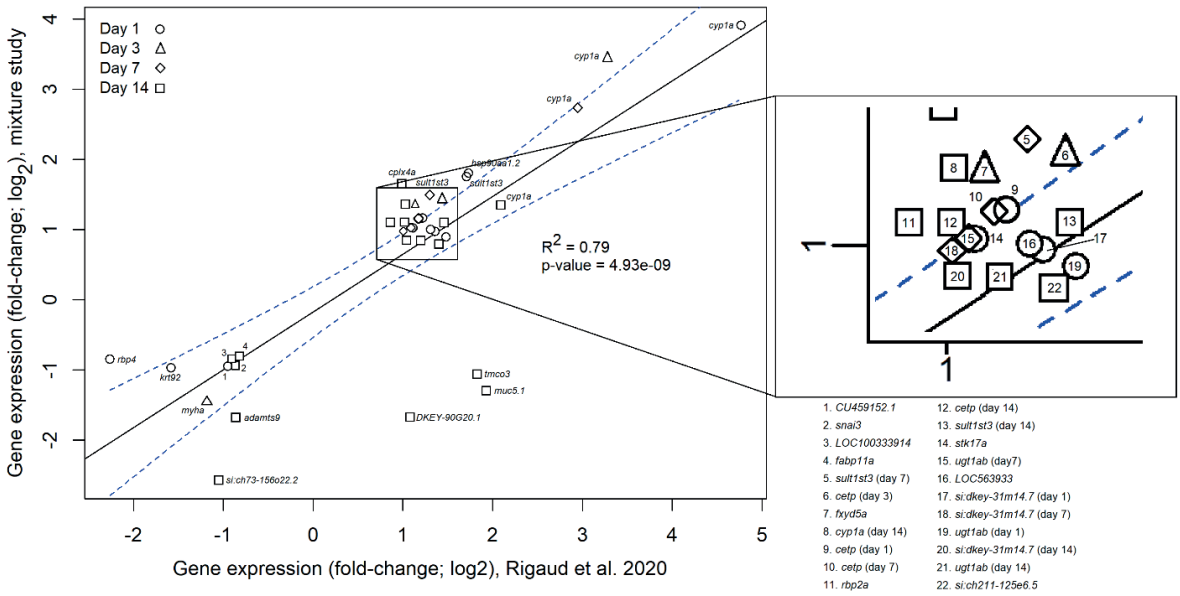

Figure s4. Spearman's rank correlation analysis (± 95% confidence interval) of differently expressed genes in developing rainbow trout alevins exposed to retene alone as per this study and those reported by Rigaud et al. (2020).

Table s3. Comparison of the direction of significantly impacted cardiac gene expressions in relation to control derived from qPCR- and microarray analysis. Gene expression was performed after 3 and 14 days of exposure. N per treatment = 3. Statistical analysis was performed using ANOVA with Tukey's post hoc test for qPCR or using Nofima's bioinformatics package for microarray analysis (Krasnov et al., 2011). Any significant difference is denoted with the arrows, the direction indicates either up- (↑) or down-regulation (↓) compared to control. Due to the low number replicates (< 3) obtained following 1 and 7 days of exposure, only the results from 3 and 14 days of exposure are presented. Non-significantly impacted gene expression following exposure on are denoted with a minus sign (-). NA = not analyzed.

		Day 3			Day 14		
Gene ID	Analysis method	Flu	Mix	Ret	Flu	Mix	Ret
crabp	qPCR	↓	↓	↓	-	-	-
	Microarray	-	↓	-	↓	↓	-
cxcr4	qPCR	-	↑	-	-	-	-
	Microarray	-	-	-	-	-	↓
cyp1a	qPCR	↑	↑	↑	↑	↑	-
	Microarray	↑	↑	↑	↑	↑	↑
fah	qPCR	-	-	-	-	↑	-
	Microarray	↑	↑	-	↑	↑	-
frim	qPCR	-	↑	-	-	↑	-
	Microarray	↑	↑	-	↑	↑	-
mt2	qPCR	-	↑	-	-	↑	-
	Microarray	-	↑	-	-	↑	-
txn	qPCR	-	↑	-	-	-	-
	Microarray	-	↑	-	-	↑	-
txnrd	qPCR	-	-	-	-	-	-
	Microarray	-	↑	-	-	↑	-


neutral lipid metabolic process
acylglycerol metabolic process
GABA receptor complex
GABA-A receptor complex
transmembrane signaling receptor activity
signaling receptor activity
molecular transducer activity
GABA-A receptor activity
extracellular ligand-gated ion channel activity
transmembrane transporter activity
aromatic amino acid family catabolic process
aromatic amino acid family metabolic process
lipid binding
chondrocyte morphogenesis involved in endochondral bone morphogenesis
growth plate cartilage chondrocyte morphogenesis
chondrocyte development involved in endochondral bone morphogenesis
chondrocyte differentiation involved in endochondral bone morphogenesis
growth plate cartilage chondrocyte differentiation
chondrocyte morphogenesis
growth plate cartilage morphogenesis
skeletal muscle contraction
endochondral bone growth
growth plate cartilage development
bone growth
multicellular organismal movement
musculoskeletal movement
chondrocyte development
cartilage development involved in endochondral bone morphogenesis
endochondral bone morphogenesis
cholesterol transporter activity
G protein-coupled receptor signaling pathway
transmembrane transport
neuron recognition
ion transport
cation transport
cell recognition
ion transmembrane transport
regulation of blood circulation
integral component of plasma membrane
intrinsic component of plasma membrane
G protein-coupled receptor activity
secondary active transmembrane transporter activity
G protein-coupled peptide receptor activity
cation transmembrane transporter activity
channel activity
passive transmembrane transporter activity
substrate-specific channel activity
inorganic molecular entity transmembrane transporter activity
solute:cation antiporter activity
peptide receptor activity
cation channel activity
potassium ion transmembrane transporter activity
voltage-gated cation channel activity
ion transmembrane transporter activity
voltage-gated ion channel activity
ion gated channel activity
voltage-gated channel activity
inorganic cation transmembrane transporter activity
metal ion transmembrane transporter activity
ion channel activity
voltage-gated potassium channel activity
gated channel activity
potassium ion antiporter activity
monovalent inorganic cation transmembrane transporter activity
calcium:cation antiporter activity
cation:cation antiporter activity
antiporter activity
active transmembrane transporter activity
bioactive lipid receptor activity
coreceptor activity
calcium ion transmembrane transporter activity
response to xenobiotic stimulus
response to heat
cellular response to xenobiotic stimulus
cellular response to chemical stimulus
cellular response to heat
response to temperature stimulus
gastrulation
xenobiotic metabolic process
protein folding
regulation of nodal signaling pathway
regulation of retinoic acid receptor signaling pathway
regulation of activin receptor signaling pathway
protein refolding
mesendoderm development
response to cadmium ion
endoderm development
embryonic morphogenesis
nodal signaling pathway
misfolded protein binding
unfolded protein binding
glutathione metabolic process
developmental growth
oxidation-reduction process
growth
response to wounding
sulfur compound metabolic process
sulfur compound biosynthetic process
cellular modified amino acid metabolic process
cysteine metabolic process
cell redox homeostasis
wound healing
cofactor metabolic process
alpha-amino acid metabolic process
cellular homeostasis
negative regulation of nervous system development
regulation of cell differentiation
regeneration
cellular amino acid metabolic process
extracellular structure organization
regulation of nervous system development
regulation of cell development
sulfur amino acid metabolic process
regulation of response to external stimulus
negative regulation of neuron differentiation
regulation of response to wounding
negative regulation of hydrolase activity
regulation of multicellular organismal process
regulation of neuron projection development
regulation of neuron differentiation
serine family amino acid metabolic process
extracellular space
extracellular region
extracellular region part
oxidoreductase activity
transferase activity, transferring alkyl or aryl (other than methyl) groups
oxidoreductase activity, acting on a sulfur group of donors
glutathione transferase activity
disulfide oxidoreductase activity
cofactor binding
electron transfer activity
coenzyme binding
flavin adenine dinucleotide binding
antioxidant activity
iron ion binding
Flu.3 Flu.7 Flu.14 Ret.1 Ret.3 Ret.7 Ret.14 Mix.1 Mix.3 Mix.7 Mix.14
p.adjust
0.04
0.03
0.02
0.01
Count
20
40
60

Figure s5. Complete over-representation analysis of figure 4. Fry were exposed towards retene (Ret), fluoranthene (Flu) and the binary mixture (Mix) for 1, 3, 7 and 14 days. Data was analyzed, p-value adjusted and plotted using clusterProfiler. The size of each dot equals the number of genes involved in each GO-term.

Supplementary references

Colby, G.A., 2019. Deposition of Polycyclic Aromatic Hydrocarbons (PAHs) into Northern Ontario Lake Sediments. bioRxiv , 786913.

Krasnov, A., Timmerhaus, G., Afanasyev, S., Jørgensen, S.M., 2011. Development and assessment of oligonucleotide microarrays for Atlantic salmon (*Salmo salar* L.). Comparative Biochemistry and Physiology Part D: Genomics and Proteomics; This Special Issue contains papers which stem from a presentation at the Genomics in Aquaculture symposium held in Bodø¸ on 5th-7th July 2009 6, 31-38.

Rigaud, C., Eriksson, A., Krasnov, A., Wincent, E., Pakkanen, H., Lehtivuori, H., Ihalainen, J., Vehniäinen, E., 2020. Retene, pyrene and phenanthrene cause distinct molecular-level changes in the cardiac tissue of rainbow trout (*Oncorhynchus mykiss*) larvae, part 1 – Transcriptomics. Sci. Total Environ. 745, 141031.

Sivula, L., Vehniäinen, E., Vehniäinen, E., Kukkonen, J.V.K., 2018. Toxicity of biomining effluents to *Daphnia magna*: Acute toxicity and transcriptomic biomarkers. Chemosphere 210, 304-311.

Sørensen, L., Silva, M.S., Booth, A.M., Meier, S., 2016. Optimization and comparison of miniaturized extraction techniques for PAHs from crude oil exposed Atlantic cod and haddock eggs. Analytical and Bioanalytical Chemistry 408, 1023-1032.

Sørensen, L., Sørhus, E., Nordtug, T., Incardona, J.P., Linbo, T.L., Giovanetti, L., Karlsen, Ø, Meier, S., 2017. Oil droplet fouling and differential toxicokinetics of polycyclic aromatic hydrocarbons in embryos of Atlantic haddock and cod. PLOS ONE 12, e0180048.

II

CHANGES IN CARDIAC PROTEOME AND METABOLOME FOLLOWING EXPOSURE TO THE PAHS RETENE AND FLUORANTHENE AND THEIR MIXTURE IN DEVELOPING RAINBOW TROUT ALEVINS

by

Andreas N.M. Eriksson, Cyril Rigaud., Anne Rokka, Morten Skaugen, Jenna H. Lihavainen & Eeva-Riikka Vehniäinen 2022

Science of the Total Environment 830: 154846.

https://doi.org/10.1016/j.scitotenv.2022.154846

Science of the Total Environment 830 (2022) 154846

Contents lists available at ScienceDirect

Science of the Total Environment

journal homepage: www.elsevier.com/locate/scitotenv

Changes in cardiac proteome and metabolome following exposure to the PAHs retene and fluoranthene and their mixture in developing rainbow trout alevins

Andreas N.M. Eriksson [a,*], Cyril Rigaud [a], Anne Rokka [b], Morten Skaugen [c], Jenna H. Lihavainen [d], Eeva-Riikka Vehniäinen [a]

[a] Department of Biological and Environmental Science, University of Jyväskylä, P.O. Box 35, FI-40014, Finland
[b] Turku Proteomics Facility, Turku University, Tykistökatu 6, 20520 Turku, Finland
[c] Faculty of Chemistry, Biotechnology and Food Science, Norwegian University of Life Sciences, Campus Ås, Universitetstunet 3, 1430 Ås, Norway
[d] Umeå Plant Science Centre, Umeå University, KB. K3 (Fys. Bot.), Artedigränd 7, Fysiologisk botanik, UPSC, KB. K3 (B3.44.45) Umeå universitet, 901 87 Umeå, Sweden

HIGHLIGHTS

- Rainbow trout alevins were exposed to retene and/or fluoranthene for 7 and 14 days.
- PAH exposure resulted in treatment specific cardiac proteome and metabolome.
- Exposure specific phase II metabolism and body burdens profiles.
- Exposure to the binary mixture disrupted energy and iron metabolism.
- Impaired cellular integrity as per depletion of intermediate filaments and tubulins.

GRAPHICAL ABSTRACT

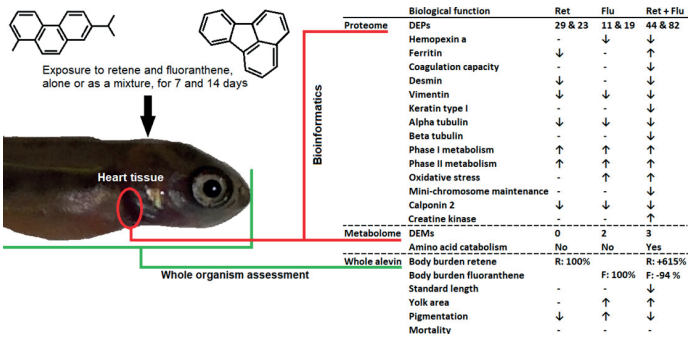

	Biological function	Ret	Flu	Ret + Flu
Proteome	DEPs	29 & 23	11 & 19	44 & 82
	Hemopexin a	-	↓	↓
	Ferritin	↓	-	↑
	Coagulation capacity	-	-	↓
	Desmin	↓	-	↓
	Vimentin	↓	↓	↓
	Keratin type I	-	-	↓
	Alpha tubulin	↓	↓	↓
	Beta tubulin	-	-	↓
	Phase I metabolism	↑	↑	↑
	Phase II metabolism	↑	↑	↑
	Oxidative stress	-	↑	↑
	Mini-chromosome maintenance	-	-	↓
	Calponin 2	↓	↓	↓
	Creatine kinase	-	-	↑
Metabolome	DEMs	0	2	3
	Amino acid catabolism	No	No	Yes
Whole alevin	Body burden retene	R: 100%		R: +615%
	Body burden fluoranthene		F: 100%	F: -94 %
	Standard length	-	-	↓
	Yolk area	-	↑	↑
	Pigmentation	↓	↑	↓
	Mortality	-	-	-

ARTICLE INFO

Article history:
Received 26 January 2022
Received in revised form 11 March 2022
Accepted 23 March 2022
Available online 26 March 2022

Editor: Daqiang Yin

Keywords:
PROTEOMICS
Metabolomics
PAH
Mixture
Developmental toxicology
Rainbow trout

ABSTRACT

Exposure to polycyclic aromatic hydrocarbons (PAHs) is known to affect developing organisms. Utilization of different omics-based technologies and approaches could therefore provide a base for the discovery of novel mechanisms of PAH induced development of toxicity. To this aim, we investigated how exposure towards two PAHs with different toxicity mechanisms: retene (an aryl hydrocarbon receptor 2 (Ahr2) agonist), and fluoranthene (a weak Ahr2 agonist and cytochrome P450 inhibitor (Cyp1a)), either alone or as a mixture, affected the cardiac proteome and metabolome in newly hatched rainbow trout alevins (*Oncorhynchus mykiss*). In total, we identified 65 and 82 differently expressed proteins (DEPs) across all treatments compared to control (DMSO) after 7 and 14 days of exposure. Exposure to fluoranthene altered the expression of 11 and 19 proteins, retene 29 and 23, while the mixture affected 44 and 82 DEPs by Days 7 and 14, respectively. In contrast, only 5 significantly affected metabolites were identified. Pathway over-representation analysis identified exposure-specific activation of phase II metabolic processes, which were accompanied with exposure-specific body burden profiles. The proteomic data highlights that exposure to the mixture increased oxidative stress, altered iron metabolism and impaired coagulation capacity. Additionally, depletion of several mini-chromosome maintenance components, in combination with depletion of several intermediate filaments and microtubules, among alevins exposed to the mixture, suggests compromised cellular integrity and reduced rate of mitosis, whereby affecting heart growth and development. Furthermore, the combination of proteomic and metabolomic data indicates altered energy metabolism, as per amino acid catabolism among mixture exposed alevins;

* Corresponding author at: P.O. Box 35, FI-40014 University of Jyväskylä, Finland.
E-mail addresses: andreas.n.m.eriksson@jyu.fi (A.N.M. Eriksson), cyril.c.rigaud@jyu.fi (C. Rigaud), anne.rokka@bioscience.fi (A. Rokka), morten.skaugen@nmbu.no (M. Skaugen), jenna.lihavainen@umu.se (J.H. Lihavainen), eeva-riikka.vehniainen@jyu.fi (E.-R. Vehniäinen).

http://dx.doi.org/10.1016/j.scitotenv.2022.154846

plausibly compensatory mechanisms as to counteract reduced absorption and consumption of yolk. When considered as a whole, proteomic and metabolomic data, in relation to apical effects on the whole organism, provides additional insight into PAH toxicity and the effects of exposure on heart structure and molecular processes.

1. Introduction

Polycyclic aromatic hydrocarbons (PAHs) are a diverse group of pollutants of either natural or anthropogenic origin; the principal sources of the latter are industrial activities, urban sprawl and petroleum-related contamination (Behera et al., 2018; Pasparakis et al., 2019). Increased levels of PAH contamination has been linked to increased stress to the local environment and negative impacts on organismal health (Wickström and Tolonen, 1987; Kim et al., 2013; dos Santos et al., 2018). Newly hatched and developing fish larvae are especially sensitive to the influence PAH(s); symptoms of PAH toxicity include yolk sac and pericardial edema, spinal and craniofacial deformities, as well as hemorrhaging (these symptoms are referred to as blue sac disease (BSD) (Billiard et al., 1999)) and plausibly slower development (Eriksson et al., 2022). Yet, heart structure and function are especially sensitive to the influence of PAHs during early life development, as per improper development, and induction of bradycardia and arrythmia (Incardona et al., 2004; Scott et al., 2011; Van Tiem and Di Giulio, 2011).

It is unclear exactly how exposure to PAH(s) induce developmental and cardiotoxicity in fish larvae. The best-known and most studied molecular pathway is the interaction between certain PAHs and subsequent activation of the aryl hydrocarbon receptor 2 (Ahr2), which in turn controls (among multiple processes) the induction of the cytochrome P450a1 (Cyp1a); a phase I xenobiotic metabolic enzyme (Köhle and Bock, 2007). Activation of phase I metabolism serves to increase the hydrophilicity of the substrate by addition of hydroxyl group(s), thus promoting further phase II metabolism and ultimately, excretion. This is perfectly exemplified by the stepwise metabolism of the PAH retene (Huang et al., 2017). Furthermore, developmental PAH toxicity is Ahr2 dependent, as knockdown of the *ahr2*, but not *cyp1a*, has been reported to prevent the formation toxicity in fish larvae (Incardona et al., 2006; Scott et al., 2011). Additional pathways governed by Ahr2 activation, such as cyclooxygenase-2, have also been suggested to contribute PAH mediated toxicity (Adverse Outcome Pathway 21 (Doering et al., 2019)). However, it has to be noted that not every PAH induce toxicity through improper activation of Ahr2. Rather, some PAHs induce toxicity non-specifically (narcosis), whereby the PAH induce cellular damages by impairing normal cell membrane function and disrupting ion homeostasis (Incardona et al., 2006; Meador and Nahrgang, 2019). However, the hypothesis of narcosis induced PAH toxicity has been questioned by Incardona (2017), who suggest that PAH-specific hydrophobicity, in relation to lipoproteins in the cell membrane, as the primary factor of non-specific PAH toxicity in fish larvae.

Two PAHs that can interact with, and activate Ahr2 signaling are retene and fluoranthene (Barron et al., 2004). Retene, also known as 1-methyl-7-isopropyl phenanthrene, is a common environmental pollutant, which is typically associated with effluents from pulp and paper industry, but also generated during forest fires, and by microbial degradation of resin acids, such as dehydroabietic acid (Leppänen and Oikari, 1999, 2001). The exact mechanisms by which retene induces toxicity in developing fish larvae are currently unknown, but activation of Ahr2 is required (Scott et al., 2011). In contrast, the PAH fluoranthene, which is a weaker Ahr2 agonist than retene (Barron et al., 2004), is a common component in crude oil and any mixture of PAHs (Baquer et al., 1988; Page et al., 1999). Mechanistically, fluoranthene can inhibit the function of Cyp1A by physically blocking the active site of the enzyme (Willett et al., 1998; Fent and Bätscher, 2000). Exposure to fluoranthene can therefore slow down its own metabolism, which in turn promotes temporal accumulation (Eriksson et al., 2022).

However, PAHs always occur as complex mixtures in the nature. Therefore, it is important to understand how complex and simple mixtures of PAHs induce toxicity at multiple levels of biological organization in developing fish larvae. The few controlled laboratory studies available have reported potentized mixture toxicity relative to the components (Willett et al., 1998; Wassenberg and Di Giulio, 2004a, 2004b; Wills et al., 2009; Garner et al., 2013; Geier et al., 2018). This suggests that toxicity is induced through multiple simultaneous mechanisms and processes, all of which contribute to the induction of toxicity (Doering et al., 2019; Meador and Nahrgang, 2019).

In our previous studies on PAH-induced developmental toxicity, we observed that rainbow trout alevins (*Oncorhynchus mykiss*) exposed to the PAHs retene and fluoranthene (alone or as a mixture) (2022), or retene, pyrene and phenanthrene alone (2020a), developed unique cardiac transcriptomics, toxicity and body burden profiles. These results confirming the notion that PAHs toxicity is both compound, and potentially mixture-specific (Geier et al., 2018). Additionally, mixture toxicity could not have been predicted from the additive potential of the two components.

Even so, transcriptomic up-regulation does not necessarily result in an equally enriched protein expression (Vogel and Marcotte, 2012). It is unclear how exposure to a binary mixture of PAHs (with different mode of actions) would affect the cardiac proteome and metabolome, relative to the components, as no such study has been performed to the knowledge of the authors. Additionally, a number of studies on the proteomic and metabolomic responses in PAH exposed fish larvae report both species, developmental stage and compound specific alterations (Bohne-Kjersem et al., 2010; Elie et al., 2015; Doering et al., 2016; Rigaud et al., 2020b).

Therefore, the aims of this study were to investigate how the cardiac proteome and metabolome of newly hatched rainbow trout alevins responded to exposure, in vivo, to a binary mixture of retene and fluoranthene, relative to the components. Through such an approach, known mechanisms of toxicity could be validated, while unknown and novel mechanisms of cardiac toxicity could be discovered. We hypothesized that exposure to the individual PAHs, or the mixture, would generate unique cardiac proteomic and metabolomic profiles, in a similar fashion as was observed in our transcriptomic study (Eriksson et al., 2022). Investigating the cardiac metabolome could provide additional support to the alterations identified in the cardiac proteome and transcriptome. Therefore, by employing two different omic-approaches concurrently, in relation to developmental toxicity and PAH accumulation, it could be possible to shed new light on the impact of these pollutants on the underlying mechanisms of PAH induced cardiotoxicity in newly hatched and developing fish larvae.

2. Materials and methods

2.1. Exposure setup and maintenance

Alevins sampled for their cardiac proteome and metabolome are not from the same batch but exposed and sampled according to the same methodology, although 2.5 months apart. The cardiac proteome originates from the same alevins as those sampled for their cardiac transcriptome; for methodology and results, see Eriksson et al. (2022).

In short, newly hatched (<24 h) rainbow trout alevins (*Oncorhynchus mykiss*) were exposed semi-statically (water and chemicals were completely renewed on a daily basis) to dimethyl sulfoxide as control (DMSO), retene (32 $\mu g \cdot l^{-1}$), fluoranthene (50 $\mu g \cdot l^{-1}$) or the binary mixture of the two PAHs. The 360-degree-days old alevins were obtained from Hanka-Taimen, Hankasalmi, Finland. Stock solutions were prepared by dissolving each PAH in pure DMSO. Chemical parameters and information are presented in Table 1. Nominal exposure concentrations were selected to induce toxicity, but not mortality, as per previous studies (retene) (Billiard et al., 1999; Vehniäinen et al., 2016) and preliminary testing (fluoranthene; ≤

Table 1
Exposure related information on stock solution concentrations (μM), volume of stock solution added per exposure bowl (μl), nominal exposure concentration (nM) of retene (Ret), fluoranthene (Flu) and the mixture (Mix), chemical purity (%), suppliers and CAS-numbers. Note: 136.6 nM of retene equals to 32 $\mu g \cdot l^{-1}$, while 247.2 nM of fluoranthene equals to 50 $\mu g \cdot l^{-1}$. Note that the volume of DMSO added to each exposure replicate is far below the upper limited of 100 $\mu g \cdot l^{-1}$ recommended by the OECD (2013). NA = not applicable.

Exposure	PAH Stock solution concentration (μM)	Volume added (μl)	Nominal PAH exposure concentration (nM)	Purity (%)	Supplier	CAS Number
DMSO	Pure DMSO	20	NA	≥ 99.9	Sigma Aldrich	67–68-5
Ret + DMSO	13,655	10 + 10	136.6	98	MP Biomedical	483–65-3
Flu + DMSO	24,720	10 + 10	247.2	≥ 98	Sigma Aldrich	206–44-0
Mix	Same as above	10 + 10	136.6 + 247.2		|--- Same as above ---|	

500 μg l^{-1} did not cause elevated mortality relative to DMSO exposed control, unpublished data).

Exposures were conducted in 1.5 l Pyrex glass trays, which had been presaturated for 24 h prior to the initiation of exposure with the corresponding chemicals. Every exposure replicate was filled with 1 l of filtered lake water (obtained at a depth of 6 m from Konnevesi Research Station, Central Finland; the levels PAHs in the water were negligible and below the level of detection of synchronous fluorescence spectroscopy (SFS)) and continuously aerated through glass Pasteur pipettes connected to an air pump. Alevins were exposed for and sampled after 7 and 14 days. The exposure (proteomics) which lasted for 7 days consisted of 12 replicates per treatment, while the 14 days exposure consisted of 8 replicates per treatment (proteomics; plus one additional replicate per treatment without alevins). The exposure meant for obtaining the cardiac tissue for metabolomics utilized 12 replicates per treatment, each containing 15 alevins, plus on set of trays without fish). At the start of the exposure, each replicate held 15 newly hatched and healthy rainbow trout alevins (free from signs of deformities). This corresponds to 720 and 480 alevins for the 7 and 14 days exposures, respectively.

Water temperature, measured daily, averaged 11.62 ± 0.32 °C, while a 16:8 light (from yellow fluorescent tubes) to darkness ratio was maintained throughout the exposure period. Any alevins found dead during exposure were recorded and assessed for symptoms of blue sac disease. Water quality (relative oxygen saturation (> 100%), pH (7.16 ± 0.10) and conductivity (26.83 ± 4.35 mS m^{-1})) of stock water were measured on Day 1, 3, 7, 10 and 14. The quality of the lake water (ammonium, alkalinity and Ca + Mg hardness) is considered as good, as per the Finnish Environment Institute (Hertta database; (Eriksson et al., 2022)). The concentration of PAH(s) in exposure water was assessed on the same days as water quality was checked. Five milliliters of exposure water, collected prior to the renewal of water and PAH(s), from 4 randomly selected tanks per treatment, were diluted 1:1 in ethanol (99.5% purity) and stored at 4 °C for later synchronous fluorescence spectroscopy analysis (results are presented in Table s1, while SFS methodology is presented in both Rigaud et al. (2020a) and Eriksson et al. (2022).

At sampling, alevins were first photographed next to a millimeter scale paper and visually scored (0 or 1) for each symptom of blue sac disease investigated (hemorrhages, and yolk sac and pericardial edemas) according to standards set by Villalobos et al. (2000) and Scott and Hodson (2008). Alevins were decapitated using a scalpel blade, and the heart excided with forceps (Dumont #5, Fine Science Tools, Heidelberg, Germany). Hearts from 2 (Day 14) or 3 (Day 7) replicates were pooled in 1.5 ml microcentrifuge tubes (N = 4 per treatment with 30 (day 14) or 45 (day 7) hearts per N), snap frozen in liquid nitrogen and stored at −80 °C for later proteomics analysis. In the case of cardiac metabolomics, sampled after 14 days of exposure, heart tissue from alevins of the same treatment, from 3 replicates, were pooled together (generating 4 replicates (N) per treatment; each replicate consisting of 45 hearts). The remaining carcasses were pooled based upon replicate in 1.5 ml microcentrifuge tubes for later body burden analysis (N = 8 per treatment; see Eriksson et al. (2022) or Rigaud et al. (2020a) for methodology).

2.2. Morphological analysis

Photographed alevins (N = 18 per treatment, 3 per replicate) were analyzed in silico using ImageJ (v1.51j8, National Institutes of Health, USA). Using the millimeter scale as a known length reference, standard length and planar yolk area were measured. Pigmentation intensity of the lateral side and dorsal fin were assessed as a measurement of development (methodology described in Eriksson et al. (2022) and based upon Vernier's salmonid developmental catalog (Vernier, 1977)).

2.3. Proteomic analysis

Cardiac protein samples (N = 4 per treatment) were prepared following the extraction of RNA with TRI Reagent (Molecular Research Center, Cincinnati, OH, USA) as presented in Eriksson et al. (2022). Following the removal of the aqueous phase, ethyl-alcohol (99.5% purity) was added to precipitate DNA from the remaining organic and interphase, and the DNA was discarded. Proteins were then precipitated using isopropanol. The protein pellets were washed, first in 0.3 M guanidine hydrochloride (in 95% ethyl alcohol) and ethanol (99.5% purity). Finally, the proteins were dissolved using a solution of 8 M urea and 2 M thiourea in a 1 M Tris-HCl buffer (pH 8.0). Protein samples (15 μg) were reduced for 1 h using dithiothreitol (37 °C), then alkylated by iodoacetamide (1 h at room temperature) and the urea concentration diluted below 1 M using 50 mM Tris-HCl. By adding trypsin (1:30 *w*/w), protein samples were digested for 16 h at 37 °C and then desalted with SepPak C18 96-well plate (Waters, Milford, MA, USA) according to manufacturer's instructions and evaporated to dryness using a SpeedVac (Thermo Fisher Scientific) and dissolved in 0.1% formic acid before mass spectrometry (MS) analysis. The peptide concentrations were determined using a NanoDrop™ (Thermo Fisher Scientific) by measuring absorbance at 280 nm and the concentrations of every sample adjusted to 100 ng μl^{-1}.

The LC-ESI-MS/MS (Liquid Chromatography-Electrospray Ionization-Mass Spectrometry/ Mass Spectrometry) analysis and measurements were performed using a nanoflow HPLC system (Easy-nLC1200, Thermo Fisher Scientific) coupled to the Q Exactive HF mass spectrometer (Thermo Fisher Scientific) equipped with a nano-electrospray ionization source. The solutions containing cardiac peptides were first injected on to a trapping column and separated inline on a 15 cm C18 column (75 μm × 15 cm, ReproSil-Pur 5 μm 200 Å C18-AQ, Dr. Maisch HPLC GmbH, Ammerbuch-Entringen, Germany). The mobile phase was constructed as follows: solution 1) de-ionized water spiked with 0.1% formic acid; and solution 2) was based upon an 80:20 mix of acetonitrile/water (v/v) with 0.1% formic acid added. Each run took 125 min; 85 min where solution 2 increased from 5% to 28% followed by an additional increase from 28% to 40% over 35 min. Finally, the samples were washed for 5 min with 100% solution 2 before the next run. This process was repeated twice for each sample as technical replicates.

2.4. Metabolomic analysis

2.4.1. Homogenization and metabolite extraction

The cardiac metabolome was analyzed, through untargeted metabolite profiling, in alevins exposed for 14 days. The same methodology was utilized by Rigaud et al. (2020b). In short: hearts from every alevin from 3 replicates of the same treatment were pooled (each pool thus contained 45 hearts), which equals 4 pooled replicates per treatment available for analysis. Cold methanol (CAS number: 67-56-1, Merck, Germany) with 0.1% of formic acid (300 μl; CAS number: 64-18-6, Sigma) and internal standard

solution (10 μl; 0.4 mg/ml of benzoic-d5 acid (CAS number: 1079-02-3, Sigma), 0.2 mg/ml of glycerol-d8 (CAS number: 7325-17-9, Sigma), 0.4 mg/ml of 4-methylumbelliferone (CAS number: 90-33-5, Sigma) in methanol) were added, and samples were homogenized with a bead mill (2 × 2 mm and 1 × 5 mm stainless steel beads, 2 × 15 s, 20 Hz, Qiagen TissueLyser II). The metabolites were extracted by vortexing the samples for 15 min at 4 °C. After a short centrifugation (2 min, 4 °C, 13500 ×g), the supernatant was transferred to a fresh test tube and cold methanol (80% aqueous) with 0.1% formic acid (300 μl) was added, and samples were again vortexed for 15 min at 4 °C. Samples were then centrifuged (short program, as above), and the two supernatants combined. Aliquots (200 μl) were transferred to vials and dried in a vacuum at 35 °C for 40 min.

2.4.2. GC–MS analysis

Samples were derivatized by adding 50 μl (20 mg/ ml) of methoxyamine hydrocloride (CAS number: 593-56-6, Sigma) in pyridine (CAS number: 110-86-1, VWR) at 37 °C for 90 min under continuous shaking (170 rpm). Samples were silylated with 50 μl of MSTFA (CAS number: 24589-78-4, Thermo Scientific) with 1% of TMSC (CAS number: 106018-85-3, Thermo Scientific) at 37 °C for 60 min under continuous shaking (170 rpm). Alkane series in hexane (5 μl; C7-C30) and 100 μl of hexane were added to each sample before GC–MS analysis.

GC–MS analysis was performed with an Agilent 7890A chromatography system coupled with an Agilent 7000 Triple quadrupole mass spectrometer and GC PAL autosampler and injector (CTC Analytics). For each run of analysis, 1 μl of sample was injected with pulsed splitless mode with a 30 psi pulse for 0.60 min and purge flow at 0.50 min in a single tapered liner with glass wool (Topaz 4 mm ID, Restek). Inlet temperature was set to 260 °C.

Helium flow in the guard column (Agilent Ultimate Plus deactivated fused silica, length 5 m, 0.25 mm ID) and in the analytical column (Agilent HP-5MS UI, length 30 m, 0.25 mm ID, 0.25 μm film thickness) was 1.2 ml min^{-1} and purge flow was 46 ml min^{-1}. Helium flow in the restrictor column (deactivated silica, length 1.5 m, 0.15 mm ID) was 1.3 ml min^{-1}. MSD interface temperature was 280 °C, MS source 230 °C and quadrupole 150 °C. The oven temperature program was set at: 50 °C for 3 min, 7 °C min^{-1} ramp to 240 °C, 10 °C min^{-1} ramp to 330 °C, 2 min at 330 °C and post-run at 50 °C for 4 min. Mass spectra were collected with a scan range of 55–550 *m/z*.

AMDIS (version 2.68, NIST) and Metabolite Detector (versions 2.06 beta and 2.2 N (Hiller et al., 2009)) were used for deconvolution, component detection and quantification. Metabolite levels were calculated using the internal standard, benzoic-d5 acid, in relation to both normalized metabolite peak, and dry and fresh weight of the sample. Metabolites were annotated based on spectra and retention index matched to reference compounds and the Golm Metabolome database (GMD) (Hummel et al., 2007), NIST Mass Spectral database (version 2.0, Agilent) and Fiehn library (Agilent).

2.5. Bioinformatics

The raw proteomics output, from LC-ESI-MS/MS, was processed for protein identification and label-free quantification using MaxQuant (v1.6.2.3) (Cox and Mann, 2008). MaxQuant allowed for the assignment of proteins to their respective RefSeq codes for both *O. mykiss* and Atlantic salmon (*Salmo salar*) through the integrated Andromeda search engine (Cox et al., 2011). In short: the MaxQuant derived output was exported to, and analyzed, using the Perseus platform (v1.6.14.0) (Tyanova et al., 2016). Data was log_2-adjusted, filtered and protein (UniProt) annotations for Atlantic salmon, due to the better coverage compared to rainbow trout, added (obtained from datashare.biochem.mpg.de). Proteins with a significantly different abundance, compared to control, were identified using the built-in ANOVA + Tukey's post hoc test function, and the data output exported to Excel for manual sorting, analysis and comparisons.

Each differently expressed protein's (DEP) UniProt code was translated to the equivalent zebrafish gene symbol (obtained at zfin.org). Gene ontology (GO) term and KEGG pathway over-representation analysis was performed using the online platform Metascape (Zhou et al., 2019). Identified terms and pathways were considered over-represented if both the p and q-value were ≤ 0.05.

The proteomic dataset is available through the repository service PRIDE, and accessible under the project code: PXD026443.

2.6. Statistics

Every statistical test, unless stated otherwise, was performed in R-studio (v1.2.5042), with significance cut-off set at $p \leq 0.05$. The effects of exposure on mortality and pigmentation intensity (in relation to control) were analyzed using Fisher's exact test. As neither standard length nor planar yolk area were normally distributed (as per Shapiro-Wilkss test), Kruskal-Wallis test combined with Dunn's post hoc test, combined with Bonferroni's adjustment method, was employed. Due to the low N (4) per treatment, enrichment or depletion of metabolites, relative to control, were assessed using Mann-Whitneys *U* test corrected for multiple comparisons using the Bonferroni's adjustment method. Principal Component Statistical analysis of the cardiac metabolome was performed using Simca P^+ (version 16, Umetrics) but visualized using R-studio.

3. Results and discussion

3.1. Mortality and morphology

The exposure of newly hatched and developing rainbow trout alevins to retene and fluoranthene (alone or as a mixture) did not significantly affect mortality; be that in relation to control or between the PAH treatments ($p > 0.05$; Table 2). This was expected as the concentrations of the PAHs were selected as to avoid elevated mortality (based upon preliminary experiments and previous studies (Billiard et al., 1999; Vehniäinen et al., 2016); for SFS quantified exposure concentrations, see Table s1). Measurement of actual exposure concentrations, sampled just before renewal of water and chemicals, yielded similar results (percentage of nominal concentration), as those reported in Eriksson et al., 2022.

Morphologically, alevins sampled for their cardiac metabolome presented similar alterations as observed among alevins sampled for their

Table 2
Summary of mortality (percentage, ± 95% confidence interval) and morphological endpoints (mean ± s.d.) in 14 days old rainbow trout alevins exposed to control (DMSO), retene (Ret), fluoranthene (Flu) or the binary mixture of the two (Mix). Dorsal fin- and yolk sac pigmentation intensity and mortality were assessed using Fisher's exact test, while standard length and yolk area were analyzed using Kruskal-Wallis' test combined with Dunn's post hoc test. Significant differences with regards to the standard length and planar yolk area are denoted using different Latin letters (lower and uppercase, respectively). In contrast, differences in pigmentation are denoted by different Greek letters and numbers, respectively. Note: these results are only representative for the alevins sampled for their cardiac metabolome. For results on alevins sampled for their cardiac proteome, see Eriksson et al. (2022).

		Morphological[¤]		Pigmentation[¤]	
Treatment	Mortality (%)[#]	Standard length (mm)	Planar yolk area (mm^2)	Dorsal fin (%)	Lateral side (%)
DMSO	3.89 (1.07–7.71)	22.76 ± 1.24^{a}	8.75 ± 4.14^{AB}	100%$^{\alpha}$	61%^{1}
Ret	1.11 (0–3.98)[Δ]	22.44 ± 1.13^{ab}	7.51 ± 1.88^{A}	100%$^{\alpha}$	17%^{2}
Flu	3.89 (1.07–7.71)	22.43 ± 1.12^{ab}	10.08 ± 2.63^{B}	89%$^{\beta}$	83%^{3}
Mix	1.11 (0–3.98)[Δ]	21.58 ± 1.11^{b}	9.99 ± 3.64^{AB}	78%$^{\beta}$	11%^{2}

[#] $N = 180$ per treatment and 15 per replicate.
[¤] $N = 18$ per treatment and 3 per replicate.
[Δ] True 95% confidence interval is −6.68 to +3.98; lowest limit is set to 0 as mortality cannot be negative.

cardiac transcriptome and proteome, after 14 days of exposure (Eriksson et al. (2022). Nevertheless, and among alevins sampled for their cardiac metabolome, no reduction in standard length was observed following exposure to retene for 14 days (significantly reduced standard length was observed among retene exposed alevins sampled for their cardiac proteome and transcriptome; Eriksson et al. (2022)) or fluoranthene (not affected in either study). Alevins exposed to the binary mixture were significantly shorter and presented a significantly greater planar yolk area than control. Similar results, with regards to standard length, but not planar yolk area, were observed among alevins sampled for their cardiac transcriptome and proteome (Eriksson et al. (2022).

An interesting aspect on the impact of exposure upon growth and development was the observation of hypopigmentation of the lateral side among retene and mixture exposed alevins and hyperpigmentation among fluoranthene exposed alevins, relative to control. Pigmentation of the dorsal fin on the other hand was significantly reduced among fluoranthene and mixture exposed alevins, but not retene, relative to control. These results are relatively similar to those reported by Eriksson et al. (2022), albeit variation exist. It is therefore plausible that pigmentation is influenced by seasonality and batches differences. Further assessment of pigmentation as an endpoint, in relation to exposure, seasonality and batch quality is required before any definitive conclusion can be established.

The combined results on the impact of exposure upon growth and pigmentation suggests that mixture exposed alevins might be at an earlier developmental stage at sampling, rather than just being shorter, compared to control alevins (Table 2), as pigmentation is, to a certain degree, controlled by Ahr activation in fish (Zodrow and Tanguay, 2003). It is also possible that retene exposed alevins were at an earlier developmental stage as well, based upon pigmentation intensity. What exactly caused the reduction in developmental gain and growth is unknown, although multiple processes are likely to be involved. The most plausible underlying processes are related to the reallocation of energy expenditures, plausibly away from growth and development to xenobiotic metabolism (Yue et al., 2021), potentially impairment of heart function (Vehniäinen et al., 2019; Ainerua et al., 2020) and structure (Incardona et al., 2011), which subsequently translates into a weakened cardiac output (Incardona, 2017), reduced absorption of yolk and fatty acids (Sørhus et al., 2021), circulation of nutrients and gas exchange. Significantly elevated pigmentation of the lateral side among fluoranthene exposed alevins (compared to control), in contrast, is plausibly a consequence of increased body burden and therefore, a potentially stronger Ahr-activation (Table 4).

3.2. Proteomic responses

3.2.1. General findings

The cardiac proteome, just like the cardiac transcriptome, responded in an exposure-specific manner to the influence of PAHs during early life development; similar results were reported by Rigaud et al. (2020a, 2020b). In total, 65 and 82 DEPs were identified after 7 and 14 days of exposure, respectively. Filtered per treatment, fluoranthene affected 11 and 19 proteins on Day 7 and 14; retene: 29 and 23; mixture: 44 and 82 (Fig. 1a and b; Tables s2 and s3). Interestingly, exposure to fluoranthene did not result in any unique DEP(s) by Day 7, while exposure to retene produced 20, and the mixture 29 unique expressions (Fig. 1a). Nevertheless, 3 DEPs were shared between the different PAH treatments on Day 7: Cyp1a (enriched relative to control; ↑), tubulin alpha chain (depleted relative to control; ↓) and methylosome subunit pICln (↓). No unique cardiac DEPs were identified among fluoranthene and retene exposed alevins sampled after 14 days, while exposure to mixture induced 47 unique DEPs (Fig. 1b). Seven DEPs were shared between the different treatments relative to control: one uncharacterized protein (↑), Cyp1a (↑), UDP-glucuronosyltransferase (↑), vesicle amine transport 1 (↑), vimentin (↓), protein 4.1 isoform X5(↓) and 60S ribosomal protein L22 (↓). When the cardiac proteomes were compared between alevins sampled after 7 and 14 days of exposure, 24 shared DEPs were identified: exposure to fluoranthene resulted in 3 shared DEPs between Day 7 and 14, retene 4 and mixture 23 (Table s3).

Following bioinformatic analysis of the DEPs, and by Day 7, no over-represented pathways or terms were identified among alevins exposed to fluoranthene (every p and q-value >0.05), while exposure to retene caused the over-representation of plasma lipoprotein assembly (R-DRE-8963898; Tables 3 and s5). In contrast, exposure to the mixture over-represented xenobiotics metabolism (dre00980) and DNA replication (GO:0006267). After 14 days of exposure, fluoranthene over-represented the xenobiotic metabolism pathway (dre00980; Table s6). Alevins exposed to retene did not over-represent any term or pathway. Exposure to the mixture gave rise to a broader over-representation profile, which encompassed xenobiotic metabolism, DNA replication, regulation of coagulation (GO:0050878), cell redox homeostasis (GO:0045454) and a few other terms, which to a large extent, overlapped with the coagulation GO-term (e.g., GO:0010466, GO:0031589 and GO:0072376).

3.2.2. PAHs body burden, proteins involved in PAHs metabolism

Exposure to the binary mixture of retene and fluoranthene resulted in different body burden profiles of the PAHs when compared to those developed among alevins exposed to the individual components. By Day 14, the

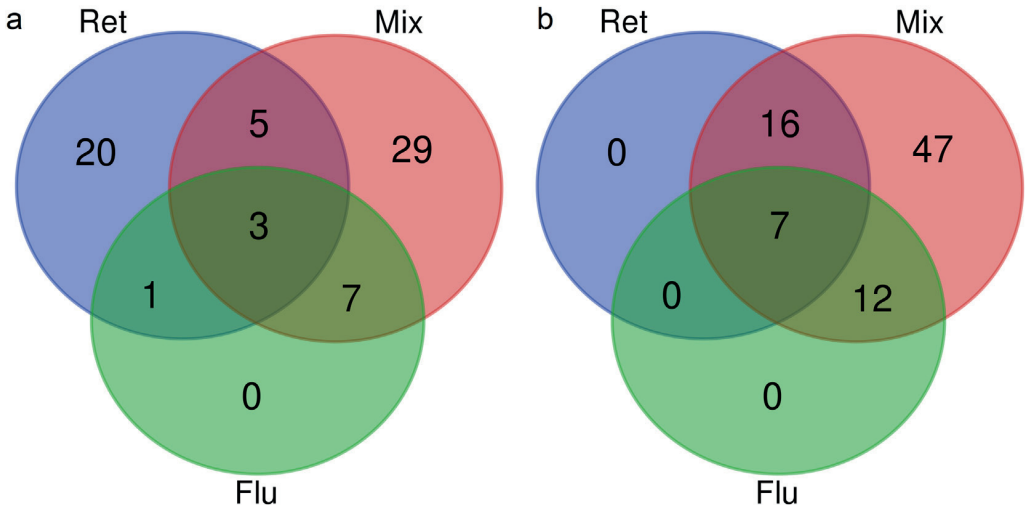

Fig. 1. Venn-diagram representations of differently expressed proteins following 7 (a) and 14 days (b) of exposure to retene (Ret), fluoranthene (Flu) and the binary mixture of the two PAH (Mix). The Venn-diagrams were created using the online tool provided by: http://bioinformatics.psb.ugent.be/webtools/Venn/.

Table 3
Over-represented GO-terms, as well as KEGG and reactome pathways, with a p and q-value ≤0.05 (as per Metascape) in rainbow trout alevins exposed to fluoranthene (Flu), retene (Ret) and the binary mixture of the two PAHs (Mix) and sampled after 7 and 14 days. For a detailed list of the depleted and enriched proteins governing these over-representations, see table s5 (Day 7) and s6 (Day 14), respectively. Note, in order to avoid reporting redundant pathways and terms, over-represented terms and pathways are those reported as "summary" by Metascape. For a complete list of over-represented terms and pathways, irrespective of q-value, see the file: Supplementary_file-Summary_Metascape.xlxs. NA = not applicable.

Sampled	Exposure	Term ID	Term description	*p*-Value	q-Value
Day 7	Flu		No over-representations identified		
	Ret	R-DRE-8963898	Plasma lipoprotein assembly	<0.0001	0.003
	Mix	dre00980	Metabolism of xenobiotics by cytochrome P450	<0.0001	<0.0001
		GO:0006267	pre-replicative complex assembly involved in nuclear cell cycle DNA replication	<0.0001	0.001
Day 14	Flu	dre00980	Metabolism of xenobiotics by cytochrome P450	<0.0001	0.018
	Ret		No over-representations identified		
	Mix	GO:0050878	regulation of body fluid levels	<0.0001	<0.0001
		GO:0010466	negative regulation of peptidase activity	<0.0001	<0.0001
		dre00980	Metabolism of xenobiotics by cytochrome P450	<0.0001	<0.0001
		GO:0045454	cell redox homeostasis	<0.0001	<0.0001
		GO:0006267	pre-replicative complex assembly involved in nuclear cell cycle DNA replication	<0.0001	0.002
		GO:0031589	cell-substrate adhesion	<0.0001	0.013
		GO:0072376	protein activation cascade	0.0001	0.037

body burden of retene had increased by 615%, while that of fluoranthene decreased by 94.4% in mixture exposed alevins compared to the body burden profiles of alevins exposed to the components (Table 4). These trends are in accordance with what was observed in our transcriptomic mixture study (Eriksson et al., 2022). These differences in body burden relates well to the exposure-specific up-regulation of proteins involved in xenobiotic metabolism. In total, eight DEPs known to be involved in phase I and II metabolism were identified among alevins exposed to the mixture: Cyp1a, UDP-glucuronosyltransferase (Ugt), 2 isoforms of sulfotransferase (Sult) and 4 isoforms of glutathione S-transferase (Gst). Furthermore, the mixture induced a stronger Cyp1a expression than the combined, additive effect of the components by Day 7, but not Day 14, as well as activation of a wider suit of phase II metabolic processes than the components. These exposure-specific differences in phase II metabolic responses confirm our previous transcriptomic findings on the relationship between the exposure-specific up-regulation of phase II metabolic processes and the corresponding body burden of the PAHs (Eriksson et al., 2022). Similar exposure-specific enrichment of phase I and II metabolic processes has been identified in the cardiac proteome of rainbow trout alevins exposed to retene, pyrene and phenanthrene individually (Rigaud et al., 2020b).

Interestingly, fluoranthene was detected and quantified in the cardiac metabolome among alevins exposed to fluoranthene alone, but below the limit of detection in the metabolome of alevins exposed to DMSO, retene and the binary mixture. This finding would imply that the fluoranthene, once absorbed, is distributed throughout the organism via the cardiovascular system. Alevins exposed to the mixture, by comparison, did not present detectable accumulation in heart tissue, whereby providing additional support to the notion of enhanced phase II metabolic capacity, and plausibly less uptake of fluoranthene in cardiovascular tissue.

Table 4
Average body burden of retene (Ret) and fluoranthene (Flu) per fish (± standard deviation) in 14 days old rainbow trout alevins exposed to the PAHs alone or as a binary mixture (Mix) and sampled for their cardiac metabolome. Body burden is background compensated. Statistically significant differences between the mixture and its components are denoted using lower and uppercase letters and established using Mann-Whitney's U test. N = 8 per treatment.

Treatment	Average retene body burden (pmol per alevins)	Average fluoranthene body burden (pmol per alevins)
Ret	1.77 ± 0.48[a]	0
Flu	0	3967 ± 960[A]
Mix	10.93 ± 3.90[b]	222 ± 73[B]

3.2.3. Iron metabolism and oxidative stress

Even though neither exposure over-represented any term or pathway related to iron metabolism, two DEPs essential for iron (Fe^{3+}) metabolism and homeostasis were identified in the cardiac proteome. These two proteins were hemopexin a (Hpxa; depleted by exposure to fluoranthene and the mixture on Day 7 and 14) and ferritin (depleted by retene on Day 7 and enriched by mixture on Day 7 and 14). Hemopexin is a plasma protein that efficiently sequesters free heme, thereby preventing oxidative damage to cells (Tolosano and Altruda, 2002). Depletion of hemopexin has previously been reported in both juvenile Atlantic cod (*Gadus morhua*) exposed to North Sea oil (Bohne-Kjersem et al., 2009), and in newly hatched rainbow trout alevins exposed to pyrene (Rigaud et al., 2020b). In humans, depletion of plasma hemopexin is clinically associated with an increase in circulating free heme, which in turn can be caused by ongoing hemolysis (Delanghe and Langlois, 2001). In contrast to hemopexin, ferritin has previously been observed to increase with increasing dose of oil (Troisi et al., 2007; Olsvik et al., 2012) or during anoxia (Larade and Storey, 2004). The primary function of ferritin is to store biologically available iron, making it non-reactive, as free and circulating iron is toxic and can act as a substrate for the formation of reactive oxygen species (Halliwell and Gutteridge, 1985). As the amount of circulating heme, normally, is maintained under strict homeostasis, there are two possible processes that could increase the concentration of circulating heme in plasma: leakage of newly produced and unbound heme, or following the dissociation from hemoproteins during oxidative stress (Sawicki et al., 2015). Hence, it seems plausible to assume that exposure to fluoranthene alone, or as part of a mixture, increased the rate at which hemopexin is depleted which in turn suggests increased availability of freely circulating heme (Delanghe and Langlois, 2001). However, the experimental protocol does not allow for the identification of the source of the free heme, but the effects of PAHs on erythrocytes should be investigated further.

As previously mentioned, un-scavenged free heme can aggravate oxidative stress by acting as a substrate for the generation of oxygen radicals (Halliwell and Gutteridge, 1985). We know from our transcriptomic dataset that exposure to fluoranthene and the binary mixture over-represented the GO-term oxidoreductase activity (GO:0016491) which involved the up-regulation of thioredoxin reductase 1, thioredoxin-like and peroxiredoxin 2 (Eriksson et al., 2022). Over-representation analysis of the cardiac proteome among mixture exposed alevins identified the GO-term cell redox homeostasis (GO:0045454), which suggests enrichment of anti-oxidative processes. Manual assessment of the involved genes revealed that exposure to the mixture enriched peroxiredoxin (also enriched by fluoranthene), peptide methionine sulfoxide reductase, thioredoxin reductase 1 and thioredoxin. These specific enrichments provide additional support to the possibility that fluoranthene and the mixture induced oxidative stress as part of the toxicity profiles and that it may take an extended exposure duration for

enrichment of certain proteins to reach detectable levels in the cardiac proteome. Furthermore, exposure-specific enrichment of anti-oxidative enzymes overlapped with the disrupted iron metabolism and homeostasis. It is unclear whether the oxidative stress is a consequence of, or exasperated by, increased amount of free and circulating heme; further studies on the relationship between PAH toxicity and oxidative stress is required.

Exposure for 14 days to the mixture, but not the components, resulted in the over-representation of the GO-term regulation of body fluid levels (GO:0050878; every protein involved in this term was depleted; Table s5). The functions of the involved proteins are primarily related to coagulation, as per the depletion of antithrombin, plasminogen, protein C (vitamin K-dependent) and fibrinogen (gamma chain-like). Combined, these depletions suggest impaired anti-coagulation regulation and capacity. This is further supported by the depletion of pro-coagulant proteins, such as von Willebrand factor(−like; VVF) and coagulation factor VIII(−like). During normal circumstances, the latter protein is always associated in an inactive form with the former, but dissociates and becomes active upon blood vessel injury, thus triggering clotting mechanisms (Zimmerman and Edgington, 1973; Weiss et al., 1977;). Hence, depletion could indicate ongoing or past injuries to the cardiovascular system, which could in turn contribute to the formation of PAH induced cardiotoxicity. The negative effect of PAH(s) upon coagulation capacity has previously been reported in mummichog embryos (*Fundulus heteroclitus*) exposed to PAH-contaminated sediment extracts, as per an observed correlation between downregulation of *vvf* and cardiotoxicity (Bozinovic et al., 2021). However, the identification of abovementioned coagulation-related proteins is a novel finding, which could contribute to, or even aggravate cardiotoxicity. How and why exposure affected coagulation-related proteins is, however, unknown and requires further inquiry.

3.2.4. Proteomic responses in relation to cellular stability and proliferation

Several significantly altered proteins, involved in cellular integrity and proliferation, were identified following exposure to the PAHs. With respect to cellular proliferation, over-representation of DNA replication (dre03030) was observed in mixture exposed alevins sampled after both 7 and 14 days. This specific over-representation implies restricted DNA replication and cellular division at an early checkpoint, as per significant depletion of 4 components of mini-chromosome maintenance proteins (Mcm; type 4, 6, and 7 by Day 7; and type 5, 6 and 7 by Day 14). During normal conditions, the Mcm components form the pre-replication complex together with Cdc6- and Cdt1 proteins; a molecular complex that is essential for the initiation of DNA replication (Dutta and Bell, 1997; Cvetic and Walter, 2006). Depletion of several types of Mcm would thus suggest that exposure to this mixture restricted organ growth at an early molecular stage, which could potentially translate to smaller heart due to fewer rounds of cellular division. Reduced heart size and fewer cardiomyocytes have been observed before in developing rainbow trout (Hornung et al., 1999) and zebrafish (Antkiewicz et al., 2005) exposed to the dioxin TCDD (which also induces toxicity through Ahr2 agonism (Tanguay et al., 2003)). A decreased expression of *mcm2* has previously been reported in Atlantic cod larvae (*Gadus morhua*) exposed to weathered crude oil (Olsvik et al., 2012). Why and how depletion of abovementioned Mcm-components occurred are beyond the scope of this manuscript, but should be investigated further.

No over-representation related to cellular integrity was identified. However, assessment of the individual DEPs highlighted additional effects of exposure on processes related to cellular integrity and proliferation. The abundance of cardiac tubulin alpha- (all treatments on Day 7 but only mixture by Day 14) and beta chain proteins (mixture on Day 7 and 14) were found to be depleted relative to control. Together, the alpha- and beta tubulins form the basis of the cytoskeleton, the microtubules (Nogales, 2000). Depletion of tubulins has previously been linked to decreased rate of mitosis, as the alpha chain tubulin acts as the microtubule anchor during mitosis from which beta tubulins extend (Mitchison and Kirschner, 1984; Meunier and Vernos, 2012). Therefore, it is plausible that these depletions are in related to the depletion of Mcm-components.

The cytoskeleton stability and integrity were further affected by exposure, as per the depletion of keratin type I cytoskeletal 18(−like), desmin (−like) and Vimentin. Keratin type I cytoskeletal 18(−type), which was depleted following exposure to the mixture, is a low molecular weight simple keratin, which together with keratin 8 (a type II keratin) form some of the most abundant intermediate filaments (Paramio and Jorcano, 2002). Altered abundance of keratin 18 could thus contribute to impaired cardiomyocyte structure following exposure to PAH, and thereby to altered heart morphology (Scott et al., 2011).

Desmin and vimentin, in contrast, are both type III intermediate filaments; the former was depleted following exposure to retene and the mixture, while the latter was depleted irrespective of exposure. Desmin is required for the maintenance of muscle structure and function, where it connects the myofibril to the *Z*-lines (Sequeira et al., 2014). The depletion of desmin draws attention to an interesting finding from our transcriptomic dataset: the down-regulated nebulette (*nebl*) by every PAH treatment (Eriksson et al., 2022). As a protein, Nebl is, together with desmin, important for the formation of the Z-line in heart musculature. Knockdown of *nebl* in mice is associated with broadening of the Z-line, but does not affect the lifespan (Mastrototaro et al., 2015). Hence, there is a good probability that exposure to PAHs altered the Z-line and therefore cardiac muscle morphology. What the consequences are for the heart is unknown, but the depletion could be either compensatory, as to offset altered action potential (Vehniäinen et al., 2019), or a direct effect of PAH(s) toxicity.

Vimentin (Vim), which is also a type III intermediate filament, serves to anchor organelles and allows for the cell to be dynamic and maintain structural cohesion (Katsumoto et al., 1990). It is unknown how (or even if) depletion of Vim contributed to PAH-induced cardiotoxicity. A previous study on *Vim*-null mice reported no changes in the structural phenotypes of multiple organs, nor did the lack of the *vim*-gene affect breeding capacity (Colucci-Guyon et al., 1994). The authors hypothesized that other intermediate filaments could compensate for the lack of *vim*/Vim. However, in our PAH exposed rainbow trout alevins, multiple cardiac intermediate filaments were depleted, and it is thus plausible that no such compensatory mechanisms can occur, and if they do, the compensatory mechanism would be limited, as several types of filaments are depleted, especially among mixture exposed alevins.

Additionally, we found that 7 days of exposure to the mixture, and every PAH treatment on Day 14, significantly depleted calponin 2 (Cnn2), which is one among many important factors involved in vascular development, cytoskeletal organization and heart function (Fukui et al., 1997; Tang et al., 2006). Knockdown of *cnn2* in zebrafish produces deleterious phenotypes as per increased occurrence of pericardial- and hindbrain edemas, while decreasing the heart rate and restricting the circulation of erythrocytes, and consequently resulting in high mortality rates (Tang et al., 2006).

Collectively, these abovementioned results suggest a decreased rate of cellular proliferation, as well as impaired cellular structure and stability. The depletion of abovementioned intermediate filaments, in combination with the down-regulation of *nebl*, alongside the known impact of PAHs on cardiac ion channels and subsequently altered repolarization of the action potential could all contribute to impaired heart morphology and function as well as overall cardiotoxicity. The slower growing and developing heart could cause downstream consequences for the whole organism as circulation of nutrients, oxygen and hormones becomes restricted (Incardona et al., 2009; de Soysa et al., 2012; Sørhus et al., 2017); factors that potentially could be related to slower development among mixture, and potentially retene, exposed alevins.

3.3. Metabolomic responses

Exposure to the PAH(s) alone, or as a mixture, resulted in few significantly impacted cardiac metabolites after 14 days of exposure, as per the untargeted metabolite profiling approach. Using principal component analysis (PCA), we found that components 1 and 2 explained 50.1% of the variation and thus highlighted a shift in the cardiac metabolome composition in PAH exposed alevins compared to control (Fig. 2a; fresh weight adjusted). In contrast, components 1 and 3 revealed that the cardiac metabolome composition among mixture exposed alevins were more akin to that of

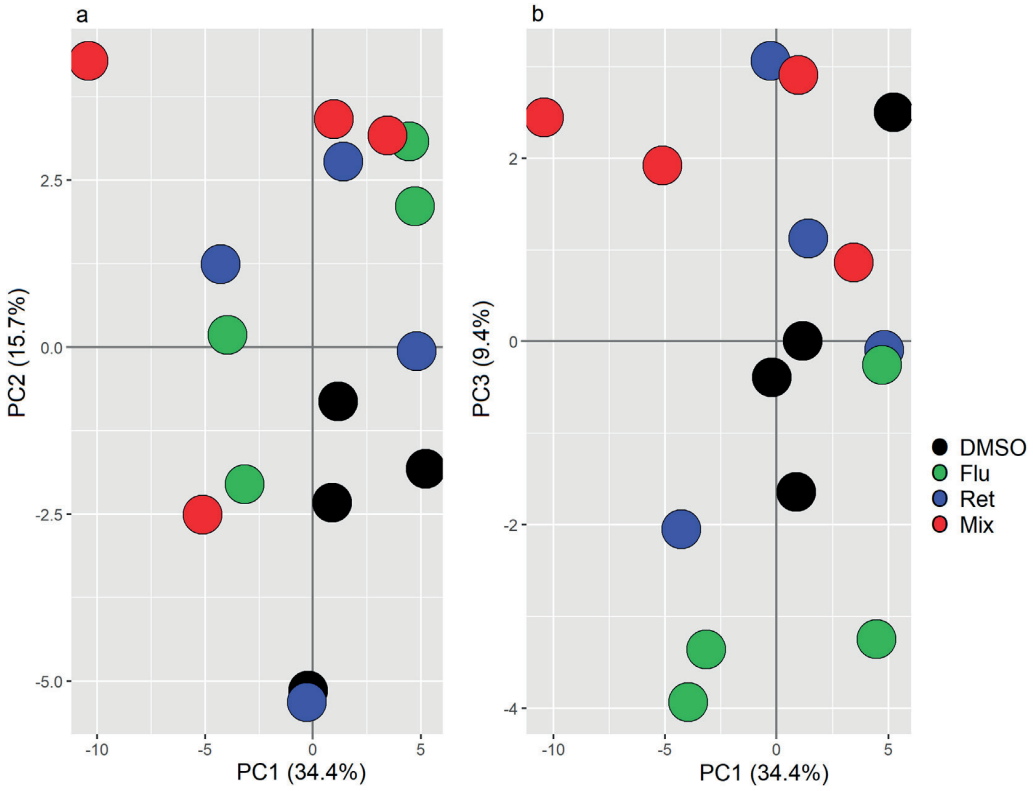

Fig. 2. Principal Component Analysis of the cardiac metabolome from 14-days old rainbow trout alevins exposed to either DMSO (black; control), retene (blue; Ret), fluoranthene (green; Flu) and the binary mixture of the two (red; Mix). Plot a) represents comparison between principal component 1 and 2 while b) the comparison between component 1 and 3. Results are compensated for fresh weight.

retene exposed alevins, than those exposed to fluoranthene (Fig. 2b). Metabolite levels, adjusted for dry weight, were excluded from the analysis due to an outlying control replicate, and poorer separation of the components (Figs. s1; s2a and s2b). Additionally and for the sake of simplicity, the impact of the mixture on energy metabolism in heart tissue (proteomics and metabolomics) is visualized in Fig. 3.

In total, 60 cardiac metabolites were detected, identified and annotated. However, three metabolites were omitted from analysis due to abundances being lower than the limit of detection in control. These were hypoxanthine, hydroxyfluorene and fluoranthene. Among the remaining 57 metabolites, 5 were found at significantly different abundance relative to control (Mann-Whitney with Bonferroni adjustment method). Exposure to retene did not significantly affect any metabolite relative to control. Fluoranthene enriched glucuronic acid and the sugar alcohol arabitol, while the binary mixture depleted methionine, putrescine and hypotaurine significantly, and phenylalanine near-to-significantly ($p = 0.0535$). By comparison, Rigaud et al. (2020b) did not observe any significantly impacted cardiac metabolite in rainbow trout alevins exposed to retene for 14 days, but among those exposed to pyrene and phenanthrene (albeit using a different statistical approach); exposure to the latter two PAHs altered the abundance of a minor number of metabolites: e.g. depletion of valine and alanine, which indicated amino acid catabolism. They also reported that exposure to phenanthrene enriched glucuronic acid and arabitol, just like fluoranthene; an observation that would suggest that these two PAHs affect similar type of processes. Decreased abundance of amino acids has also been observed in the metabolome of newly hatched zebrafish exposed to benz[*a*]anthracene (BAA) and its oxidized form (Elie et al., 2015).

Out of the 5 significantly and differently abundant metabolites, only one amino acid was observed at altered abundance: methionine, significantly depleted following exposure to the mixture. Depletion of methionine is plausibly a consequence of increased demand for cysteine (which is required in glutathione metabolism). The biotransformation is facilitated by the S-Adenosyl methionine (SAM-e) cycle where methionine is metabolized in a three-step reaction to homocysteine, which can then be transformed to cysteine in two steps (Finkelstein and Martin, 2000) (Fig. 3). Depletion of hypotaurine among mixture exposed alevins could, just like methionine, could be linked to cysteine. During normal cellular functionality, taurine is produced from hypotaurine, which in turn is derived from cysteine. The amount of taurine in the cardiac metabolome was also (on average, but not significantly) depleted among mixture exposed alevins relative to control. Hence, the depletion of hypotaurine is plausibly linked to restrictions in the enzymatic conversion rate of cysteine, as the latter could be in demand for glutathione metabolism rather than the biosynthesis of taurine. Alternatively, cysteine can be catabolized following biotransformation to pyruvate. Hence, exposure-specific whole body quantification of cysteine, and other amino acids, could therefore shed additional light on these aspects.

The near-to-significant depletion of phenylalanine could imply ongoing amino acid catabolism. This notion is indirectly supported by data from our transcriptomic study (Eriksson et al., 2022), as exposure to the mixture caused up-regulation of tyrosine aminotransferase (*tat*; up-regulated on Day 3) and fumarylacetoacetate hydrolase (*fah*; up-regulated on Day 3, 7 and 14). The corresponding proteins are involved in the biotransformation of phenylalanine to tyrosine by Tat (Dietrich, 1992), which is then transformed into fumarate by Fah (Bateman et al., 2001). Fumarate, in turn, can be utilized in the citric acid cycle for the generation of both energy and reducing agents. The absence of enriched Tat and Fah proteins is most likely related to quantification rather than temporal aspects, especially since the heart is less metabolically active than other organs.

Furthermore, exposure to the mixture enriched four proteins essential in aerobic energy metabolism: phosphofructokinase (PFK), 2-oxoglutarate dehydrogenase (OGDC; also enriched by retene), dihydrolipoamide acetyltransferase (a component of the pyruvate dehydrogenase complex) and glucan phosphorylase (alpha-1,4). PFK is essential in the glycolysis as it catalyze the reaction: D-fructose 6-phosphate + ADP → fructose 1,6-

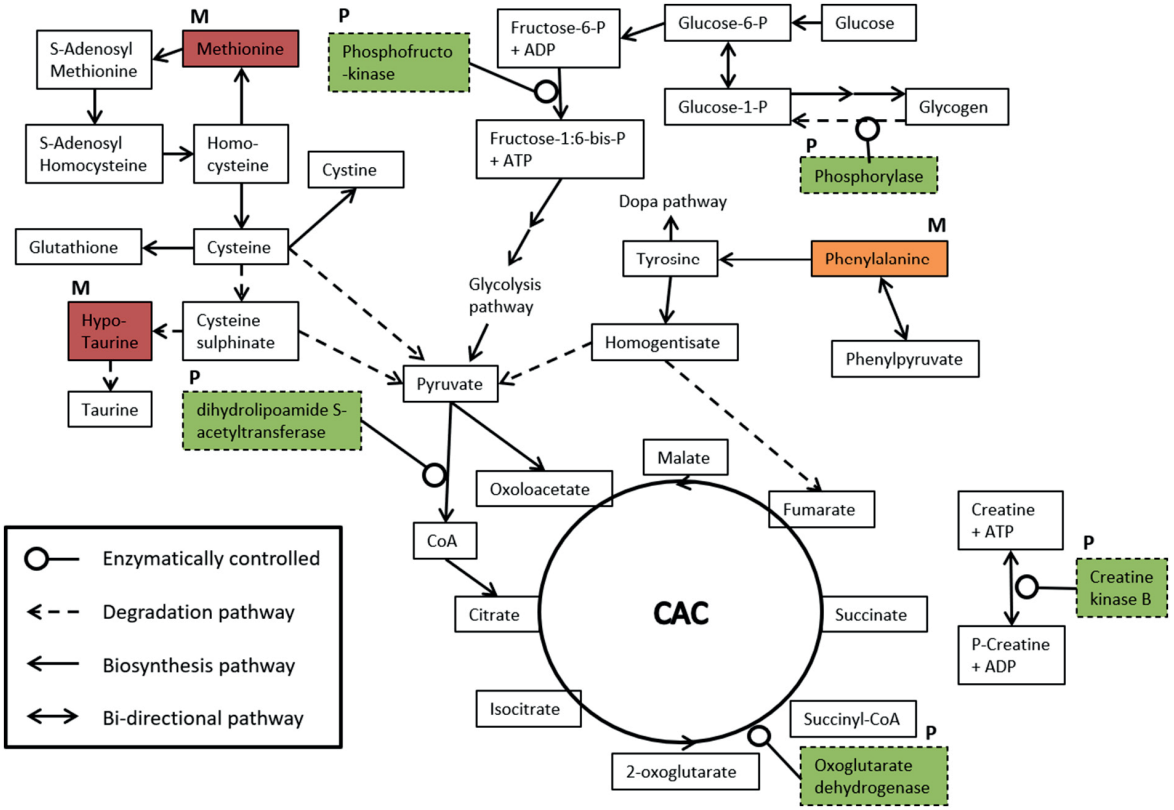

Fig. 3. A simplified visualization representing the impact of mixture on energy metabolism in heart tissue, as per the cardiac proteome (P) and metabolome (M). Boxes with a solid boarder represent products, while boxes with dashed boarders represent enzymes. Boxes colored in green indicate enrichments, while red and orange represent significantly and near-to-significant depletions, respectively. CAC = Citric Acid Circle.

bisphosphate + ATP (Uyeda, 1979). In contrast, OGDC catalyzes an essential reaction in the citric acid cycle: α-ketoglutarate + NAD^+ + Acetyl-CoA (CoA) → Succinyl CoA + CO_2 + NADH (Williamson, 1979). Alpha-glucan phosphorylase on the other hand is involved in multiple biochemical reactions, including carbohydrate metabolism, as per UniProt. Enrichment of dihydrolipoamide acetyltransferase suggests increased rate of conversion of pyruvate to CoA, indicative of increased demand for energy.

Additional support for increased and altered metabolic activity is provided by the enrichment of creatine kinase B(−type). This enzyme facilitates the reversible and ATP/ADP dependent conversion of creatin ↔ phosphocreatine (PCr) (Oliver, 1955). Hence, PCr can be reverted back to creatin by the same enzyme and thus generate a localized burst of ATP, when required. Combined, the proteomic-, transcriptomic- and metabolomic data suggests that exposure to this mixture increases energy requirements, be that aerobically or catabolically (Fig. 3). However, and due to the poorer metabolic capacity of the heart, relative to the liver, these results on amino acid metabolism could indicate a systemic energy deficit in mixture exposed alevins rather than a localized deficit, as our data indicate. These results are especially relevant since heart tissue primarily utilize β-oxidation of fatty acids to cover energy expenses, rather than glycolysis and amino acid catabolism (Grynberg and Demaison, 1996).

Enrichment of arabitol and glucuronic acid following exposure to fluoranthene indicates either increased rate of formation, decreased rate of utilization or both. Arabitol is a sugar alcohol that can be utilized in energy metabolism through the pentose phosphate pathway (Bateman et al., 2001) (PPP). The primary outcome of PPP is the formation of NADPH, which in turn is important in multiple biological processes, including counteracting oxidative stress. Hence, enrichment could suggest that increased oxidative stress had occurred and that accumulation of arabitol could therefore be left-over material that can be utilized for the formation of NADPH from $NADP^+$ as well as maintaining the equilibrium between oxidized- and reduced glutathione (Stanton, 2012). Glucuronic acid on the other hand is primarily utilized in phase II metabolism by UDP-glucuronosyltransferase (UGT). Exposure to fluoranthene induced a weak but statistically significant enrichment of UGT by Day 14 (a 64.9% stronger induction relative to control). It is possible that partial inhibition of Cyp1a by fluoranthene could limit the utilization of glucuronic acid and thus force its enrichment.

However, metabolomic investigations at earlier timepoints are required to confirm and assess the trends temporally. Furthermore, the low number of metabolomic replicates and material ($N = 4$ per treatment) limits the statistical analysis. It is likely that a greater number of replicates with more material per replicate could produce a more precise assessment of the impact of exposure on the cardiac metabolome. Likewise, sampling and assessment of other tissues, with higher metabolic capacity than cardiac tissue, could highlight other impacted metabolic pathways and processes.

4. Conclusion

We found that the exposure to retene, fluoranthene and their binary mixture produced exposure-specific toxicity profiles in newly hatched rainbow trout alevins with regards to development, growth and body burden, alongside exposure-specific cardiac proteome and metabolome profiles. Additionally, the effects exerted by the mixture on the growing and developing alevins could not be predicted from the additive effect of the components as only mixture exposed alevins were significantly shorter compared to control, while impacting a broader repertoire of cardiac proteins and pathways. Exposure-specific changes in the cardiac proteome, just like in the transcriptome (Eriksson et al., 2022), could explain the exposure-specific body burden profiles, as per PAH-specific induction of phase II metabolic processes and inhibition of Cyp1a by fluoranthene. When alevins were exposed to the mixture, a stronger and more diverse induction of phase I and II metabolic responses was observed which facilitated

decreasing body burden of fluoranthene, while the body burden of retene increased compared to the alevins exposed to the individual components. Exposure to the mixture increased the abundance of ferritin, while decreasing hemopexin (the latter was also depleted following exposure to fluoranthene) which would suggest disrupted iron metabolism and potentially increased oxidative stress. It is plausible that the altered iron metabolism is related to impaired coagulation as well as impacted erythrocyte cell membrane components. Exposure to the mixture caused decreased abundance of several components affecting cell proliferation and structure, and depletion of alpha- and beta tubulin chains, which suggests impaired cellular integrity. This is further supported by depletion of several components of intermediate filaments that are involved in cell structure, vimentin and desmin for example. In contrast, analysis of the cardiac metabolome revealed few impacts following 2 weeks of exposure, although exposure to the mixture suggests increased energy demand as per methionine depletion. Indirect support for increased demand for energy is present in the cardiac proteome as enzymes and enzyme components involved in energy metabolism were enriched. Combined, these findings highlight that no one single pathway is responsible for the development of toxicity following exposure to retene, fluoranthene or their combined binary mixture. Rather, it is likely that exposure induced toxicity through multiple mechanisms.

Ethical approval

Under the European Union Directive 2010/63/EU (*On the Protection of Animals Used for Scientific Purposes*), Chapter 1, Article 1, point 3: no ethical approval is required for in vivo experiments on non-human vertebrate animals deriving their energetic needs from the consumption of yolk.

Funding sources

Academy of Finland project number: 285296, 294066 and 319284 granted to Eeva-Riikka Vehniäinen.

Author contributions

Andreas N. M. Eriksson: Exposure maintenance; sampling; proteomics and metabolomics data analysis; tissue extraction and HPLC analysis; photo-analysis; primary author.

Cyril Rigaud: Experiment design; sampling; exposure maintenance; protein and metabolite extraction; SFS-analysis; Review & Editing.

Anne Rokka: Proteomics;

Morten Skaugen: Proteomics;

Jenna Lihavainen: Metabolomics preparation and principal component analysis; Review & Editing.

Eeva-Riikka Vehniäinen: Group leader; experimental design; Review & Editing.

Declaration of competing interest

The authors declare that they have no known competing financial interests or personal relationships that could have appeared to influence the work reported in this paper.

Acknowledgment

We would like to acknowledge the contribution of laboratory technicians Mervi Koistinen, Emma Pajunen, Hannu Pakkanen and laboratory personnel at Konnevesi research station for technical support. We also like to thank Hanka-Taimen OY fish farm for supplying us with rainbow trout alevins for scientific purposes and research.

Appendix A. Supplementary data

Supplementary data to this article can be found online at https://doi.org/10.1016/j.scitotenv.2022.154846.

References

Ainerua, M.O., Tinwell, J., Kompella, S.N., Sørhus, E., White, K.N., van Dongen, B.E., Shiels, H.A., 2020. Understanding the cardiac toxicity of the anthropogenic pollutant phenanthrene on the freshwater indicator species, the brown trout (Salmo trutta): from whole heart to cardiomyocytes. Chemosphere 239, 124608. https://doi.org/10.1016/j.chemosphere.2019.124608.

Antkiewicz, D.S., Burns, C.G., Carney, S.A., Peterson, R.E., Heideman, W., 2005. Heart malformation is an early response to TCDD in embryonic zebrafish. Toxicol. Sci. 84, 368–377. https://doi.org/10.1093/toxsci/kfi073.

Baquer, N.Z., Hothersall, J.S., McLean, P., 1988. Function and regulation of the pentose phosphate pathway in brain. In: Horecker, B.L., Stadtman, E.R. (Eds.), Current Topics in Cellular Regulation. Academic Press, pp. 265–289 https://doi.org/10.1016/B978-0-12-152829-4.50008-2.

Barron, M.G., Heintz, R., Rice, S.D., 2004. Relative potency of PAHs and heterocycles as aryl hydrocarbon receptor agonists in fish. Mar. Environ. Res. 58, 95–100. https://doi.org/10.1016/j.marenvres.2004.03.001.

Bateman, R.L., Bhanumoorthy, P., Witte, J.F., McClard, R.W., Grompe, M., Timm, D.E., 2001. Mechanistic inferences from the crystal structure of fumarylacetoacetate hydrolase with a bound phosphorus-based inhibitor. J. Biol. Chem. 276, 15284–15291. https://doi.org/10.1074/jbc.m007621200.

Behera, B.K., Das, A., Sarkar, D.J., Weerathunge, P., Parida, P.K., Das, B.K., Thavamani, P., Ramanathan, R., Bansal, V., 2018. Polycyclic aromatic hydrocarbons (PAHs) in inland aquatic ecosystems: perils and remedies through biosensors and bioremediation. Environ. Pollut. 241, 212–233. https://doi.org/10.1016/j.envpol.2018.05.016.

Billiard, S.M., Querbach, K., Hodson, P.V., 1999. Toxicity of retene to early life stages of two freshwater fish species. Environ. Toxicol. Chem. 18, 2070–2077. https://doi.org/10.1002/etc.5620180927.

Bohne-Kjersem, A., Skadsheim, A., Goksøyr, A., Grøsvik, B.E., 2009. Candidate biomarker discovery in plasma of juvenile cod (Gadus morhua) exposed to crude North Sea oil, alkyl phenols and polycyclic aromatic hydrocarbons (PAHs). Mar. Environ. Res. 68, 268–277. https://doi.org/10.1016/j.marenvres.2009.06.016.

Bohne-Kjersem, A., Bache, N., Meier, S., Nyhammer, G., Roepstorff, P., Sæle, Ø., Goksøyr, A., Grøsvik, B.E., 2010. Biomarker candidate discovery in Atlantic cod (Gadus morhua) continuously exposed to North Sea produced water from egg to fry. Aquat. Toxicol. 96, 280–289. https://doi.org/10.1016/j.aquatox.2009.11.005.

Bozinovic, G., Shea, D., Feng, Z., Hinton, D., Sit, T., Oleksiak, M.F., 2021. PAH-pollution effects on sensitive and resistant embryos: integrating structure and function with gene expression. PLoS ONE 16, e0249432.

Colucci-Guyon, E., Portier, M.-M., Dunia, I., Paulin, D., Pournin, S., Babinet, C., 1994. Mice lacking vimentin develop and reproduce without an obvious phenotype. Cell 79, 679–694. https://doi.org/10.1016/0092-8674(94)90553-3.

Cox, J., Mann, M., 2008. MaxQuant enables high peptide identification rates, individualized p.p.b.-range mass accuracies and proteome-wide protein quantification. Nat. Biotechnol. 26, 1367–1372. https://doi.org/10.1038/nbt.1511.

Cox, J., Neuhauser, N., Michalski, A., Scheltema, R.A., Olsen, J.V., Mann, M., 2011. Andromeda: a peptide search engine integrated into the MaxQuant environment. J. Proteome Res. 10, 1794–1805. https://doi.org/10.1021/pr101065j.

Cvetic, C.A., Walter, J.C., 2006. Getting a grip on licensing: mechanism of stable Mcm2-7 loading onto replication origins. Mol. Cell 21, 143–144. https://doi.org/10.1016/j.molcel.2006.01.003.

de Soysa, T.Y., Ulrich, A., Friedrich, T., Pite, D., Compton, S.L., Ok, D., Bernardos, R.L., Downes, G.B., Hsieh, S., Stein, R., Lagdameo, M.C., Halvorsen, K., Kesich, L.-R., Barresi, M.J.F., 2012. Macondo crude oil from the Deepwater Horizon oil spill disrupts specific developmental processes during zebrafish embryogenesis. BMC Biol. 10, 40. https://doi.org/10.1186/1741-7007-10-40.

Delanghe, J.R., Langlois, M.R., 2001. Hemopexin: a review of biological aspects and the role in laboratory medicine. Clin. Chim. Acta 312, 13–23. https://doi.org/10.1016/S0009-8981(01)00586-1.

Dietrich, J.B., 1992. Tyrosine aminotransferase: a transaminase among others? Cell Mol.Biol. 38, 95–114.

Doering, J.A., Tang, S., Peng, H., Eisner, B.K., Sun, J., Giesy, J.P., Wiseman, S., Hecker, M., 2016. High conservation in transcriptomic and proteomic response of white sturgeon to equipotent concentrations of 2,3,7,8-TCDD, PCB 77, and benzo[a]pyrene. Environ. Sci. Technol. 50, 4826–4835. https://doi.org/10.1021/acs.est.6b00490.

Doering, J., Hecker, M., Villeneuve, D., Zhang, X., 2019. Adverse Outcome Pathway on Aryl Hydrocarbon Receptor Activation Leading to Early Life Stage Mortality, via Increased COX-2IS. 12. https://doi.org/10.1787/bd46b538-en.

dos Santos, I.F., Ferreira, S.L.C., Domínguez, C., Bayona, J.M., 2018. Analytical strategies for determining the sources and ecotoxicological risk of PAHs in river sediment. Microchem. J. 137, 90–97. https://doi.org/10.1016/j.microc.2017.09.025.

Dutta, A., Bell, S.P., 1997. Initiation of DNA replication in eukaryotic cells. Annu. Rev. Cell Dev. Biol. 13, 293–332. https://doi.org/10.1146/annurev.cellbio.13.1.293.

Elie, M.R., Choi, J., Nkrumah-Elie, Y., Gonnerman, G.D., Stevens, J.F., Tanguay, R.L., 2015. Metabolomic analysis to define and compare the effects of PAHs and oxygenated PAHs in developing zebrafish. Environ. Res. 140, 502–510. https://doi.org/10.1016/j.envres.2015.05.009.

Eriksson, A.N.M., Rigaud, C., Krasnov, A., Wincent, E., Vehniäinen, E.-R., 2022. Exposure to retene, fluoranthene, and their binary mixture causes distinct transcriptomic and apical outcomes in rainbow trout (Oncorhynchus mykiss) yolk sac alevins. Aquat. Toxicol. 106083. https://doi.org/10.1016/j.aquatox.2022.106083.

Fent, K., Bätscher, R., 2000. Cytochrome P4501A induction potencies of polycyclic aromatic hydrocarbons in a fish hepatoma cell line: demonstration of additive interactions. Environ. Toxicol. Chem. 19, 2047–2058. https://doi.org/10.1002/etc.5620190813.

Finkelstein, J.D., Martin, J.J., 2000. Homocysteine. Int. J. Biochem. Cell Biol. 32, 385–389. https://doi.org/10.1016/S1357-2725(99)00138-7.

Fukui, Y., Masuda, H., Takagi, M., Takahashi, K., Kiyokane, K., 1997. The presence of h2-calponin in human keratinocyte. J. Dermatol. Sci. 14, 29–36. https://doi.org/10.1016/S0923-1811(96)00545-2.
Garner, L.V.T., Brown, D.R., Di Giulio, R.T., 2013. Knockdown of AHR1A but not AHR1B exacerbates PAH and PCB-126 toxicity in zebrafish (Danio rerio) embryos. Aquat. Toxicol. 142–143, 336–346. https://doi.org/10.1016/j.aquatox.2013.09.007.
Geier, M.C., James Minick, D., Truong, L., Tilton, S., Pande, P., Anderson, K.A., Teeguardan, J., Tanguay, R.L., 2018. Systematic developmental neurotoxicity assessment of a representative PAH superfund mixture using zebrafish. Toxicol. Appl. Pharmacol. 354, 115–125. https://doi.org/10.1016/j.taap.2018.03.029.
Grynberg, A., Demaison, L., 1996. Fatty acid oxidation in the heart. J. Cardiovasc. Pharmacol. 28 (Suppl. 1), S11–S17. https://doi.org/10.1097/00005344-199600003-00003.
Halliwell, B., Gutteridge, J.M.C., 1985. The importance of free radicals and catalytic metal ions in human diseases. Mol. Asp. Med. 8, 89–193. https://doi.org/10.1016/0098-2997(85)90001-9.
Hiller, K., Hangebrauk, J., Jäger, C., Spura, J., Schreiber, K., Schomburg, D., 2009. MetaboliteDetector: comprehensive analysis tool for targeted and nontargeted GC/MS based metabolome analysis. Anal. Chem. 81, 3429–3439. https://doi.org/10.1021/ac802689c.
Hornung, M.W., Spitsbergen, J.M., Peterson, R.E., 1999. 2,3,7,8-Tetrachlorodibenzo-p-dioxin alters cardiovascular and craniofacial development and function in sac fry of rainbow trout (Oncorhynchus mykiss). Toxicol. Sci. 47, 40–51. https://doi.org/10.1093/toxsci/47.1.40.
Huang, M., Mesaros, C., Hackfeld, L.C., Hodge, R.P., Zang, T., Blair, I.A., Penning, T.M., 2017. Potential metabolic activation of a representative C4-alkylated polycyclic aromatic hydrocarbon retene (1-methyl-7-isopropyl-phenanthrene) associated with the Deepwater Horizon oil spill in human hepatoma (HepG2) cells. Chem. Res. Toxicol. 30, 1093–1101. https://doi.org/10.1021/acs.chemrestox.6b00457.
Hummel, J., Selbig, J., Walther, D., Kopka, J., 2007. The Golm Metabolome Database: a database for GC-MS based metabolite profiling. In: Nielsen, J., Jewett, M.C. (Eds.), Metabolomics: A Powerful Tool in Systems Biology. SpringerBerlin Heidelberg, Berlin, Heidelberg, pp. 75–95 https://doi.org/10.1007/4735_2007_0229.
Incardona, J.P., 2017. Molecular mechanisms of crude oil developmental toxicity in fish. Arch. Environ. Contam. Toxicol. 73, 19–32. https://doi.org/10.1007/s00244-017-0381-1.
Incardona, J.P., Collier, T.K., Scholz, N.L., 2004. Defects in cardiac function precede morphological abnormalities in fish embryos exposed to polycyclic aromatic hydrocarbons. Toxicol. Appl. Pharmacol. 196, 191–205. https://doi.org/10.1016/j.taap.2003.11.026.
Incardona, J.P., Day, H.L., Collier, T.K., Scholz, N.L., 2006. Developmental toxicity of 4-ring polycyclic aromatic hydrocarbons in zebrafish is differentially dependent on AH receptor isoforms and hepatic cytochrome P4501A metabolism. Toxicol. Appl. Pharmacol. 217, 308–321. https://doi.org/10.1016/j.taap.2006.09.018.
Incardona, J.P., Carls, M.G., Day, H.L., Sloan, C.A., Bolton, J.L., Collier, T.K., Scholz, N.L., 2009. Cardiac arrhythmia is the primary response of embryonic Pacific herring (Clupea pallasi) exposed to crude oil during weathering. Environ. Sci. Technol. 43, 201–207. https://doi.org/10.1021/es802270t.
Incardona, J.P., Linbo, T.L., Scholz, N.L., 2011. Cardiac toxicity of 5-ring polycyclic aromatic hydrocarbons is differentially dependent on the aryl hydrocarbon receptor 2 isoform during zebrafish development. Toxicol. Appl. Pharmacol. 257, 242–249. https://doi.org/10.1016/j.taap.2011.09.010.
Katsumoto, T., Mitsushima, A., Kurimura, T., 1990. The role of the vimentin intermediate filaments in rat 3Y1 cells elucidated by immunoelectron microscopy and computer-graphic reconstruction. Biol. Cell. 68, 139–146. https://doi.org/10.1016/0248-4900(90)90299-I.
Kim, K.-H., Jahan, S.A., Kabir, E., Brown, R.J.C., 2013. A review of airborne polycyclic aromatic hydrocarbons (PAHs) and their human health effects. Environ. Int. 60, 71–80. https://doi.org/10.1016/j.envint.2013.07.019.
Köhle, C., Bock, K.W., 2007. Coordinate regulation of Phase I and II xenobiotic metabolisms by the Ah receptor and Nrf2. Biochem. Pharmacol. 73, 1853–1862. https://doi.org/10.1016/j.bcp.2007.01.009.
Larade, K., Storey, K.B., 2004. Accumulation and translation of ferritin heavy chain transcripts following anoxia exposure in a marine invertebrate. J. Exp. Biol. 207, 1353. https://doi.org/10.1242/jeb.00872.
Leppänen, H., Oikari, A., 1999. Occurrence of retene and resin acids in sediments and fish bile from a lake receiving pulp and paper mill effluents. Environ. Toxicol. Chem. 18, 1498–1505. https://doi.org/10.1002/etc.5620180723.
Leppänen, H., Oikari, A., 2001. Retene and resin acid concentrations in sediment profiles of a lake recovering from exposure to pulp mill effluents. J. Paleolimnol. 25, 367–374. https://doi.org/10.1023/A:1011120426661.
Mastrototaro, G., Liang, X., Li, X., Carullo, P., Piroddi, N., Tesi, C., Gu, Y., Dalton, N.D., Peterson, K.L., Poggesi, C., Sheikh, F., Chen, J., Bang, M.-L., 2015. Nebulette knockout mice have normal cardiac function, but show Z-line widening and up-regulation of cardiac stress markers. Cardiovasc. Res. 107, 216–225. https://doi.org/10.1093/cvr/cvv156.
Meador, J.P., Nahrgang, J., 2019. Characterizing crude oil toxicity to early-life stage fish based on a complex mixture: are we making unsupported assumptions? Environ. Sci. Technol. 53, 11080–11092. https://doi.org/10.1021/acs.est.9b02889.
Meunier, S., Vernos, I., 2012. Microtubule assembly during mitosis – from distinct origins to distinct functions? J. Cell Sci. 125, 2805. https://doi.org/10.1242/jcs.092429.
Mitchison, T., Kirschner, M., 1984. Dynamic instability of microtubule growth. Nature 312, 237–242. https://doi.org/10.1038/312237a0.
Nogales, E., 2000. Structural insights into microtubule function. Annu. Rev. Biochem. 69, 277–302. https://doi.org/10.1146/annurev.biochem.69.1.277.
OECD, 2013. Test No. 236: Fish Embryo Acute Toxicity (FET) Test. OECDiLibrary https://doi.org/10.1787/9789264203709-en.
Oliver, I.T., 1955. A spectrophotometric method for the determination of creative phosphokinase and myokinase. Biochem. J. 61, 116–122. https://doi.org/10.1042/bj0610116.
Olsvik, P.A., Lie, K.K., Nordtug, T., Hansen, B.H., 2012. Is chemically dispersed oil more toxic to Atlantic cod (Gadus morhua) larvae than mechanically dispersed oil? A transcriptional evaluation. BMC Genomics 13, 702. https://doi.org/10.1186/1471-2164-13-702.
Page, D.S., Boehm, P.D., Douglas, G.S., Bence, A.E., Burns, W.A., Mankiewicz, P.J., 1999. Pyrogenic polycyclic aromatic hydrocarbons in sediments record past human activity: a case study in Prince William sound,Alaska. Mar. Pollut. Bull. 38, 247–260. https://doi.org/10.1016/S0025-326X(98)00142-8.
Paramio, J.M., Jorcano, J.L., 2002. Beyond structure: do intermediate filaments modulate cell signalling? Bioessays 24, 836–844. https://doi.org/10.1002/bies.10140.
Pasparakis, C., Esbaugh, A.J., Burggren, W., Grosell, M., 2019. Physiological impacts of Deepwater Horizon oil on fish. Comp. Biochem. Physiol. C: Toxicol. Pharmacol. 224, 108558. https://doi.org/10.1016/j.cbpc.2019.06.002.
Rigaud, C., Eriksson, A., Krasnov, A., Wincent, E., Pakkanen, H., Lehtivuori, H., Ihalainen, J., Vehniäinen, E.-R., 2020a. Retene, pyrene and phenanthrene cause distinct molecular-level changes in the cardiac tissue of rainbow trout (Oncorhynchus mykiss) larvae, part 1 – transcriptomics. Sci. Total Environ. 745, 141031. https://doi.org/10.1016/j.scitotenv.2020.141031.
Rigaud, C., Eriksson, A., Rokka, A., Skaugen, M., Lihavainen, J., Keinänen, M., Lehtivuori, H., Vehniäinen, E.-R., 2020b. Retene, pyrene and phenanthrene cause distinct molecular-level changes in the cardiac tissue of rainbow trout (Oncorhynchus mykiss) larvae, part 2 – proteomics and metabolomics. Sci. Total Environ. 746, 141161. https://doi.org/10.1016/j.scitotenv.2020.141161.
Sawicki, K.T., Hsiang-Chun, Chang, Hossein, A., 2015. Role of heme in cardiovascular physiology and disease. J. Am. Heart Assoc. 4, e001138. https://doi.org/10.1161/JAHA.114.001138.
Scott, J.A., Hodson, P.V., 2008. Evidence for multiple mechanisms of toxicity in larval rainbow trout (Oncorhynchus mykiss) co-treated with retene and α-naphthoflavone. Aquat. Toxicol. 88, 200–206. https://doi.org/10.1016/j.aquatox.2008.04.007.
Scott, J.A., Incardona, J.P., Pelkki, K., Shepardson, S., Hodson, P.V., 2011. AhR2-mediated, CYP1A-independent cardiovascular toxicity in zebrafish (Danio rerio) embryos exposed to retene. Aquat. Toxicol. 101, 165–174. https://doi.org/10.1016/j.aquatox.2010.09.016.
Sequeira, V., Nijenkamp, L.L.A.M., Regan, J.A., van der Velden, J., 2014. The physiological role of cardiac cytoskeleton and its alterations in heart failure. 1838, 700–722. https://doi.org/10.1016/j.bbamem.2013.07.011 Reciprocal influences between cell cytoskeleton and membrane channels, receptors and transporters.
Sørhus, E., Incardona, J.P., Furmanek, T., Goetz, G.W., Scholz, N.L., Meier, S., Edvardsen, R.B., Jentoft, S., 2017. Novel adverse outcome pathways revealed by chemical genetics in a developing marine fish. eLife 6, e20707. https://doi.org/10.7554/eLife.20707.
Sørhus, E., Meier, S., Donald, C.E., Furmanek, T., Edvardsen, R.B., Lie, K.K., 2021. Cardiac dysfunction affects eye development and vision by reducing supply of lipids in fish. Sci. Total Environ. 800, 149460. https://doi.org/10.1016/j.scitotenv.2021.149460.
Stanton, R.C., 2012. Glucose-6-phosphate dehydrogenase, NADPH, and cell survival. IUBMB Life 64, 362–369. https://doi.org/10.1002/iub.1017.
Tang, J., Hu, G., Hanai, J., Yadlapalli, G., Lin, Y., Zhang, B., Galloway, J., Bahary, N., Sinha, S., Thisse, B., Thisse, C., Jin, J.-P., Zon, L.I., Sukhatme, V.P., 2006. A critical role for calponin 2 in vascular development. J. Biol. Chem. 281, 6664–6672. https://doi.org/10.1074/jbc.m506991200.
Tanguay, R.L., Andreasen, E.A., Walker, M.K., Peterson, R.E., 2003. Dioxin toxicity and aryl hydrocarbon receptor signaling in fish.Dioxins and Health. Wiley Online Books, pp. 603–628 https://doi.org/10.1002/0471722014.ch15.
Tolosano, E., Altruda, F., 2002. Hemopexin: structure, function, and regulation. DNA Cell Biol. 21, 297–306. https://doi.org/10.1089/104454902753759717.
Troisi, G., Borjesson, L., Bexton, S., Robinson, I., 2007. Biomarkers of polycyclic aromatic hydrocarbon (PAH)-associated hemolytic anemia in oiled wildlife. Environ. Res. 105, 324–329. https://doi.org/10.1016/j.envres.2007.06.007.
Tyanova, S., Temu, T., Sinitcyn, P., Carlson, A., Hein, M.Y., Geiger, T., Mann, M., Cox, J., 2016. The Perseus computational platform for comprehensive analysis of (prote)omics data. Nat. Methods 13, 731–740. https://doi.org/10.1038/nmeth.3901.
Uyeda, K., 1979. Phosphofructokinase. Adv. Enzymol. Relat. Areas Mol. Biol., 193–244 https://doi.org/10.1002/9780470122938.ch4.
Van Tiem, L.A., Di Giulio, R.T., 2011. AHR2 knockdown prevents PAH-mediated cardiac toxicity and XRE- and ARE-associated gene induction in zebrafish (Danio rerio). Toxicol. Appl. Pharmacol. 254, 280–287. https://doi.org/10.1016/j.taap.2011.05.002.
Vehniäinen, E.-R., Bremer, K., Scott, J.A., Junttila, S., Laiho, A., Gyenesei, A., Hodson, P.V., Oikari, A.O.J., 2016. Retene causes multifunctional transcriptomic changes in the heart of rainbow trout (Oncorhynchus mykiss) embryos. Environ. Toxicol. Pharmacol. 41, 95–102. https://doi.org/10.1016/j.etap.2015.11.015.
Vehniäinen, E.-R., Haverinen, J., Vehniäinen, E.-R., 2019. Polycyclic aromatic hydrocarbons phenanthrene and retene modify the action potential via multiple ion currents in rainbow trout Oncorhynchus mykiss cardiac myocytes. Environ. Toxicol. Chem. 38, 2145–2153. https://doi.org/10.1002/etc.4530.
Vernier, J.M., 1977. Chronological Table of the Embryonic Development of Rainbow Trout, Salmo Gairdneri Rich. 1836. Fisheries and Marine Service. Translation Series. Department of the Environment, Fisheries and Marine Service, Pacific Biological Station, Canada.
Villalobos, S.A., Papoulias, D.M., Meadows, J., Blankenship, A.L., Pastva, S.D., Kannan, K., Hinton, D.E., Tillitt, D.E., Giesy, J.P., 2000. Toxic responses of medaka, D-rR strain, to polychlorinated naphthalene mixtures after embryonic exposure by in ovo nanoinjection: a partial life-cycle assessment. Environ. Toxicol. Chem. 19, 432–440. https://doi.org/10.1002/etc.5620190224.
Vogel, C., Marcotte, E.M., 2012. Insights into the regulation of protein abundance from proteomic and transcriptomic analyses. Nat. Rev. Genet. 13, 227–232. https://doi.org/10.1038/nrg3185.
Wassenberg, D., Di Giulio, R., 2004a. Synergistic embryotoxicity of polycyclic aromatic hydrocarbon aryl hydrocarbon receptor agonists with cytochrome P4501A inhibitors in

Fundulus heteroclitus. Environ. Health Perspect. 112, 1658–1664. https://doi.org/10.1289/ehp.7168.
Wassenberg, D., Di Giulio, R., 2004b. Teratogenesis in Fundulus heteroclitus embryos exposed to a creosote-contaminated sediment extract and CYP1A inhibitors. Mar. Environ. Res. 58, 163–168. https://doi.org/10.1016/j.marenvres.2004.03.012.
Weiss, H.J., Sussman, I.I., Hoyer, L.W., 1977. Stabilization of factor VIII in plasma by the von Willebrand factor. Studies on posttransfusion and dissociated factor VIII and in patients with von Willebrand's disease. J. Clin. Invest. 60, 390–404. https://doi.org/10.1172/JCI108788.
Wickström, K., Tolonen, K., 1987. The history of airborne polycyclic aromatic hydrocarbons (PAH) and perylene as recorded in dated lake sediments. Water Air Soil Pollut. 32, 155–175. https://doi.org/10.1007/BF00227691.
Willett, K.L., Randerath, K., Zhou, G.-D., Safe, S.H., 1998. Inhibition of CYP1A1-dependent activity by the polynuclear aromatic hydrocarbon (PAH) fluoranthene. Biochem. Pharmacol. 55, 831–839. https://doi.org/10.1016/S0006-2952(97)00561-3.
Williamson, J.R., 1979. Mitochondrial function in the heart. Annu. Rev. Physiol. 41, 485–506. https://doi.org/10.1146/annurev.ph.41.030179.002413.
Wills, L.P., Zhu, S., Willett, K.L., Di Giulio, R.T., 2009. Effect of CYP1A inhibition on the biotransformation of benzo[a]pyrene in two populations of Fundulus heteroclitus with different exposure histories. Aquat. Toxicol. 92, 195–201. https://doi.org/10.1016/j.aquatox.2009.01.009.
Yue, M.S., Martin, S.E., Martin, N.R., Taylor, M.R., Plavicki, J.S., 2021. 2,3,7,8-Tetrachlorodibenzo-p-dioxin exposure disrupts development of the visceral and ocular vasculature. Aquat. Toxicol. 234, 105786. https://doi.org/10.1016/j.aquatox.2021.105786.
Zhou, Y., Zhou, B., Pache, L., Chang, M., Khodabakhshi, A.H., Tanaseichuk, O., Benner, C., Chanda, S.K., 2019. Metascape provides a biologist-oriented resource for the analysis of systems-level datasets. Nat. Commun. 10, 1523. https://doi.org/10.1038/s41467-019-09234-6.
Zimmerman, T.S., Edgington, T.S., 1973. Factor VIII coagulant activity and factor VIII-like antigen: independent molecular entities. J. Exp. Med. 138, 1015–1020. https://doi.org/10.1084/jem.138.4.1015.
Zodrow, J.M., Tanguay, R.L., 2003. 2,3,7,8-Tetrachlorodibenzo-p-dioxin inhibits zebrafish caudal fin regeneration. Toxicol. Sci. 76, 151–161. https://doi.org/10.1093/toxsci/kfg205.

SUPPORTING INFORMATION

Changes in cardiac proteome and metabolome following exposure to the PAHs retene and fluoranthene and their mixture in developing rainbow trout alevins

Andreas N.M. Eriksson[a,*], Cyril Rigaud[a], Anne Rokka[b], Morten Skaugen[c], Jenna H. Lihavainen[d], Eeva-Riikka Vehniäinen[a]

a Department of Biological and Environmental Science, University of Jyväskylä, P.O. Box 35, FI-40014, Finland

b Turku Proteomics Facility, Turku University, Tykistökatu 6, 20520 Turku, Finland

c Faculty of Chemistry, Biotechnology and Food Science, Norwegian University of Life Sciences, Campus Ås, Universitetstunet 3, 1430 Ås, Norway

d Umeå Plant Science Centre, Umeå University, KB. K3 (Fys. Bot.), Artedigränd 7, Fysiologisk botanik, UPSC, KB. K3 (B3.44.45) Umeå universitet, 901 87 Umeå, Sweden

* Corresponding author: Andreas N.M. Eriksson. andreas.n.m.eriksson@jyu.fi.

Supplementary material

Table s1. Average concentration (± sd; $\mu g \cdot L^{-1}$) of retene (Ret) and fluoranthene (Flu), alone or as mixture (Mix) in exposure water after 1, 3, 7, 10 and 14 days. Water samples were analyzed using synchronous fluorescence spectroscopy. For details, see Rigaud *et al.* 2020[1].

Sampling day	Retene	Ret. Mix	Fluoranthene	Flu. Mix
1	6.00 ± 1.79	7.66 ± 2.19	9.15 ± 4.68	6.23 ± 2.68
3	8.07 ± 2.79	8.92 ± 2.97	6.60 ± 0.46	11.22 ± 2.85
7	8.02 ± 2.65	15.82 ± 9.00	11.64 ± 1.25	15.34 ± 3.84
10	10.00 ± 3.72	10.22 ± 2.37	10.00 ± 0.77	7.68 ± 0.89
14	14.00 ± 4.24	14.09 ± 0.73	14.00 ± 2.22	15.00 ± 3.56

Table 2. Protein expression fold changes (log_2) in fry exposed to fluoranthene (Flu), retene (Ret) or the combination of the two PAHs (Mix) relative to control after 7 days. Yellow filled cells (UniProt- and zebrafish gene IDs) denote significantly impacted proteins shared between Day 7 and 14. Color gradient filled and boxed cells indicate proteins significantly different relative to control as per Perseus (build-in ANOVA + Tukey's test). The proteins are presented with their corresponding UniProt ID, the zebrafish gene ID equivalent as well as the corresponding functional protein name. Data is sorted from highest to lowest protein expression among mixture exposed fry.

UniProt	Gene ID	Flu	Mix	Ret	UniProt name
B5X3P7	cyp1a	3.818	5.194	3.758	Cytochrome P450 (EC 1.14.14.1)
B5X3C0	gsr	0.234	2.623	-0.195	Glutathione reductase (EC 1.8.1.7)
B5XGZ2	GSTP1	0.562	2.247	-0.175	Glutathione S-transferase P
B5XDY6	st1s3	0.425	2.241	1.385	Sulfotransferase (EC 2.8.2.-)
A0A1S3NX81	ugt1a1	0.474	2.115	0.517	UDP-glucuronosyltransferase-like
A0A1S3NMZ6	clip1	1.959	1.944	-0.183	CAP-Gly domain-containing linker protein 1-like isoform X6
B9EM96	GSTA	0.414	1.502	0.068	Glutathione S-transferase A
B5X9Y8	GSTO1	0.113	1.224	-0.201	Glutathione transferase omega-1 (glutathione S-transferase omega 1) (EC 2.5.1.18)
B5X793		0.070	1.202	-0.562	Ferritin
B5X8H5	prdx1	0.366	1.149	-0.101	Peroxiredoxin
A0A1S3NWP8	ATP5J	0.850	1.054	-0.326	calphotin-like isoform X2
A0A1S3MS25	selenbp1	-0.015	0.764	-0.240	selenium-binding protein 1-like isoform X3
A0A1S3KK03	LncRNA	0.530	0.699	1.637	uncharacterized protein LOC106560505 isoform X1
B5X317	bcap31	0.756	0.670	-0.440	B-cell receptor-associated protein 31
A0A1S3RPZ1	tstd2	0.341	0.632	-0.209	thiosulfate sulfurtransferase/rhodanese-like domain-containing protein 1
B5DH21	rplp1	0.220	0.484	-0.695	60S acidic ribosomal protein P1-like (Ribosomal protein, large, P1 like 2)
A0A1S3L7A3	apoa1	0.607	0.483	-1.073	Ribosomal protein
C0H850	ctsba	0.070	0.314	0.401	Cathepsin B (cathepsin B-like)
A0A1S3L5F6	get3	0.355	0.305	-0.640	ATPase LOC106564561 (EC 3.6.-.-) (Arsenical pump-driving ATPase) (Arsenite-stimulated ATPase)
A0A1S3Q618	adss2	0.005	0.149	-0.366	Adenylosuccinate synthetase (AMPSase) (AdSS) (EC 6.3.4.4) (IMP--aspartate ligase)
B5X0Q5		0.218	-0.002	-0.458	ATP-binding cassette sub-family E member 1
B9EL79	TCP4	0.006	-0.015	0.484	Activated RNA polymerase II transcriptional coactivator p15 (activated RNA polymerase II transcriptional coactivator p15-like)
B5XBL0	ssrd	0.246	-0.037	-0.638	Translocon-associated protein subunit delta precursor

A0A1S3LXJ6	prkacbb	0.090	-0.038	-0.786	cAMP-dependent protein kinase catalytic subunit beta isoform X2
A0A1S3PX04	p4hb	-0.036	-0.060	0.256	Protein disulfide-isomerase (EC 5.3.4.1)
A0A1S3N6M0	polr2a	0.172	-0.067	0.959	DNA-directed RNA polymerase subunit (EC 2.7.7.6)
A0A1S3RP65	tmed9	-0.108	-0.072	-0.702	transmembrane emp24 domain-containing protein 9-like
A0A1S3NJ33	txndc5	-0.085	-0.119	0.199	thioredoxin domain-containing protein 5-like
A0A1S3S5F2	smndc1	0.191	-0.142	0.549	survival of motor neuron-related-splicing factor 30-like isoform X1
A0A1S3M538	col1a2	0.218	-0.148	0.816	collagen alpha-2(I) chain isoform X1
C0HA50	eif2s3	0.108	-0.172	-0.579	Eukaryotic translation initiation factor 2 subunit 3
A0A1S3RPC5	TCERG1	-0.136	-0.197	0.374	transcription elongation regulator 1-like
A0A1S3PXF3	cars1	-0.436	-0.237	-0.310	cysteine--tRNA ligase, cytoplasmic
A0A1S3RRH9	npm1b	-0.148	-0.258	-0.037	nucleophosmin-like
B5X6J4	nifk	-0.026	-0.267	0.543	MKI67 FHA domain-interacting nucleolar phosphoprotein-like
C0HBD9	elf2b	0.016	-0.276	-0.254	Elongation factor 2 (elongation factor 2-like isoform X1)
C0HA19	hdlbpa	-0.066	-0.300	-0.069	Vigilin
A0A1S3RQL9	mcm7	-0.040	-0.303	-0.133	DNA replication licensing factor MCM7 (EC 3.6.4.12)
B5DGE8	tuba8l2	-0.350	-0.305	-0.203	Tubulin alpha chain
B5DH01	tba	-0.181	-0.305	-0.154	Tubulin alpha chain
B5X0U5	tbb5	-0.106	-0.307	-0.037	Tubulin beta chain
A0A1S3PZA6		-0.242	-0.311	0.534	chromosomal protein D1-like
B5X3R8	CNN2	0.042	-0.399	0.104	Calponin
A0A1S3ND03	nid1a	-0.170	-0.403	0.191	nidogen-1-like isoform X1
A0A1S3LZP6	mcm6	-0.116	-0.424	-0.068	DNA helicase (EC 3.6.4.12)
A0A1S3LXE0	mcm4	-0.104	-0.450	-0.061	DNA helicase (EC 3.6.4.12)
A0A1S3LMW6	dpysl3	-0.078	-0.455	-0.156	dihydropyrimidinase-related protein 3-like isoform X3
C0HAV9	FKB10	-0.062	-0.460	0.376	Peptidylprolyl isomerase (EC 5.2.1.8)
B5X1U2	ILF2	-0.329	-0.463	-0.631	Interleukin enhancer-binding factor 2 homolog
A0A1S3MBU2	meis2a	-0.130	-0.471	0.222	homeobox protein Meis2-like
B5XDM7	clns1a	-0.376	-0.500	-0.221	Methylosome subunit pICln (methylosome subunit pICln-like isoform X1) (methylosome subunit pICln-like isoform X2)
B5DGA5	txndc9	-0.163	-0.527	0.114	ATP binding protein associated with cell differentiation (Thioredoxin domain-containing

					protein 9) (thioredoxin domain-containing protein 9-like)
A0A1S3R5X8	rcn3	-0.034	-0.617	0.464	reticulocalbin-3 isoform X2
A0A1S3KYN8	hapln1b	-0.372	-0.655	-0.178	hyaluronan and proteoglycan link protein 1
A0A1S3MYT8		-0.343	-0.684	0.334	non-muscle caldesmon-like isoform X1
A0A1S3MYU3		-0.342	-0.704	0.284	non-muscle caldesmon-like isoform X3
C0HBH7	fkbp10b	-0.343	-0.740	0.224	Peptidylprolyl isomerase (EC 5.2.1.8)
B9ELG2	cnn1b	-0.061	-0.750	-0.245	Calponin
A0A1S3L6X2	myh11	-0.290	-0.831	0.014	myosin-11 isoform X2
A0A1S3LSF4	vcanb	-0.365	-0.955	0.646	versican core protein-like
A0A1S3NRT6		-0.442	-1.015	-0.063	alpha-2-macroglobulin-like
A0A1S3RGV3	wdhd1	-0.755	-1.167	0.196	WD repeat and HMG-box DNA-binding protein 1 isoform X2
A0A1S3SZ54		-0.265	-1.396	0.432	latent-transforming growth factor beta-binding protein 4-like isoform X2
A0A1S3PQV6	hpxa	-0.830	-1.470	0.127	Hemopexin
A0A1S3R078	ahsg2	-0.428	-1.598	0.515	alpha-2-HS-glycoprotein-like

Table 3. Protein expression fold changes (log_2) in fry exposed to fluoranthene (Flu), retene (Ret) or the combination of the two PAHs (Mix) relative to control after 14 days. Yellow filled cells (UniProt- and zebrafish gene IDs) denote significantly impacted proteins shared between day 7 and 14. Color gradient filled and boxed cells indicate proteins significantly different relative to control as per Perseus (build-in ANOVA + Tukey's test). The proteins are presented with their corresponding UniProt ID, the zebrafish gene ID equivalent as well as the corresponding functional protein name. Data is sorted from highest to lowest protein expression among mixture exposed fry.

UniProt	gene ID (DRE)	Flu	Mix	Ret	UniProt name
B5X3P7	cyp1a	3.828	4.603	3.939	Cytochrome P450 (EC 1.14.14.1)
B5XGZ2	GSTP1	1.403	3.174	0.013	Glutathione S-transferase P
B5X0S0	ckbb	0.374	3.111	0.877	Creatine kinase B-type
B5X3C0	gsr	0.344	3.066	0.019	Glutathione reductase (EC 1.8.1.7)
A0A1S3R7F8	vat1	3.332	2.872	3.248	synaptic vesicle membrane protein VAT-1 homolog
A0A1S3LHK8		0.191	2.863	2.403	Sulfotransferase (EC 2.8.2.-)
A0A1S3NX81	ugt1a1	0.721	2.362	1.302	UDP-glucuronosyltransferase-like
C0HAV9	FKB10	2.901	2.343	2.804	Peptidylprolyl isomerase (EC 5.2.1.8)
B5XDY6	st1s3	0.233	2.202	1.699	Sulfotransferase (EC 2.8.2.-)
B9EM96	GSTA	0.872	2.014	-0.095	Glutathione S-transferase A
B5X9Y8	GSTO1	0.547	1.841	0.020	Glutathione transferase omega-1 (glutathione S-transferase omega 1) (EC 2.5.1.18)
A0A1S3LCK1	pfkmb	0.126	1.760	-0.045	ATP-dependent 6-phosphofructokinase (ATP-PFK) (Phosphofructokinase) (EC 2.7.1.11) (Phosphohexokinase)
B5X8H5	prdx1	0.436	1.454	0.213	Peroxiredoxin
B5X793		0.161	1.419	0.212	Ferritin
B5XF92	txn	0.436	1.302	0.123	Thioredoxin
A0A1S3KRS1	dhtkd1	0.114	1.177	0.644	probable 2-oxoglutarate dehydrogenase E1 component DHKTD1, mitochondrial
A0A1S3LJD8	tgm2a	0.214	0.962	0.799	protein-glutamine gamma-glutamyltransferase 2-like
A0A1S3RPZ1	tstd2	0.437	0.808	0.021	thiosulfate sulfurtransferase/rhodanese-like domain-containing protein 1
A0A1S3R5X8	rcn3	1.270	0.701	1.164	reticulocalbin-3 isoform X2
B5X8R5	MSRA	0.053	0.632	-0.009	Peptide methionine sulfoxide reductase
A0A1S3SYD6	trip12	0.145	0.627	0.231	E3 ubiquitin-protein ligase TRIP12-like isoform X1
A0A1S3KK03	LncRNA	0.713	0.521	0.857	uncharacterized protein LOC106560505 isoform X1
A0A1S3T4G1	dbt	0.246	0.514	-0.188	Dihydrolipoamide acetyltransferase component of pyruvate dehydrogenase complex (EC

					2.3.1.-)
A0A1S3L9H1	txnrd3	0.034	0.509	0.037	thioredoxin reductase 1, cytoplasmic-like
A0A1S3SSM2	fgfbp2a	0.039	0.481	-0.456	fibroblast growth factor-binding protein 2-like
C0H8W5	PYGM	0.026	0.417	0.272	Alpha-1,4 glucan phosphorylase (EC 2.4.1.1)
B5DFT9	ckmt2	-0.137	0.393	0.284	Creatine kinase, mitochondrial 2 (creatine kinase S-type, mitochondrial) (EC 2.7.3.2)
A0A1S3Q775	rrbp1a	-0.159	0.336	-0.096	ribosome-binding protein 1-like isoform X3
A0A1S3MRL7	desmb	-0.052	0.308	0.224	desmin-like
A0A1S3T350	bckdha	0.002	0.290	0.255	2-oxoisovalerate dehydrogenase subunit alpha (EC 1.2.4.4)
A0A1S3NC52	bves	-0.196	-0.251	-0.110	blood vessel epicardial substance-like isoform X3
A0A1S3RRE0	f8	-0.032	-0.254	0.121	coagulation factor VIII-like
A0A1S3PSE3		0.047	-0.289	-0.035	Tubulin alpha chain
A0A1S3T1E0		-0.036	-0.295	0.023	Tubulin beta chain
B5DH01	tba	-0.131	-0.326	-0.065	Tubulin alpha chain
A0A1S3L9E0	krt18b	-0.121	-0.330	-0.167	keratin, type I cytoskeletal 18-like
A0A1S3MQ74	ncl	-0.120	-0.340	-0.093	nucleolin
B5XG75	RL22	-0.237	-0.367	-0.198	60S ribosomal protein L22
A0A1S3R1A2	lamc1	-0.145	-0.396	-0.066	laminin subunit gamma-1-like
A0A1S3N7H0	trip6	-0.219	-0.401	-0.101	thyroid receptor-interacting protein 6-like
B5X9G8	mrto4	0.323	-0.403	-0.067	Ribosome assembly factor mrt4
B5DGK7	rs8	-0.136	-0.410	-0.083	40S ribosomal protein S8
A0A1S3SMP0	ppm1g	-0.063	-0.416	-0.039	protein phosphatase 1G-like
A0A1S3RQL9	mcm7	-0.132	-0.420	-0.060	DNA replication licensing factor MCM7 (EC 3.6.4.12)
B5X1Q5	serph1	-0.007	-0.421	-0.212	Collagen-binding protein
A0A1S3S809	lama4	-0.171	-0.429	-0.111	laminin subunit alpha-4-like
A0A1S3LZP6	mcm6	-0.151	-0.433	-0.023	DNA helicase (EC 3.6.4.12)
A0A1S3MYT8		-0.142	-0.435	-0.297	non-muscle caldesmon-like isoform X1
A0A1S3MEJ6	agrn	0.021	-0.442	0.002	agrin-like isoform X3
A0A1S3MLE6	dnaja2b	-0.199	-0.459	-0.022	dnaJ homolog subfamily A member 2-like
B5X369	rpl17	-0.203	-0.465	-0.171	60S ribosomal protein L17-like (Ribosomal protein L17)
A0A1S3N022	itih2	-0.306	-0.478	0.562	inter-alpha-trypsin inhibitor heavy chain H2-like

A0A1S3NAJ6	EIF3C	-0.218	-0.484	-0.115	Eukaryotic translation initiation factor 3 subunit C (eIF3c) (Eukaryotic translation initiation factor 3 subunit 8)
Q9PTA8	serpinc1	-0.182	-0.516	0.236	Antithrombin (antithrombin protein precursor)
B5X0U5	tbb5	-0.050	-0.523	-0.073	Tubulin beta chain
B5XCV0	fabp11a	-0.271	-0.524	-0.547	Fatty acid-binding protein, heart
A0A1S3PE97	dnaja4	-0.160	-0.531	-0.164	dnaJ homolog subfamily A member 4-like
A0A1S3KK24	fetub	-0.470	-0.542	0.018	histidine-rich glycoprotein-like
A0A1S3PBB7		-0.275	-0.542	0.147	kininogen-1-like
B5X105	mcm5	-0.154	-0.543	-0.174	DNA helicase (EC 3.6.4.12)
B5DG79	rbm4.3	-0.106	-0.545	0.018	RNA-binding protein 4B-like isoform X1 (Zgc:56141-like)
A0A1S3LMW6	dpysl3	-0.353	-0.596	-0.274	dihydropyrimidinase-related protein 3-like isoform X3
P21848	alb1	-0.273	-0.598	0.086	Serum albumin 1
B5X3R8	CNN2	-0.186	-0.608	-0.243	Calponin
B5X4G3	vim	-0.445	-0.623	-0.410	Vimentin
A0A1S3S8H0	plg	-0.373	-0.682	0.169	Plasminogen (EC 3.4.21.7)
A0A1S3KTG6	vwf	-0.399	-0.708	0.099	von Willebrand factor-like
A0A1S3QR20	cfh	-0.361	-0.719	0.036	complement factor H-like
A0A1S3RF10	fgg	-0.378	-0.766	-0.081	fibrinogen gamma chain-like
A0A1S3KYN8	hapln1b	-0.286	-0.792	-0.336	hyaluronan and proteoglycan link protein 1
A0A1S3LUK3	proca	-0.395	-0.824	0.455	vitamin K-dependent protein C
A0A1S3QRL5	C3	-0.713	-0.841	0.216	complement C3
A0A1S3LV03		-0.314	-0.842	-0.140	lysosome membrane protein 2-like
A0A1S3S885	epb41l2	-0.312	-0.858	-0.386	protein 4.1 isoform X5
A0A1S3LBU1	NUCKS1	-0.296	-0.868	-0.438	nuclear ubiquitous casein and cyclin-dependent kinase substrate 1-like isoform X1
B5X672	crp	-0.268	-0.930	0.169	Pentaxin (Pentraxin)
A0A1S3PQV6	hpxa	-0.560	-1.034	0.120	Hemopexin
A0A1S3P2D1	si:ch211-222l21.1	-0.576	-1.119	-0.606	parathymosin-like
A0A1S3LT49	c9	-0.378	-1.188	0.059	complement component C9
A0A1S3NRT6		-0.562	-1.412	0.013	alpha-2-macroglobulin-like

A0A1S3SY27	a2ml	-0.493	-1.697	0.057	alpha-2-macroglobulin-like
A0A1S3R078	ahsg2	-0.760	-2.255	0.159	alpha-2-HS-glycoprotein-like

16

17

Table s4. Differently expressed proteins (log_2 fold change) shared between Day 7 and 14 following exposure to fluoranthene (Flu), retene (Ret) and the binary mixture of the two PAHs (Mix). Colored cells with full borders are significantly affected compared to control (DMSO) fry.

		Day 7			Day 14			
UniProt ID	Gene ID	Flu	Ret	Mix	Flu	Ret	Mix	Protein name
B9EM96	*gsta*	0.414	0.068	1.502	0.872	-0.095	2.014	Glutathione S-transferase A
B5X9Y8	*gsto1*	0.113	-0.201	1.224	0.547	0.020	1.841	Glutathione transferase omega-1
B5XGZ2	*gstp1*	0.562	-0.175	2.247	1.403	0.013	3.174	Glutathione S-transferase P
B5X3C0	*gshr*	0.234	-0.195	2.623	0.344	0.019	3.066	Glutathione reductase
A0A1S3RPZ1	*tstd2*	0.341	-0.209	0.632	0.437	0.021	0.808	Thiosulfate sulfurtransferase/rhodanese-like domain-containing protein 1
B5XDY6	*st1s3*	0.425	1.385	2.241	0.233	1.699	2.202	Sulfotransferase
A0A1S3NX81	*ugt1a1*	0.474	0.517	2.115	0.721	1.302	2.362	UDP-glucuronosyltransferase-like
B5X3P7	*cp1a1*	3.818	3.758	5.194	3.828	3.939	4.603	Cytochrome P450 1A1
A0A1S3LZP6	*mcm6*	-0.116	-0.068	-0.424	-0.151	-0.023	-0.433	DNA helicase
A0A1S3RQL9	*mcm7*	-0.040	-0.133	-0.303	-0.132	-0.060	-0.420	DNA replication licensing factor MCM7
B5DH01	*tba*	-0.181	-0.154	-0.305	-0.131	-0.065	-0.326	Tubulin alpha chain
B5X0U5	*tbb5*	-0.106	-0.037	-0.307	-0.050	-0.073	-0.523	Tubulin beta chain
B5X3R8	*cnn2*	0.042	0.104	-0.399	-0.186	-0.243	-0.608	Calponin
A0A1S3KYN8	*hapln1*	-0.372	-0.178	-0.655	-0.286	-0.336	-0.792	Hyaluronan and proteoglycan link protein 1
A0A1S3MYT8	*loc106576070**	-0.343	0.334	-0.684	-0.142	-0.297	-0.435	Non-muscle caldesmon-like isoform X1
A0A1S3R5X8	*rcn3*	-0.034	0.464	-0.617	-0.218	-0.324	-0.786	Reticulocalbin-3 isoform X2
B5X8H5	*tdx*	0.366	-0.101	1.149	0.436	0.213	1.454	Peroxiredoxin
B5X793	*frim*	0.070	-0.562	1.202	0.161	0.212	1.419	Ferritin
A0A1S3PQV6	*hpxa*	-0.830	0.127	-1.470	-0.560	0.120	-1.034	Hemopexin
A0A1S3KK03	*lncrna*	0.530	1.637	0.699	0.713	0.857	0.521	Uncharacterized protein LOC106560505 isoform X1
C0HAV9	*fkb10*	-0.062	0.376	-0.460	-0.124	-0.221	-0.682	Peptidylprolyl isomerase
A0A1S3LMW6	*dpysl3*	-0.078	-0.156	-0.455	-0.353	-0.274	-0.596	Dihydropyrimidinase-related protein 3-like isoform X3
A0A1S3R078	*ahsg2*	-0.428	0.515	-1.598	-0.562	0.013	-1.412	Alpha-2-HS-glycoprotein-like
A0A1S3NRT6	*loc106580921**	-0.442	-0.063	-1.015	-0.760	0.159	-2.255	Alpha-2-macroglobulin-like

* No relevant zebrafish gene available.

Table s5. Summary table of over-represented terms and pathways, as per Metascape, in 7-days old rainbow trout fry exposed to retene (Ret), fluoranthene (Flu) and the mixture (Mix). Terms and pathways were considered over-represented if both the p and q value ≤ 0.05. Significantly depleted (crimson filled cells) or enriched (green filed cells) cardiac proteins (log_2) involved in the over-represented term and pathways are highlighted.

Exposure	Term / Pathway ID code	Term / pathway function	p-value	q-value	Protein name	UniProt code	Gene (Dre-ID)	Protein Expression (log_2) Flu	Mix	Ret
Ret	R-DRE-8963898	Plasma lipoprotein assembly	< 0.0001	0.003	Ribosomal protein	A0A1S3L7A3	*apoa1a*	0.607	0.483	-1.073
					Protein disulfide-isomerase (EC 5.3.4.1)	A0A1S3PX04	*p4hb*	-0.036	-0.060	0.256
					cAMP-dependent protein kinase	A0A1S3LXJ6	*prkacbb*	0.090	-0.038	-0.786
					Activated RNA polymerase II transcriptional coactivator p15	B9EL79	*TCP4*	0.006	-0.015	0.484
Mix	dre00980	Metabolism of xenobiotics by cytochrome P450	< 0.0001	< 0.0001	Glutathione S-transferase P	B5XGZ2	*gstp1*	0.562	2.247	-0.175
					Cytochrome P450 (EC 1.14.14.1)	B5X3P7	*cyp1a*	3.818	5.194	3.758
					Glutathione S-transferase A	B9EM96	*gsta.1*	0.414	1.502	0.068
					Glutathione transferase omega-1	B5X9Y8	*gsto1*	0.113	1.224	-0.201
					UDP-glucuronosyltransferase-like	A0A1S3NX81	*ugt1a1*	0.474	2.115	0.517
					Sulfotransferase (EC 2.8.2.-)	B5XDY6	*sult1st2*	0.425	2.241	1.385
					Glutathione reductase (EC 1.8.1.7)	B5X3C0	*gsr*	0.234	2.623	-0.195
					Hemopexin	A0A1S3PQV6	*hpxa*	-0.830	-1.470	0.127
					Peroxiredoxin	B5X8H5	*prdx1*	0.366	1.149	-0.101
Mix	GO:0006267	Pre-replicative complex assembly involved in nuclear cell cycle DNA replication	< 0.0001	0.001	DNA replication licensing factor MCM7 (EC 3.6.4.12)	A0A1S3RQL9	*mcm7*	-0.040	-0.303	-0.133
					DNA helicase (EC 3.6.4.12)	A0A1S3LXE0	*mcm4*	-0.104	-0.450	-0.061
					DNA helicase (EC 3.6.4.12)	A0A1S3LZP6	*mcm6*	-0.116	-0.424	-0.068
					WD repeat and HMG-box DNA-binding protein 1 isoform X2	A0A1S3RGV3	*wdhd1*	-0.755	-1.167	0.196
					Tubulin alpha chain	B5DGE8	*tuba8l2*	-0.350	-0.305	-0.203
					Tubulin alpha chain	B5DH01	*tba*	-0.181	-0.305	-0.154

Table s6. Summary table of over-represented terms and pathways, as per Metascape, in 14-days old rainbow trout fry exposed to retene (Ret), fluoranthene (Flu) and the mixture (Mix). Terms and pathways were considered over-represented if both the p and q value ≤ 0.05. Significantly depleted (crimson filled cells) or enriched (green filed cells) cardiac proteins (log_2) involved in the over-represented term and pathways are highlighted.

Exposure	Term / Pathway ID code	Term / pathway function	p-value	q-value	Protein name	UniProt code	Gene (Dre-ID)	Protein Expression (log2) Flu	Mix	Ret
Flu	dre00980	Metabolism of xenobiotics by cytochrome P450	< 0.0001	0.018	Glutathione S-transferase P	B5XGZ2	*gstp1*	1.403	3.174	0.013
					Cytochrome P450 (EC 1.14.14.1)	B5X3P7	*cyp1a*	3.828	4.603	3.939
					UDP-glucuronosyltransferase-like	A0A1S3NX81	*ugt1a1*	0.721	2.362	1.302
Mix	GO:0050878	Regulation of body fluid levels	< 0.0001	< 0.0001	Antithrombin (antithrombin protein precursor)	Q9PTA8	*serpinc1*	-0.182	-0.516	0.236
					Plasminogen (EC 3.4.21.7)	A0A1S3S8H0	*plg*	-0.373	-0.682	0.169
					vitamin K-dependent protein C	A0A1S3LUK3	*proca*	-0.395	-0.824	0.455
					fibrinogen gamma chain-like	A0A1S3RF10	*fgg*	-0.378	-0.766	-0.081
					blood vessel epicardial substance-like isoform X3	A0A1S3NC52	*bves*	-0.196	-0.251	-0.110
					von Willebrand factor-like	A0A1S3KTG6	*vwf*	-0.399	-0.708	0.099
					coagulation factor VIII-like	A0A1S3RRE0	*f8*	-0.032	-0.254	0.121
					Vimentin	B5X4G3	*vim*	-0.445	-0.623	-0.410
					dihydropyrimidinase-related protein 3-like isoform X3	A0A1S3LMW6	*dpysl3*	-0.353	-0.596	-0.274
					alpha-2-HS-glycoprotein-like	A0A1S3R078	*ahsg2*	-0.760	-2.255	0.159
					histidine-rich glycoprotein-like	A0A1S3KK24	*fetub*	-0.470	-0.542	0.018
					Tubulin alpha chain	B5DH01	*tba*	-0.131	-0.326	-0.065
Mix	GO:0010466	Negative regulation of peptidase activity	< 0.0001	< 0.0001	Antithrombin (antithrombin protein precursor)	Q9PTA8	*serpinc1*	-0.182	-0.516	0.236
					inter-alpha-trypsin inhibitor heavy chain H2-like	A0A1S3N022	*itih2*	-0.306	-0.478	0.562
					agrin-like isoform X3	A0A1S3MEJ6	*agrn*	0.021	-0.442	0.002
					alpha-2-HS-glycoprotein-like	A0A1S3R078	*ahsg2*	-0.760	-2.255	0.159

					histidine-rich glycoprotein-like	A0A1S3KK24	*fetub*	-0.470	-0.542	0.018
					alpha-2-macroglobulin-like	A0A1S3SY27	*a2ml*	-0.493	-1.697	0.057
					Collagen-binding protein	B5X1Q5	*SERPH*	-0.007	-0.421	-0.212
					laminin subunit gamma-1-like	A0A1S3R1A2	*lamc1*	-0.145	-0.396	-0.066
					Plasminogen (EC 3.4.21.7)	A0A1S3S8H0	*plg*	-0.373	-0.682	0.169
					fibrinogen gamma chain-like	A0A1S3RF10	*fgg*	-0.378	-0.766	-0.081
					E3 ubiquitin-protein ligase TRIP12-like isoform X1	A0A1S3SYD6	*trip12*	0.145	0.627	0.231
					blood vessel epicardial substance-like isoform X3	A0A1S3NC52	*bves*	-0.196	-0.251	-0.110
Mix	dre00980	Metabolism of xenobiotics by cytochrome P450		< 0.0001	< 0.0001	Glutathione S-transferase P	B5XGZ2	*gstp1*	1.403	3.174	0.013
						Cytochrome P450 (EC 1.14.14.1)	B5X3P7	*cyp1a*	3.828	4.603	3.939
						Glutathione S-transferase A	B9EM96	*gsta.1*	0.872	2.014	-0.095
						Glutathione transferase omega-1 (EC 2.5.1.18)	B5X9Y8	*gsto1*	0.547	1.841	0.020
						UDP-glucuronosyltransferase-like	A0A1S3NX81	*ugt1a1*	0.721	2.362	1.302
						Sulfotransferase (EC 2.8.2.-)	B5XDY6	*sult1st2*	0.233	2.202	1.699
						Glutathione reductase (EC 1.8.1.7)	B5X3C0	*gsr*	0.344	3.066	0.019
						Creatine kinase B-type	B5X0S0	*ckbb*	0.374	3.111	0.877
						Creatine kinase, mitochondrial 2 (creatine kinase S-type, mitochondrial) (EC 2.7.3.2)	B5DFT9	*ckmt2b*	-0.137	0.393	0.284
Mix	GO:0045454	Cell redox homeostasis		< 0.0001	< 0.0001	thioredoxin reductase 1, cytoplasmic-like	A0A1S3L9H1	*txnrd3*	0.034	0.509	0.037
						Thioredoxin	B5XF92	*txn*	0.436	1.302	0.123
						Peroxiredoxin	B5X8H5	*prdx1*	0.436	1.454	0.213
						Glutathione reductase (EC 1.8.1.7)	B5X3C0	*gsr*	0.344	3.066	0.019
						Cytochrome P450 (EC 1.14.14.1)	B5X3P7	*cyp1a*	3.828	4.603	3.939
						Peptide methionine sulfoxide reductase	B5X8R5	*msra*	0.053	0.632	-0.009
Mix	GO:0006267	Pre-replicative complex assembly involved in nuclear cell cycle		< 0.0001	0.002	DNA replication licensing factor MCM7 (EC 3.6.4.12)	A0A1S3RQL9	*mcm7*	-0.132	-0.420	-0.060
						DNA helicase (EC 3.6.4.12)	B5X105	*mcm5*	-0.154	-0.543	-0.174
						DNA helicase (EC 3.6.4.12)	A0A1S3LZP6	*mcm6*	-0.151	-0.433	-0.023
						nuclear ubiquitous casein and cyclin-	A0A1S3LBU1	*nucks1a*	-0.296	-0.868	-0.438

					dependent kinase substrate 1-like isoform X1					
					E3 ubiquitin-protein ligase TRIP12-like isoform X1	A0A1S3SYD6	*trip12*	0.145	0.627	0.231
Mix	GO:0031589	Cell-substrate adhesion	< 0.0001	0.013	laminin subunit gamma-1-like	A0A1S3R1A2	*lamc1*	-0.145	-0.396	-0.066
					fibrinogen gamma chain-like	A0A1S3RF10	*fgg*	-0.378	-0.766	-0.081
					blood vessel epicardial substance-like isoform X3	A0A1S3NC52	*bves*	-0.196	-0.251	-0.110
					laminin subunit alpha-4-like	A0A1S3S809	*lama4*	-0.171	-0.429	-0.111
					von Willebrand factor-like	A0A1S3KTG6	*vwf*	-0.399	-0.708	0.099
					Alpha-1,4 glucan phosphorylase (EC 2.4.1.1)	C0H8W5	*pygma*	0.026	0.417	0.272
					desmin-like	A0A1S3MRL7	*desmb*	-0.052	0.308	0.224
					agrin-like isoform X3	A0A1S3MEJ6	*agrn*	0.021	-0.442	0.002
Mix	GO:0072376	Protein activation cascade	0.0001	0.037	complement C3	A0A1S3QRL5	*c3a.1*	-0.713	-0.841	0.216
					Antithrombin (antithrombin protein precursor)	Q9PTA8	*serpinc1*	-0.182	-0.516	0.236
					fibrinogen gamma chain-like	A0A1S3RF10	*fgg*	-0.378	-0.766	-0.081
					complement component C9	A0A1S3LT49	*c9*	-0.378	-1.188	0.059
					Hemopexin	A0A1S3PQV6	*hpxa*	-0.560	-1.034	0.120
Mix	GO:0051186	Cofactor metabolic process	0.0002	0.040	Glutathione S-transferase P	B5XGZ2	*gstp1*	1.403	3.174	0.013
					Hemopexin	A0A1S3PQV6	*hpxa*	-0.560	-1.034	0.120
					Glutathione S-transferase A	B9EM96	*gsta.1*	0.872	2.014	-0.095
					probable 2-oxoglutarate dehydrogenase E1 component DHKTD1, mitochondrial	A0A1S3KRS1	*dhtkd1*	0.114	1.177	0.644
					Peroxiredoxin	B5X8H5	*prdx1*	0.436	1.454	0.213
					Glutathione reductase (EC 1.8.1.7)	B5X3C0	*gsr*	0.344	3.066	0.019
					ATP-dependent 6-phosphofructokinase (ATP-PFK) (Phosphofructokinase) (EC 2.7.1.11) (Phosphohexokinase)	A0A1S3LCK1	*pfkmb*	0.126	1.760	-0.045
					Alpha-1,4 glucan phosphorylase (EC 2.4.1.1)	C0H8W5	*pygm*	0.026	0.417	0.272

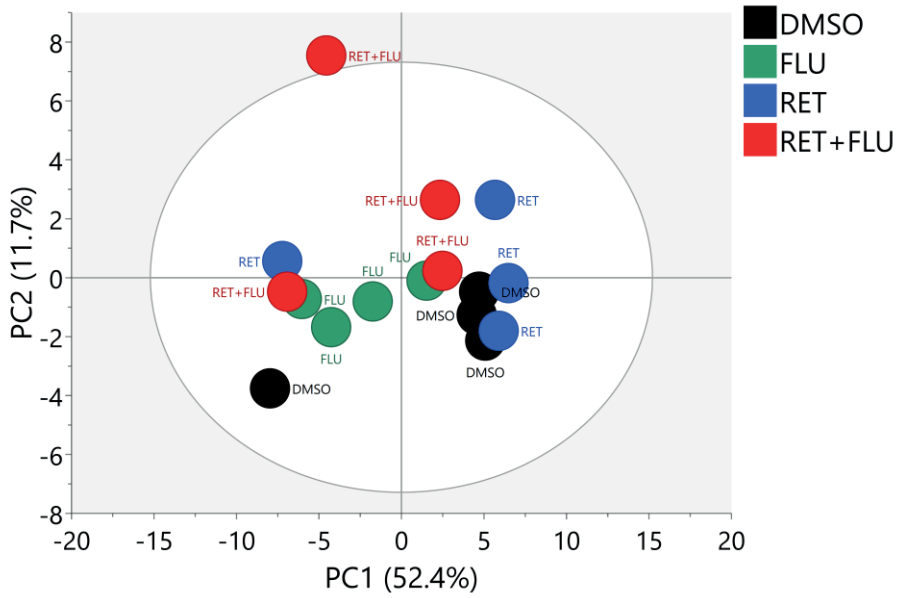

Figure s1. Principal Component Analysis of the cardiac metabolome from 14-days old rainbow trout fry exposed to either DMSO (black; control), retene (blue; Ret), fluoranthene (green; Flu) and the binary mixture of the two (red; Mix). Compensation for dry weight resulted in a poorer separation of results and an outlaying DMSO replicate, and therefore the results from dry weight compensation were excluded from our analysis.

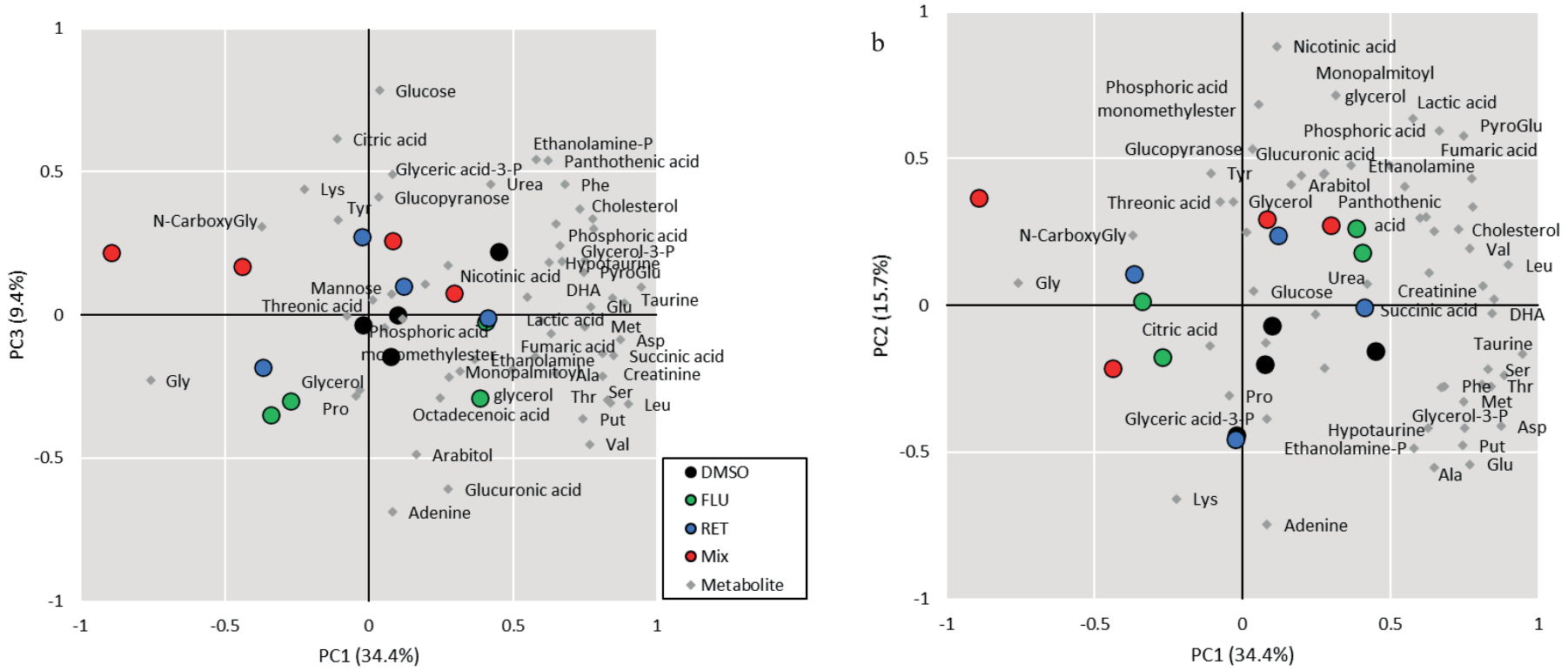

Figure s2a and b. Biplot displays the sample scores and metabolite loadings (57 metabolites) of principal component analysis (PCA). Profiling of alevin cardiac metabolome was performed with GC-MS. Each sample (n=4 in each treatment) consists of pooled hearts of alevins after 14 days of PAH exposure. PCA was performed with Simca P+ (version 16, Umetrics, Umeå, Sweden).

III

ENDOGENOUS AHR AGONIST FICZ ACCUMULATES IN RAINBOW TROUT (*ONCORHYNCHUS MYKISS*) ALEVINS EXPOSED TO A MIXTURE OF TWO PAHS, RETENE AND FLUORANTHENE

by

Andreas N.M. Eriksson, Cyril Rigaud, Emma Wincent, Hannu Pakkanen, Pihla Salonen & Eeva-Riikka Vehniäinen

Submitted manuscript

Request a copy from author.